

# **FH2-dependent Localization of FHOD Formins in the Sarcomere**

By

Elisabeth C. Hamilton

A Dissertation in Cell and Developmental Biology

Submitted in partial fulfillment of the requirements for the degree of Doctor of  
Philosophy in the School of Graduate Studies at the State University of New  
York, Upstate Medical University

Approved\_\_\_\_\_

Date\_\_\_\_\_

## TABLE OF CONTENTS

<b>Acknowledgements</b> .....	iv
<b>List of Figures</b> .....	vi
<b>Abbreviations</b> .....	ix
<b>Thesis Abstract</b> .....	xi
<b>Chapter 1: General Introduction</b> .....	1
<b>Chapter 2: The multiplicity of human formins: Expression patterns in cells and tissues</b> .....	31
Abstract.....	32
Introduction.....	33
Methods.....	37
Results.....	63
Discussion.....	78
References.....	117
<b>Chapter 3: Immunohistochemical Localization of Fhod1 and Fhod3 in the Sarcomere</b> .....	122
Introduction.....	123
Methods.....	125
Results.....	128
Discussion.....	139
References.....	141
<b>Chapter 4: Exogenous Fhod1 and Fhod3 in the Sarcomere</b> .....	143
Introduction.....	144
Methods.....	145
Results.....	151
Discussion.....	164
References.....	168
<b>Chapter 5: General Discussion</b> .....	171
References.....	189

<b>Chapter 6: Localization of Exogenous FMNL1</b> .....	192
Introduction.....	193
Methods.....	194
Results.....	197
Discussion.....	201
References.....	203

## ACKNOWLEDGEMENTS

First and foremost I want to thank my thesis advisor and mentor, Dr. Scott Blystone for providing me the opportunity to learn and grow while pursuing a graduate degree in Cell & Developmental Biology in his lab. His guidance, insight, patience and sense of humor have been an invaluable resource on this journey to become an independently thinking scientist and individual.

I would also like to thank the members of my thesis committee for offering up their time and expertise: Dr. Brian Haarer, Dr. David Pruyne, Dr. Jennifer Schwarz, Dr. Jean Sanger and Dr. Andrea Viczian. I am especially grateful to Dr. Jean Sanger and Dr. David Pruyne for providing guidance, knowledge and motivation throughout my graduate career.

Dr. Joseph Sanger and the Department of Cell & Developmental Biology have provided resources and support throughout my time as a graduate student.

I could not have completed this project without the help and previous work of all of the members of the Blystone laboratory past and present. Thank you to Ginny Graczyk for keeping the lab running smoothly, and most importantly for her untiring efforts to help clone cDNAs. I also want to thank my fellow graduate students in the lab, Dr. Akos Mersich, Dr. Matthew Miller and Eric Miller for their support and friendship inside and outside of the lab. A special thank you to Dr. Jessica Pecone for helping to get the project analyzing formin expression started that contributed to Chapter 2 of this thesis, and to Dr. George Contantineau for laying the groundwork in the lab for work with FHOD1 and skeletal muscle.

The work in Chapter 2 could not have been completed without the generous help and sharing of equipment of Dr. Thomas Welch's lab. I owe a special thank you to Lisa Blystone for her help with the RT-PCR experiments.

I would also like to thank the people behind the scenes, my friends and family. The unwavering support and open doors of friends nearby have made the past seven years a joy. My parents and siblings, though far away, have been nothing but supportive of my pursuit of a graduate degree and my parents have been incredibly generous in their efforts to help me achieve my goals. Last, but

not least, I would like to thank my husband, Bill for always believing in me and for taking care of our daughter, giving me the time and space to finish my project and write this thesis.

## LIST OF FIGURES & TABLES

### Chapter 1: General Introduction

Figure 1: Actin nucleation, elongation, hydrolysis and dissociation.....	3
Figure 2: Domain organizations of formin families.....	5
Figure 3: Actin polymerization by formins.....	7
Figure 4: Autoinhibition and activation of mDIA2.....	8
Figure 5: Model of FHOD1 activation in endothelial cells.....	11
Figure 6: Electron micrograph of a sarcomere.....	15
Figure 7: Sarcomere structure in skeletal muscle.....	16

### Chapter 2: The multiplicity of human formins: Expression patterns in cells and tissues

Table 1: Human formin family nomenclature and sequence references.....	35
Figure 1A: Formin alignments.....	43
Figure 1B: PCR products.....	44
Figure 1C: Complete Formin Alignment with Primers.....	45
Table 2: Expression level of human formins in cell and tissue types.....	65
Figure 2: Homeostatic formins expressed at detectable levels in all cells and tissue types.....	67
Figure 3: Least and most commonly expressed formins are closely related	68
Figure 4: Formin family expression is elevated in hematopoietic cells.....	70
Figure 5: Expression of most formins is similar between cells and tissues of mesenchymal, epithelial and neural origins.....	72
Figure 6A: Total expression of all formins varies in human cell and tissue types.....	74
Figure 6B: Variation of individual formin expression in human cell and tissue types.....	75

### **Chapter 3: Immunohistochemical Localization of Fhod1 and Fhod3 in the Sarcomere**

Figure 1: FHOD1 and FHOD3 expression in 22 cell types and tissues.....	128
Figure 2: Formin expression in cardiac and skeletal muscle.....	129
Figure 3A: FHOD1 and FHOD3 during C2C12 differentiation .....	130
Figure 3B: FHOD1 and FHOD3 intensity throughout C2C12 differentiation.	131
Figure 4: FHOD1 immunohistochemistry in C2C12 cells with myomesin....	133
Figure 5: FHOD3 immunohistochemistry in C2C12 with alpha actinin.....	135
Figure 6: FHOD3 immunohistochemistry in C2C12 cells.....	136
Figure 7: Endogenous FHOD1 and FHOD3 localization in the sarcomere...	137
Figure 7a: Components of the Sarcomere .....	137
Figure 7b: FHOD1 and FHOD3 localization in the sarcomere model 1.....	137
Figure 7c: FHOD1 and FHOD3 localization in the sarcomere model 2.....	137

### **Chapter 4: Exogenous Fhod1 and Fhod3 in muscle**

Figure 1: GFP-tagged plasmids expressed in HeLa cells.....	151
Figure 2: Localization of GFP-Fhod1 and GFP-Fhod1 actin-binding mutants.....	153
Figure 3: Width of Intensity Profile Peaks at mid-point with standard deviation .....	155
Figure 4: Localization of GFP-Fhod3 and GFP-Fhod3 actin-binding mutants.....	157
Figure 5: Average Number of Nuclei per Myotube for Fhod1 and Fhod3 siRNA treatments and controls.....	159
Figure 6: Exogenous FHOD1 and FHOD3 localization in the sarcomere...	161
Figure 6a: Components of the Sarcomere .....	161
Figure 6b: GFP-FHOD1 and GFP-FHOD3 in the Sarcomere Model 1.....	161
Figure 6c: GFP-FHOD1 and GFP-FHOD3 in the Sarcomere Model 2.....	161

## **Chapter 5: Discussion**

Figure 1 - Proposed localization of endogenous FHOD1 and FHOD3, and GFP- FHOD1, GFP-FHOD3 and GFP-FMNL1.....	187
Figure 1a – Components of the Sarcomere .....	187
Figure 1b – Formin localization in the sarcomere model 1.....	187
Figure 1c – Formin localization in the sarcomere model 2.....	187

## **Appendix 1: Localization of Exogenous FMNL1**

Figure 1 – GFP-FMNL1 localization with sarcomeric alpha-actinin .....	198
Figure 2 – GFP-FMNL1 in the Sarcomere.....	200
Figure 2a – Components of the Sarcomere .....	200
Figure 2b – Model of GFP-FMNL1 Localization in the Sarcomere.....	200

## LIST OF ABBREVIATIONS

Arp2/3	Actin-Related Proteins 2/3
BLASTp	Basic Local Alignment Search Tool for proteins
BSA	Bovine serum albumin
CC	Coiled coil domain
cDNA	Complementary DNA
Cobl	Cordon-bleu
COBALT	Constraint-based Multiple Alignment Tool
CK2	Casein kinase 2
CRISPR	Clustered Regularly Interspaced Short Palindromic Repeats
DAAM 1, 2	Disheveled-associated activators of morphogenesis 1, 2
DAD	Diaphanous-autoinhibitory-domain
DAPI	4',6-diamidino-2-phenylindole
DD	Dimerization domain
DEL	Delphinin
DID	Diaphanous inhibitory domain (DID) also known as FH3
Dia1, 2, 3	Diaphanous formin 1, 2, 3
DMEM	Dulbecco's Modified Eagle Medium
DMSO	Dimethyl sulfoxide
DNA	Deoxyribonucleic acid
EDTA	Ethylenediaminetetraacetic acid
FSI	Formin-Spire interaction domain
FH1	Formin homology domain 1
FH2	Formin homology domain 2
FH3	Formin homology domain 3, also known as DID
FHOD1, 3	Formin homology domain containing proteins 1, 3
FITC	Fluorescein isothiocyanate
FMN 1, 2	Original formins 1, 2
FRAP	Fluorescence Recovery after Photobleaching
FRL1, 2, 3	Formin-related proteins identified in leukocytes 1, 2, 3
GBD	GTPase-binding domain
GFP	Green fluorescent protein
HS	Horse serum
INF 1, 2	Inverted formins 1, 2
Lmod	Tropomodulin-related leomodulin-2
N-WASP	Neuronal Wiskott–Aldrich Syndrome protein
PBS	Phosphate-buffered saline
PCR	Polymerase chain reaction
PDZ	Postsynaptic density protein, Discs large, Zona occludens 1 domain
PMSF	phenylmethanesulfonyl fluoride
qRT-PCR	Quantitative Real-time polymerase chain reaction
ROCK	Rho-associated protein kinase
RT-PCR	Reverse transcription polymerase chain reaction
SDS-PAGE	Sodium dodecyl sulfate polyacrylamide gel electrophoresis
TRITC	Tetramethylrhodamine

WASP      Wiskott–Aldrich Syndrome protein  
WH2      WASP homology 2 domain

## **THESIS ABSTRACT**

### **FH2-dependent Localization of FHOD Formins in the Sarcomere**

**Author: Elisabeth C. Hamilton**

**Sponsor: Scott D. Blystone, Ph.D.**

Formins are a class of actin nucleating factors containing a highly-conserved FH2 domain, which binds actin. There are 15 mammalian formin proteins in seven sub-families that have been found to nucleate, cap, sever, bundle, and polymerize linear actin filaments. An expression analysis of all 15 human formins across 22 different cell and tissue types showed high levels of expression for one formin sub-family in striated muscle: FHOD. While FHOD1 is highly expressed across many cell and tissue types, FHOD3 is only found at comparatively high levels in striated muscle cells.

The mature structure of skeletal muscle is a very recognizable periodic repetition of filaments that allows muscles to contract. The sarcomere is the smallest contractile unit of skeletal muscle, with the two main filaments, the thick filament containing myosin, and the thin filament containing actin moving back and forth via the interaction of myosin heads with the thin filament, which allows muscles to contract. While the molecular functioning and the mature structure of skeletal muscle is well understood, the exact mechanism by which the sarcomere is assembled, and specifically, how the actin-core of the thin filament is formed and incorporated into the thin filament remains unknown. The high levels of expression of FHOD formins in striated muscle, combined with their ability to

interact with filamentous actin warranted a closer look at FHOD1 and FHOD3 in the sarcomere.

In this study we found that FHOD1 and FHOD3 have distinct sarcomeric localizations in C2C12 cells. FHOD1 localizes to the barbed end of the actin filament at the Z-disk and FHOD3 localizes to the pointed end of the actin filament near the center of the sarcomere. Full-length cDNA constructs for FHOD1 and FHOD3 were introduced into skeletal muscle cells, and we were able to recreate the endogenous localization of FHOD3 with the exogenous cDNA. The FHOD1 cDNA localized not to the barbed end of the actin filament, as endogenous FHOD1 does, but instead to the pointed end of the actin filament, where endogenous and exogenous FHOD3 were found. We hypothesized that FHOD binding to actin is dependent upon two highly conserved actin-binding sites in the FH2 domain. Mutations of the actin-binding residues in the FH2 domain impaired the actin-binding ability of both exogenous FHOD1 and FHOD3 and showed that the localization of FHOD1 and FHOD3 in the sarcomere is actin-binding dependent.

## **Chapter 1:**

## **General Introduction**

## **Overview**

This introduction provides a brief overview of the actin cytoskeleton in mammalian cells, including actin monomers, actin polymerization and actin modification, an overview of mammalian formins with a special focus on the human formins Fhod1 and Fhod3 and an overview of muscle cytoskeletal development and mature structure.

## **Actin Cytoskeleton**

The ability of cells to change shape, retain their structure, move and divide depends on their internal cytoskeleton, which consists of three types of filaments: microfilaments, intermediate filaments and microtubules. This thesis will focus on microfilaments and the protein that comprises them, actin.

Actin is a globular 42kDa protein that is able to polymerize and form double-stranded helical filaments (Kabsch, et al., 1990). Globular actin, also called G-actin or monomeric actin is the smallest building block of actin filaments (Holmes, et al., 1990). Actin filament assembly begins with actin nucleation, the formation of actin dimers and trimers, which then elongate through polymerization into polarized actin filaments at a rate dependent on the availability of G-actin (Wegner and Engel, 1975; Sept, et al., 1999). The polarized nature of the actin filament results in a fast-growing barbed or plus-end and a slow-growing pointed or minus-end as shown in Figure 1 (Pollard, TD, 1986). After spontaneous formation of actin dimers and trimers, polymerization of actin filaments is enhanced by actin nucleation factors.

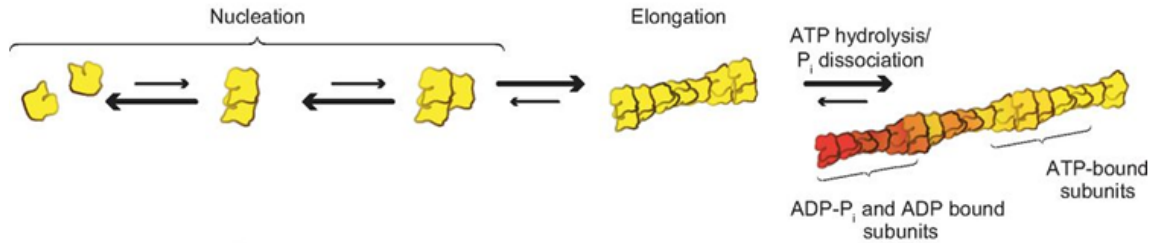


**Figure 1: Actin nucleation, elongation, hydrolysis and dissociation**

Globular actin forms dimers and trimers and then elongates into filaments.

Adapted from Blanchoin et al., 2014.

There are three classes of actin assembly factors that facilitate actin polymerization: Arp2/3, formins and Spire/Cordon bleu/Leimodin (Spire/Cobl/Lmod). Arp2/3 initiates the formation of branched actin filaments at a 70° angle from an existing mother filament and stays associated with the slow-growing pointed end (Pollard and Borisy, 2003). Spire/Cobl/Lmod form polymerization seeds to kick-start the polymerization of actin filaments (Chesarone and Goode, 2009). Formins, which are the focus of this study, nucleate filamentous actin *de novo* and remain associated with the fast-growing barbed end (Pruyne, et al., 2002; Goode and Eck, 2007).

## Formins

Formins are a class of actin-modifying proteins that play a role in cell morphology, cell migration, cell invasion, cytokinesis, microtubule dynamics, phagocytosis, intracellular transport, plasma membrane blebbing, filopodia, invadopodia and podosome formation and focal adhesions (Wallar and Alberts, 2003; Kovar, 2006; Goode and Eck, 2007; Chesarone et al., 2010). They have been shown to nucleate, cap, sever, bundle, and polymerize actin *in vitro*, with

their main function being the polymerization of linear actin filaments (Wallar and Alberts, 2003; Kovar, 2006; Goode and Eck, 2007; Chesarone et al., 2010).

Formin proteins are highly conserved and in humans consist of 15 formins in seven sub-families, based on the phylogeny of the highly conserved FH2 domain, shown as follows and as in Figure 2 (Schönichen and Geyer, 2010; Campellone and Welch, 2010):

- Diaphanous formins (DIA)
  - o mDia1
  - o mDia2
  - o mDia3
  
- formin-related proteins identified in leukocytes or formin-like (FRL or FMNL)
  - o FRL1 or FMNL1
  - o FRL2 or FMNL2
  - o FRL3 or FMNL3
  
- disheveled-associated activators of morphogenesis (DAAM)
  - o DAAM1
  - o DAAM2
  
- formin homology domain containing proteins (FHOD)
  - o Fhod1
  - o Fhod3
  
- original formins (FMN)
  - o FMN1
  - o FMN2
  
- delphilin (DEL)
  
- inverted formins (INF)
  - o INF1
  - o INF2

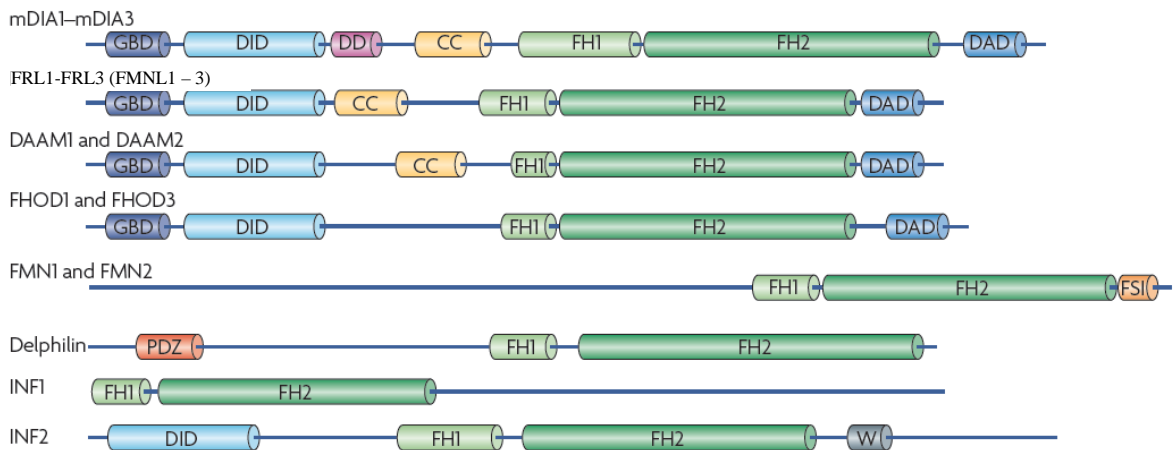


**Figure 2: Domain organizations of formin families.**

All 15 mammalian formins contain formin homology 1 and 2 (FH1, FH2) domains, along with family and protein-specific regulatory and binding domains:

- GTPase-binding domain (GBD)
- Diaphanous inhibitory domain (DID) also known as FH3 domain
- Dimerization domain (DD)
- Coiled coil domain (CC)
- Formin homology 1 domain (FH1)
- Formin homology 2 domain (FH2)
- Diaphanous-autoinhibitory-domain (DAD)
- Postsynaptic density protein, Discs large, Zona occludens 1 domain (PDZ)
- WASP homology 2 domain (W)
- Formin-Spire interaction domain (FSI)

Adapted from: Campellone and Welch, 2010.

### **Actin polymerization by formins**

All formins have two domains in common, the formin homology domain 1 (FH1) and formin homology domain 2 (FH2), which are the key domains involved in formins' actin polymerization activity. After the formation of actin dimers and trimers, the FH2 domain forms a homo-dimer that remains associated with the fast-growing barbed end of the actin filament (Pruyne, et al., 2002). As shown in Figure 3, The FH2 domains form a head-to-tail homo-dimer and associates with the fast-growing, barbed end of the actin filament. The FH1 domain recruits profilin-bound globular actin via its proline-rich stretches, and delivers the actin monomers to the FH2 domain at the barbed end of the actin filament (Zigmond, et al., 2003; Baarlink C and Grosse R, 2008). The two FH2 domains from the two dimerized formin proteins then processively step up the growing actin filament and bind to the newly added actin monomer (Campellone and Welch, 2010). Highly conserved Isoleucine and Lysine residues in the FH2 have been shown to be required for proper actin-binding (Xu, et al., 2004; Otomo, et al., 2005; Lu, et al., 2007).

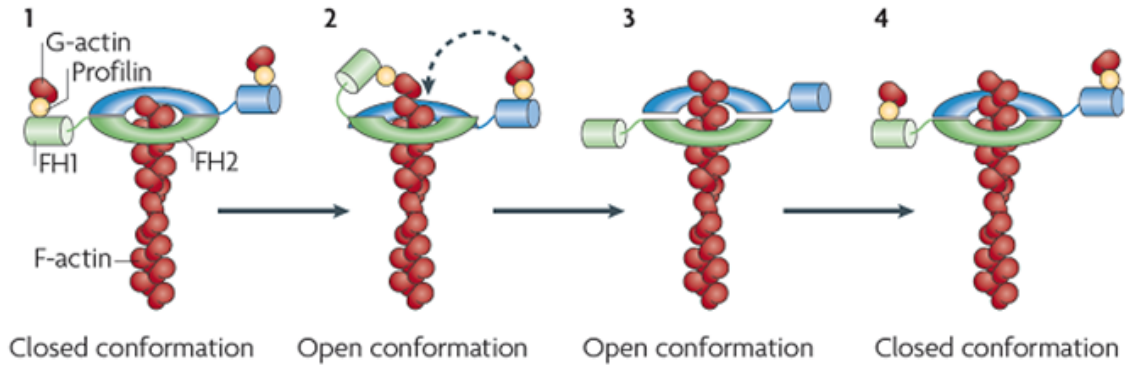


### Figure 3: Actin polymerization by formins

The FH2 domain forms a homo-dimer and associates with the fast-growing, barbed end of the actin filament. (1) Globular actin monomers bound to profilin are recruited by the proline-rich FH1 domain and are delivered to the barbed end of the actin filament. (2+3) The FH2 domains step up processively to remain associated with the barbed end of the actin filament. The closed/open conformational change allows for the addition of actin monomers, while also ensuring that the barbed end is not capped or otherwise modified.

Adapted from: Campellone and Welch, 2010.

## Activation of Formins

*In vitro*, the purified FH2 domain is sufficient to attain actin polymerization (Chesarone, et al., 2010), but the activation of full-length formins *in vivo* varies between sub-families. This section will focus on the autoinhibitory mechanism of activation seen in most formins that contain DIDs and DADs, as shown in figure 2. The most well-studied group, the diaphanous related formins (DRFs) Dia1, 2 and 3, exist in an autoinhibited state created by the interaction of the DID and DAD. This autoinhibition is relieved by the binding of RhoGTPases to the GBD, resulting in a conformational change that allows the FH2 domain to interact with actin monomers, as shown in Figure 4 (Li and Higgs, 2005; Lammers, et al., 2005).

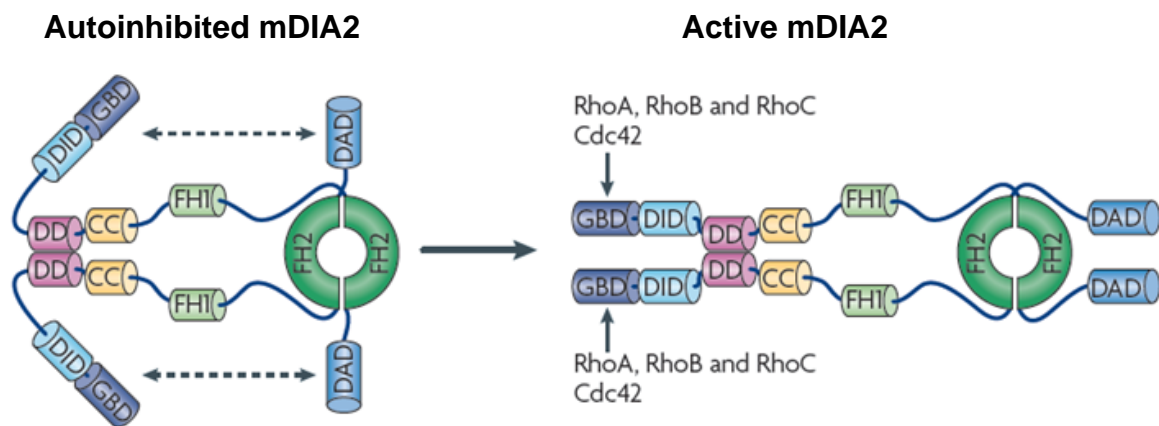


**Figure 4: Autoinhibition and Activation of mDIA2**

The binding of the DID and DAD result in an autoinhibited state. To activate diaphanous related formins, a Rho-GTPase binds to the GBD, relieving the autoinhibition.

Adapted from Campellone and Welch, 2010.

## **Formin homology domain containing proteins (FHOD)**

FHOD proteins are highly conserved, with the simplest ortholog found in the single-celled eukaryote *Capsaspora owczarzaki* (Bechtold, et al., 2014), and contain the formin-specific FH1 and FH2 domains (Westendorf, et al., 1999). The FHOD formins are diaphanous-related formins (DRFs), which are defined by the presence of two domains: the diaphanous inhibitory domain (DID) and the diaphanous auto-regulatory domain (DAD) (Bechtold, et al., 2014; Rivero, et al., 2005). Two FHOD proteins have been identified in humans: FHOD1 and FHOD3.

### **FHOD1**

FHOD1 is a 128kDa 1165 amino acid DRF that maps to chromosome 16q22. (Westendorf, et al., 1999).

### **FHOD1 activation**

As the presence of the diaphanous-related autoinhibitory domains suggests, FHOD1 is autoinhibited by the interaction of the N-terminal DID and C-terminal DAD (Westendorf JJ, 2001). FHOD1 interacts with the RhoGTPase Rac1 in a guanine-nucleotide independent manner, and does not interact with the other RhoGTPases Rho or Cdc42 (Gasteier, et al., 2003; Westendorf JJ, 2001). Interaction with Rac1 has been shown to result in increased levels of FHOD1 in the actin fibers of lamellipodia and membrane ruffles (Gasteier, et al.,

2003), but it is unclear how exactly Rac1 affects FHOD1's autoinhibited state, since no Rac1-binding sites have been found in FHOD1's DID, making it highly unlikely that Rac1 binds directly to the DID to relieve autoinhibition (Schönichen, et al., 2006). Most likely, binding of Rac1 to the GBD causes a conformational change in the adjacent DID to relieve the autoinhibitory binding to the DAD. Constitutively active FHOD1 lacking a DAD domain has been shown to increase actin stress fiber formation *in vitro* via the Rho-ROCK cascade in NIH3T3 cells, and *in vitro* studies have shown that FHOD1's auto-inhibition is relieved by a single mutation in the DID domain of Valine 228 to Glutamate (Koka, et al., 2003; Schulte, et al., 2008), which confirms that FHOD1 does indeed rely on the reversal of its autoinhibition to carry out its cellular functions.

In addition to this activation by reversal of the autoinhibition as is the norm among DRFs, FHOD1 can also be activated by phosphorylation of three residues in the DAD domain, as shown in Figure 5. *In vivo*, FHOD1's autoinhibition can be relieved by the phosphorylation of Ser1131, Ser1137, and Thr1141, all located within the DAD, by the Rho-dependent protein kinase ROCK in endothelial cells, resulting in increased stress fiber formation (Takeya, et al., 2008). This mechanism of activation proposes that thrombin binds to its G-protein coupled receptor (GPCR), which activates the Rho-ROCK cascade, and ROCK phosphorylates three residues in the C-terminal DAD, Ser1131, Ser1137 and Thr1141, which relieves the DID-DAD autoinhibition of FHOD1 and activates it, as shown in figure 5. This Rho-dependence has also been shown in *Drosophila melanogaster*. The FHOD1 ortholog Knittrig has been shown to be activated by

Rho-dependent Rok and a constitutively active form of Knittrig results in an increase in stress fiber formation in macrophages and epithelial cells (Lammel, et al., 2014).

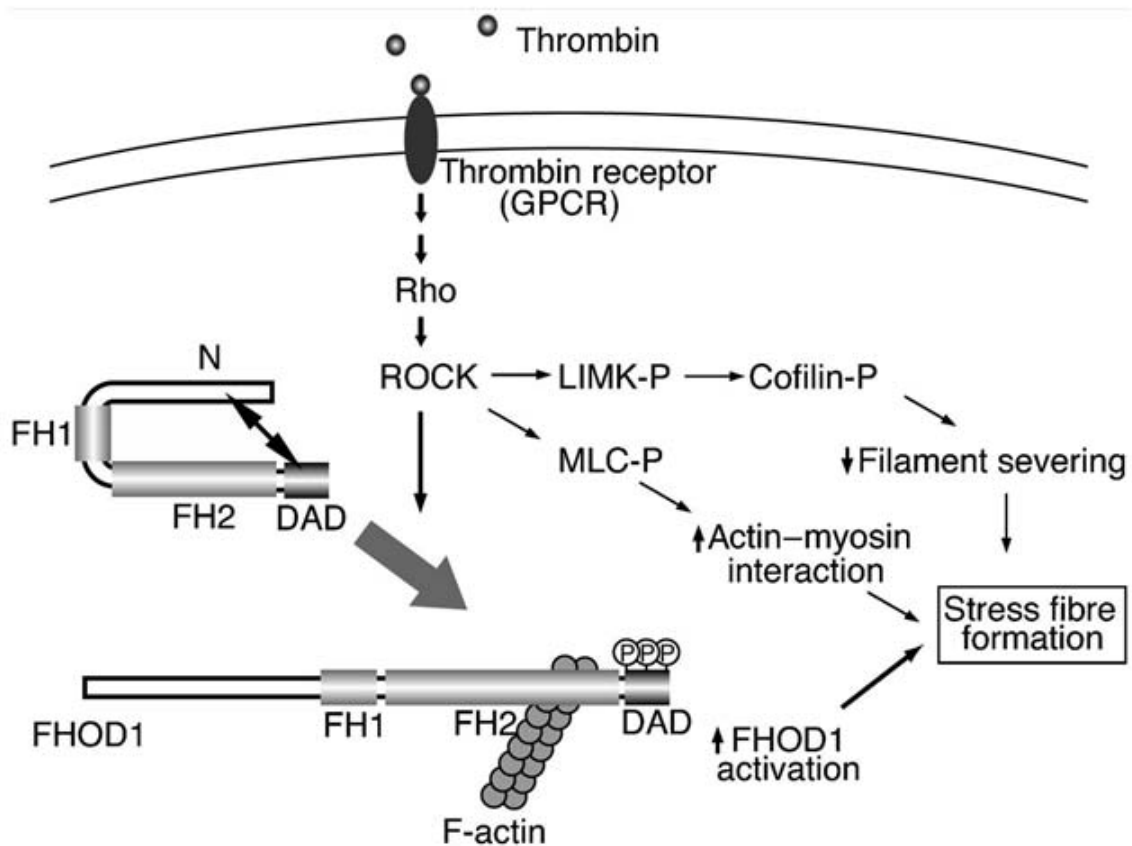


**Figure 5: Model of FHOD1 activation in endothelial cells**

Thrombin binds to the G-protein coupled receptor (GPCR), activating Rho, which in turns activates ROCK, which then phosphorylates Ser1131, Ser1137 and Thr1141, relieving the DID-DAD autoinhibition of FHOD1, activating it.

Adapted from Takeya, et al., 2008.

## **FHOD1 Interaction with Actin**

The exact mechanism by which FHOD1 interacts with actin filaments *in vivo* has yet to be determined. *In vitro*, full length FHOD1 does not enhance actin filament polymerization, but has been found to inhibit actin polymerization (Schönichen, et al., 2013). Truncated FHOD1 without a DAD, considered to be constitutively active, has been shown to bundle 5-10 parallel actin filaments into filament bundles in lamellipodia and accumulates in actin arcs and stress fibers, where it has been suggested, it helps to stabilize actin filaments (Schönichen, et al., 2013). This localization is in line with the inability of FHOD1 to enhance actin filament polymerization. This *in vitro* inhibition of actin polymerization holds true for full-length FHOD1, FHOD1 lacking the DAD, as well as a mutant containing only the N-terminal portion from the FH1 domain onward (FH1-FH2 and DAD domains) (Schönichen, et al., 2013). A construct lacking the FH2 domain had no effect on actin polymerization, suggesting a capping role of actin filaments involving the FH2 domain (Schönichen, et al., 2013). Furthermore, an N-terminal construct lacking the FH1, FH2 and DAD domains still bound to actin *in vitro*, which could mean a secondary actin binding site in the N-terminus (Schönichen, et al., 2013). The higher ratio of this N-terminal mutant found in high-speed centrifugation assays compared with the ratio of FH2-binding mutants suggests that this secondary binding site allows FHOD1 to interact with the sides of actin filaments (Schönichen, et al., 2013). These results are based on mutants lacking the DAD, which renders formins constitutively active, but the DAD has also been shown to be involved in actin nucleation (Gould, et al., 2011). Specifically, the

DAD has been shown to bind globular actin, both as part of an actin-binding mutant with an FH2 domain that is incapable of binding actin, and by itself as a DAD-only construct (Gould, et al., 2011). This concept that DRFs have other actin-binding sites outside the FH2 is supported by additional findings of another DRF: full-length FMNL1, with mutations in the FH2 domain that interfere with actin binding has been shown to rescue an actin-dependent function *in vivo* (Blystone Lab, unpublished observations).

### **FHOD3**

Formin Homology Domain Containing Protein 3 (FHOD3) is a 1439 residue protein that maps to chromosome 18q12.2 (Katoh and Katoh, 2004). It is most closely related to FHOD1, but has been studied less, which is likely due to the fact that it shows significant expression levels in fewer tissues than FHOD1 and that there are fewer orthologs to FHOD3 than there are to FHOD1 (Krainer, et al., 2013).

### **FHOD3 Activation**

FHOD3 is a diaphanous-related formin, which suggests its activation occurs via the relief of the auto inhibitory interaction between the DID and DAD domains. While no specific GTPase has been identified as the activator of FHOD3, it can be activated by the ROCK-dependent phosphorylation of three amino acids in the DAD domain (Paul, et al., 2015). This phosphorylation-dependent activation was confirmed by phosphorylation of S1590, S1596 and

T1600 by casein kinase 2 (CK2), which activates a cardiomyocyte-specific isoform of FHOD3 and leads to an increase in actin filaments (Iskratsch, et al., 2010). The exact molecular mechanism by which these phosphorylation events activate FHOD3 is still unclear, but the most likely explanation is an interruption of the DID-DAD binding, thus activating FHOD3, since these residues are located toward the center of the DAD.

### **FHOD3 Interaction with Actin and other Cytoskeletal Filaments**

Overexpression of FHOD3 has been found to increase stress fiber formation in HeLa cells (Kanaya, et al., 2005). FHOD3 was found to co-localize with the intermediate filament marker nestin in rat neonatal cardiomyocytes (Kanaya, et al., 2005). Constitutively active FHOD3 resulted in the increased formation of spike-like actin structures in an ovarian cancer cell line, indicating that FHOD3 may have an effect on the formation of actin structures involved in cell migration and invasion (Paul, et al., 2015).

## Skeletal Muscle

The structure of striated muscle is highly conserved across species. This overview focuses on mammalian skeletal muscle.

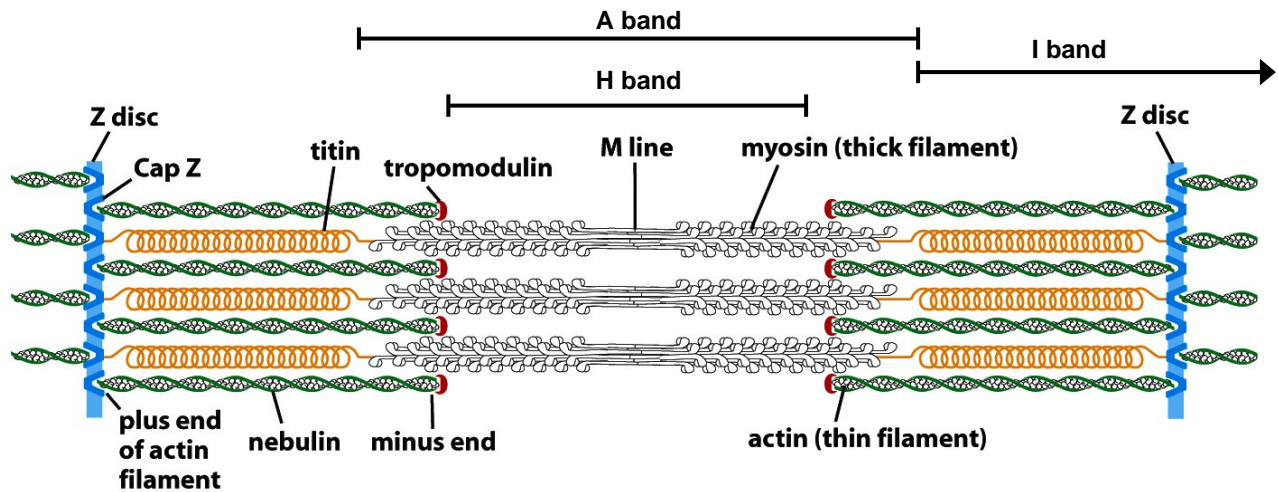


**Figure 6 – Sarcomere structure in skeletal muscle**

Adapted from Alberts, et al, 2003, p 963.

Schematic representation of the main parts of the sarcomere.

### Sarcomere Structure

The sarcomere is the smallest contractile unit in muscles and its areas are named based on their appearance in electron and polarized light micrographs, as shown in Figure 7. The dark region indicating the boundaries of one sarcomere is referred to as the Z-disk, named for the German word “Zwischenscheibe” or “in between disk”, since it is in between two sarcomeres (Luther, PK, 2009). I-bands are named for their isotropic appearance, and represent the region of the thin filament, spanning the thin filaments of two adjacent sarcomeres across the Z-

disk. Next to the I-band is the A-band, named for its anisotropic or directional organization, and it consists of the functional region of the thick filament that binds to the thin filament (Ehler and Gautel, 2008). The H-band encompasses the region between thick filaments, referring to the German word “heller”, meaning lighter. In the center of the sarcomere is the M-line, the “Mitte” or “middle” of the sarcomere. (Kontrogianni-Konstantopoulos, et al., 2009).

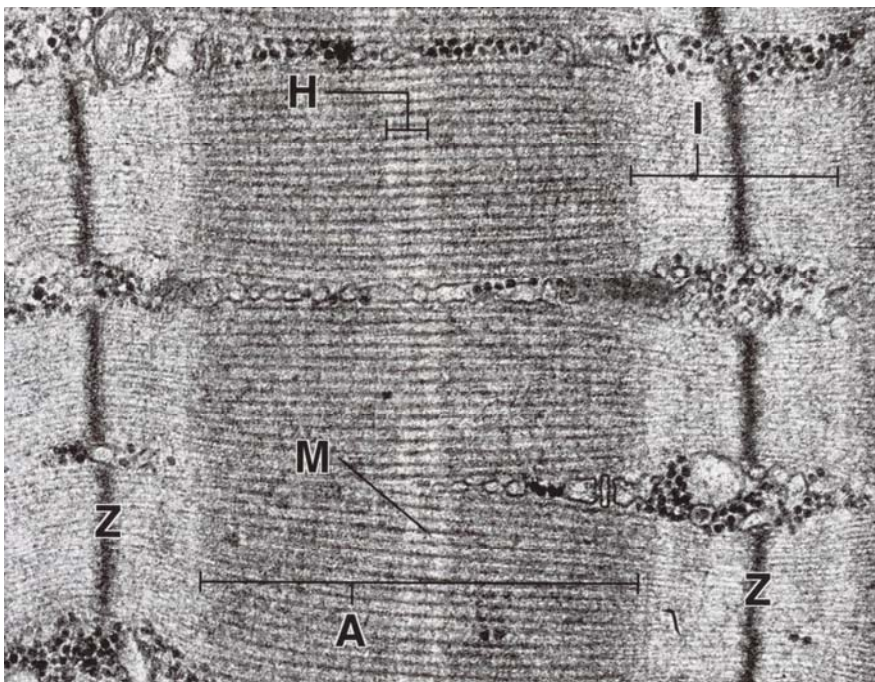


**Figure 7 – Electron micrograph of a sarcomere**

Adapted from Ross, et al., 2003, p 253.

The sarcomere as it appears in an electron micrograph. The H and A bands received their names from their appearance in microscopy images – H for heller, the German word for lighter, and A for anisotropic.

### **Thick Filament**

The thick filament is 1.59 $\mu\text{m}$  long in human skeletal muscles, consisting of 294 myosin II molecules. It interacts with titin, which binds the thick filament to the Z-disk (Ehler and Gautel, 2008). Each myosin molecule is comprised of two heavy and four light chains (Clark, et al., 2002). The myosin heavy chains bind the filamentous actin in the thin filaments, and through ATP hydrolysis and the subsequent conformational change in the myosin heads, contractile forces are created, resulting in muscle contraction and relaxation (Clark, et al., 2002). The thick filament is anchored to the thin filament and the Z-disk by titin (Clark, et al., 2002).

### **Thin Filament**

Thin filaments consist of an actin filament that is approximately 1 $\mu\text{m}$  long and is surrounded by a tropomyosin-troponin complex, which has a regulatory role in the interaction of the thick and thin filaments (Clark, et al., 2002). The fast-growing, barbed end of the actin filament is capped by CapZ and anchored to the Z-disk via alpha-actinin, while the slow-growing, pointed end of the actin filament is capped by tropomodulin, which also controls the length of the thin filament (Luther, PK, 2009, Gregorio, et al., 1995). CapZ prevents the actin filament from depolymerizing (Faulkner, et al., 2001). The turnover rate of thin filament proteins has been suggested to be quite fast with a half-life of 3 days (Martin, AF, 1981).

## **Sarcomerogenesis**

Striated muscle has a highly preserved microscopic structure, due to the repetitive arrangement of its smallest contractile unit, the sarcomere, as shown in Figure 6 (Huxley H and Hanson J, 1954). The arrangement of actin in muscle cells is one of the most prominent cytoskeletal structures, yet it is not entirely clear how the actin structure in muscles is formed and maintained. On a cellular level, myoblasts fuse to form multinucleated myotubes, which attach to each other and the extracellular matrix before assembling into myotubes (Ehler and Gautel, 2008). Within myofibrils, the formation of sarcomeres involves several large proteins, including titin and nebulin, which act as molecular scaffolds for myosin and actin, respectively, onto which other essential components of the sarcomere assemble (Sanger, et al., 2005; Clark, et al., 2002). However, the exact mechanism by which the actin filaments are nucleated and incorporated into the developing muscle is still unclear.

On a microscopic level, it has been shown that sarcomere assembly begins at integrin-based sites where Z-disk precursors called Z-bodies anchor stress fiber-like actin filament at the barbed end (Sparrow and Schöck, 2009; Moerman and Williams, 2006; Volk, et al., 1990). The first myofibrils most likely originate from these integrin-based adhesion sites and thus form near the cell membrane. They have an irregular arrangement of alpha-actinin and titin, resembling non-muscle cell actin stress fibers, and are referred to as premyofibrils (Rhee, et al., 1994; Sanger, et al., 2005). These premyofibrils contain Z-bodies and thin filaments made up of actin with tropomyosin and

troponin, as well as non-muscle myosin II filaments (Sanger, et al., 2005). During the maturation of these premyofibrils, the Z-bodies in adjacent myofibrils align and fuse into mature Z-disks, and other sarcomeric proteins, such as titin, M-band proteins and muscle myosin II are incorporated into the mature myofibril (Sanger, et al., 2005). This process of maturation has been confirmed in cardiac muscle cells as well (Du, et al., 2008).

While the microscopic appearance of sarcomere development is fairly well understood, the exact molecular mechanism by which actin is recruited to and nucleated in this structure remains unknown. Based on their known nucleation activity, three actin nucleation factors (ANFs) have been suggested in striated muscle actin nucleation: neuronal Wiskott–Aldrich Syndrome protein (N-WASP), tropomodulin-related leomodulin-2 (Lmod), and formins (Takano, et al., 2010; Chereau, et al., 2008; Tanaguchi, et al., 2009). This study focuses on formins.

### **FHOD1 in Muscle**

The level of expression of FHOD1 in cardiac and skeletal muscle was found to be high or higher than most other formins, suggesting that FHOD1 proteins may play a role in muscle development and maintenance (Krainer, et al., 2013). FHOD1 was found to localize to the intercalated discs as well as to the Z-disks in frozen sections of murine heart muscle (Dwyer, et al., 2014). This coincides with the localization of the *Caenorhabditis elegans* FHOD1 ortholog to newly forming Z-bodies and close to Z-disks (Mi-Mi, et al., 2012). FHOD1 allele deletion in *Caenorhabditis elegans* showed a narrowing of body wall muscles

and wider spaces between muscle pairs, as well as fewer overall striations, indicating a necessary function of FHOD1 in proper muscle formation (Mi-Mi, et al., 2012). A *Caenorhabditis elegans* mutant lacking FHOD1 showed a disruption of Z-bodies and narrower sarcomeres, but did not completely inhibit sarcomere formation (Mi-Mi and Pruyne, 2015). In cardiac muscle, FHOD1 has been found to localize to intercalated discs and costameres (Al Haj, et al., 2015). The expression of constitutively active FHOD1 in cultured smooth muscle cells has shown an involvement in the differentiation of smooth muscle cells. However, this finding could not be replicated with full-length FHOD1 (Staus, et al., 2011).

### **FHOD3 in Muscle**

FHOD3 has been found to be highly expressed in cardiac muscle, and most studies involving FHOD3 have been conducted in cardiac rather than skeletal muscle. However, the role of FHOD3 in striated, and specifically, cardiac muscle has not been clearly determined and its localization remains somewhat disputed. Studies in cardiac muscle have shown conflicting evidence, placing Fhod3 near the center of the sarcomere at the pointed end of actin, as two closely spaced lines on either side of the central M-line (Taniguchi, et al., 2009, Kan-o, et al., 2010) but also at the Z-disk, at the barbed end of actin in mature cardiomyocytes (Iskratsch, et al., 2010, 2013). Domain-based studies suggest that an N-terminal motif, rather than the FH2 domain may be responsible for the localization to the pointed end of actin (Taniguchi, et al., 2009). As for its function, FHOD3 has been found to promote myofibril maintenance in cardiac

muscle, specifically at the barbed end at the Z-disk, as actin-binding mutants were not able to rescue the effect of FHOD3 knock-down on the sarcomere (Iskratsch, et al., 2010).

Two splicing isoforms of FHOD3 have been identified, a long version and a short version, with the long version specific to cardiac muscle (Taniguchi, et al., 2009, Kan-o, et al., 2010). Mutations in cardiac FHOD3 have been associated with a form of dilated cardiomyopathy and hypertrophic cardiomyopathy (Arimura, et al., 2013; Wooten, et al., 2013).

## **Thesis Overview**

This thesis begins with an expression analysis of all 15 human formins across 22 different cell and tissue types using real-time quantitative PCR (rtPCR) in Chapter 2. The purpose of this study was to determine complete expression profiles across a wide variety of commonly cultured cell lines and tissues to provide a basis for further studies. Chapters 3 and 4 on the localization of endogenous and exogenous FHOD1 and FHOD3 in skeletal muscle are based on the findings of FHOD1 and FHOD3 expression in Chapter 2. Chapter 5 provides a summative conclusion with suggestions for further experimentation, and appendix 1 contains additional data on the localization of FMNL1 in striated muscles.

## References

Al Haj A, Mazur AJ, Radaszkiewicz K, Radaszkiewicz T, Makowiecka A, Stopschinski BE, Schonichen A, Geyer M and Mannherz HG. 2015. Distribution of formins in cardiac muscle: FHOD1 is a component of intercalated discs and costameres. *Eur J Cell Biol Elsevier GmbH*94:2101-113.

Alberts B, Johnson A, Lewis J, Raff M, Roberts K and Walter P. 2002. *Molecular Biology of the Cell*. Garland Science, p963.

Arimura T, Takeya R, Ishikawa T, Yamano T, Matsuo A, Tatsumi T, Nomura T, Sumimoto H and Kimura A. 2013. Dilated cardiomyopathy-associated FHOD3 variant impairs the ability to induce activation of transcription factor serum response factor. *Circ J* 77:122990-2996.

Baarlink C and Grosse R. 2008. A GBD uncovered: the FHOD1 N terminus is formin'. *Structure* 16:91287-1288.

Bechtold M, Schultz J and Bogdan S. 2014. FHOD proteins in actin dynamics--a formin' class of its own. *Small GTPases* 5:211.

Blanchoin L, Boujemaa-Paterski R, Sykes C and Plastino J. 2014. Actin dynamics, architecture, and mechanics in cell motility. *Physiol Rev* 94:1235-263.

Campellone KG and Welch MD. 2010. A nucleator arms race: cellular control of actin assembly. *Nat Rev Mol Cell Biol* 11:4237-251.

Chereau D, Boczkowska M, Skwarek-Maruszczyńska A, Fujiwara I, Hayes DB, Rebowski G, Lappalainen P, Pollard TD and Dominguez R. 2008. Leiomodin is an actin filament nucleator in muscle cells. *Science* 320:5873239-243.

Chesarone MA, DuPage AG and Goode BL. 2010. Unleashing formins to remodel the actin and microtubule cytoskeletons. *Nat Rev Mol Cell Biol* 11:162-74.

Chesarone MA and Goode BL. 2009. Actin nucleation and elongation factors: mechanisms and interplay. *Curr Opin Cell Biol* 21:128-37.

Clark KA, McElhinny AS, Beckerle MC and Gregorio CC. 2002. Striated muscle cytoarchitecture: an intricate web of form and function. *Annu Rev Cell Dev Biol* 18:637-706.

Du A, Sanger JM and Sanger JW. 2008. Cardiac myofibrillogenesis inside intact embryonic hearts. *Dev Biol* 318:2236-246.

Dwyer J, Pluess M, Iskratsch T, Dos Remedios CG and Ehler E. 2014. The formin FHOD1 in cardiomyocytes. *Anat Rec (Hoboken) Wiley Periodicals, Inc* 297:91560-1570.

Ehler E and Gautel M. 2008. The sarcomere and sarcomerogenesis. *Adv Exp Med Biol* 642:1-14.

Faulkner G, Lanfranchi G and Valle G. 2001. Telethonin and other new proteins of the Z-disk of skeletal muscle. *IUBMB Life* 51:5275-282.

Gasteier JE, Madrid R, Krautkramer E, Schroder S, Muranyi W, Benichou S and Fackler OT. 2003. Activation of the Rac-binding partner FHOD1 induces actin stress fibers via a ROCK-dependent mechanism. *J Biol Chem* 278:4038902-38912.

Goode BL and Eck MJ. 2007. Mechanism and function of formins in the control of actin assembly. *Annu Rev Biochem* 76:593-627.

Gould CJ, Maiti S, Michelot A, Graziano BR, Blanchoin L and Goode BL. 2011. The formin DAD domain plays dual roles in autoinhibition and actin nucleation. *Curr Biol Elsevier Ltd* 21:5384-390.

Gregorio CC, Weber A, Bondad M, Pennise CR and Fowler VM. 1995. Requirement of pointed-end capping by tropomodulin to maintain actin filament length in embryonic chick cardiac myocytes. *Nature* 377:654483-86.

Holmes KC, Popp D, Gebhard W and Kabsch W. 1990. Atomic model of the actin filament. *Nature* 347:628844-49.

Huxley H and Hanson J. 1954. Changes in the cross-striations of muscle during contraction and stretch and their structural interpretation. *Nature* 173:4412973-976.

Iskratsch T, Reijntjes S, Dwyer J, Toselli P, Degano IR, Dominguez I and Ehler E. 2013. Two distinct phosphorylation events govern the function of muscle FHOD3. *Cell Mol Life Sci* 70:5893-908.

Iskratsch T, Lange S, Dwyer J, Kho AL, dos Remedios C and Ehler E. 2010. Formin follows function: a muscle-specific isoform of FHOD3 is regulated by CK2 phosphorylation and promotes myofibril maintenance. *J Cell Biol* 191:61159-1172.

Kabsch W, Mannherz HG, Suck D, Pai EF and Holmes KC. 1990. Atomic structure of the actin:DNase I complex. *Nature* 347:628837-44.

Kanaya H, Takeya R, Takeuchi K, Watanabe N, Jing N and Sumimoto H. 2005. Fhos2, a novel formin-related actin-organizing protein, probably associates with the nestin intermediate filament. *Genes Cells* 10:7665-678.

Kan-o M, Takeya R, Taniguchi K, Tanoue Y, Tominaga R and Sumimoto H. 2012. Expression and subcellular localization of mammalian formin Fhod3 in the embryonic and adult heart. *PLoS One* 7:4e34765.

- Katoh M and Katoh M. 2004. Identification and characterization of human FHOD3 gene in silico. *Int J Mol Med* 13:4615-620.
- Koka S, Neudauer CL, Li X, Lewis RE, McCarthy JB and Westendorf JJ. 2003. The formin-homology-domain-containing protein FHOD1 enhances cell migration. *J Cell Sci* 116:Pt 91745-1755.
- Kontrogianni-Konstantopoulos A, Ackermann MA, Bowman AL, Yap SV and Bloch RJ. 2009. Muscle giants: molecular scaffolds in sarcomerogenesis. *Physiol Rev* 89:41217-1267.
- Kovar DR. 2006. Molecular details of formin-mediated actin assembly. *Curr Opin Cell Biol* 18:111-17.
- Krainer EC, Ouderkirk JL, Miller EW, Miller MR, Mersich AT and Blystone SD. 2013. The multiplicity of human formins: Expression patterns in cells and tissues. *Cytoskeleton (Hoboken) Wiley Periodicals, Inc.* 70(8):424-38.
- Lammers M, Rose R, Scrima A and Wittinghofer A. 2005. The regulation of mDia1 by autoinhibition and its release by Rho\*GTP. *EMBO J* 24:234176-4187.
- Lammel U, Bechtold M, Risse B, Berh D, Fleige A, Bunse I, Jiang X, Klambt C and Bogdan S. 2014. The *Drosophila* FHOD1-like formin Knittrig acts through Rok to promote stress fiber formation and directed macrophage migration during the cellular immune response. *Development* 141:61366-1380.
- Li F and Higgs HN. 2005. Dissecting requirements for auto-inhibition of actin nucleation by the formin, mDia1. *J Biol Chem* 280:86986-6992.
- Lu J, Meng W, Poy F, Maiti S, Goode BL and Eck MJ. 2007. Structure of the FH2 domain of Daam1: implications for formin regulation of actin assembly. *J Mol Biol* 369:51258-1269.

Luther PK. 2009. The vertebrate muscle Z-disk: sarcomere anchor for structure and signaling. *J Muscle Res Cell Motil* 30:5-6171-185.

Martin AF. 1981. Turnover of cardiac troponin subunits. Kinetic evidence for a precursor pool of troponin-I. *J Biol Chem* 256:2964-968.

Mi-Mi L and Pruyne D. 2015. Loss of Sarcomere-associated Formins Disrupts Z-line Organization, but does not Prevent Thin Filament Assembly in Muscle. *J Cytol Histol* 6:2318.

Mi-Mi L, Votra S, Kempfues K, Bretscher A and Pruyne D. 2012. Z-line formins promote contractile lattice growth and maintenance in striated muscles of *C. elegans*. *J Cell Biol* 198:187-102.

Moerman DG and Williams BD. 2006. Sarcomere assembly in *C. elegans* muscle. *WormBook* 1-16.

Otomo T, Tomchick DR, Otomo C, Panchal SC, Machius M and Rosen MK. 2005. Structural basis of actin filament nucleation and processive capping by a formin homology 2 domain. *Nature* 433:7025488-494.

Paul NR, Allen JL, Chapman A. 2015. alpha5beta1 integrin recycling promotes Arp2/3-independent cancer cell invasion via the formin FHOD3. *J Cell Biol* Paul et al 210:61013-1031.

Pollard TD and Borisy GG. 2003. Cellular motility driven by assembly and disassembly of actin filaments. *Cell* 112:4453-465.

Pollard TD. 1986. Rate constants for the reactions of ATP- and ADP-actin with the ends of actin filaments. *J Cell Biol* 103:6 Pt 22747-2754.

Pruyne D, Evangelista M, Yang C, Bi E, Zigmund S, Bretscher A and Boone C. 2002. Role of formins in actin assembly: nucleation and barbed-end association. *Science* 297:5581612-615.

Quinlan ME, Heuser JE, Kerkhoff E and Mullins RD. 2005. Drosophila Spire is an actin nucleation factor. *Nature* 433:7024382-388.

Rhee D, Sanger JM and Sanger JW. 1994. The premyofibril: evidence for its role in myofibrillogenesis. *Cell Motil Cytoskeleton* 28:11-24.

Rivero F, Muramoto T, Meyer AK, Urushihara H, Uyeda TQ and Kitayama C. 2005. A comparative sequence analysis reveals a common GBD/FH3-FH1-FH2-DAD architecture in formins from Dictyostelium, fungi and metazoa. *BMC Genomics* 6:28.

Ross M, Kaye G and Pawline W. 2003. *Histology - A Text and Atlas*. Baltimore, MD: Lippincott Williams & Wilkins, 4th ed.

Sanger JW, Kang S, Siebrands CC, Freeman N, Du A, Wang J, Stout AL and Sanger JM. 2005. How to build a myofibril. *J Muscle Res Cell Motil* 26:6-8343-354.

Schönichen A, Mannherz HG, Behrmann E. 2013. FHOD1 is a combined actin filament capping and bundling factor that selectively associates with actin arcs and stress fibers. *J Cell Sci* 126:Pt 81891-1901.

Schönichen A and Geyer M. 2010. Fifteen formins for an actin filament: a molecular view on the regulation of human formins. *Biochim Biophys Acta* 1803:2152-163.

Schönichen A, Alexander M, Gasteier JE, Cuesta FE, Fackler OT and Geyer M. 2006. Biochemical characterization of the diaphanous autoregulatory interaction in the formin homology protein FHOD1. *J Biol Chem* 281:85084-5093.

Schulte A, Stolp B, Schönichen A, Pylypenko O, Rak A, Fackler OT and Geyer M. 2008. The human formin FHOD1 contains a bipartite structure of FH3 and GTPase-binding domains required for activation. *Structure* 16:91313-1323.

Sept D, Elcock AH and McCammon JA. 1999. Computer simulations of actin polymerization can explain the barbed-pointed end asymmetry. *J Mol Biol Academic Press* 294:51181-1189.

Sparrow JC and Schock F. 2009. The initial steps of myofibril assembly: integrins pave the way. *Nat Rev Mol Cell Biol* 10:4293-298.

Squire JM. 1997. Architecture and function in the muscle sarcomere. *Curr Opin Struct Biol* 7:2247-257.

Staus DP, Blaker AL, Medlin MD, Taylor JM and Mack CP. 2011. Formin homology domain-containing protein 1 regulates smooth muscle cell phenotype. *Arterioscler Thromb Vasc Biol* 31:2360-367.

Takano K, Watanabe-Takano H, Suetsugu S, Kurita S, Tsujita K, Kimura S, Karatsu T, Takenawa T and Endo T. 2010. Nebulin and N-WASP cooperate to cause IGF-1-induced sarcomeric actin filament formation. *Science* 330:60101536-1540.

Takeya R, Taniguchi K, Narumiya S and Sumimoto H. 2008. The mammalian formin FHOD1 is activated through phosphorylation by ROCK and mediates thrombin-induced stress fibre formation in endothelial cells. *EMBO J* 27:4618-628.

Taniguchi K, Takeya R, Suetsugu S, Kan-O M, Narusawa M, Shiose A, Tominaga R and Sumimoto H. 2009. Mammalian formin fhod3 regulates actin assembly and sarcomere organization in striated muscles. *J Biol Chem* 284:4329873-29881.

Tokuyasu KT and Maher PA. 1987. Immunocytochemical studies of cardiac myofibrillogenesis in early chick embryos. II. Generation of alpha-actinin dots within titin spots at the time of the first myofibril formation. *J Cell Biol* 105:6 Pt 12795-2801.

Volk T, Fessler LI and Fessler JH. 1990. A role for integrin in the formation of sarcomeric cytoarchitecture. *Cell* 63:3525-536.

Waller BJ and Alberts AS. 2003. The formins: active scaffolds that remodel the cytoskeleton. *Trends Cell Biol* 13:8435-446.

Wegner A and Engel J. 1975. Kinetics of the cooperative association of actin to actin filaments. *Biophys Chem* 3:3215-225.

Westendorf JJ. 2001. The formin/diaphanous-related protein, FHOS, interacts with Rac1 and activates transcription from the serum response element. *J Biol Chem* 276:4946453-46459.

Westendorf JJ, Mernaugh R and Hiebert SW. 1999. Identification and characterization of a protein containing formin homology (FH1/FH2) domains. *Gene* 232:2173-182.

Wooten EC, Hebl VB, Wolf MJ. 2013. Formin homology 2 domain containing 3 variants associated with hypertrophic cardiomyopathy. *Circ Cardiovasc Genet* 6:110-18.

Xu Y, Moseley JB, Sagot I, Poy F, Pellman D, Goode BL and Eck MJ. 2004. Crystal structures of a Formin Homology-2 domain reveal a tethered dimer architecture. *Cell* 116:5711-723.

Zigmond SH, Evangelista M, Boone C, Yang C, Dar AC, Sicheri F, Forkey J, Pring M. Formin leaky cap allows elongation in the presence of tight capping proteins. *Curr Biol*. 2003 Oct 14; 13(20): 1820-1823.

## **Chapter 2:**

# **The multiplicity of human formins: Expression patterns in cells and tissues**

**This chapter was published in its entirety as:**

Krainer EC, Ouderkirk JL, Miller EW, Miller MR, Mersich AT and Blystone SD.  
2013. The multiplicity of human formins: Expression patterns in cells and tissues.  
Cytoskeleton (Hoboken) Wiley Periodicals, Inc. 70(8):424-38.

## **Abstract**

Formins are actin binding proteins conserved across species from plants to humans. The formin family is defined by their common FH2 domains. The 15 distinct human formins are involved in a broad range of cellular functions, including cell adhesion, cytokinesis, cell polarity, and cell morphogenesis. Their commonality is actin polymerization activity inherent to FH2 domains. While still requiring much study, biochemical activity of formins has been carefully described. In contrast, much less is known of their activities in complex living systems. With the diversity of the formin family and the actin structures that they affect, an extensive future of study beckons. In this study, we report the expression level of all 15 formins in 22 different human cell and tissue types using quantitative real-time PCR (qPCR). Identification of major themes in formin expression and documentation of expression profiles should facilitate the cellular study of formins.

## Introduction

Formins are a class of actin-modifying proteins participating in cell adhesion, cytokinesis, cell polarity, and cell morphogenesis. Similar to other actin-assembly proteins such as Arp2/3, Spire or Cobl, formins have been shown to nucleate, cap, sever, bundle, and polymerize actin *in vitro*, but unlike other actin-modifying proteins, formins polymerize linear actin filaments [Wallar and Alberts, 2003; Kovar, 2006; Goode and Eck, 2007; Chesarone et al., 2010]. Most formins have been genetically characterized in significant detail, allowing for functional analysis and classification based on domain structure. All formins contain a characteristic Formin Homology 2 (FH2) domain, which nucleates actin and remains associated with the fast-growing, barbed end of the actin filament throughout elongation [Higgs, 2005; Kovar, 2006; Paul and Pollard, 2009]. The C-terminally located Formin Homology 1 (FH1) domain is proline rich and sequesters profilin-actin for facilitated use by the FH2 domain [Evangelista et al., 2003]. The FH2 domain forms a head-to-tail dimer, which is necessary for formins to carry out their actin-polymerizing function and moves with the growing filament, processively capping the barbed end and protecting it from capping proteins [Zigmond, et al., 2003; Copeland et al., 2004; Campellone and Welch, 2010]. Formin function is regulated at several levels, including recruitment to specific cellular locations and the timing of the functional stages of autoinhibition, activation, and the actin nucleating and elongating activity [Goode and Eck, 2007; Aspenstrom, 2010; Chesarone, et al., 2010]. Formin function varies in efficiency between family members.

On a molecular level, the genomes of humans, mice, chickens, protists and yeast have been analyzed for the presence of FH2 domains and the resulting 15 formins identified in humans are the only existent human formins. These 15 formins are divided into seven groups based on domain similarities and phylogenetic relationships (Table 1) [Higgs and Peterson, 2005; Schönichen and Geyer, 2010].

Documentation of the cellular functions and distribution of formins lags far behind the advances of formin biochemistry and genetic identification. To facilitate the cellular study of formins, we have analyzed the expression levels of all 15 human formins in 22 different human cell and tissue types, using qPCR with Western blot confirmations where available.

## Chapter 2: Formin expression patterns

Formin Family	Formin Name	Alternate Name(s) + References	Protein Accession #	Gene Name	Gene Accession #
Diaphanous formins (Dia)	<b>Dia1</b>	Protein diaphanous homolog 1 = DIAP1, DIAPH1 Diaphanous-related formin 1 = DRF1 [Castrillon and Wasserman, 1994].	NP_005210	diaphanous homolog 1 (DIAPH1)	NM_005219
	<b>Dia2</b>	Protein diaphanous homolog 2 = DIAP2, DIAPH2 Diaphanous-related formin 2 = DRF2 [Chae et al., 1998]	NP_006720	diaphanous homolog 3 (DIAPH3)	NM_001042517
	<b>Dia3</b>	Protein diaphanous homolog 3 = DIAP3, DIAPH3 Diaphanous-related formin 3 = DRF3 [Peng et al., 2003]	NP_001035982	diaphanous homolog 2 (DIAPH2)	NM_007309
formin-related proteins identified in leukocytes (FRL)	<b>FRL1</b>	formin-like protein 1 = FMNL1 formin homology domain containing protein 4 = FHOD4 [Katoh and Katoh, 2003a]	NP_005883	formin-like 1 (FMNL1)	NM_005892
	<b>FRL2</b>	formin-like protein 2 = FMNL 2 formin-like protein 3 = FRL3 formin homology domain containing protein 2 = FHOD2 [Block, et al., 2012; Harris, et al., 2010, Katoh and Katoh, 2003a]	NP_443137	formin-like 2 (FMNL2)	NM_052905
	<b>FRL3</b>	formin-like protein 3 = FMNL 3 formin-like protein 2 = FRL2 formin homology domain containing protein 3 = FHOD3 [Block, et al., 2012; Harris, et al., 2010, Katoh and Katoh, 2003a]	Q8IVF7	formin-like 3 (FMNL3)	NM_175736
disheveled-associated activators of morphogenesis (DAAM)	<b>DAAM1</b>	disheveled-associated activators of morphogenesis 1 = DAAM1 [Habas et al., 2001]	NP_055807	dishevelled associated activator of morphogenesis 1 (DAAM1)	NM_014992
	<b>DAAM2</b>	disheveled-associated activators of morphogenesis 2 = DAAM2 [Katoh and Katoh, 2003b]	NP_001188356	dishevelled associated activator of morphogenesis 2 (DAAM2)	NM_015345
delphilin	<b>Delphilin</b>	Glutamate receptor, ionotropic, delta 2-interacting protein 1 = GRID2IP [Miyagi et al., 2002 Katoh and Katoh, 2003c]	NP_001138590	glutamate receptor, ionotropic, delta 2 (Grid2) interacting protein (GRID2IP)	NM_001145118

## Chapter 2: Formin expression patterns

inverted formins (INF)	<b>INF1</b>	FH2 domain-containing protein 1 = FHDC1 [Katoh and Katoh, 2004a]	Q9C0D6	FH2 domain containing 1 (FHDC1)	NM_033393
	<b>INF2</b>	WASp homology 2 (WH2) domain-containing formin 1 = WHIF1 [Chhabra and Higgs, 2006]	NP_071934	inverted formin, FH2 and WH2 domain containing (INF2)	NM_022489
formin homology domain containing proteins (FHOD)	<b>FHOD1</b>	formin homolog over-expressed in spleen 1 = FHOS1 [Westendorf et al., 1999]	NP_037373	formin homology 2 domain containing 1 (FHOD1)	NM_013241
	<b>FHOD3</b>	formin homolog over-expressed in spleen 2 = FHOS2 [Westendorf et al., 1999]	NP_079411	formin homology 2 domain containing 3 (FHOD3)	NM_025135
original formins (FMN)	<b>FMN1</b>	FMN1 = Formin 1 [Katoh and Katoh, 2004b]	NP_001096654	formin 1 (FMN1)	NM_001103184
	<b>FMN2</b>	FMN2 = Formin 2 [Katoh and Katoh, 2004c]	NP_064450	formin 2 (FMN2)	NM_020066

**Table 1 – Human formin family nomenclature and sequence references.**

The seven formin families with all their members are listed, as well as the alternate nomenclature for each formin. The 15 mammalian formins analyzed in this study are grouped into families based on FH2 phylogeny with gene names and accession numbers provided. The amino acid and genomic accession sequences used for alignment and oligonucleotide design are listed.

## **Materials and Methods**

### **Protein alignment**

The 15 members of the human formin family of actin binding proteins (Table 1, Fig. 1A) were aligned using Constraint-based Multiple Alignment Tool (COBALT). For individual comparisons Basic Local Alignment Search Tool for proteins (BLASTp) was used with gapping of 10%.

### **Cells and RNA**

The following cells were purchased from ATCC (Manassas, VA): HeLa (immortalized human cervical cancer cell line), Meg-01 (human megakaryocytes from chronic myelogenous leukemia), U2OS (human osteosarcoma cell line), HCN (human cortical neurons), THP-1 (acute human monocytic leukemia cell line), K562 (immortalized human myelogenous leukemia cell line), U937 (monocytic human cell line of myeloid lineage from histiocytic lymphoma), and HUVEC (human umbilical vein endothelial cells). Total human RNA of cerebellum, skeletal muscle, and cardiac tissue was purchased from Clontech Laboratories (Mountain View, CA). The following cells were gifts: HK-2 (immortalized proximal tubule epithelial cell line from human kidney) from Thomas R. Welch, M.D.; MDA-MB-231 (human breast cancer cell line from epithelial adenocarcinoma) and HT1080 (human fibrosarcoma cell line) from Christopher E. Turner, Ph.D.; Jurkat (immortalized line of human T-lymphocytes) from Andras Perl, M.D., Ph.D., all at SUNY Upstate Medical University in

Syracuse, NY. HEK (primary human keratinocyte cell line from neonatal foreskin) and HaCaT (human immortalized keratinocyte cell line) were gifts from Andrew P. Kowalczyk, Ph.D. in the department of Cell Biology at Emory University in Atlanta, GA. Monocytes that were differentiated into macrophages and platelets and neutrophils were isolated from healthy human blood as previously described [Mersich et al., 2010; Blystone et al., 1997; Jones et al., 1998].

### **RNA purification**

RNA was extracted and purified from  $5 \times 10^6$  to  $20 \times 10^6$  cells using RNeasy<sup>®</sup>Mini Kit from QIAGEN (Valencia, CA), in keeping with clinical laboratory standards for qPCR as laid out in “Quantification of mRNA using real-time RT-PCR” and “The MIQE guidelines: minimum information for publication of quantitative real-time PCR experiments” [Bustin et al., 2009; Nolan et al., 2006]. Cells grown in suspension were pelleted at 1000 rpm for 5 minutes using a Hermle Z400K centrifuge (Hermle Labortechnik, Wehingen, GERMANY) at room temperature (RT). For adherently grown cells, growth media was removed and cells were incubated at 37°C in 0.25% Trypsin-EDTA (1X), Phenol Red (GIBCO<sup>®</sup> Life Technologies, Grand Island, NY) for 5 minutes and pelleted at 1000 rpm for 5 minutes at RT. Cell pellets were disrupted by adding 600µl QIAGEN buffer RLT, containing a high concentration of guanidine isothiocyanate to facilitate RNA binding to a silica membrane in subsequent steps, and the resulting lysate was homogenized by passing it through a blunt 20-gauge needle 5 times. Subsequently 600µl 70% ethanol from Pharmaco-AAPER (Pharmaco, Brookfield,

CT; AAPER, Shelbyville, KY) was added to the lysate and mixed by pipetting. The sample was then transferred to the RNeasy spin column, which was placed in a collection tube and centrifuged for 15 seconds at 14,000 rpm using an Eppendorf 5415C centrifuge (Hamburg, GERMANY). To remove non-specifically bound carbohydrates, proteins, fatty acids and RNA molecules smaller than 200 bases from the silica membrane, 700µl QIAGEN buffer RW1, containing guanidine salt and ethanol, was added to the column and centrifuged at 14,000 rpm for 15 seconds. Next, 500µl buffer RPE is added to the column and centrifuged at 14,000 rpm for 15 seconds, followed by another 500µl of buffer RPE and centrifugation at 14,000 rpm for 2 minutes. After placing the column in a new collection tube, it was centrifuged for 1 minute at 14,000 rpm to ensure the elimination of ethanol. 30µl RNase-free water were then added to the column, which was placed in a new collection tube and centrifuged at 14,000 rpm for 1 minute, and repeated with the eluate from this step.

### **RNA quantification**

RNA was quantified using Agilent RNA 6000 Nano Kit in the Agilent 2100 Bioanalyzer (Santa Clara, CA). RNA Nano 6000 reagents were warmed to RT for 30 minutes in the dark. Prior to running the experimental chip, the electrodes of the bioanalyzer were decontaminated by adding 350µl RNaseZap and 350µl RNase-free DI water into the RNaseZap and RNase-free DI water electrode cleaner chip, respectively. The RNaseZap electrode cleaner chip was placed into the bioanalyzer, and incubated with the lid closed for 1 minute, and the chip was

removed and replaced with the RNase-free DI water electrode cleaner chip, which was incubated for 10 seconds with the lid closed. After removing the chip the bioanalyzer was left open to dry for 10 seconds. To prepare the Gel Matrix, 550 $\mu$ l of gel was filtered through the filter column and centrifuged at 4000 rpm for 10 minutes, and once filtered, 65 $\mu$ l of gel were put into one tube. Next the Dye Concentrate was vortexed for 10 seconds and 1 $\mu$ l was added to the 65 $\mu$ l of filtered gel matrix. After vortexing thoroughly, the mixture was centrifuged at 13,000 g for 10 minutes. A new chip was placed on the chip priming station and 9 $\mu$ l of the gel-dye mixture were added to the G well, the plunger was pulled up to the 1ml mark, the station closed, and the plunger depressed and incubated for 30 seconds. A properly sealed syringe gasket was indicated by the plunger's retraction to 0.3ml and after 5 seconds the plunger was pulled back to 1ml and the priming station was opened. 9 $\mu$ l of gel-dye mixture were added to each G well and 5 $\mu$ l of nano marker buffer was added to each of the 12 sample wells and the ladder well. 1 $\mu$ l of 150  $\mu$ g/ml RNA 6000 ladder was added to the ladder well and 1 $\mu$ l of sample into each sample well, and the chip was vortexed at 240 rpm for 1 minute before it was inserted into the bioanalyzer. The assay for total eukaryote RNA was selected in the 2100 Expert Software for each analysis, which calculated RNA quality and concentration, expressed as an RNA Integrity Number (RIN) using an algorithm based on a Bayesian analysis of nine distinct features of the electropherogram of 1208 samples of RNA of varying degrees of degradation using the Agilent 2100 bioanalyzer system. The RNA extracted from some cell types was found to have a low RIN, which was due to the low

concentration of RNA in the sample, and not due to degraded RNA as can be seen from gels showing integrity of major 28s and 18S RNA (Fig. 2S). However, since the algorithm used to compute the RIN incorporates 9 features of the electropherogram, the low concentration yielded a low RIN. [Schroeder et al., 2006]

### **Reverse Transcription PCR (RT-PCR)**

For reverse transcription PCR, 1ug of RNA, determined as described above, was used to prepare DNA using the SuperScript®III First Strand Synthesis System for RT-PCR from Invitrogen (St. Louis, MO) [Ståhlberg, et al., 2004]. For each reaction, 1µg of RNA, 2.5µl dNTP mix and 2.5µl oligo(dT)<sub>20</sub> were added to a final volume of 25µl diethylpyrocarbonate-treated water and incubated first at 70°C for 5 minutes, and then on ice for 5 minutes. Following these incubations, 22.5µl 10x RT buffer, 20µl MgCl<sub>2</sub>, 10µl DTT and 5µl RNase OUT were added and the mixture was incubated at 42°C for 2 minutes. After adding 2.5µl of SuperScript®III, the mixture was incubated at 42°C for 50 minutes, 70°C for 15 minutes to terminate the reaction and on ice for 5 minutes. Next, 2.5µl of RNase H were added to degrade any remnant RNA and incubated at 37°C for 20 minutes.

### **Qualitative PCR**

For each qualitative PCR reaction, 1µl each of specific forward and reverse primers at 20pM were mixed with 2ul of cDNA. PCR was run using MJ Research PTC-100 Programmable Thermal Controller from Bio-Rad (Hercules, CA). After 1 minute at 94°C, 94µl of the following was added: 10µl TAQ DNA Polishing Buffer B, 6µl MgCl<sub>2</sub>, 2µl dNTP, 0.8µl of 5,000 units/ml Taq DNA Polymerase, all from Fisher Scientific (Hampton, NH), 5µl dimethyl sulfoxide (DMSO) from Sigma-Aldrich (St. Louis, MO), and 71.2µl water, followed by a drop of mineral oil from Fisher Scientific. After a total of 2 minutes at 94°C followed 35 cycles of 0:30 at 55°C, 1:00 at 72°C, and 1:00 at 92°C, and one 2:00 cycle at 94°C.

### **Quantitative real-time PCR (qPCR)**

Quantitative real-time PCR was performed using Eco Real-Time PCR System from Illumina, Inc. (San Diego, CA) and iQ™SYBR®Green Supermix from BIO-RAD (Hercules, CA). For each qPCR cell analysis 500µl of iQ™SYBR®Green Supermix was combined with 50µl of cDNA and 360µl of distilled water and mixed carefully. For each formin analyzed, 1µl of forward specific primer, 1µl of reverse specific primer, each at 1.25pM, the design of which is detailed in Methods, and 18µl of the cDNA mixture were combined. 1µL of forward and reverse 18S primer was used at a concentration of 10pM. The qPCR reaction was programmed as follows: 2:30 at 95°C, 40 cycles of 0:15 at 95°C, 0:20 at 55°C, 0:30 at 72°C, concluded with 0:15 each at 55°C, 60°C and 95°C. The data was analyzed and graphed using Microsoft Excel (Redmond, WA).

Figure 1A

DIA1	402	--KDSKAEPHFLSILQHLLLRND-----YEARPQYYKLIIEEC--	437
DIA2	429	--KETRAEGYFISILQHLLLRND-----YFIRQYFKLIDEC--	464
DIA3	417	--KDTAAENYFLSILQHFLLRND-----YYIRPQYYKIIIEEC--	452
DAAM1	372	--THSEAYPHFMSILHHCLQMPYKR-----SGNTVQYWLLLDRI--	408
DAAM2	368	--KYTEAYPCLLSVLHHCLQMPYKR-----NGGYFQQWQLLDRI--	404
FRL1	393	--TKNAVLEHMEELQEQVALLTER-----LRD----	417
FRL2	387	--TKNAALERVEELENISHLSEK-----LQD----	411
FRL3	390	--TKNVALEKVEELEEHVSHLSEK-----LLD----	414
WHIF1	283	--SCSPVSAQLLSVLQGLLHLEPT-----LRSSQLLWEALESL--	318
INF1		-----	
FHOD1	384	GPASVPGPT-----SSTG-----	396
FHOD3	379	SPCSQSAPSFKNQVRDLREKYSN-----FGNNSYHSSRPSSG----	416
DELPH	308	SPADNAALKSGDRILFLNGLDMRN-----CSHDKVVSMLQSGSAM--	347
FMN1	236	GEEGSQDLPAVTNQNSSVG-----ITESASSKKEVSGEKSFQLPAFFSGLRVLKKGATAEG--	291
FMN2	266	SPDTEQALSALSDLPESLAAEPREPQQPPSPGGPLVSEAPSLPAAQPAAKDSPSSTAFPFPEAGPGEAAAGAPVRGAGDT	345
DIA1	438	-----ISQIVLHKN-GADPDFKCR-HLQIE-----IEGL	464
DIA2	465	-----VSQIVLHRD-GMDPDFTYRKRDLDD-----LTQF	492
DIA3	453	-----VSQIVLHCS-GMDPDFKYRQRDLID-----LTHL	480
DAAM1	409	-----IQQIVIQNDKGGQDPDSTPLENFNIK-----NV	435
DAAM2	405	-----LQQIVLQDERGVDPDLAPLENFNVK-----NI	431
FRL1	418	-----AENE-----	421
FRL2	412	-----TENE-----	415
FRL3	415	-----LENE-----	418
WHIF1	319	-----VNRAVLLAS-----DAQ-----ECT	333
INF1		-----	
FHOD1	397	-----PALLTGPASSVGP-----PSGLQASVNL	420
FHOD3	417	-----SSVPTTPTSSVSPPEARLERS-----SPSGLLTSSFR	449
DELPH	348	-----PTLVVEEGLVPFASDSDSLSDSP-----NPSSALTSLQW	380
FMN1	292	-----GETITIEIKPKDGLLALLKLTQPQVQKSLVQAGLQTVKSEKKATDPKA-----TPTLEQLSLL	348
FMN2	346	DEEGEEDAFEDAPRGPGEWAVEVGEDAPQRLGEEPEEEAQPDAPAAASLPGSPAPSQRCFKPYPLITPCYIKTTTRQ	425
...			
DIA1	761	QLRRPNWSKLVAEDLSQ-DC-----FWTKVKEDRFEN-NELFAK---LTLTFSAQTKTS-----KAKKDQEGGE	836
DIA2	629	SMRRLNWLKIRPHEMTE-NC-----FWTKVVENKYEN-VDLLCK---LENTFCQQKER-----RE---EEDIE	702
DIA3	620	SMKRINWSKLEPTEELSE-NC-----FWLRVKEDKFEN-PDLFAK---LALNFATQIKVQ-----KN---AEALE	692
DAAM1	598	ALKSFNWSKLPENKLE--GT-----VWTEIDDTKVFK-ILDLED---LERTFSAYQRQDDFFVNSNSKQKEADAID	673
DAAM2	593	PLKSFNWWKLNLERVPE--GT-----VWNEIDDMQVFR-ILDLED---FEKMFSAAYQRHQ-----KELGSTE	658
FRL1	630	RMPLLNWWALKPSQIT--GT-----VFTLNDKQVLE-ELDMSD---FEEQFKTKSQGP-----SLDLSALK	696
FRL2	613	RMPVFNWVALKPNQIN--GT-----VFNIEIDDERILE-DLNVDE---FEEIFKTKAQGP-----AIDLSSK	680
FRL3	558	RLPVFNWTALKPNQIS--GT-----VFSELDDKILE-DLDDLK---FEELFKTKAQGP-----ALDLICSK	625
WHIF1	546	RMKKNLWQKLPNSVAREHNS-----MWASLSSPDAAEAVPDFSS---IERLFSFPAKP-----KEP	616
INF1	82	RMRSFFWKTIP--EEQVRGKTN-----IWTLAARQEHHYQ-IDTKT---IEELFQQQEDTT-----KSSLPRRG	153
FHOD1	618	KTVKLFWRKELKLAGHGHSASRFGPCAT-LWASLDPVSV---DTAR---LEHLFESRAKEV-----LPS----	681
FHOD3	901	KTIRLFWNEVRPFDPWCKNNRR--CREFLWSKLEPIKV---DTSR---LEHLFESKSKEL-----SVS----	963
DELPH	820	SVKRLRWEQVENSEGT-----IWGQLGEDSDYDKLSDMVKYLDLELHFGTQKPAK-----PVP----	881
FMN1	735	PMKPLYWTRIQSDRSQNTPT-----LWDSLEEPDIRDP-SEFEY---LFSKDTTQQKKK-----PLS---ETY	815
FMN2	1262	PMKPLYWTRIQLHSKRDSSTSL-----IWEKIEEESI-DC-HEFEE---LFSKTAVKERKK-----PIS---DTI	1348
<b>FH2</b>			
DIA1	837	EKKS-VQKKVKELKVLDSKTAQNLSIFLGSFRMPYQEIKNVILEVNEAV-LTESMIQNLIKQMPPEPEQLKMLSEL--	910
DIA2	703	EKKS--IKKKIKELKFLDSKIAQNLSIFLSSFRVPYEEIRMMILEVDETR-LAESMIQNLIKHLDPQEQLNSLSQF--	773
DIA3	693	EKKTGPTKKKVKELRILDPKTAQNLSIFLGSYRMPYEDIRNVILEVNEDM-LSEALIQNLVKHLPEQKILNELAEL--	767
DAAM1	674	DTLS--SKLKVKELSVIDGRRACNILLRSLKLSNDEIKRAILTMDEQEDLPKDMLEQLLKVFPEKSDIDLLEEH--	747
DAAM2	659	DIYL--ASRKVKELSVIDGRRACNIIILLSKLKSNEEIRQAILKMDQEDLAKDMLEQLLKFIPEKSDIDLLEEH--	732
FRL1	697	SKAA--QKAPSKATLIEANRAKNLAITLRKGNLGAERICQAI EAYDQA-LGLDFLELLMRFLPTEYERSLITRF--	768
FRL2	681	QKIP--QKGSNKVTLLEANRAKNLAITLRKAGKTADEICKAIHVFDLKT-LPVDFVECLMRFLPTEVENVKVLRLY--	752
FRL3	626	NKTA--QKAASKVTLLEANRAKNLAITLRKAGRSAAEIEICRAIHTFDLQT-LPVDFVECLMRFLPTEAEVKLLRQY--	697
WHIF1	617	TMVAPRAKPEKEITFLDAKKSLLNLIIFLKQFKCSNEEVAAMIRAGDTTK-FDVEVLKQLLKLLEPKHEIENLRAF--	691
INF1	154	RTLNSFREAREEITILDAKRSMNIGIFLKQFKKSPRSIVEDIHQGKSEH-YGSETLREFLKFLPESEEVKCLKAF--	229
FHOD1	682	-KK-AGEG-RRMTTVLDPKRSNAINIGLTTL-PPVHVIAKALLNFDEFA-VSKDGIKLLTMMPTEEERKIEEA--	752
FHOD3	964	-KTTAADG-KRQEIIVLDSKRSNAINIGLTVL-PPPTIKIAILNFDEYA-LNKEGIEKLLTMIPTDEEKQIQEA--	1035
DELPH	882	-GP-EPPR-KKEVVEILSHKAYNTSILLAHLKLSPAELRQVLMSEPRR-LEPAHLAQLLLEFAPDADEEQRQY--	951
FMN1	816	EKKNK--VKKIKLLDGKRSQTVGILISSLHLEMKDIQQAIFNVDDSV-VDLETLAALYENRAQDELVKIRKYEE	888
FMN2	1349	SKTKA--KQVVKLLSNKRSQAVGILMSSLHLMKDIQHAVVNLDSV-VDLETLQALYENRAQSELEKIEKHGR	1420

**Figure 1A: Formin alignments** - Formin protein sequences from Table 1 were analyzed using COBALT. Amino acids highlighted in light grey are translations of forward primers and amino acids highlighted in black are translations of reverse primers used for PCR and qPCR as described in Methods. The vertical line indicates the start of the FH2 domain. The C-terminal end of the FH1 domain is not depicted in this alignment, and is located upstream of the amino acids indicating the forward primers used for qPCR (Fig. 1S). The underlined amino acids indicate the location of intron-exon borders between forward and reverse primers. For information regarding intron and exon length and position, see Methods.

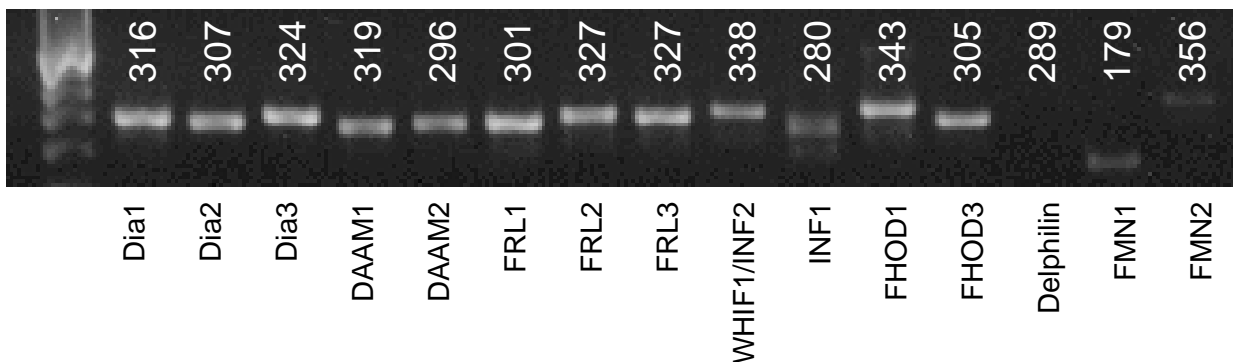


**Figure 1B: PCR products** – PCR performed on DNA from RT-PCR to demonstrate that the primer pairs for each formin, as listed in Methods, produce unique and specific products of predicted sizes. Product sizes are above each band in number of base pairs. PCR products of formin primers were analyzed using electrophoresis on a 2% agarose gel and visualized using ethidium bromide under ultraviolet light. The gel was photographed using Polaroid GelCam (Minnetonka, MN) and Fujifilm FP-3000B (Tokyo, Japan) instant black and white film. The resulting image was scanned using an HP ScanJet5300C (Palo Alto, CA) and processed using the Microsoft Scanning Wizard and Microsoft Powerpoint (Redmond, WA). A single example from U2OS cells of multiple trials in several cell types is shown as a representative example.

Figure 1C – Complete Formin Alignment with Primers

DIA1	1	ME-----PPGGSLGPG---RGTDRKK---KGRSPDELPSAGGDGGKSK---KFTLKRMLADELERFTSMRI	57
DIA2	1	MERHQPRLHHHPAQGSAAGTPYPSSASLRGCRESKMPRRKGPQHPPPPSGPEEPGEKRPKFHLNIRTLTDDMLDKFASIRI	80
DIA3	1	ME---QPGA--AASGAGGGSEEPG-----GGRSNK--RSAGNR-----AANEETKKNPKLNIQIKTLADDVRDRITTSFRK	64
DAAM1		-----M	
DAAM2		-----M	
FRL1		-----	
FRL2		-----	
FRL3		-----	
WHIF1		-----	
INF1		-----	
FHOD1		-----M	
FHOD3		-----	
DELPH		-----	
FMN1		-----	
FMN2		-----	
DIA1	58	K-KEKEKPNSAH-RNSSASYGDDPTAQ-----SLQDVSDEQVLVLFQMLLDMNLNEEKQQPLREKDI	119
DIA2	81	PGSKKERPLPN-LKTAFASSDCSAAPLEM-----MENFPKPLSENELLELFKEMMEDMNLNEDKKAPLREKDFS	149
DIA3	65	STVKKEKPLIQHPIDSQVAMSEFPAAQ-PL-----YDERSLNLSEKEVLDLFEKMMEDMNLNEEKAPLRNKDFT	133
DAAM1	2	APRKRGGRGISF-IFCCFRNNDHPEITYRLRNDNSNFALQTMEPALPMPVVEELDVMFSELVDELDTDKHREAMFALPAE	80
DAAM2	2	APRKRSHHGLGF-L-CCFGSDIPEINLR---DNHPLQFMFESSPIPNAEELNIRFAELVDELDTDKNREAMFALPPE	75
FRL1	1	-----MGNAAGSAEQPAGPAAP---PPKQPAPP-KQMPAAGELEERFNALNCMNLPPDKVQLLSQYDNE	62
FRL2	1	-----MGNAGSMDSQOTDFRAH---NVPL---KLPMPPEPGELEERFAIVLNAMNLPPDKARLLRQYDNE	58
FRL3	1	-----MGNLESAEGVPGE--PP---SVPLLLPPGKMPPEPCELEERFALVLSMNLPPDKARLLRQYDNE	61
WHIF1	1	-----MSVKEGAQ	8
INF1		-----	
FHOD1	2	AGGEDRGDGEVSVVTVRVQYLEDTDPFACAN-FPEP-----RRAPTCSLD-----GALPLGAQIPAVHRLLGAP	65
FHOD3	1	-----MATLACRVQFLDDTDPFNSTN-FPEP-----SRPPLFTFR-----EDLALGTQLAGVHRLQAP	53
DELPH	1	-----MATTATPATNQG-WPEDFGFRLGGSGPCFVLEVAKGSSAHAGGLRPGDQILEVEGLAVGG	59
FMN1		-----	
FMN2		-----	
DIA1	120	IKREMSVQYLYTSKAGMSQKESK---SAMMYIQELRSGLRDMPLLS---C-----LE-SLRV	170
DIA2	150	IKKEMVMQYINTASKTGSGLKRSRQ---ISPQEFIHLEKMGSADERLVT---C-----LE-SLRV	201
DIA3	134	TKREMVVQYISATAKSGGLKNSKHECTLSSQEYVHELRSGISDEKLLN---C-----LE-SLRV	188
DAAM1	81	KKWQIYCSKKKQEE-NKGATSWP-----EFYIDQLNSMAARKSLLA---LE-----KEEEERSKTIE-SLKT	139
DAAM2	76	KKWQIYCSKKKEQEDPNKLATSWP-----DYIDRINSMAAMQSLYA---FD-----EEETEMRNQVVE-DLKT	135
FRL1	63	KKWELICDQERFQVK-----NP---PAAIYQKLKSYVDTGGVSR---KVAADWMSNLGFKRRVQESTQVLR-ELET	126
FRL2	59	KKWELICDQERFQVK-----NP---PHTYIQKLKGYLDPVTRK---K-----FRRRVQESTQVLR-ELEI	112
FRL3	62	KKWELICDQERFQVK-----NP---PHTYIQKLKGYLDPVTRK---K-----FRRRVQESTQVLR-ELEI	115
WHIF1	9	RKWAALKEKLGPDSDPTEANLES-----ADPELCIR--LLQMPVSVN-----YS-GLRK	55
INF1		-----	
FHOD1	66	LKLEDCAQVSPSGYYLDTELSLEEQREMLEGFYEEISKGRKPTLILRTQLSVRVNAILEKLYSSSGPELRRSLF-SLK-	143
FHOD3	54	HKLDDCTLQLSHNGAYLDLEATLAEQRDELEGFQDDAGRGKHSIILRTQLSVRVHACIEKLYNSSGRDLRRALF-SLK-	131
DELPH	60	LSRER-LVRLARCRVPPSLGVLPAPD---GGPGPGSGPAAPTTLVLRAPRCGRGLALGRELRLLAGRKRPDVHRERR-	134
FMN1		-----	
FMN2		-----	
DIA1	171	SLNNNPVSWVQTFGA-E--GLASLLDILKRLHDEKEETAGSYDSRNKHE-----	216
DIA2	202	SLTSNPVSWVESFGH-E--GLGLLLDILEKLI SGIQE--KVVKKNQHK-----	245
DIA3	189	SLTSNPVSWVNNFGH-E--GLGLLLDLEKLLDKKQOE--NIDKKNQYK-----	232
DAAM1	140	ALRTKPMRFVTRFIDLDD--GLSCILNFKTMDYETSES-----RIHTS-----	180
DAAM2	136	ALRTQPMRFVTRFIELE--GLTCLLNFLRSMDHATCES-----RIHTS-----	176
FRL1	127	SLRTNHIGWVQEFVLENEENRGLDVLLEYLAFQAQSVTYDMESTDNGASNS-EKNKPLEQSVEDLSKGGPPSSVP-----K	198
FRL2	113	SLRTNHIGWVREFLNEENKGLDVLVEYLSFAQYAVTFDFESVESTVSSVDKSKPWSRSIEDLHRGSNLPSPVGNVSRS	192
FRL3	116	SLRTNHIGWVREFLNDENKGLDVLVDYLSFAQCSVMDFEGLESGDDGAFDKLRSWSRSIEDLQPPSALSAPFTNSLARS	195
WHIF1	56	RLEGSDDGWMVQFLEQS--GLDLLLEALARLSGRGVARI--SDALLQLT-----	100
INF1		-----	
FHOD1	144	QIFQEDKDLVPEFVHSE--GLSCLIRVGAADHNYQSY-----	179
FHOD3	132	QIFQDDKDLVHEFVVAE--GLTCLIKVGAEADQNYQNY-----	167
DELPH	135	RKAQEF SRKLVDEILGDQ--PTA--KEQ-----	157
FMN1		-----	
FMN2		-----	

## Chapter 2: Formin expression patterns

DIA1	217	-----IIRCLKAFMNNKFGIKTMLETEEGILLVLRAMPDPAVPMNMIDAAKLLSA	265
DIA2	246	-----VIQCLKALMNTQYGLERIMSEERSLSLLAKAVDRHPNMMDVVKLLSA	294
DIA3	233	-----LIQCLKAFMNNKFGIQRILGDERSLLLARADPKQPNMTEIVKILSA	281
DAAM1	181	-----LIGCIKALMNNQGRAHVLAHSESINVAQSLSTENIKTKVAVLEILGA	229
DAAM2	177	-----LIGCIKALMNNQGRAHVLAQPEAISTIAQSLRTENSKTAVLEILGA	225
FRL1	199	SRHLTIKLTPAHSRKALRNSRIVSQKDDVHVCIMCLRAIMNYQSGFSLVMNHPACVNEIALSLNNKNPRTKALVLELLAA	278
FRL2	193	GRHSALRYNTLPSRRTLKNSRLVSKKDDVHVCIMCLRAIMNYQYGFNMVMSHPHAVNEIALSLNNKNPRTKALVLELLAA	272
FRL3	196	ARQSVLRYSTLPGRRALKNSRLVSKKDDVHVCILCLRAIMNYQYGFNLVMSHPHAVNEIALSLNNKNPRTKALVLELLAA	275
WHIF1	101	-----CVSCVRAVMNSRQGIIFYILSNQGGYVRQLSQALDTSNVMVKKQVFELLAA	149
INF1		-----	
FHOD1	180	-----ILRALGQLMLFVDGMLGVVAHSDTIQWLYTLCASLSRLVVKTKALKLLV	228
FHOD3	168	-----ILRALGQIMLYVDGMNGVINRNETIQWLYTLIGSKFRLVVKTKALKLLV	216
DELPH	158	-----VFAALKQF-----AAEQRVDDLVTTLT--ALPREACGPLLDNLRI	196
FMN1		-----	
FMN2		-----	
DIA1	266	LCILP---QPEDMNERVLEAMTE-RAEMDEVERFQPLLDGL----KSGTTIALKVGCLQLINALI---TPAEELDFRVH	333
DIA2	295	VCIVG---E-ESILEEVLEALTS-AGEEKKIDRFFCIVEGL----R-HNSVQLQVACMQFINALV---TSPDDLDFRLH	360
DIA3	282	ICIVG---E-ENILDKLLGAIIT- AAERNRERFSPIVEGL----ENQEALQVACMQFINALV---TSPYELDFRLH	348
DAAM1	230	VCLVP---G---GHKKVLQAMLHYQKYASERTRFOTLINDLDKSTGRYRDEVSLKTAIMSFINAVLSQAGVESLDFRLH	303
DAAM2	226	VCLVP---G---GHKKVLQAMLHYQVYAAERTRFOTLLNELDRSLGRYRDEVNLKTAIMSFINAVLNAGAGEDNLEFRLH	299
FRL1	279	VCLVR---G---GHEIIILAAFDNFKEVCGEQHRFEKLEMEYFR---NEDSNIDFMVACMQFINIVV---HSVENMNFVRV	345
FRL2	273	VCLVR---G---GHEIIILSAFDNFKEVCGEQHRFEKLEMEYFR---NEDSNIDFMVACMQFINIVV---HSVEDMNFVRV	339
FRL3	276	VCLVR---G---GHEIIILAAFDNFKEVCKELHRFEKLEMEYFR---NEDSNIDFMVACMQFINIVV---HSVEDMNFVRV	342
WHIF1	150	LCIYS---P---EGHVLTLDALDHYKTVCSSQYRFSIVMNELS-----GSDNVPYVVTLTLLSVINAVI---LGPEDLRARTQ	216
INF1		-----	
FHOD1	229	FV-----EYSENNAPLFIKAVNSVASTTGAPPWANLVSILEE---KNGADPELLVYTVTLINKTL---AALPDQDSFYD	296
FHOD3	217	FV-----EYSESNAPLLIQAVTAVDTKRGVWPWSNIMEILEE---KDGVDTELLVYAMTLVNKTL---SGLPDQDTFYD	284
DELPH	197	FIPKXHRARFDEVVSQGLLGLKCRARRAQGAQ-----RLRRS---RSEERPERL-----LVSTRA---SAPPRP-----	255
FMN1	1	-----MENVDNSLDGSDVSEPAKPE---AGLEVAQSILS	31
FMN2	1	-----MGNQDQGLKRSAGDALHEGG---GGAEDALGPRD	31
DIA1	334	IRSELMRLGLH-QVLQDLREIE-----NEDMRVQLNVFDEQG-EEDSYDLKGRLLDDI-	383
DIA2	361	IRNEFMRCGLK-EILPNLKCIC-----NDGLDIQLKVFDEHK-EEDLFELSHRLEDI-	410
DIA3	349	LRNEFLRSGLK-TMLPDLKEKE-----NDELDIQLKVFDENK-EDDLTELSHRLNDI-	398
DAAM1	304	LRYEFLMLGIQ-PVIDKLRHE-----NSTLDRHLDFEFEMLR-NEDELEFAKRFELV-	353
DAAM2	300	LRYEFLMLGIQ-PVIDKLRQHE-----NAILDKHLDFEFEMVR-NEDDLELARRFDMV-	349
FRL1	346	LQYEFTHLGLD-LYLERLRLTE-----SDKLQVQIQAY-----	377
FRL2	340	LQYEFTKLGLD-EYLDKLRKHE-----SDKLQVQIQAY-----	371
FRL3	343	LQYEFTKLGLE-EFLQKSRHTE-----SEKLQVQIQAY-----	374
WHIF1	217	LRNEFIGLQLL-DVLARLRDLE-----DADLLIQLEAFEEAK-AEDEEELLR--VSG-	264
INF1		-----	
FHOD1	297	VTDALQQGMEALVQRHLGTAG-----TDVDLRTQLVLYENAL-----KLEDG-	339
FHOD3	285	VVDCLEELGIAAVSQRHLNKKG-----TDLDLVEQLNIYEVAL-----RHEDG-	327
DELPH	256	-----DEPPRRASLLVGGL-----A-----	271
FMN1	32	KFSMKSFLG---FTSKLESVNPPEEEDAVLKAFHSLDVNPTSQQDDSSNGLDPQEAGSRVSPDLGNDEKIASVETESEGS	107
FMN2	32	VEATKKGSG---GKKALGKHGKGGGGGGGGESGKKSXSDRASVFSNLRIRKNLSKGGKAGGSRREDVLDLSQLQGTG-	106
DIA1	384	-----RMEMDDFN-----	391
DIA2	411	-----RAELDEAY-----	418
DIA3	399	-----RAEMDDMN-----	406
DAAM1	354	-----HIDTKSAT-----	361
DAAM2	350	-----HIDTKSAS-----	357
FRL1	378	-----LDNIF-----	382
FRL2	372	-----LDNVF-----	376
FRL3	375	-----LDNVF-----	379
WHIF1	265	-----GVDMSHQ-----	272
INF1		-----	
FHOD1	340	-----DIEEAPGAGGRERRRKPSS-----	357
FHOD3	328	-----DETTEPPPSGCRDRRRASVCSGGG	352
DELPH	272	-----GPGGARTRVRY-----	283
FMN1	108	QRKEAGTSLLAQELLPLSTLKGTKDDVICVRG-----TLVHTTSDSDSDGGGQEPPEEGS-STNGPK	167
FMN2	107	ELDSAHSLLTKTPDLSLDAEAGLSDTECADPFEVTPGGPGPAEARVGGRIADVEDVETAAGAQQGQRTSSGS-DTDIYS	185

## Chapter 2: Formin expression patterns

DIA1	392	-EVFQILLNTV-----	401
DIA2	419	-DVYNMVWSTV-----	428
DIA3	407	-EVYHLLYNML-----	416
DAAM1	362	-QMFELTRKRL-----	371
DAAM2	358	-QMFELIHKKL-----	367
FRL1	383	-DVGALLEDETE-----	392
FRL2	377	-DVGALLEDAE-----	386
FRL3	380	-DVGGLLEDAE-----	389
WHIF1	273	-EVFASLPHKV-----	282
INF1		-----	
FHOD1	358	SEEGKRSRRSL-----EGGCPARAPEPGPT	383
FHOD3	353	EHRGLDRRRSR-----RHSVQSIKSTLSAPT	378
DELPH	284	--KGNKSPGF-----LRGHGPVWLVESVLPV	307
FMN1	168	SPSGVLSEP-----SQESKENPGGFRENTVTGEMNGAELCAEDPQRIPPEMSSKLEAGNGGLQTERRPSQDQV	235
FMN2	186	FHSATEQEDLLSDIQQAIRLQQQQQQQLQLQLQQQQQQQLQGAEEPAAPPTAVSPQPGAFGLDRFLLGSPSGGAGEAPG	265
DIA1	402	--KDSKAEPHFLSILQHLLLVNRD-----YEARPQYYKLIIEC--	437
DIA2	429	--KETRAEGYFISILQHLLLIRND-----YFIRQQYFKLIDEC--	464
DIA3	417	--KDTAAENYFLSILQHFLLRND-----YYIRPQYYKIIIEC--	452
DAAM1	372	--THSEAYPHFMSILHHCLQMPYKR-----SGNTVQYWLLLDRI--	408
DAAM2	368	--KYTEAYPCLLSVLHHCLQMPYKR-----NGGYFQQWQLLDRI--	404
FRL1	393	--TKNAVLEHMEELQEQVALLTER-----LRD--	417
FRL2	387	--TKNAALERVEELENISHLSEK-----LQD--	411
FRL3	390	--TKNVALEKVEELEEHVSHLTEK-----LLD--	414
WHIF1	283	--SCSPVSAQLLSVLQGLLHLEPT-----LRSSQLLWEALES--	318
INF1		-----	
FHOD1	384	GPASPVGPT-----SSTG--	396
FHOD3	379	SPCSQSAPSFKNQVRDLREKYSN-----FGNNSYHSSRPSSG--	416
DELPH	308	SPADNAALKSGDRILFLNGLDMRN-----CSHDKVVSMLQSGSAM--	347
FMN1	236	GEEGSQDLPAVNTQNSSVG-----ITESASSKKEVSGEKSFLPAFFSGLRVLKKGATAEG--	291
FMN2	266	SPDTEQALSALSDLPESLAAEPREPQQPPSPGGLPVSEAPSLPAAQPAKADSPSSTAFFPPEAGPGEEAAGAPVRGAGDT	345
DIA1	438	-----ISQIVLHKN-GADPDFKCR-HLQIE-----IEGL	464
DIA2	465	-----VSQIVLHRD-GMDPDFTYRKRDLDD-----LTQF	492
DIA3	453	-----VSQIVLHCS-GMDPDFKYRQLDID-----LTHL	480
DAAM1	409	-----IQQIVIQNDKGQDPDSTPLENFNIK-----NV	435
DAAM2	405	-----LQQIVLQDERGVDPDLAPLENFNVK-----NI	431
FRL1	418	-----AENE-----	421
FRL2	412	-----TENE-----	415
FRL3	415	-----LENE-----	418
WHIF1	319	-----VNRAVLLAS-----DAQ-----ECT	333
INF1		-----	
FHOD1	397	-----PALLTGPASSPVGP-----PSGLQASVNL	420
FHOD3	417	-----SSVPTPTSSVSPQEARLERS-----SPSGLLTSSFR	449
DELPH	348	-----PTLVVEEGLVPFASDSLSLSP-----NPSSALTSLQW	380
FMN1	292	-----GETITEIKPKDGLALLKLTQPVQKSLVQAGLQTVKSEKATDPKA-----TPTLEQLSLL	348
FMN2	346	DEEGEEDAFEDAPRGSPEEWAPEVGEDAPQRLGEEPEEEAQGPDAPAAASLPGSPAPSQRCKPYPLITPCYIKTTTRQ	425
DIA1	465	IDQMIDKTKVEKSEAK-----	480
DIA2	493	VDICIDQAKLEEFEEK-----	508
DIA3	481	IDSCVNKAKVEESEKQ-----	496
DAAM1	436	VRMLVNEVEVKQWKEQ-----	451
DAAM2	432	VNMLINENEVKQWRDQ-----	447
FRL1	422	-----SMAKIAELEKQ-----	432
FRL2	416	-----AMSKIVELEKQ-----	426
FRL3	419	-----NMMRVAELEKQ-----	429
WHIF1	334	LEEVEVERLLSVKGRPR-----	349
INF1		-----	
FHOD1	421	FPTI---SVAPSADTS-----SERSIY-----KARFL	444
FHOD3	450	QHQE---SLAAERERRRQEREERLQRIER-----EERNKFSRDYLDKREEQRQA-----REERYKYL	503
DELPH	381	VAEILPSSIRVQGRFTFSQQLEHLLTPPERYGVCRALESFFOHRNIDTLIVDVYPVLDTPA-----KQVLWQFI	448
FMN1	349	LNIDMPKTEPKGADPESPREEM-----GCNADQESQSGPGVPQTQGGVEVKPKSPETALEAFKALFIRPPRKGTTADT	421
FMN2	426	LS--SPNHSPSQSPNQSPRIKRREPEPSLSRGSRTALASVAAPAKKHRADGGLAAGLSRSA-DWTEELGARTPRVGGSAHL	502

## Chapter 2: Formin expression patterns

DIA1	481	-----AAELEKKLDSELTA-----	494
DIA2	509	-----ASELYKKFEKEFTD-----	522
DIA3	497	-----AAEFSSKPFDEEFTA-----	510
DAAM1	452	-----AEKMRKE-----	458
DAAM2	448	-----AEKFRKE-----	454
FRL1	433	-----LSQARKELETLRER-----	446
FRL2	427	-----LMQRNKELDVVREI-----	440
FRL3	430	-----LLQREKELESIKET-----	443
WHIF1	350	-----PSPLVKAHKSVQAN-----	363
INF1		-----	
FHOD1	445	ENVAAAETEKQV--ALA-----QGRA-----	463
FHOD3	504	EQLAAEEHEKELRSRSVS-----RGRADLSLDLTSPAAPACLAPLSH-----SPSSSDSQEAL	556
DELPH	449	YQLLTYE-EQELCQEKIACFLG-----YTAMTAEPEPELDLESEPTPEP-QPRSS-----LRASSMCRSL	507
FMN1	422	SELEALKRKRMRHEKESL-----RAVFERSNSKPADGPPSDS-----	456
FMN2	503	LERGVASDSGGGVSPALAAKASGAPAAADGFQNVFTGRTLLEKLFSSQENGPPEEAKEFCSRI IAMGLLLPFSDCFREPC	582
DIA1	495	-----	510
DIA2	523	-----RHELQVEMKMMESDFE-----	510
DIA3	511	-----HQETAELQKKEA---	535
DAAM1	459	-----RQEAQAELOKRDE---	523
DAAM2	455	-----HNELQKLEKKERECD	474
FRL1	447	-----HMELVSRLEKERECE	470
FRL2	441	-----FSESTAMGASRRPPEP	462
FRL3	444	-----YKDANTQVHTLRKMVK	456
WHIF1	364	-----YENTSHQVHTLRRLIK	459
INF1	1	-----LDQSQRGSSPQNTTTP	379
FHOD1	464	-----MHVMN-----	5
FHOD3	557	-----ETLAGAMPNEAGG--	476
DELPH	508	TVSASSPGTPH-----HPQASAGDPEPES---EAEPEAEAGAGQVADEAGQDI	601
FMN1	457	RSQGLEAGLSC-----GPSECEMPLPLI---PGE-----RQAGDG-	540
FMN2	583	-----KSPDHSLTEQDDRTPGRLQAVWPPPKTKDTEEKVGLKYTEAEYQAAIHLHKREHKEEI	514
		NQNAQTNAASFDQDQLYTWAAVSQPTHSLDYSEGQFPRRVPSMGPPSKPPDEEHR--LEDAETESQSAVSETPQKRSDAV	660
<b>FH1</b>			
DIA1	511	QKLQ-----DLQGEKDALHSEKQQLATEKQDLEAEVSQLTGEVAK-----LTKELE	556
DIA2	536	-KIN-----ELQAELOAFKSQFGAL-----	554
DIA3	524	-KIK-----ELEAEIQQLRRTQAQVL-----	542
DAAM1	475	AKTQ-----EKEEMMQTLNKMKEKLEKETTEHK---QVKQVAD-----LTAQL-	515
DAAM2	471	TKTL-----EKEEMMRTLNKMKDKLARESQELR---QARGQVAE-----LVAQL-	511
FRL1	463	EKAPP-----AAPTRPSALELKVVEELEEKGL-----IR	490
FRL2	457	EKE-----EAIQRQSTLEKKIHELEKQGT-----IK	482
FRL3	460	EKE-----EAFQRRCHLEPNVRGBLE-----	479
WHIF1	380	KPSV-----EGQQPAAAAACEPVDHAQSESI-----LK	407
INF1	6	-----CV-----	7
FHOD1	477	-----HPDA-RQ-----	482
FHOD3	602	ASAH-----EGAETEVEQALEQEPEE-RASLSEKERQ-----NEGVNERDNCSSASSV	647
DELPH	541	TSLP-----ETPNPKMMSAVYAELES-RLNSSFKGKM-----GTVSKSRASPPGP	584
FMN1	515	E NLQAQFELRAFHIRGEHAMITARLEETIENLKHELEHRWR-----GGCEERKDVCI	566
FMN2	661	QK-----EVDVDMKSEGQ-ATVIQQLEQTIEDLRTKIAELERQYPALDTEVASGHQGLENGVTASGDVCLALRLEEKEVR	734
DIA1	557	-----DA-----	558
DIA2		-----	
DIA3		-----	
DAAM1		-----	
DAAM2		-----	
FRL1	491	-----IL-----	492
FRL2	483	-----IQ-----	484
FRL3		-----	
WHIF1	408	-----VS-----	409
INF1		-----	
FHOD1	483	-----LWD-----SPET	489
FHOD3	648	-----SSSSSTLEREEKEDKLSRDRTTGLWPAGVQDAGVNGQ-----CGDIL--TNKRFMLDMLYAHN-----RKSPDD	709
DELPH	585	-----SPAVTTGPRTLSGVSWPSE---LLPSPCYHPLCSGG-----LASPS--SSESHPYASLDSSR-----APSPQP	643
FMN1		-----	
FMN2	735	HHRILEAKSIQTSPTTEGGVLTLPVVDGLPGRPPCPPGAESGPQTKFCSEISLIVSPRRISVQLDSHQPTQSISQPPPPP	814

## Chapter 2: Formin expression patterns

DIA1	559	-----KKEMASLSAAAITV-----	572
DIA2		-----	
DIA3		-----	
DAAM1		-----	
DAAM2		-----	
FRL1	493	-----R-GPGD-AVSIEI-----	503
FRL2	485	-----KKGDDG-----IAI-----	493
FRL3		-----	
WHIF1	410	-----Q-----	410
INF1	8	-----S-----	8
FHOD1	490	-----AP-AARTP-----QSPAPCVLLRAQR-----	509
FHOD3	710	E-----EKGDGE-AGRTQ-----QE-AEAVASLATRIS-----TLQANSQTQDESVRVDV-----GCLDNRGS	761
DELPH	644	-----GPGPICPDSF-----PSPDPTRPPSRRKLF-----TFSHPVRSRDTD-RFLDV-----	685
FMN1	567	-----STDDDCPPKTRFNVCVQTDRETFLKPCSESESKT-----	602
FMN2	815	SLLWSAGQGQPGSQPPHSISTEFQTSHEHSVSSAFKNSCNIPSPPL--PCTESSSSMPGLGMVPPPPPLPGMTVPTLP	892
DIA1	573	-----PPSVPS-----	578
DIA2		-----	
DIA3		-----	
DAAM1		-----	
DAAM2		-----	
FRL1	504	-----LPV-AV-----	508
FRL2	494	-----LPVVAS-----	499
FRL3		-----	
WHIF1		-----	
INF1	9	--LVSDKEN-----	15
FHOD1	510	-----SLAP-EPKE-----PL--IPASPKAEP-IW-----ELPTRA--PR-LSIGDLDFSDL	549
FHOD3	762	VKAFAEKFNISGDLGRGSI SPDAEPND-----KVPETAPVQPKTESDYIW-----DQLMAN--PRELRIQDMDFSDL	825
DELPH	686	---LSEQ-----LGPRVTIVD-----DF--LTPENDYEEMSFHD-----DQGSFV--TNERSSASDCISS	734
FMN1	603	NQLVPKKNLIS--SLSQLSPNDHKDIHAALQPMEGMASNQKALPP--	647
FMN2	893	STAIPQPPPLQ--GTEMLPPPPPLP-GAGIPPPPLPGAGILPLPLPGAGIPPPPLPGAAIPPPPLPGAGIPLPPP	969
DIA1	579	-----RAPVPPAPPLPGD-----SGTIIIP-----	598
DIA2		-----	
DIA3		-----	
DAAM1		-----	
DAAM2		-----	
FRL1	509	-----ATPSGGDAPTPGV-----P-TGSPS-----	527
FRL2	500	-----GTLSMGSEVVAGN-----S-VG-----	515
FRL3	480	-----SVDSEALA-----R-VG-----	490
WHIF1		-----	
INF1		-----	
FHOD1	550	GEDEDQ-----	555
FHOD3	826	GEEDDI-----	831
DELPH	735	EEGSSL-----	740
FMN1		-----	
FMN2	970	LPGAGIPPPPLPGAGIPPPPLPGAGIPPPPLPGAGIPPPPLPGAGIPPPPLPGAGIPPPPLPGAGIPPPPLPG	1049
DIA1	599	-----PPAPGDSTTPPPPPPPPPPLPGGVCISSPPSLPGGTAI	639
DIA2	555	-----PAD--CNIPL-----PPSKEGGTGH	572
DIA3	543	-----SSSGIGPPA-----APPLPG-VGP	562
DAAM1	516	-----HELSRRAVCA-----	525
DAAM2	512	-----SELSTGPV-----	519
FRL1	528	-----P--DLAPAAEPAPGAAPPP-----PPLPG-----	550
FRL2	516	-----P---TMGAASS--GPLPPPP-----PPLPP-----	535
FRL3	491	-----P-----AELS--EGMPPSD-----LDLLA-----	507
WHIF1	411	-----PR-----ALEQQASTPPPPPP-----PLLPGSSAE	436
INF1	16	-----GN-----	17
FHOD1	556	-----DMLNVESVEAGKDIPA-----PS-----PPLPLLSGV	582
FHOD3	832	-----DVLDVDL--GHREAPG-----PPP-----PPPPTFLGL	857
DELPH	741	-----TYSSISDHIPPPPLSP-----PPP-----PPLPFHDA-	767
FMN1	648	-----PPASIPPP-----PPLPSGLGS	664
FMN2	1050	AGIPPPPLPGAGIPPPPLPGAGIPPPPLPGAGIPPPPLPGAGIPPPPLPGVGIPPP-----PPLPG--AG	1117

## Chapter 2: Formin expression patterns

DIA1	640	SPPPPLSGDATIPPPPLPEGV-----GIPSPSSLPGGTAIPPPPLPGSARIPP-PPPP-LPGSA-GIPPPPPPLPGEA	711
DIA2	573	SAL-----PPPPPLPSGG-----GVPPPPP-----PPPPPLPG-MRM-P-FSGP-VP-----PPPLGFLGGQ	622
DIA3	563	PPP-----PPAPPLPGA-----PL-----PPPPPLPGMMGI-P-PPPP-PLLF-GGPPPPPLGG--	611
DAAM1	526	-----SIPGGPS-----PGAPGP--FPSS-VPGSL-LPPPPPLPGGM	561
DAAM2	520	-----SS-----PPPPGGLTLSSS-MTND-LPPPPPLPFACC	552
FRL1	551	LPSP-----QEAPP-----SAPPQAPPLGSEPPPP-APP-LPGDLPPPPPPPPPGTD	598
FRL2	536	SSDT-----PETVQ-----NGPV-TPPMPPPPPPP-PPP-PP-----PPPPPPPLPGA	578
FRL3	508	PAPP-----PEEVL-----PLPPPAPPL-PPP-PP-----PLPDKCPP-----	539
WHIF1	437	PPPP-----PPPPPLPSVGAKALPTAPPPPL-----PGLGAMAPPAPP-LPPP-LPGSCEFLPPPPPLPLGLG	498
INF1	18	IATAPGFMIGQTPPPAPP-----PPPPPP-----SPPCSCSRECP-SSPP-PP-----PPPPPLG--	68
FHOD1	583	PPPP-----L-PPPPPIKGF-----PPPPPL-----PLAAP-LPHS-VPDS-----	617
FHOD3	858	PPPPPPPLDS-IPPPVPGNLL-----VPPPPVF-----NAPQG-LGWSQVPRG-----	900
DELPH	768	-KPSRSSDGSRGPAQALAKPLTQLSHVPPPP-----PP-LPPP-VPCA-----PPMLSR--	816
FMN1	665	LSPAPPMPVVSAGPPPLPP-----PPPPPL-----PPSSAGPPPP-PPPP-LPN-----SPAPPNP	717
FMN2	1118	IPPPPLPGAGIPPPPLPGAGI-----PPPPPLPRVG-----	
DIA1	712	GMPPPPPLPGGPGIPPPPP-----FPGGPGIP-----PPPPGMGMPPPP-----PFGFGVPA	760
DIA2	623	NSPPLP-----VPPPPGI-----S-----	628
DIA3	612	-----VPPPPGI-----S-----	619
DAAM1	562	LPPPPPLPPGGPPPPPGPP-----P-LGAIMP-----PP---GAPM-----GLA-----	597
DAAM2	553	PPPPPPPLPPGGPPTPPGAP-----PCLGMGLP-----LP---QDPYPS-----S---DVP-----	592
FRL1	599	GPVPPP--PPPPPPPGGPP-----DALG-----RRD-----S-----ELGPG-----DTAR	629
FRL2	579	AETVPA--PPLAPPLSAPP-----L--PGTS-----SPT-----V-----VFNGLA-----	612
FRL3	540	-----APP-----L--PG-A-----APS-----V-----VLTVGLS-----	557
WHIF1	499	CPPPPPPLPGMGWPPPP-----PPLLPTC-----SPPV--AGGMEE-----VIVAQVDHG	545
INF1	69	-EPIP--PPPPGL-PP-----	81
FHOD1		-----	
FHOD3		-----	
DELPH	817	-----GLG-----	819
FMN1	718	-GPPPA--PPPPGLAPPPPP-----	734
FMN2	1184	IPPPPP--LPVVGIPPPPLPGAGIPPPPLPGMIPPAPAPPLPPPGTGIPPPPLPVSGPPLLQVGSSTLPTPQVCG	1261
DIA1	761	---PVLPFGLT-----PKKLYKPEVQLRRPNWSKLVAEDLSQ-DC-----FWTKVKEDRFEN-NELFAK-	814
DIA2	629	---ILPFGLK-----PKKEFKPEISMRLNLWKLIRPHEMTI-NC-----FWIKVNNENKYEN-VDLLCK-	681
DIA3	620	---LNLPGYGMK-----QKKMYKPEVSMKRINWSKIEPTIELSE-NC-----FWLRVKEDKFEN-PDLFAK-	673
DAAM1	598	-----LK-----KKSIPQPTNALKSFNWSKLPENKLE--GT-----VWTEIDDTKVFK-ILDLED-	644
DAAM2	593	-----LR-----KKRVPQPSHPLKSFNWKLNLERV--GT-----VWNEIDDMQVFR-ILDLED-	639
FRL1	630	-----VK-----AKKPIQTKFRMPLLNWVALKPSQIT--GT-----VFTELNDEKVLQ-ELDMSD-	676
FRL2	613	-----AVK-----IKKPIKTKFRMPVFNWVALKPNQIN--GT-----VFNEDDERILE-DLNVED-	660
FRL3	558	-----AIR-----IKKPIKTKFRLPVFNWVALKPNQIS--GT-----VFSELDEKILE-DLDDLK-	605
WHIF1	546	---LGSAWVPS-----HRRVNPPTLRMKLNWQKLPNSVAREHNS-----MWASSLSPDAEAEVPDFSS-	601
INF1	82	-----TTHMNGYSHLGKKRMRSFVFKTIP--EEQVRGKTN-----IWTLAARQEHYQ-IDTKT-	133
FHOD1	618	-----S-ALPTKRKTVKLFWRELKLAGGHVGSASRFGPCAT-LWASLDPSV-----DTAR-	666
FHOD3	901	-----QPTFTKKKKTIRLFWNEVRPFDWPCNNRR---CREFLWSKLEPIKV-----DTSR-	948
DELPH	820	-----HRRSETSHMSVKRLRWQVENSEGT-----IWGQLGEDSDYDKLSDMVKY	864
FMN1	735	-----GLFFGLGSSSSQCPRKPAIEPSCPMPLYWTRIQISDRSQNATPT-----LWDSLEEDIRDP-SEFEY-	797
FMN2	1262	FLPPPLPSGLF-GLGMNQDKGSRKQPIEPCRPMKPLYWTRIQIHSKRDSSTSL-----IWEKIEEPSI-DC-HEFEE-	1330
<b>FH2</b>			
DIA1	815	--LTLTFSAQTKTS-----KAKKDQEGGEEKS-VQKKVKELKVLDSKTAQNLSIFLGSFRMPYQEIKNVILEVNEA	884
DIA2	682	--LENTFCCQOKER-----RE---EEDIEEKS--IKKKIKELKFLDSKIAQNLSIFLSSFRVPEEIRMMILEVDET	747
DIA3	674	--LALNFATQIKVQ-----KN---AEALEKKTGPTKKKKVKELRILDPKTAQNLSIFLGSYRMPYEEIRNVILEVNEA	741
DAAM1	645	--LERTFSAYQRQDDFFVNSNSKQKEADAIDDTLS--SKLKVKELSVIDGRRQNCNILLSRLKLSNDEIKRAILTMDEQ	720
DAAM2	640	--FEKMFSAQRHQ-----KELGSTEDIYL--ASRKVKELSVIDGRRQNCIILLSKLLSNEEIRQAILKMDEQ	705
FRL1	677	--FEEQFKTKSQGP-----SLDLSALKSKAA--QKAPSKATLLEANRAKNLAITLRKGNLGAERICQAI EAYDLQ	742
FRL2	661	--FEEIFKTKAQGP-----AIDLSSSKQIP--QKGSNKVTLLEANRAKNLAITLRKAGKTADEICKAIHVFDLK	726
FRL3	606	--FEELFKTKAQGP-----ALDLICSKNKTA--QKAASKVTLLEANRAKNLAITLRKAGRSAAEICRAIHTFDLQ	671
WHIF1	602	--IERLFSFPAKP-----KEPTMVAPRARKEPKEITFLDAKKSLLNLI FLKQFKCSNEEVAAMIRAGDIT	665
INF1	134	--IEELFGQEDTT-----KSSLPRRGRTLNSSFREAREEITILDAKRSMNIGIFLKQFKKSPRSIVEDIHQKSE	202
FHOD1	667	--LEHLFESRAKEV-----LPS-----KK-AGEG-RRTMTTVLDPKRSNAINIGLTTL-PPVHVIKAAALLNFDEF	726
FHOD3	949	--LEHLFESKSKEL-----SVS-----KKTADG-KRQEIIVLDSKRSNAINIGLTVL-PPPRTIKIAILNFDEY	1009
DELPH	865	LDLELHFGTQKPAK-----PVP-----GP-EPFR-KKEVVEILSHKKAYNTSILLAHLKLSPAELRQVLMSEPR	927
FMN1	798	--LFSKDTTQKKK-----PLS---ETYEKNK--VKKIKLLDGKRSQTVGILISSLHLEMKDIQQAIFNVDDS	860
FMN2	1331	--LFSKTAVKERKK-----PIS---DTISKTKA--KQVVKLLSNKRSQAVGILMSSLHLDMKDIQHAVVNLDSN	1392

## Chapter 2: Formin expression patterns

DIA1	885	V-LTESMIGNLIKQMPPEPEQLKMLSEL---KDE---YDDLAESEQFVVMGTVPRLRPRLNAILFKLQFSEQVENIKPEI	957
DIA2	748	R-LAESMIGNLIKHLDPQEQLNLSLSQF---KSE---YSNLCEPEQFVVMNSVKRLRPRLSAIIFKLQFEEQVNNIKPDI	820
DIA3	742	M-LSEALIGNLVKHLPEQKILNELAEL---KNE---YDDLCEPEQFVVMSSVKMLQPRSSILFKLTFEEHINNPKPSI	814
DAAM1	721	EDLPEKDMLEQQLKFFVPEKSDIDLLEEH---KHE---LDRMAKADRFLFEMSRINHYQQRLLQSLYFKKKFAERVAEVKPKV	794
DAAM2	706	EDLAKDMLEQQLKFFIPEKSDIDLLEEH---KHE---IERMARADRFLYEMSRIDHYQQRLLQALFFKKKFAERVAEAKPKV	779
FRL1	743	A-LGLDFLELLMRFLPTEYERSLITRF---EREQRPMEELSEDRFMLCFSRIPRLPERMTTLTFLGNFPDTAQLLMPQL	818
FRL2	727	T-LPVDFVECLMRFLPTENEVQLVRLY---ERERKPLENLSDEDRFMMQFSKIERLMQKMTIMAFIGNFAESIQLMTPQL	802
FRL3	672	T-LPVDFVECLMRFLPTEAEVKLLRQY---ERERQPLEELAAEDRFMLLFSKVERLRTQRMAGMAFLGNFQDNLQMLTPQL	747
WHIF1	666	K-FDVEVLKQLLKLLEPKHEIENLRAF---TEE---RAKLASADHFYLLLLAIPCYQLRIECLMLCEGAAAVLDMVRPKA	738
INF1	203	H-YGSETIREFLKFLPESEEVKLLKAF-----SGDVSKLSLSDSFLYGLIQVPNYSLRIEAMVLKKEFLPSCSSLYTDI	275
FHOD1	727	A-VSKDGIKELLTMMPTEEERQKIEEA-----QLANPDIPLGPAENFLMTLASIGGLAARLQLWAFKLDYDSMEREIAEPL	801
FHOD3	1010	A-LNKEGIEKILTWIPTDEEKQKIQEA-----QLANPEIPLGSAEQFLLTLSSISELSARLHLWAFKMDYETTEKEVAEPL	1084
DELPH	928	R-LEFAHLAQLLAFAPDADEEQRYQ-----AFREAPGRLESDQFVLQMLSVPEYKTRLRSLHFQATLQEQTEEIRGSL	1000
FMN1	861	V-VDLETALYENRAQDEDELVKIRKYETSKEEELKLLDKPEQFLHELALQIPNFAERAQCIIFRSVFSFSEGTSLHRKV	938
FMN2	1393	V-VDLETALYENRAQSDLELEKIEKHGRSSKDKENAKSLDKPEQFLYELSLIPNFSERVFCILFQSTFSESICSIIRKLL	1471
DIA1	958	VSVTAACEELRKSEFSFNSLLEITLLVGNMNMAGSRN-AGAFGFNIFLCKLRDTKST-DQKMTLLHFALAEFCEN-----D	1030
DIA2	821	MAVSTACEEIKKSKSFSKLELLEVLMMGNMNMAGSRN-AQTFGNLSSCKLKDTKSA-DQKTTLLHFVLEICEE-----K	893
DIA3	815	IAVTLACEELKKSSEFNRLLELVLVGNMNMAGSRN-AQSLGFKINFCKIRDTKSA-DQKTTLLHFADICEE-----K	887
DAAM1	795	EAIRSGSEEVFRSGALKQLLEVLAFGNMYMNGSRN-GNAYGFKISSLNKIADTKSSIDKNIITLLHYLITIVEN-----K	867
DAAM2	780	EAILLASRELVRSKRLRQMLEVILAIGNFMNKGSR--GGAYGFRVASLNKIADTKSSIDRNIITLLHYLIMILEK-----H	852
FRL1	819	NAIIAASMIKSSDKLRQILEIVLAFGNMNSKR--GAAYGFRVLSLADALLEMKST-DRKQTLNHHYLVKVIKAE-----K	890
FRL2	803	HAI I AASVSIKSSQKLLKILEIILALGNMNSKR--GAVYGFKLQSLDLDLDTKST-DRKQTLNHHYISNVVKE-----K	874
FRL3	748	NAIIAASASVKSQKLLKQMLEIILALGNMNSKR--GAVYGFKLQSLDLDLDTKST-DRKMTLLHFIALTVKE-----K	819
WHIF1	739	QLVLAACESLLTSRQLPFCQLILRIGNFLNYGSHT-GDADGFKISTLLKLETETKSQ-QNRVTLNHHVLEEAEK-----S	811
INF1	276	TVLRTAIKELMSCEELHSILHLVLQAGNIMNAGGYA-GNAVGFKLSSLLKLDADTKAN-KPGMNLHVFVAQEAQK-----K	348
FHOD1	802	FDLKVGMEQLVQNAATFRCILATLLAVGNFLNGSQ-----SSGFELSYLEKVSEVKDT-VRRQSLHHLCSLVLQ-----T	870
FHOD3	1085	LDLKEGIDQLENNKTLGFILSTLLAIGNFLNGTN-----AKAFELSYLEKVPVVKDT-VHKQSLHHLVCTMVE-----N	1153
DELPH	1001	ECLRQASLELKNRKLAKILEFVLAMGNVLDGQPKNTTGFKINFLELSTKTV-DGKSTFLHILAKLSLQ-----H	1074
FMN1	939	EIITRASDLHLHVSVKDIILALILAFGNMNMGNRTRGQADGYSLEIILPKLKDVKSR-DNGINLVVYVVKYYLRYDQEA	1017
FMN2	1472	ELLQKLCETLKNPGVGMQVLGLVLAFGNMYMNGNKRTRGQADGFLDILPKLKDVKSS-DNSRSLLSYIVSYLNRNDFEDA	1550
DIA1	1031	YPDVLKFP-DELAHVEKASRVSAENLQKNLDQMKQISDVERDVQNFPA--ATDEKDKFVEKMTSFVKDAQEQYNKLRMM	1107
DIA2	894	YPDILNFV-DDLEPLDKASKVSVETLEKNLRQMRGQLQLEKELETFFP--PEDLHDKFVTMKSRLFVISAKEYETLSKL	970
DIA3	888	YRDILKFP-ELEHVESASKVSAQILKSNLASMEQIVHLERDIKFKFPQ--AENQHDKFVEKMTSFTKTAREQYKELSTM	964
DAAM1	868	YPSVLNLN-EELRDIPQAAKVNMTELDKEISTLRSGLKAVETELEYQKSQ-PPQPGDKFVSVVSQFITVASFSFSDVDEL	945
DAAM2	853	FPDILNMP-SELQHLPEAAKVNLAELEKEVEGNLRRGLRAVEVELEYQRRQ-VREPSDKFVVPVMSDFITVSSFSFSELEDQ	930
FRL1	891	YPQLTGFH-SDLHFLDKAGSVSLDSVLADVRSLQRGLTQREFVVRQD-----CMVLFKFLRANSPMTDKLLAD	959
FRL2	875	YHQVSLFY-NELHYVEKAAAVSLENVLLDVKELQRGMDLTKREYTMHDH-----NTLLKEFIIINNEGKLLKQLDD	943
FRL3	820	YPDLANFW-HELHFVEKAAAVSLENVLLDVKELGRGMELIRRECSIHD-----NSVLRNFLTSTNEGKLDKQLDQ	887
WHIF1	812	HPDLLQLP-RDLEQPSQAAGINLEIRSEASSNLKLLLETERKVSASVA---EVQEYQYTERLQASISA---FRALDEL	882
INF1	349	DTILLNFS-EKLHHVQKTARLSLENTEAELHLFLVTRTKSLKENQRDGE-----LCQQMEFLQFAIEKLRCEW	418
FHOD1	871	RPSSDLY-SEIPALTRCAKVDQFQLTENLQGLERRSRAAEEESLRSIAK---HELAPALRARLTHFLDQCARRVAMLRIV	946
FHOD3	1154	FPSSDLY-SEIGAITRSKVDQDQDNLQCMERRCKASWDHLKAIK---HEMMPVLRQMSSEFLKDCAERI I I L K I V	1229
DELPH	1075	FPELLGFA-QDLPTVPLAAKVNQRALTSDLADLHGTISEIQDACQSI SP---SSEDKFAMVMSFLETAQPALRALDGL	1149
FMN1	1018	GTEKSVFPLPEPQDFFLASQVKFEDLIKDLRKLKRQLEASEKQMVVCKESPKEYLQPFKDKLEEFFQKAKKEHKMEESH	1097
FMN2	1551	GKEQCLFPLPEPQDLFQASQMKFEDFQKDLRKLKDLKACEVEAGKVYQVSSKEHMQPFKENMEQFI I QAKI DQEAENS	1630
DIA1	1108	HSNMETLYKELGEYFLFDPK-----LSVEEFFMDLHNFNMFLQAVKEN-QKRRETEEKMRRAKLAKAKA-----	1172
DIA2	971	HENMEKLYQSIIGYYAIDVKK-----VSVEDFLDLNFRFTTFMQAIKEN- IKKREAEKEKRVRIAKELA-----	1035
DIA3	965	HNNMMKLYENLGEYFIFDSKT-----VSEIEFFGLNFRFTLFLAVREN-NKRREMEKTRRAKLAKAKA-----	1029
DAAM1	946	LAEAKDLFTKAVKHFGEEAGK-----IQPDEFFGIFDQFLQAVSEAKQENENMRKKKEEERRARMEAQLK-----	1011
DAAM2	931	LNEARDKFAKALMHFGHEHDSK-----MQPDEFFGIFDQFLQAVSEARQDLEAMRRRKEEERRARMEAMLK-----	996
FRL1	960	SKTAQAEAFESVVEYFGENPKT---TSPGLFSLFSRFIKAYKQAEQEV-EQWKK-EAAAQEAQDTPGKGEPPAPKSP	1033
FRL2	944	AKIAQDAFDDVVYFGENPKT---TPPSVFFPVFVRFVVKAYKQAEQEV-ELRKKQEALMEKLLQEALMEQDQPKSP	1018
FRL3	888	AKTAEAYNAVVRVYFGENPKT---TPPSVFFPVFVRFVRSYKAEQEN-EARKKQEEVMREKQLAQEA--KKLDAKTPS	960
WHIF1	883	FEAIEQKQRELADYLCEDAQQ-----LSLEDTFSTMKAFRDLFLRALKEN---KDRKEQAAKAERRKQQLA-----	945
INF1	419	KRELQDEAYTLIDFFCEDKKT---MKLDECFQIFRDFCTKFNKAVKDN--HDREAQELRQLRQLEQEQ-KORSWATGE	491
FHOD1	947	HRRVQNREAFLLYLGYTPQAA-REVRIMQFQHLRFALEYRTRERV--LQQQKQATYERENKTRGR-MITE--TEK	1020
FHOD3	1230	HRRINRPHSFLFLFMGHPYAI-REVNINKFCRIISEFALEYRTRERV--LQQQKQKRNHRERENKTRGR-MITD--SGK	1303
DELPH	1150	QREAMEELGKALAFFGEDSKA---TTSEAFFGIFAEFMSKF---ERA--LSDLQA-----GE-GLRS--SGM	1205
FMN1	1098	LENAQKSFETTTRYFGMKPKSKEKIEITPSYVFMVWYEFCSDFK-----	1140
FMN2	1631	LTETHKCFLETTAYFFMKPKLGEKVESPNAFFSIIWHEFSDFK-----	1673

## Chapter 2: Formin expression patterns

DIA1	1173	-----EKERLEKQQKREQLIDMNAEGDETVGMDLLEALQSGAAF-----R--RKRGPQA-----	1221
DIA2	1036	-----ERERLERQKKKRLLEMKTEGDETVGMDNLLLEALQSGAAF-----RDRRKRTMPKDVQRQSLSPMSQRPV	1100
DIA3	1030	-----EQEKLERQKKKQLIDINKEGDETVGMDNLLLEALQSGAAF-----RDRRKRI PR-----	1078
DAAM1	1012	-----EQRERERKMRKAK-----ENSEESGEFDDLVSALRSGEVFDKDL SKL--KRNRKRI TNQM----TDSSRERPI	1073
DAAM2	997	-----EQRERERWQRQRKVLAAAGSSLEEGGEFDDLVSALRSGEVFDKDLCKL--KRSRKRSGSQA-----LEVTRERAI	1063
FRL1	1034	-KARRPQMDLISELKRQQKEPLIYESDRDGAIEDIITVIKTVPFT-----A--RTGKRTS--RLLCEASL----GEEM	1098
FRL2	1019	HKSKRQQQELIAELRRRQVKDNRHVYEGKDGAIEDIITDLRNQPYR-----R--ADAVRRSVRRRFDDQNLRVNGAEI	1090
FRL3	961	QRNKWQQQELIAELRRRQAKEHRPVYEGKDGITIEDIITVLKSVFPT-----A--RTAKRGS--RFFCD----AAHDES	1026
WHIF1	946	-----EEEARRPRGEDGKPVVRKGPVKQEEVVCIDALLADIRKGFQLRKTA-----RGRGDTDGGSKAASMDPPRATFP	1013
INF1	492	LGAFGRSSSENDVELLTKKGAEG-----LLPFLHPRPISPSSPSYRPPNTRRSRLSLGPSADRELLTFLESST	559
FHOD1	1021	FSGVAGEAPSNPSVPVAVSSGPRGDADSHASKSLL--TSRP--EDTT-----HNRRSRGMVQSSSP--IMPTVGPST	1088
FHOD3	1304	FSG--SSPAPPSQPQGLSYAE--DAAEHENMKAVLKTSSPSVEDATPALGVTRSRASRGSTSSW-----T	1365
DELPH	1206	VSPLAW-----	1211
FMN1		-----	
FMN2		-----	
DIA1	1222	-----NRKAGCAVTSLLASELTKDDAMAAPAKVSKNSETFPTI-----LEEAKELVGRAS-----	1272
DIA2	1101	LKVCNHNQKVQLTEGSRSHYNINCNSTRTPVAKELNYLDTHSTGRIKAAEKKEACNVESNRKKETELLSGFSKNESV	1180
DIA3	1079	----NPDNRRVPL-ERSRSRHN-----GAISSK----	1101
DAAM1	1074	TKL-NF-----	1078
DAAM2	1064	NRL-NY-----	1068
FRL1	1099	PL-----	1100
FRL2	1091	TM-----	1092
FRL3	1027	NC-----	1028
WHIF1	1014	VATSNPAGDPVVGSTRCPASEPGLDATTASESRGWLVDVAVTPGPQP-TLEQLEEGGPRPLERRSSWYVDASDVLTTEDPQ	1092
INF1	560	GSPEEPNK-----FHSLPRSSPRQARPTIA--CLEPAEVRHQDSSFAHK--PQASGGQEEAPNPPSAQAHQLA	623
FHOD1	1089	ASPEEPPGSSLPDSTSEIMDLLVQSVTKSSPRALA--ARERKRSRGNRKSRLRRT--LKSGLGDDLQALGLSKGPGLE	1163
FHOD3	1366	MGTDDSP--NVTDDAADEIMDRIVKSATQVPSQRVV--PRERKRSRANRKSRLRRT--LKSGLTPPEARALGLVGTSELO	1438
DELPH		-----	
FMN1		-----	
FMN2		-----	
DIA1		-----	
DIA2	1181	PEVEALLARLRAL-----	1193
DIA3		-----	
DAAM1		-----	
DAAM2		-----	
FRL1		-----	
FRL2		-----	
FRL3		-----	
WHIF1	1093	CPQPLEGAWPVTLGDAQALKPLKFSSNQPPAAGSSRQDAKDPTSLGLVQAEADTSEGLEDAVHSRGARPPAAGPGGDE	1172
INF1	624	AAQPENHASAFPRARRQGVSVLRKRYSEPVSLGSAQSPPLSPALAL-GIKEHEL-VTGLAQFNLQGSQGMEETSQTLTSDF	701
FHOD1	1164	V-----	1164
FHOD3	1439	L-----	1439
DELPH		-----	
FMN1		-----	
FMN2	1674	-----DF-----	1675
DIA1		-----	
DIA2		-----	
DIA3		-----	
DAAM1		-----	
DAAM2		-----	
FRL1		-----	
FRL2		-----	
FRL3		-----	
WHIF1	1173	DEDEEDTAPESALDTSLDKSFSEDAVTDSSSGSGLPRARGRASKGTGKRRKKRPSRSQEEVPPDSDDNKTKKLCVIQ---	1249
INF1	702	SPMELESVGHGRG-PQSLASASSSLTPMGRDALGSLSPALEDGKAAPDEPGSAALGSVGSDDPENKDPRLFCISDTTDCS	780
FHOD1		-----	
FHOD3		-----	
DELPH		-----	
FMN1		-----	
FMN2		-----	

## Chapter 2: Formin expression patterns

DIA1		-----	
DIA2		-----	
DIA3		-----	
DAAM1		-----	
DAAM2		-----	
FRL1		-----	
FRL2		-----	
FRL3		-----	
WHIF1		-----	
INF1	781	LTLDCSEGTDSDRPRGGDPEEGEGDGSMSGSGEMGDSQVSSNPTSSPPGEAPAPVSVSDSEPSCKGGLPRDKPTKRKDVV	860
FHOD1		-----	
FHOD3		-----	
DELPH		-----	
FMN1		-----	
FMN2		-----	
DIA1		-----	
DIA2		-----	
DIA3		-----	
DAAM1		-----	
DAAM2		-----	
FRL1		-----	
FRL2		-----	
FRL3		-----	
WHIF1		-----	
INF1	861	APKRGSLKEASPGASKPGSARRSQGAVAKSVRTLTAASENESMRKVMPITKSSRGAGWRRPELSSRGPSQNPPTSSTDTVWS	940
FHOD1		-----	
FHOD3		-----	
DELPH		-----	
FMN1	1141	-----	-----TIWK 1144
FMN2	1676	-----	-----WK 1677
DIA1		-----	
DIA2		-----	
DIA3		-----	
DAAM1		-----	
DAAM2		-----	
FRL1		-----	
FRL2		-----	
FRL3		-----	
WHIF1		-----	
INF1	941	RQNSVRRASTGAEEQRLPRGSSGSSSTRPGRDVPLQPRGSFKKPSAKPLRNLPQKPEENKTCRAHSEGPESPKKEEPKTP	1020
FHOD1		-----	
FHOD3		-----	
DELPH		-----	
FMN1	1145	RE-----SKNISKERL-----KMAQESVSKLTSEKKVETK-----	1174
FMN2	1678	KENKL-----LLQERV-----KEAEVCRQKKGKSLY-----	1704
DIA1		-----	
DIA2		-----	
DIA3		-----	
DAAM1		-----	
DAAM2		-----	
FRL1		-----	
FRL2		-----	
FRL3		-----	
WHIF1		-----	
INF1	1021	SVPSVPHELPRVPSFARNTVASSSRSMRTDLPPVAKAPGITRTVTSQRQLRVKGPEDAAPKDSSTLRRASSARAPKKRPE	1100
FHOD1		-----	
FHOD3		-----	
DELPH		-----	
FMN1		-----	
FMN2		-----	

```

DIA1      -----
DIA2      -----
DIA3      -----
DAAM1     -----
DAAM2     -----
FRL1      -----
FRL2      -----
FRL3      -----
WHIF1     -----
INF1      1101  SAEGPSANTEAPLKARGAGERASLRRKDSRRTLGRILNPLRK  1143
FHOD1     -----
FHOD3     -----
DELPH     -----
FMN1      1175  -----KINPTASLKER-----LRQKEASVTTN-----  1196
FMN2      1705  -----KIKPR---HDSGIKAKISMKT-----  1722

```

**Figure 1C – Complete human formin amino acid alignment.**

Formin alignment was performed using COBALT on 3/30/2012 with the accession numbers listed in Methods. Amino acids highlighted in yellow are translations of forward primers and amino acids highlighted in green are translations of reverse primers used for PCR and qPCR as described in Methods. Two additional sets of primers were made against delphilin, with the amino acids encoded by the forward primers highlighted in pink and those encoded by the reverse primers highlighted in blue.

### Primer design

Custom primer pairs were designed and synthesized for each formin to span the FH1 and FH2 domain linkage of each formin. The products of each primer pair range from 179 to 355 base pairs, averaging 307 bp. Oligonucleotide annealing locations are indicated in Figure 1A and in the complete proteins in Figure 1C. Each set of formin primers, except for FMN1 spans at least one intron, with an average intron size of 9745 bp, and ranging from 83 bp to 107733 bp. The product sizes corresponded to the combined size of the exons, showing that no genomic DNA was present in the PCR reactions. Intron-exon boundaries in the primer product regions are indicated by an underlined amino acid. Oligo(dT)<sub>20</sub> was used for RT-PCR, resulting in retro-transcription starting from the C-terminal end only. The primers used for qPCR and qualitative PCR are equidistant from the C-terminus, with the exception of the inverted formin INF1 and FMN1. A component of the oligo design stemmed from our search for comparable regions within target templates across all formins, following RNA and DNA alignments, as performed using COBALT.

### Primers used for qPCR

#### DAAM1

NP\_055807            1078 aa            linear    PRI 28-JAN-2012

NM\_014992            4256 bp    mRNA    I

inear    PRI 28-JAN-2012

5'- GCC CGA GAA CAA ACT GGA AGG -3'

Bp 1979 - 1999

AA 620 - 627

5'-GGG CAG ATC TTC CTG TTC GTC C -3'

Bp 2276 - 2297

AA 718 - 724

product size 319 bp, spans exons 15-19, spans introns sized 1659, 7358, 4902, 1243

### **DAAM2**

NP\_001188356          1068 aa          linear    PRI 09-SEP-2011

NM\_015345            6252 bp    mRNA    linear    PRI 28-NOV-2011

5'- GGA GCG TGT CCC TGG CAC CGT ATG G -3'

Bp 2048-2072

AA 616-623

5'- CCA GCA TGT CCT TAG CAA GGT CCT CC -3'

Bp 2318-2343

AA 706-713

product size 296 bp, spans exons 16-18, bridges introns sized 1086, 2577

### **Delphillin**

NP\_001138590          1211 aa          linear    PRI 15-AUG-2011

NM\_001145118        4632 bp    mRNA    linear    PRI 15-AUG-2011

5'- GGC ACC ATC TGG GGT CAG CTC GGG G -3'

Bp 2527 - 2551

AA 843 - 850

5'- GCC CGC ACA TCT CGC GCA GCT GCT GC -3'

Bp 2790 – 2815

AA 932 – 940

product size 289 bp, spans exons 13-16, bridges introns sized 2077, 949, 1105

### **Delphillin**

NP\_001138590          1211 aa          linear    PRI 15-AUG-2011

NM\_001145118 4632 bp mRNA linear PRI 15-AUG-2011

5'- GCG TCA AGC GCT TGC GGT GGG AAC AGG -3'

Bp 2486-2512

AA 831-838

5'- GGA CCA GTT CGT CCT GCA GGT GC -3'

Bp 2889-2911

AA 964-970

product size 426 bp

### **Delphillin**

NP\_001138590 1211 aa linear PRI 15-AUG-2011

NM\_001145118 4632 bp mRNA linear PRI 15-AUG-2011

5'- GGA CAT GAG GTC AGA GGC TAT TGG (sequence =  
AACTGCTCCCACGA) -3'

Bp 981-990

AA 328-331

5'- CCA GCA CAG GAA CAT CGA CAC CC -3'

Bp 1260-1282

AA 421-427

product size 301 bp

### **Dia 1**

NP\_005210 1272 aa linear PRI 18-DEC-2011

NM\_005219 5804 bp mRNA linear PRI 18-DEC-2011

5' – GCTTGTGGCTGAGGACCTCTCCC - 3'

Bp 2499 - 2521

AA 786 - 793

5' – GCTGTTCTGACTGAGTCTATGATC – 3'

Bp 2791 - 2814

AA 884 - 891

product size 316 bp, spans exons 16-20, bridges introns sized 1451, 489, 36994,  
4637

**Dia 2**

NP\_006720            1101 aa            linear    PRI 04-MAR-2012

NM\_001042517        4812 bp    mRNA    linear    PRI 21-NOV-2011

5' – GATCAGACCTCATGAAATGACTG – 3'

Bp 2178 - 2200

AA 645 - 652

5' – CGGTTGGCAGAGTCTATGATTCAG – 3'

Bp 2461 - 2484

AA 742 - 749

product size 307 bp, spans exons 17-20, bridges introns sized 45073, 8525, 4318

**Dia 3**

NP\_001035982        1193 aa            linear    PRI 21-NOV-2011

NM\_007309            3782 bp    mRNA    linear    PRI 04-MAR-2012

5' – GGTCAAAGATTGAACCCACAG – 3'

Bp 2324 - 2344

AA 652 - 657

5' – GCTGAGTGAGGCTTTAATTCAGAACC – 3'

Bp 2622 - 2647

AA 749 - 756

product size 324 bp, spans exons 16-20, bridges introns sized 6944, 107733, 2124, 24432

**FHOD1**

NP\_037373            1164 aa            linear    PRI 05-FEB-2012

NM\_013241            3865 bp    mRNA    linear    PRI 05-FEB-2012

5' – CGTGACGTGAAGCTGGCTGGGGG – 3'

Bp 2006 - 2028

AA 632 - 638

5' – CCATGATGCCACGGAGGAAGAGC – 3'

Bp 2325 - 2348

AA 740 - 746

product size 343 bp, spans exons 13-14, bridges intron sized 1462

### **FHOD3**

NP\_079411            1439 aa            linear    PRI 28-JAN-2012

NM\_025135            4942 bp    mRNA    linear    PRI 28-JA N-2012

5'- CCG ACG CTG CAG AGA ATT CCT GTG G -3'

Bp 2881 - 2905

AA 929 - 936

5'- CGAT

CCACCGATGAGGAGAAGC -3'

Bp 3159 - 3185

AA 1022 - 1090

product size 305 bp, spans exons 16-17, bridges intron sized 11930

### **FMN1**

NP\_001096654        1196 aa            linear    PRI 30-JAN-2012

NM\_001103184        12355 bp    mRNA    linear    PRI 30-JAN-2012

5' – GCTGAAGAAGGGGGCTACCGC – 3'

Bp 846 – 866

AA 992 - 999

5' – GGAGAGTGGGAGTGGCCTTCG – 3'

Bp 1004 – 1024

AA 1083 - 1090

product size 179 bp

### **FMN2**

NP\_064450            1722 aa            linear    PRI 30-OCT-2011

NM\_020066            6440 bp    mRNA    linear    PRI 30-OCT-2011

5'- GCC TCT TTA CTG GAC CAG G -3'

Bp 4107 - 4215

AA 1302 - 1309

5'- CGA GTT CGT CTG ACT GTG C -3'

Bp 4444 - 4462

AA 1393 - 1399

product size 356 bp, spans exons 5-8, bridges introns sized 37845, 15638, 1895

### **FRL1**

NP\_005883            1100 aa            linear    PRI 19-NOV-2011

NM\_005892            3973 bp    mRNA    linear    PRI 19-NOV-2011

5' – GCACTGAAACCCAGCCAGATCACC – 3'

Bp 2145 - 2168

AA 649 - 656

5' – GGAAGTCCAGGCCAGAGCCTGC – 3'

Bp 2433 - 2445

AA 742 - 748

product size 301 bp, spans exons 16-18, bridges introns sized 652, 470

### **FRL2**

NP\_443137            1092 aa            linear    PRI 28-JAN-2012

NM\_052905            5575 bp    mRNA    linear    PRI 28-JAN-2012

5'- GCT CTG AAG CCC AAT CAG ATC AAT GGC -3'

Bp 2263 - 2290

AA 633 - 641

5'- GGT AGG AAC CGC ATC AAG CAT TCC -3'

Bp 2566 - 2589

AA 734 - 740

product size 327 bp, spans exons 16-18, bridges introns sized 962, 1571

### **FRL3**

Q8IVF7 FRL3\_HUMAN 1028 aa linear PRI 22-FEB-2012

NM\_175736 11192 bp mRNA linear PRI 28-JAN-2012

5'- GCA CTG AAA CCC AAC CAG ATC AGT GGC -3'

Bp 1966 - 1992

AA 579 - 587

5'- GCG CAT CAG GCA CTC CAC GAA GTC C -3'

Bp 2259 - 2292

AA 676 - 686

product size 327 bp, spans exons 16-18, bridges introns sized 289, 750

### **INF1**

Q9C0D6 FHDC1\_HUMAN 1143 aa linear PRI 22-FEB-2012

NM\_033393 6480 bp mRNA linear PRI 18-DEC-2011

5'- GGA CCT TGG CAG CCA GGC AGG -3'

Bp 425 - 441

AA 118 - 122

5'- CGC AAG GTC TCT GAT CCA TAA TGC -3'

Bp 681 - 704

AA 203 - 209

product size 280 bp, spans exons 1-3, bridges introns sized 9943, 656

### **WHIF1**

NP\_071934 1249 aa linear PRI 26-FEB-2012

NM\_022489 4725 bp mRNA linear PRI 26-FEB-2012

5'- GCT GCC ATC CAA CGT GGC ACG TGA GC -3'

Bp 1856 - 1881

AA 572 - 577

5'- CGT GCT TCT CGG GAA GGA GCT TAA GG -3'

Bp 2168 - 2193

AA 676 - 683

product size 338 bp, spans exons 8-11, bridges introns sized 433, 83, 548

### **Data analysis**

q RT-PCR analyses were run in triplicate and the results were averaged. Data within one standard deviation were used for the expression analysis. The percent of 18S expression of each formin was calculated as the inverted natural logarithm of the ratio of average formin expression to average 18S expression and multiplied by 100 ( $1 - \text{LN}(\text{average formin expression} / \text{average 18S expression}) \times 100$ ). ANOVA and T-tests were performed on raw data,  $p < 0.05$  for specific comparisons. ANOVA was performed on all data points listed in Table 2 with a p-value  $< 0.05$ .

## Results

We performed specific quantitative reverse transcription PCR (RT-PCR) on total RNA equivalently isolated from human cells and tissues as described in Methods. Total RNA was harvested to ensure that all available message was sampled, since little is known of formin transcript activators or locale.

Normalization of signal to total cellular RNA and a reference gene as applied in this study, are deemed the most reliable method of quantification [Bustin, SA 2002, Nolan et al., 2006]. Oligo(dT)<sub>20</sub>, identified as an appropriate and acceptable priming choice in “The MIQE guidelines: minimum information for publication of quantitative real-time PCR experiments,” was used for all RT reactions [Bustin et al., 2009]. Annealing to the C-terminally located Poly-A tail of intact mRNA makes Oligo(dT)<sub>20</sub> a good priming choice, since the target region of the primers used for PCR is located toward the C-terminus of each formin [Ståhlberg et al., 2004].

The sites of specific oligonucleotide primer annealing were carefully chosen based on alignment of all formin protein sequences (Fig. 1A). Between the FH1 and FH2 domains of all human formins is a region of highly divergent sequence of generally consistent length (avg. length = 100.57 amino acids with a standard deviation of 13.39; % identity = 19.11%). Amplification across this region exhibited a high specificity for individual formins. Further, with a single exception, this region also represents a splice site for mRNA synthesis, bridging non-coding introns averaging 9000 bases. Incorporating the conserved homology of the FH1

and FH2 domain termini in this analysis permitted oligonucleotide design consistency important for comparison between formins. Average product size was 307 base pairs with a standard deviation of only 41 base pairs, varying only 13% in size, yet allowing single band selectivity (Fig. 1B). The qualitative PCR products (Fig. 1B) indicated no evidence of genomic DNA, and all products were as anticipated from RNA, as there were no products that included introns, even with 35 cycles of PCR, further demonstrating the lack of genomic DNA in RNA samples. End point melt-curve analysis confirmed the presence of single amplicons in each reaction.

	HeLa	Macrophage	Cerebellum	U2OS	HCN	Skeletal muscle	THP	Diff. THP	U937	K562	Cardiac muscle	HaCaT	MDA	HK-2	HUVEC	HEK	Meg-01	Neutrophil	Platelet	Monocyte	HT1080	Jurkat
<b>DAAM1</b>	31	16	48	31	30	16	34	26	7	9	9	49	32	52	42	32	30	70	39	58	4	37
<b>DAAM2</b>	23	9	43	22	38	4	36	8	0	6	9	66	15	62	16	14	5	71	23	32	0	39
<b>Delphilin</b>	18	1	23	5	17	19	19	11	0	0	0	27	8	35	12	5	0	81	19	44	2	57
<b>Dia1</b>	50	34	42	38	38	14	46	37	21	27	15	50	47	53	44	44	56	91	51	60	15	46
<b>Dia2</b>	40	9	26	32	36	18	36	16	14	16	8	44	38	47	31	31	31	62	24	25	3	30
<b>Dia3</b>	27	20	35	28	31	33	40	29	18	4	5	38	33	48	37	30	33	81	33	45	0	37
<b>FHOD1</b>	51	38	52	45	50	20	61	49	31	33	28	58	50	68	49	49	49	111	54	63	22	72
<b>FHOD3</b>	13	0	39	14	27	32	16	3	0	0	23	48	37	49	35	23	6	68	17	29	13	41
<b>FMN1</b>	40	22	37	27	29	21	54	37	34	31	28	54	43	59	40	53	26	94	48	46	2	71
<b>FMN2</b>	30	5	50	13	33	9	34	19	63	42	3	62	18	47	18	18	17	81	32	24	0	46
<b>FRL1</b>	38	26	41	24	26	20	33	33	11	7	6	30	32	45	19	25	29	87	38	60	5	52
<b>FRL2</b>	40	31	53	19	33	18	31	41	6	0	14	37	38	46	45	36	35	73	25	34	11	40
<b>FRL3</b>	44	35	54	32	35	24	41	46	18	16	11	37	46	47	44	37	39	77	45	54	12	41
<b>INF1</b>	52	26	47	34	42	24	51	37	17	23	15	46	38	59	35	34	35	101	52	39	0	49
<b>INF2/WHIF1</b>	40	28	34	31	44	10	41	37	9	9	4	35	37	49	43	23	6	68	17	29	13	41

**Table 2 – Expression level of human formins in cell and tissue types.**

qRT-PCR for 15 human formins was performed on the cell and tissue types listed as described in Methods. The data are presented as the average of samples prepared in triplicates and reported as the percent of the signal achieved for levels of 18S RNA,  $p < 0.05$ .

The detected levels of formins are presented as the percentage of expression of the 18S ribosomal subunit (Table 2). Based on previous experiments, expression levels above 30% of the 18S subunit translate to protein levels detectable via SDS PAGE and Western blotting. [Mersich et al., 2010] This expression level has been confirmed as detectable in Dia1, Dia2, FRL1, FHOD1 and FHOD3. [Mersich et al., 2010; data not shown] Therefore, expression levels above 30% likely represent functional levels of the protein. Primer pairs used for qPCR produced the predicted product and were confirmed to yield qualitative results by PCR and agarose gel electrophoresis (Fig. 1B). Each of the cell and tissue types analyzed typically showed three to six highly expressed formins (Table 1). With the exception of neutrophils (discussed below), no cell type exhibited expression of all formin family members. Expression of some formins, such as FHOD3 and INF1, showed extreme variation between cell types, suggesting very specific functions. In contrast, some formins, termed homeostatic here, were expressed roughly equally in all cells. For qPCR, all reactions were run in triplicates, using DNA retro-transcribed from equal amounts of RNA, and results averaged, a standard approach detailed in "Properties of the reverse transcription reaction in mRNA quantification." [Ståhlberg et al., 2004]

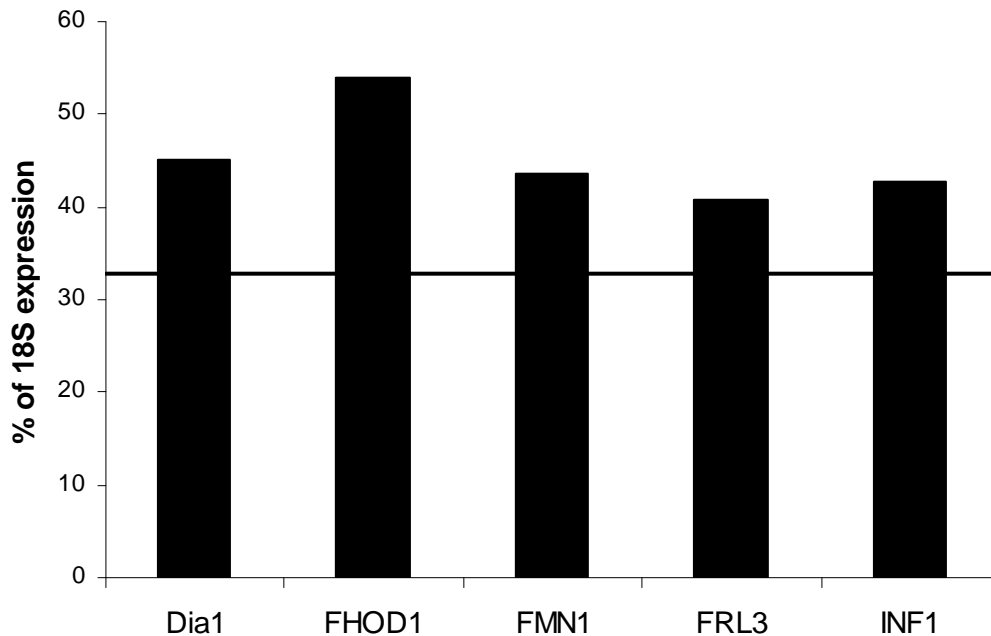


**Figure 2 – Homeostatic formins expressed at detectable levels in all cell and tissue types.**

The level of each formin's expression in all cell and tissue types listed in Table 2 was analyzed. Five formins, Dia1, FHOD1, FMN1, FRL3, and INF1 were found to exhibit a consistently elevated level of expression in all cell and tissue types, suggesting functional roles common to all cells. Line indicates the average expression of all 15 formins in all cells. Data are reported as the average percentage of expression of 18S ribosomal subunit,  $p < 0.05$ .

**Homeostatic Formins**

The level of formin expression varies greatly between different formins as well as between different cell and tissue types. Several formins exhibited a high level of expression in most cells and tissues analyzed (Fig. 2). The average expression of FHOD1, Dia1, FMN1, INF1 and FRL3 in the cells and tissues analyzed is above 40% of the expression of the 18S ribosomal subunit. The ubiquitous and consistent expression of these formins suggests potential roles in the production or maintenance of microfilament structures common to all cells, but does not

rule out additional, specific activities. Dia1 is the most-studied of these formins to date on a structural as well as cellular level. Activated by the GTPase RhoA, and catalyzed by ROCK, Dia1 is an actin nucleator that has been identified to play a role in cell adhesion, migration, and stimulation of T-cells by dendritic cells. [Li and Higgs, 2003; Tanizaki et al., 2010]

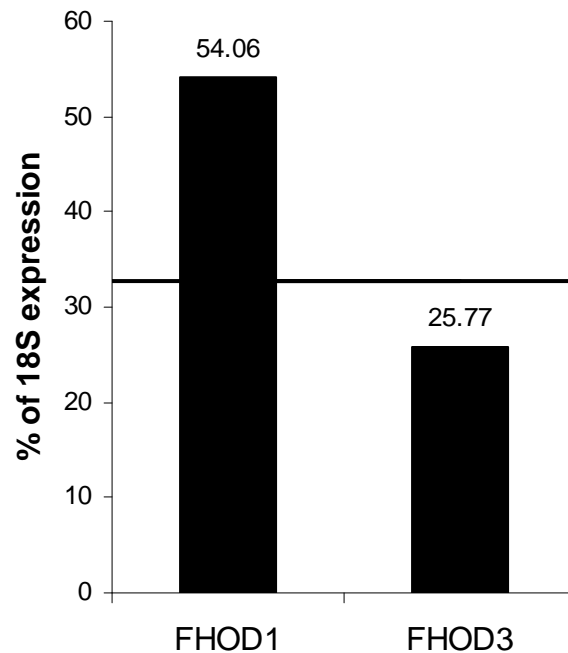


**Figure 3 – Least and most commonly expressed formins are closely related.**

The levels of formin expression in all cell and tissue types listed in Table 2 were analyzed. Two formins, FHOD1 and FHOD3, were notable for consistently high and low expression, respectively. Line indicates the average expression of all 15 formins in all cells. Data are reported as the average percentage of expression of 18S ribosomal subunit,  $p < 0.05$ . FHOD1 and FHOD3 data points have a  $p$ -value of  $< 0.05$ .

### Least and most expressed formins

Averaged across all cell and tissue types analyzed, the most highly expressed human formin is FHOD1 and the least expressed formin we were able to detect

reliably is FHOD3, with an expression of 54.06% and 25.77% of the 18S ribosomal subunit, respectively (Fig. 3). FHOD1 is expressed in all cell and tissue types analyzed, thus it is not surprising that it is the most highly expressed formin. Remarkably, the formin most structurally homologous to FHOD1, FHOD3 (50% identity, 67% similarity), is the least expressed formin, raising the question of why these two formins have such opposite expression profiles. This contrasting expression can be seen in the inverted expression patterns of FHOD1 and FHOD3 in skeletal and cardiac muscle. While FHOD1 is more highly expressed in cardiac muscle than skeletal muscle, 27.78% compared to 20.50% of the 18S ribosomal subunit, FHOD3 shows the opposite expression profiles, with 23.04% in cardiac and 31.87% in skeletal muscle (Fig. 1). These expression profiles have been confirmed by Western blotting (data not shown).

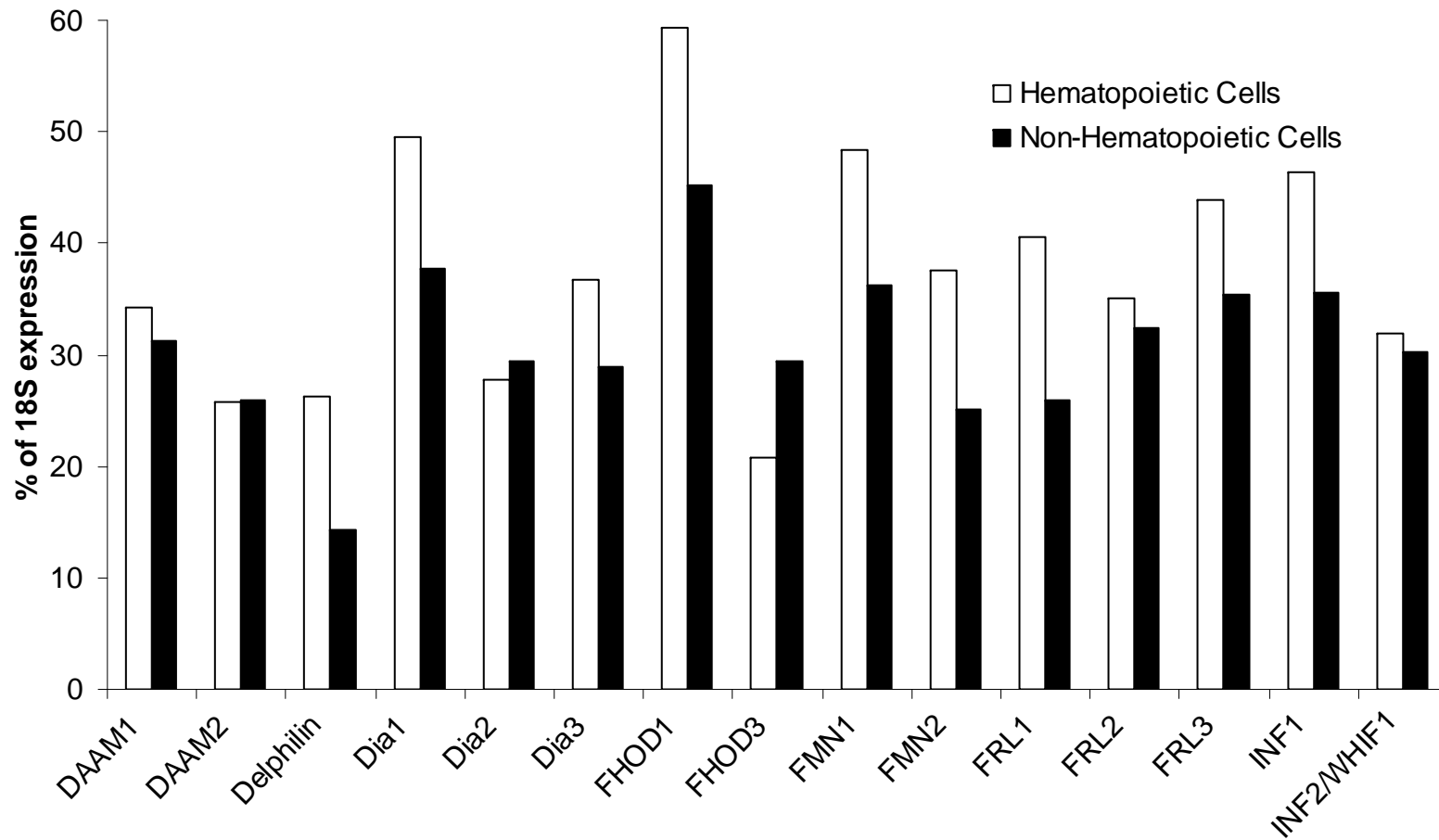


**Figure 4 – Formin family expression is elevated in hematopoietic cells.**

qPCR was performed as described in Methods. Data are reported as the average percentage of expression of 18S ribosomal subunit,  $p < 0.05$ , with experiments performed in triplicate and data within one standard deviation used for analysis. Non-hematopoietic cells and tissues include HeLa, cerebellum, U2OS, HCN, skeletal and cardiac muscle, HaCaT, MDA, HK-2, HUVEC, HEK, HT1080. All other cells and tissues are hematopoietic.

### **Formins in hematopoietic versus non-hematopoietic cells and tissues**

Formin levels in hematopoietic and non-hematopoietic cell types exhibit the expected elevated levels of expression of homeostatic formins, such as Dia1, FHOD1 and FMN1 (Fig. 4). Surprisingly, with the exception of FHOD3, formins have a higher average level of expression in hematopoietic cells than non-hematopoietic cells, despite the former typically exhibiting the greater microfilament organization. FHOD3 is closely related to FHOD1, yet their expression in hematopoietic cells versus non-hematopoietic cells is inverted when compared to the 14 other formins. This raises the question of why FHOD3 is the only formin more highly expressed in non-hematopoietic cells than in hematopoietic cells. FHOD3 has been found to promote myofibril maintenance in cardiac muscle, but no other specific cellular localization or function has been identified to provide insight into this finding [Taniguchi et al., 2009].

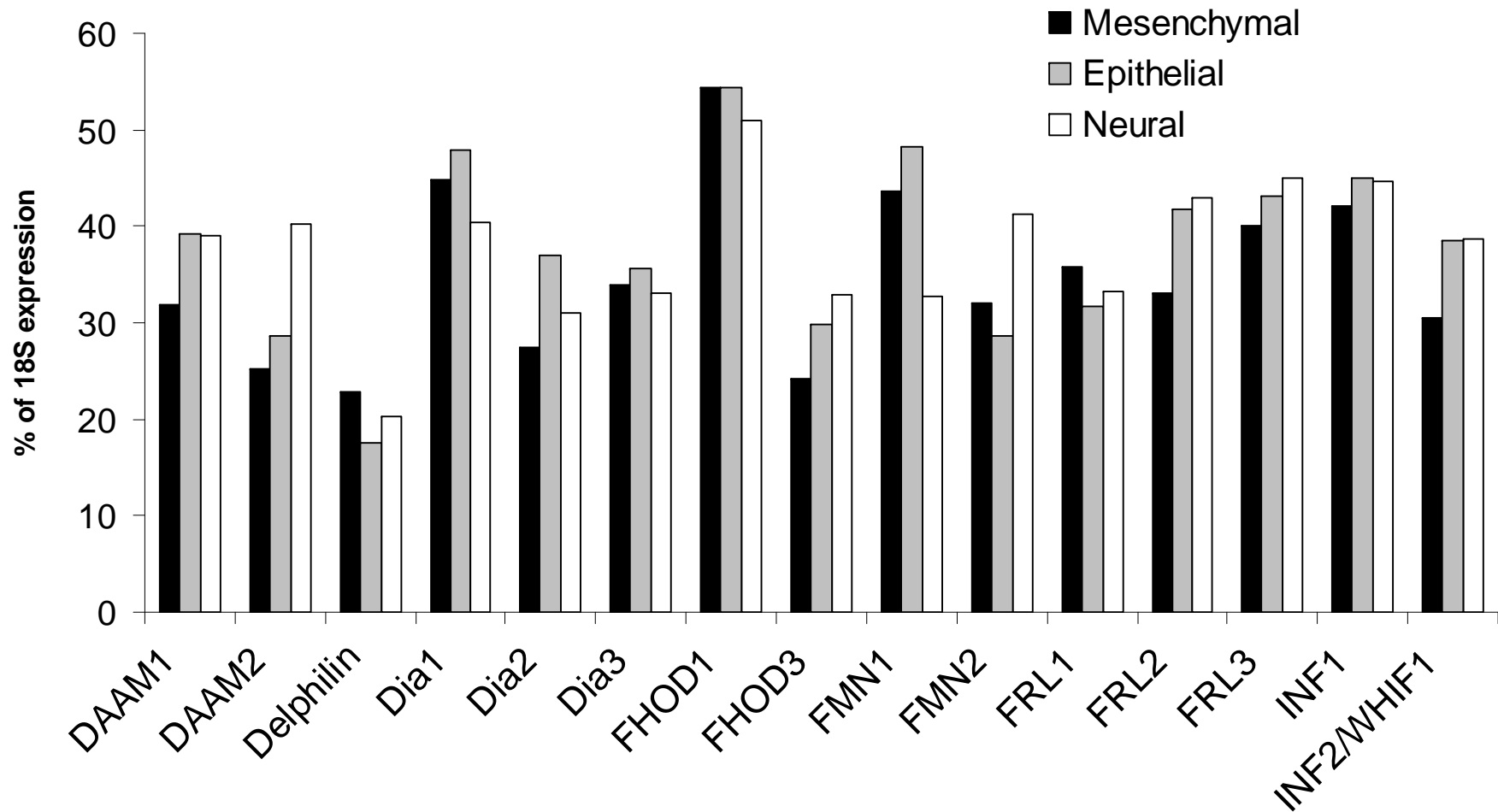


**Figure 5 – Expression of most formins is similar between cells and tissues of mesenchymal, epithelial and neural origins.**

qPCR was performed as described in Methods. Data are reported as the average percentage of expression of 18S ribosomal subunit,  $p < 0.05$ . Mesenchymal cells and tissues include MDA, macrophage, monocyte, THP, K562, U937, HT1080, neutrophil, platelet, Jurkat, megakaryocyte, U2OS, and cardiac and skeletal muscle. Epithelial cells include HeLa, HUVEC, HEK, and HK-2. Neural cells and tissues include HCN and cerebellum.

### **Mesenchymal, epithelial, and neural origins**

The average formin expression among mesenchymal, epithelial, and neural cell and tissue types follows the expected homeostatic pattern, with Dia1, FHOD1 and FMN1 having higher average levels of formin expression (Fig. 5). An unexpected finding was that the expression of each individual formin varies little between the three distinct cell and tissue embryonic origins. DAAM2, however, has a significantly higher level of expression in cells and tissues of neural origin than of mesenchymal or epithelial origin.

An analysis of DAAM1 and DAAM2 expression in the central nervous system of mouse and chick embryos showed that the two proteins have different expression profiles, with DAAM2 being expressed more highly in later developmental stages in the brain, while DAAM1 is expressed earlier overall. Kida et al., found little expression of DAAM2 in the spinal cord, while Lee and Deneen show that DAAM2 plays a role in dorsal patterning in the spinal cord through Wnt signaling [Kida et al., 2004; Lee and Deneen, 2012]. While no conclusion can be made about the localization of DAAM2 in the central nervous system based on the expression analysis presented here, the studies in chick and mice support the comparatively high level of expression of DAAM2 in neural tissues. [Kida et al., 2004; Lee and Deneen, 2012]

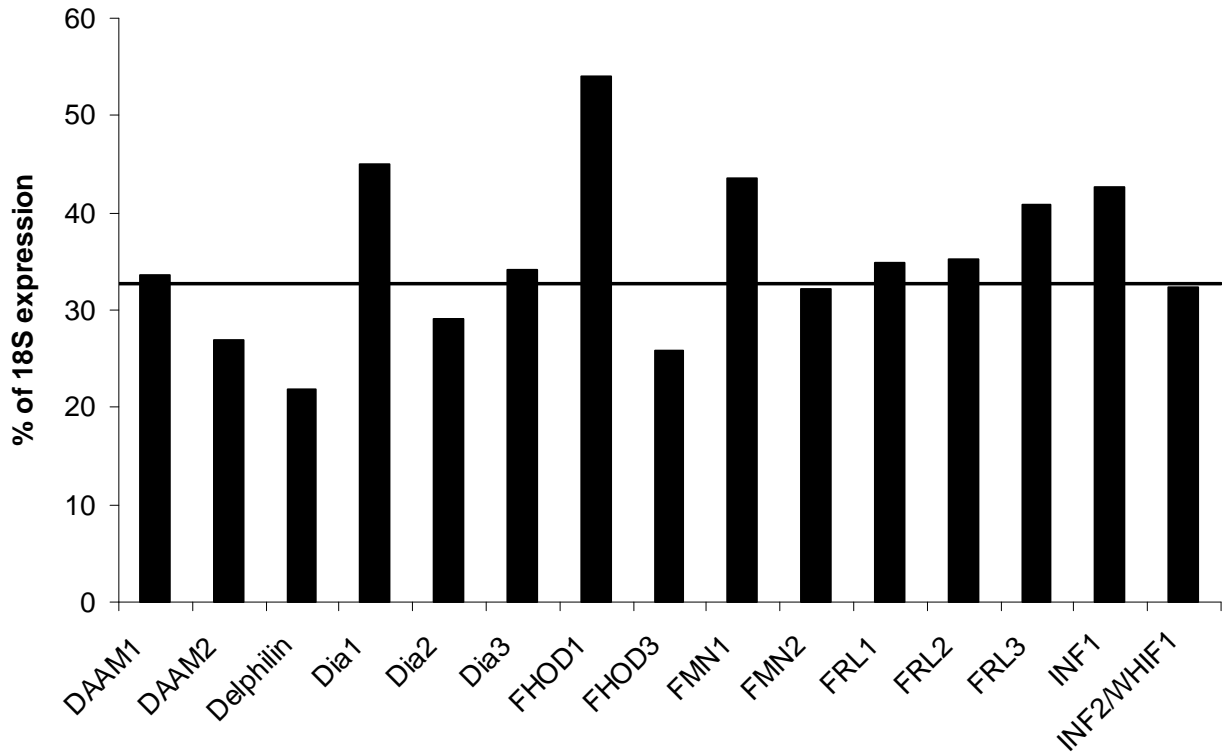


**Figure 6A – Total expression of all formins varies in human cell and tissue types.**

qPCR was performed as described in Methods. The level of expression of all formins in each individual cell and tissue type was averaged and is displayed as a percentage of expression of the 18S ribosomal subunit. The line indicates the average expression of all 15 formins in all cells. Data are reported as the average percentage of expression of 18S ribosomal subunit,  $p < 0.05$ .

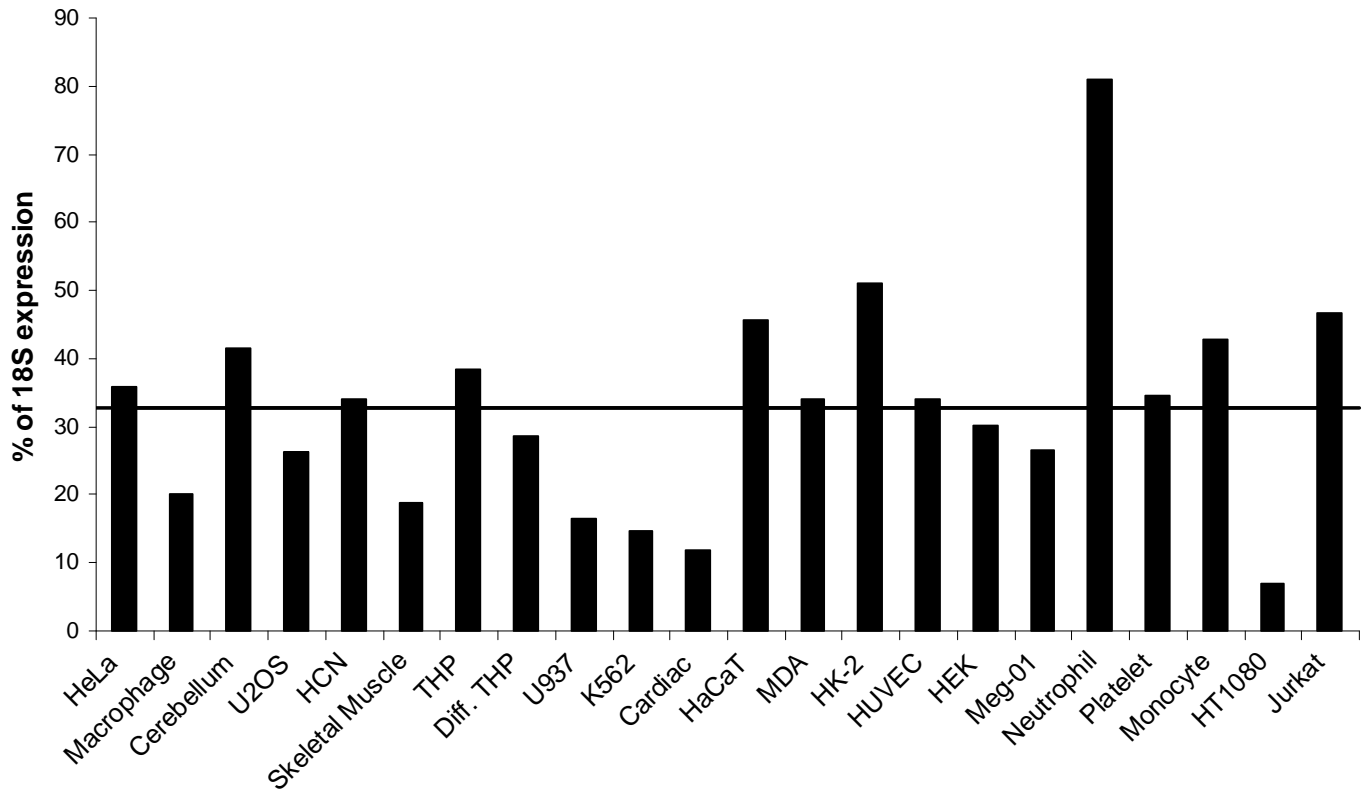


**Figure 6B – Variation of individual formin expression in human cell and tissue types.**

qPCR was performed as described in Methods. The total level of expression for each individual formin in all cell and tissue types was averaged and is displayed as a percentage of expression of the 18S ribosomal subunit. The line indicates the average expression of all 15 formins in all cells. Data are reported as the average percentage of expression of 18S ribosomal subunit,  $p < 0.05$ .

### **Formin levels in cells and tissues**

The level of formin expression for all 15 formins combined varies from barely detectable in HT1080 cells to 80% of 18S expression in neutrophils (Fig. 6A). The significantly higher level of formin expression in neutrophils was not predicted, but may be explained by considering their functions. Neutrophils are multipotent, nondividing cells that are recruited to sites of inflammation immediately after injury, and their function spans a variety of tasks including migration, phagocytosis, and degranulation. In order to carry out these tasks in a timely manner, it may be beneficial for neutrophils to have a large amount of RNA ready for translation. In turn, this reinforces a model where differentiation-based structures are constructed with the input of specific formins [Chhabra and Higgs, 2007]. Another explanation would be a lower level of 18S RNA in neutrophils than in the other cells and tissues that were analyzed, although this was not evident in qPCR of the 18S RNA. Furthermore, similar elevated expression was not seen in fully differentiated macrophages that execute comparable physiologic functions (Table 2). Regardless of the reason for the high level of expression of formins in neutrophils, all formins exhibit high message levels in neutrophils. When the expression level of individual formins is averaged for its total expression in all human cell and tissue types, we found a remarkably similar expression level for all formins with notable exceptions FHOD1 and FHOD3 discussed above and Delphilin (Fig. 6B).

### **Delphilin**

Delphilin was first identified as a glutamate receptor  $\delta 2$  (GluR $\delta 2$ ) interacting protein in parallel fiber-Purkinje cell postsynapses in the cerebellar cortex [Miyagi et al., 2002

Watanabe-Kaneko et al., 2007]. It was termed GRID2IP (glutamate receptor, ionotropic, delta 2-interacting protein 1) and delphilin from “Delta2-philic-protein”. Two differently palmitoylated isoforms of delphilin have been characterized and may be involved in controlling GluR $\delta$ 2 signaling in Purkinje cells [Matsuda et al., 2006]. Delphilin could not be detected via PCR in any tissue and cell types analyzed. The primers to confirm the presence of delphilin were designed to encompass 289 base pairs located N-terminally of the poly-proline stretch and extending into the FH2 domain. This pair of primers did not yield a DNA product detectable via agarose gel electrophoresis using DNA obtained from U2OS cells, HeLa cells and HCN cells. Since delphilin has been reported in Purkinje cells located in the cerebellar cortex, DNA obtained from total human cerebellar RNA as described in Methods was also used to detect delphilin, but PCR did not yield a product [Miyagi et al., 2002]. Two additional sets of primers to detect delphilin in these cells and tissues also did not yield a product, one starting slightly C-terminally and ending slightly N-terminally of the original primers with a 426 base pair product, and one located at the C-terminal end of delphilin with a 401 base pair product (Fig. 1S).

## Discussion

In this report we highlight several results to show the potential that exists in the field of formin research. The biochemical study of formins with regard to their actin polymerization activity and structure is quite advanced [Goode and Eck, 2007; Paul and Pollard, 2008; Paul and Pollard, 2009]. However, the cellular localization and function of most formins remain elusive. As actin modifiers, formins are present in every cell type we analyzed, and quite predictably in every other cell and tissue, providing a plethora of *in vitro* model systems.

The formin field nomenclature and classification exhibited an expected extent of disorder, complicating the pursuit of this new field. The diligent efforts of several laboratories have brought to fruition a clear nomenclature that is universally accepted among formin researchers, making the sharing of data and ideas easier (Table 1). We see similarities between the newer field of formins and the more established field of integrins. The formin and integrin families have a comparable number of molecules that are present in a multitude of cells, all of which contain several members of the protein families, with some proteins being very specific, while others are partly redundant. Considering the widespread presence of formins and the importance of the actin cytoskeleton to numerous essential physiological processes, we predict that formins harbor decades of investigative research, yielding thousands of functionally descriptive publications, comparable to integrin research efforts.

It is important to note that some formins, such as FRL1, have already been ascribed multiple alternative splice forms [Colon-Franco et al., 2011]. While these isoforms were readily detectable through PCR using isoform specific primers, the variant nature of the spliced sequences prohibited confidence in the quantitative reliability of the oligonucleotides utilized (data not shown). Detailed analysis of individual formins should include evaluation of the specific role of alternatively spliced isoforms.

As the speed of formin research is increasing exponentially due to the growing realization of the significance and widespread implications of the formin field, we are excited to witness the future of this promising field unfold. The results presented in this paper and our experience in working with formins suggest that some formins serve more general functions, while others have highly specialized functions. A complete understanding of formins will involve not only the expression profiles discussed here, but also insight into the activation and localization of formins in cells. We hope that the information provided here can be a starting point for future studies on formins. To encourage the study of the cellular aspects of the formin field, we will continue to analyze human cell and tissue types using qPCR as they become available. Please contact the corresponding author if you are interested in providing us with cells or tissues.

Figure 1S – Formin Alignment with Primers

DIA1	1	ME-----PPGSLGPG---RGTDRDK---KGRSPDELPSAGDGGKSK---KFTLKRMLADELERFTSMRI	57
DIA2	1	MERHQPRLLHHPAQGSAAGTYPYPSSASLRGCRESKMPRRKGPQHPPPPSPGPEEPGEKRPKPHLNIRTLTDDMLDKFASIRI	80
DIA3	1	ME--QPGA--AASGAGGSEEPG-----GGRSNK--RSAGNR-----AANEEETKNKPKLNIQIKTLADDVDRDRITSFVK	64
DAAM1		-----M	
DAAM2		-----M	
FRL1		-----	
FRL2		-----	
FRL3		-----	
WHIF1		-----	
INF1		-----	
FHOD1		-----M	
FHOD3		-----	
DELPH		-----	
FMN1		-----	
FMN2		-----	
DIA1	58	K-KEKEKPNSAH-RNSSASYGDDPTAQ-----SLQDVSDEQVLVLFQMLLDMNLNEEKQQLPREKDII	119
DIA2	81	PGSKKERPPLPN-LKTAFASSDCSAAPLEM-----MENFPKPLSENELELFEKMMEDMNLNEDKKAPLREKDFS	149
DIA3	65	STVKKKEKPLIQHPIDSQVAMSEFPAAQ-PL-----YDERSLNLSEKEVLDLFEKMMEDMNLNEEKKAPLRNKDFT	133
DAAM1	2	APRRKGGRGISF-IFCCFRNNDHPEITYRLRNDNSNFALQTMEPALPMPVVEELDVMSSELVDELDTDKHREAMFALPAE	80
DAAM2	2	APRRKSHHGLGF-L-CCFGSDIPEINLR---DNHPLQFMFESSPIPAEELNIRFAELVDELDTDKNREAMFALPPE	75
FRL1	1	-----MGNAAGSAEQPAGPAAP---PPKQPAPP-KQMPAAGELEERFNALNCMNLPDPKVQLLSQYDNE	62
FRL2	1	-----MGNAGSMDSQQTDFAH---NVPL---KLPMPPEGELEERFAIVLNAMNLPDPKARLLRQYDNE	58
FRL3	1	-----MGNLESAEVPGE--PP---SVPLLLPPGKMPPEPCELEERFALVLSMNLPDPKARLLRQYDNE	61
WHIF1	1	-----MSVKEGAQ	8
INF1		-----	
FHOD1	2	AGGEDRGDGEVSVVTVRVQYLEDTPFACAN-FPEP-----RRAPTCSLD-----GALPLGAQIPAVHRLLGAP	65
FHOD3	1	-----MATLACRVQFLDDTDPFNSTN-FPEP-----SRPPLFTFR-----EDLALGTQLAGVHRLLGAP	53
DELPH	1	-----MATTATPATNQG-WPEDFGFRLGGSGPCFVLEAVKGS SAHAGGLRPGDQILEVEGLAVGG	59
FMN1		-----	
FMN2		-----	
DIA1	120	IKREMSQYLYTSKAGMSQKESK---SAMMYIQELRSGLRDMPLLS---C-----LE-SLRV	170
DIA2	150	IKKEMVMQYINTASKTGSLKRSRQ---ISPQEFIHCLKMGSADERLVT---C-----LE-SLRV	201
DIA3	134	TKREMVVQYISATAKSGGLKNSKHECTLSSQYVHELRSIGSDEKLLN---C-----LE-SLRV	188
DAAM1	81	KKWQIYCSKKKQEE-NKGATSWP-----EFYIDQLNSMAARKSLLA---LE-----KEEEERSKTIE-SLKT	139
DAAM2	76	KKWQIYCSKKKEQEDPNKLATSWP-----DYIDRINSMAAMQSLYA---FD-----EETEMRNQVVE-DLKT	135
FRL1	63	KKWELICDQERFQVK-----NP-----PAAYIQKLSYVDTGVS---KVAADWMSNLGFKRRVQESTQVLR-ELET	126
FRL2	59	KKWELICDQERFQVK-----NP-----PHTYIQKLGKYLDPVTRK---K-----FRRRVQESTQVLR-ELEI	112
FRL3	62	KKWDLICDQERFQVK-----NP-----PHTYIQKLSFQVTRK---K-----FRRRVQESTQVLR-ELEI	115
WHIF1	9	RKWAALKEKLGPDSDPTEANLES-----ADPELCIR---LLQMPVVN-----YS-GLRK	55
INF1		-----	
FHOD1	66	LKLEDCALQVSPSGYYLDTELSLEEQREMLEGFYEEISKGRKPTLILRTQLSVRVNAILEKLYSSSGPELRRSLF-SLK-	143
FHOD3	54	HKLDDCTLQLSHNGAYLDLEATLAEQRDELEGFQDDAGRKKHSIILRTQLSVRVHACIEKLYNSSGRDLRRALF-SLK-	131
DELPH	60	LSRER-LVRLARRCPRVPPSLGVLPAFD---GGPGGSGPAAPTTLVLRAPRCGRGLALGRELLRAGRKRPDVHRERR-	134
FMN1		-----	
FMN2		-----	
DIA1	171	SLNNNPVSWVQTFGA-E--GLASLLDILKRLHDEKEETAGSYDSRNKHE-----	216
DIA2	202	SLTSNPVSWVESFGH-E--GLGLLLDILEKLI SGKIQE--KVVKNQHK-----	245
DIA3	189	SLTSNPVSWVNNFGH-E--GLGLLLDELEKLLDKKQEE--NIDKKNQYK-----	232
DAAM1	140	ALRTKPMRFVTRFIDL--GLSCILNFKTMDYETSES-----RIHTS-----	180
DAAM2	136	ALRTQPMRFVTRFIELE--GLTCLLNFLRSMHATCES-----RIHTS-----	176
FRL1	127	SLRTNHIGWVQEFLNENRGLDVLLEYLAFAQCSVTYDMESTDNGASNS-EKNKPLEQSVEDLSKGPSSVP-----K	198
FRL2	113	SLRTNHIGWVREFLNENRGLDVLVEYLSFAQYAVTFDFESVESTVSSVDKSKPWSRSIEDLHRGNSLPSVGNVSRS	192
FRL3	116	SLRTNHIGWVREFLNENRGLDVLVDYLSFAQCSVMFDFEGLESDDGAFDKLRSWSRSIEDLQPPSALSAPFTNSLARS	195
WHIF1	56	RLEGSDGGMVQFLEQS--GLDLLLEALARLSGRGVARI--SDALLQLT-----	100
INF1		-----	
FHOD1	144	QIFQEDKDLVPEFVHSE--GLSCLIRVGAAADHNYQSY-----	179
FHOD3	132	QIFQDDKDLVHEFVVAE--GLTCLIKVGAEADQNYQNY-----	167
DELPH	135	RKAQEF SRKVD EILGDQ--PTA-----KEQ-----	157
FMN1		-----	
FMN2		-----	

## Chapter 2: Formin expression patterns

DIA1	217	-----IIRCLKAFMNNKFGIKTMLETEEGILLVLRAMPDAVPMNMDAAKLLSA	265
DIA2	246	-----VIQCLKALMNTQYGLERIMSEERSLSLLAKAVDPRHPNMMDTVVKLLSA	294
DIA3	233	-----LIQCLKAFMNNKFLQRIIGDERSLLLLARADPKQPNMTEIVKILSA	281
DAAM1	181	-----LIGCIKALMNNQGRAHVLAHSESINVIAQSLSTENIKTKVAVLEILGA	229
DAAM2	177	-----LIGCIKALMNNQGRAHVLAQPEAISTIAQSLRTENSKTAVLEILGA	225
FRL1	199	SRHLTIKLTPAHSRKALRNSRIVSQKDDVHVCIMCLRAIMNYQSGFSLVMNHPACVNEIALSLNNKNPRTKALVLELLAA	278
FRL2	193	GRHSALRYNTLPSRRTLKNSRLVSKKDDVHVCIMCLRAIMNYQYGFNMVMSHPHAVNEIALSLNNKNPRTKALVLELLAA	272
FRL3	196	ARQSVLRYSTLPGRRALKNSRLVSKKDDVHVCILCLRAIMNYQYGFNLVMSHPHAVNEIALSLNNKNPRTKALVLELLAA	275
WHIF1	101	-----CVSCVRAVMNSRQGIIEYILSNQGYVRQLSQALDTSNMVVKQVFEELAA	149
INF1		-----	
FHOD1	180	-----ILRALGQLMLFVDGMLGVVAHSDTIQWLYTLCASLSRLVVKTKALKLLLV	228
FHOD3	168	-----ILRALGQIMLYVDGMNGVINRNETIQWLYTLIGSKFRLVVKTKALKLLLV	216
DELPH	158	-----VFAALKQF-----AAEQRVDDLVTWLTLL--ALPREACGPLLDNLRI	196
FMN1		-----	
FMN2		-----	
DIA1	266	LCILP---QPEDMNERVLEAMTE-RAEMDEVERFQPLLDGL----KSGTTIALKVGCLQLINALI---TPAEELDFRVH	333
DIA2	295	VCIVG---E-ESILEEVLEALTS-AGEEKKIDRFFCIVEGL----R-HNSVQLQVACMQLINALV---TSPDDLDFRLH	360
DIA3	282	ICIVG---E-ENILDKLLGAIIT-AAERNNRERFSPIVEGL----ENQEALQVACMQFINALV---TSPYELDFRIH	348
DAAM1	230	-----GHKKVLQAMLHYQKYASERTRFOTLINDLDKSTGRYRDEVSLKTAIMSFINAVLSPGAGVESLDFRLH	303
DAAM2	226	VCLVP---G---GHKKVLQAMLHYQVYAAERTRFOTLLNELDRSLGRYRDEVNLKTAIMSFINAVLNAGAGEDNLEFRLH	299
FRL1	279	VCLVR---G---GHDIIILAAFDFNFKEVCGEQHRFEKLEMEYFR----NEDSNIDFMVACMQFINIVV---HSVENMNFVRV	345
FRL2	273	VCLVR---G---GHEIILSAFDNFKEVCGEKQRFKLEMEHFR----NEDNNIDFMVASMQFINIVV---HSVEDMNFVRV	339
FRL3	276	VCLVR---G---GHEIILSAFDNFKEVCHELHRFEKLEMEYFR----NEDSNIDFMVACMQFINIVV---HSVEDMNFVRV	342
WHIF1	150	LCIYS---P---EGHVLTLDALDHYKTVCSSQYRFSIVMNELS----GSDNVPYVVTLLSVINAVI---LGPEDLRARTQ	216
INF1		-----	
FHOD1	229	FV-----EYSENNAPLPIRAVNSVASTTGAPPWANLVSILEE---KNGADPELLVYTVTLINKTL---AALPDQDSFYD	296
FHOD3	217	FV-----EYSESNAPLLIQAVTAVDTKRGVKNPSNIMEILEE---KDGVDTELLVYAMTLVNKTL---SGLPDQDTFYD	284
DELPH	197	FIPKXHRARFDEVVSQGLLGLKCRARRAQGAQ-----RLRRS---RSEERPERL-----LVSTRA---SAPPRRP----	255
FMN1	1	-----MENVDNSLDGSDVSEPAKPE---AGLEVAQSILS	31
FMN2	1	-----MGNQDGKLRKRSAGDALHEGG---GGAEDALGPRD	31
DIA1	334	IRSELMRLGLH-QVLQDLREIE-----NEDMRVQLNVFDEQG-EEDSYDLKGRLLDDI-	383
DIA2	361	IRNEFMRCGLK-EILPNLKCIC-----NDGLDIQLKVFDEHK-EEDLFELSHRLEDI-	410
DIA3	349	LRNEFLRSLGK-TMLPDLKEKE-----NDELDIQLKVFDEHK-EEDLTELSHRLNDI-	398
DAAM1	304	LYEFLMLGIQ-PVIDKLRHE-----NSTLDRHLDFFEMLR-NEDELEFAKRFELV-	353
DAAM2	300	LYEFLMLGIQ-PVIDKLRQHE-----NAILDKHLDFEFMVR-NEDDLELARRFDMV-	349
FRL1	346	LQYEFTHLGLD-LYLERLRLTE-----SDKLQVQIQAY-----	377
FRL2	340	LQYEFTKLGLD-EYLDKLRKHE-----SDKLQVQIQAY-----	371
FRL3	343	LQYEFTKLGLE-EFLQKSRHTE-----SEKLQVQIQAY-----	374
WHIF1	217	LRNEFIGLQLL-DVLARLRDLE-----DADLLIQLEAFEEAK-AEDEEELLR--VSG-	264
INF1		-----	
FHOD1	297	VTDALQQGMEALVQRHLGTAG-----TDVDLRTQLVLYENAL-----KLEDG-	339
FHOD3	285	VVDCLEELGIAAVSQRHLNKKG-----TDLDLVEQLNIYEVAL-----RHEDG-	327
DELPH	256	-----DEPPPRRASLLVGG-----A-----	271
FMN1	32	KFSMKSFLG---FTSKLESVNPEEEDAVLKAFHSLDVNPTSQQDSSNGLDPQEAGSRVSPDLGNDEKIASVETESEGS	107
FMN2	32	VEATKKGSG---GKKALGKHGKGGGGGGGGESGKKKSKSDSRASVFSNLRIRKNLSKKGKAGGSREDVLDLSQLQTG-	106
DIA1	384	-----RMEMDDFN-----	391
DIA2	411	-----RAELDEAY-----	418
DIA3	399	-----RAEMDDMN-----	406
DAAM1	354	-----HIDTKSAT-----	361
DAAM2	350	-----HIDTKSAS-----	357
FRL1	378	-----LDNIF-----	382
FRL2	372	-----LDNVF-----	376
FRL3	375	-----LDNVF-----	379
WHIF1	265	-----GVDMSHQ-----	272
INF1		-----	
FHOD1	340	-----DIEEAPGAGGRERRKPS-----	357
FHOD3	328	-----DETTEPPPSGCDRRRARSVCSSGGG-----	352
DELPH	272	-----GPGGARTRVRY-----	283
FMN1	108	QRKEAGTSLLAQELLPLSTLKGTKDDVICVGR-----TLVHTTSDSDSDGGQEPPEGS-STNGPK	167
FMN2	107	ELDSAHSLLTKTPDLSLSADEAGLSDTECADPFEVTPGGPGPAEARVGRPIAEDVETAAGAQDQRTSSGS-DTDIYS	185

## Chapter 2: Formin expression patterns

DIA1	392	-EVFQILLNTV-----	401
DIA2	419	-DVYNMVWSTV-----	428
DIA3	407	-EVYHLLYNML-----	416
DAAM1	362	-QMFELTRKRL-----	371
DAAM2	358	-QMFELIHKKL-----	367
FRL1	383	-DVGALLEDETE-----	392
FRL2	377	-DVGALLEDAE-----	386
FRL3	380	-DVGGLLEDAE-----	389
WHIF1	273	-EVFASLFHKV-----	282
INF1		-----	
FHOD1	358	SEEGKRSRRSL-----EGGGCPARAPEPGPT	383
FHOD3	353	EHRGLDRRRSR-----RHSVQSIKSTLSAPT	378
DELPH	284	--KGNKSGFFT-----LRGHGPVWIESVLPG	307
FMN1	168	SPSGVLSEPE-----SQESKENPGGFRENTVTGEMNGAELCAEDPQRIPPEMSSKLEAGNGLQTERRPSQDQV	235
FMN2	186	FHSATEQEDLLSDIQQAIRLQQQQQQQLQLQLQQQQQQQLQGAEEPAAPPTAVSPQPGAFLGLDRFLLGPGSGGAGEAPG	265
DIA1	402	--KDSKAEPHFLSILQHLLLRND-----YEARPQYYKLIIEEC--	437
DIA2	429	--KETRAEGYFISILQHLLLRND-----YFIRQQYFKLIDEC--	464
DIA3	417	--KDTAAENYFLSILQHFLLRND-----YYIRPQYYKIIIEEC--	452
DAAM1	372	--THSEAYPHFMSILHHCLQMPYKR-----SGNTVQYWLLLDRI--	408
DAAM2	368	--KYTEAYPCLLSVLHHCLQMPYKR-----NGGYFQQWQLLDRI--	404
FRL1	393	--TKNAVLEHMEELQEQVALLTER-----LRD----	417
FRL2	387	--TKNAALERVEELEENISHLSEK-----LQD----	411
FRL3	390	--TKNVALEKVEELEEHVSHLTEK-----LLD----	414
WHIF1	283	--SCSPVSAQLLSVLQGLLHLEPT-----LRSSQLLWEALESL--	318
INF1		-----	
FHOD1	384	GPASPVGPT-----SSTG----	396
FHOD3	379	SPCSQSAPSFKNQVRDLREKYSN-----FGNNSYHSSRPSSG----	416
DELPH	308	SPADNAALKSGDRILFLNGLDMRN-----CSHDKVVSMLOGSGAM--	347
FMN1	236	GEEGSQDLPAVTNQNSSVG-----ITESASSKKEVSGEKSFLPAFFSGLRVLKKGATAEG--	291
FMN2	266	SPDTEQALSALSDLPESLAAEPREPQQPPSPGGPLVSEAPSLPAAQPAAKDSPSSTAFFPFPEAGPGEAAAGAPVRGAGDT	345
DIA1	438	-----ISQIVLHKN-GADPDFKCR-HLQIE-----IEGL	464
DIA2	465	-----VSQIVLHRD-GMDPDFTYRKRLDLD-----LTQF	492
DIA3	453	-----VSQIVLHCS-GMDPDFKYRQRDID-----LTHL	480
DAAM1	409	-----IQQIIVIQNDKGDQDPDSTPLENFNIK-----NV	435
DAAM2	405	-----LQQIVLQDERGVDPDLAPLENFNVK-----NI	431
FRL1	418	-----AENE-----	421
FRL2	412	-----TENE-----	415
FRL3	415	-----LENE-----	418
WHIF1	319	-----VNRVALLAS-----DAQ-----ECT	333
INF1		-----	
FHOD1	397	-----PALLTGPASSPVGP-----PSGLQASVNL	420
FHOD3	417	-----SSVPTTPTSSVSPQEARLERS-----SPSGLLTSSFR	449
DELPH	348	-----PTLVVEEGLVPFASDSLSLDS-----NPSSALTSLQW	380
FMN1	292	-----GETITEIKPKDGLALLKLTQPVKSLVQAGLQTVKSEKATDPKA-----TPTLLEQLSLL	348
FMN2	346	DEEGEEDAFEDAPRGSPEEWAPEVGEDAPQRLGEEPEEEAQGPDAPAAASLPGSPAPSORCFKPYPLITPCYIKTTTRQ	425
DIA1	465	IDQMIDKTKVEKSEAK-----	480
DIA2	493	VDICIDQAKLEEFEEK-----	508
DIA3	481	IDSCVNKAKVEESEKQ-----	496
DAAM1	436	VRMLVNEVEVKQWKEQ-----	451
DAAM2	432	VNMLINENEVKQRDQ-----	447
FRL1	422	-----SMAKIAELEKQ-----	432
FRL2	416	-----AMSKIVELEKQ-----	426
FRL3	419	-----NMMRVAELEKQ-----	429
WHIF1	334	LEEYVERLLSVKGRPR-----	349
INF1		-----	
FHOD1	421	FPTI---SVAPSADTS-----SERSIY-----KARFL	444
FHOD3	450	QHQE---SLAAERERRRQEREERLQRIER-----EERNKFSRDYLDKREEQRQA-----REERYKYL	503
DELPH	381	VAEILPSSIRVQGRFTFSQQLEHLLTPPERYGVCRALESFFQHRNIDTLIVDVYPVLDTPA-----KQVLWQFI	448
FMN1	349	LNIDMPKTEPKGADPESPREEM-----GCNADQESQSGGVPQTQGGEVKPKSPETALEAFKALFIRPPRKGTADT	421
FMN2	426	LS--SPNHSPSQSPNQSPRIKRRPEPSLSRGSRTALASVAAPAKKHRADGGLAGLSRSA-DWTEELGARTPRVGGSAHL	502

## Chapter 2: Formin expression patterns

DIA1	481	----AAELEKKLDESELTA-----	494
DIA2	509	----ASELYKKFEKEFTD-----	522
DIA3	497	----AAEFSKKFDEEFTA-----	510
DAAM1	452	----AEKMRKE-----	458
DAAM2	448	----AEKFRKE-----	454
FRL1	433	----LSQARKELETLRER-----	446
FRL2	427	----LMQRNKELDVVREI-----	440
FRL3	430	----LLQREKELESIKET-----	443
WHIF1	350	----PSPLVKAHKSVQAN-----	363
INF1		-----	
FHOD1	445	ENVAAAETEKQV---ALA-----QGRA-----	463
FHOD3	504	EQLAAEEHEKELRSRSVS-----RGRADLSLDLTSAPAACLAPLSH-----SPSSSDSQEAL	556
DELPH	449	YQLLTYE-EQELCQEKIACFLG-----YTAMTAEPEPELDLESEPTPEP-QPRSS-----LRASSMCRRSL	507
FMN1	422	SELEALKRKRMRHEKESL-----RAVFERSNSKPADGPSDS-----	456
FMN2	503	LERGVASDSGGGVSPALAAKASGAPAAADGFQNVFTGRTLLEKLFSSQENGPPEAEKFCSRIIAMGLLLPFSDCFREPC	582
DIA1	495	-----RHELVEMKKMESDFE	510
DIA2	523	-----HQETQAELOKKEA---	535
DIA3	511	-----RQEAQAELOKRDE---	523
DAAM1	459	-----HNELQQKLEKKERECD	474
DAAM2	455	-----HMELVSRLEKERECE	470
FRL1	447	-----FSESTAMGASRRPPEP	462
FRL2	441	-----YKDANTQVHTLRKMVK	456
FRL3	444	-----YENTSHQVHTLRRLIK	459
WHIF1	364	-----LDQSQRGSSPQNTTTP	379
INF1	1	-----MHVMN-----	5
FHOD1	464	-----ETLAGAMPNEAGG--	476
FHOD3	557	TVSASSPPTPH-----HPQASAGDPEPES---EAEPEAEAGAGQVADEAGQDI	601
DELPH	508	RSQGLEAGLSC-----GPSECPEMPLPLI---PGE-----RQAGDG-	540
FMN1	457	-----KSPDHSLTEQDDRTPGRLQAVWPPKTKDTEEKVGLKYTEAEYQAAILHLKREHKEEI	514
FMN2	583	NQNAQTNAASFQDQLYTAAVVSQPTHSLDYSEGQFPRRVPSMGPPSKPPDEEHR--LEDAETESQSAVSETPQKRSDAV	660
<b>FH1</b>			
DIA1	511	QKIQ-----DLQGEKDALHSEKQQLATEKQDLEAEVSQLTGEVAK-----LTKELE	556
DIA2	536	-KIN-----ELQAELOAFKSFQFAL-----	554
DIA3	524	-KIK-----ELEAEIQQLRTQAQVL-----	542
DAAM1	475	AKTQ-----EKEEMMQTLNKMKEKLEKETTEHK---QVKQQVAD-----LTAQL-	515
DAAM2	471	TKTL-----EKEEMMRTLNMKDKLARESQELR---QARGQVAE-----LVAQL-	511
FRL1	463	EKAPP-----AAPTRPSALELKVEELEEKGL-----IR	490
FRL2	457	EKE-----EAIQRQSTLEKKIHELEKQGT-----IK	482
FRL3	460	EKE-----EAFQRRCHLEPNVRGLE-----	479
WHIF1	380	KPSV-----EGQQPAAAAACEPVDHAQSESI-----LK	407
INF1	6	-----CV-----	7
FHOD1	477	-----HPDA---RQ-----	482
FHOD3	602	ASAH-----EGAETEVEQALEQEPEE---RASLSEKERQ-----NEGVNERDNCSASSV-----	647
DELPH	541	TSLP-----ETPNPKMMSAVYAELES---RLNSSFKGKM-----GTVSKSRASPPGP	584
FMN1	515	E NLQAQFELRAFHIRGEHAMITARLEETIENLKHELEHRWR-----GGCEERKDVCI-----	566
FMN2	661	QK-----EVVDMKSEGG-ATVIQQLEQTIEDLRKTKIAELERQYPALDTEVASGHQGLENGVTASGDVCLALRLEEKEVR	734
DIA1	557	-----DA-----	558
DIA2		-----	
DIA3		-----	
DAAM1		-----	
DAAM2		-----	
FRL1	491	-----IL-----	492
FRL2	483	-----IQ-----	484
FRL3		-----	
WHIF1	408	-----VS-----	409
INF1		-----	
FHOD1	483	-----LWD-----SPET	489
FHOD3	648	-----SSSSSTLEREEKEDKLSRDRRTTGLWPAGVQDAGVNGQ-----CGDIL--TNKRFMLDMLYAHN-----RKSPDD	709
DELPH	585	-----SPAVTTGPRTLSGVSWPSER---LLSPCYHPLCSGG---LASPS--SSESHPYASLDSSR-----APSPQP	643
FMN1		-----	
FMN2	735	HHRILEAKSIQTSPTTEGGVLTLPVPDGLPGRPPCPPGAESGPQTKFCSEISLIVSPRRISVQLDShQPTQSI SQPPPPP	814

## Chapter 2: Formin expression patterns

DIA1	559	-----KKEMASLSAAAITV-----	572
DIA2		-----	
DIA3		-----	
DAAM1		-----	
DAAM2		-----	
FRL1	493	-----R-GPGD--AVSIEI-----	503
FRL2	485	-----KKGDDG-----IAI-----	493
FRL3		-----	
WHIF1	410	-----Q-----	410
INF1	8	-----S-----	8
FHOD1	490	-----AP-AARTP----QSPAPCVLLRAQR-----	509
FHOD3	710	E-----EKGDGE-AGRTQ---QE-AEAVASLATRIS-----TLQANSQTQDESVRVDV-----GCLDNRGS	761
DELPH	644	-----GPGPICPDSP----PSPDPTRPPSRRKLF-----TFSHPVRSRDTD-RFLDV-----	685
FMN1	567	-----STDDDCPPKTFRNVQVQTDRETFLKPCESSESKT-----TRS	602
FMN2	815	SLLWSAGQGQPGSQPPHSISTEFQTSHEHSVSSAFKNSCNIPSPPL--PCTESSSSMPGLGMVPPPPPLPGMTVPTLP	892
DIA1	573	-----PPSVPS-----	578
DIA2		-----	
DIA3		-----	
DAAM1		-----	
DAAM2		-----	
FRL1	504	-----LPV-AV-----	508
FRL2	494	-----LPVVAS-----	499
FRL3		-----	
WHIF1		-----	
INF1	9	--LVSDKEN--	15
FHOD1	510	-----SLAP--EPKE-----PL--IPASPKAEP--IW-----ELPTRA--PR-LSIGDLDFSDL	549
FHOD3	762	VKAFAEKFNSGDLGRGSI SPDAEPND-----KVPETAPVQPKTESDYIW-----DQLMAN--PRELRIQDMDFTDL	825
DELPH	686	--LSEQ-----LGPRVTIVD-----DF--LTPENDYEEMSFHD-----DQGSFV--TNERSSASDCISSS	734
FMN1	603	NQLVPPKKNLIS--SLSQLSPNDHKDIHAALQPMEGMASNQKALPP	647
FMN2	893	STAIPQPPPLQ--GTEMLPPPPPLP-GAGIPPPPLPGAGILPLPPLPGAGIPPPPLPGAAI PPPPLPGAGIPLPPP	969
DIA1	579	-----RAPVPPAPPLPGD-----SGTIIPP-----	598
DIA2		-----	
DIA3		-----	
DAAM1		-----	
DAAM2		-----	
FRL1	509	-----ATPSGGDAPTPGV-----P-TGSPS-----	527
FRL2	500	-----GTLSMGSEVVAGN-----S-VG-----	515
FRL3	480	-----SVDSEALA-----R-VG-----	490
WHIF1		-----	
INF1		-----	
FHOD1	550	GEDEDQ-----	555
FHOD3	826	GEEDDI-----	831
DELPH	735	EEGSSL-----	740
FMN1		-----	
FMN2	970	LPGAGIPPPPLPGAGIPPPPLPGAGIPPPPLPGAGIPPPPLPGAGIPPPPLPGAGIPPPPLPGAGIPPPPLPG	1049
DIA1	599	-----PPAPGDSTTPPPPPPPPPPPPLPGVCISSPPSLPGGTAI	639
DIA2	555	-----PAD--CNIPL-----PPSKEGGTGH	572
DIA3	543	-----SSSSGIPGPPA-----APPLPG-VGP	562
DAAM1	516	-----HELSRRAVCA-----	525
DAAM2	512	-----SELSTGPV-----	519
FRL1	528	-----P---DLAPAAEPAPGAAPPPP-----PPLPG-----	550
FRL2	516	-----P---TMGAASS---GPLPPPP-----PPLPP-----	535
FRL3	491	-----P---AELS---EGMPPSD-----LDLLA---	507
WHIF1	411	-----PR---ALEQQASTPPPPPPP-----PLLPGSSAE	436
INF1	16	-----GN	17
FHOD1	556	-----DMLNVESVEAGKDIPA-----PS-----PPLPLLSGV	582
FHOD3	832	-----DVLVDVL--GHREAPG-----PPP-----PPPPTFLGL	857
DELPH	741	-----TYSSISDHIPPPPLSP-----PPP-----PPLPFHDA-	767
FMN1	648	-----PPASIPPP-----PPLPSGLGS	664
FMN2	1050	AGIPPPPLPGAGIPPPPLPGAGIPPPPLPGAGIPPPPLPGAGIPPPPLPGVGI PPP-----PPLPG--AG	1117

## Chapter 2: Formin expression patterns

DIA1	640	SPPPPLSGDATIPPPPLPEGV-----GIPSPSSLPGGTAIPPPPLPGSARIPP-PPP-LPGSA-GIPPPPPPLPGEA	711
DIA2	573	SAL-----PPPPPLPSGG-----GVPPPPP-----PPPPPLPG-MRM-P-FSGP-VP-----PPPLGFLGGQ	622
DIA3	563	PPP-----PPAPPLPGBA-----PL-----PPPPPLPGMMGI-P-PPP-PLL-F-GGPPPPPLGG--	611
DAAM1	526	-----SIPGGPS-----PGAPGGP--FPSS-VPSSL-LPPPPPPPLPGGM	561
DAAM2	520	-----SS-----PPPPGGPLTLSSS-MTND-LPPPPPLPFACC	552
FRL1	551	LPSP-----QEAPP-----SAPPQAPPLPGSPEPPP--APP-LPGDLPPPPPPPPPPGTD	598
FRL2	536	SSDT-----PETVQ-----NGPV-TPPMPPPPPPP-PPP-PP----PPPPPPPLPGPA	578
FRL3	508	PAPP-----PEEVL-----PLPPPPAPPL--PPP-PP----PLPDKCPP-----	539
WHIF1	437	PPP-----PPPPPLPSVGAKALPTAPPPPL-----PGLGAMAPPAPP-LPPP-LPGSCEFLPPPPPLPLGLG	498
INF1	18	IATAPGMIGQTTPPPAPP-----PPPPPPP-----SPPCSRSRECP-SSPP-PP-----PPPLPG--	68
FHOD1	583	PPPPP-----L-PPPPPIKGF-----PPPPPL-----PLAAP-LPHS-VPDS-----	617
FHOD3	858	PPPPPPPLDS-IPPPVPGNLL-----VPPPVF-----NAPQG-LGWSQVPRG-----	900
DELPH	768	-KPSRSSDGSRGPAQALAKPLTQLSHVPPPP-----PP-LPPP-VPCA-----PPMLSR--	816
FMN1	665	LSAPPMPVVSAGPPLPP-----PPPPPL-----PPSSAGPPPPP-PPP-LPN-----SPAPPNG--	717
FMN2	1118	IPPPPLPGAGIPPPPLPGAGI---PPPPPLPRVG-----	
DIA1	712	GMPPPPPLPGGPGIPPPPP-----FPGGGIP-----PPPPGMGMPPPP-----PFGFVPA-----	760
DIA2	623	NSPLP-----	628
DIA3	612	-VPPPPGI-----S-----	619
DAAM1	562	LPPPPPLPGGPPPPPGPP-----P-LGAIMP-----PP---GAPM-----GLA-----	597
DAAM2	553	PPPPPPPLPGGPPPTPGAP-----PCLGMGLP-----LP---QDPYPS-----S---DVP-----	592
FRL1	599	GPVPPP--PPPPPPPGGPP-----DALG-----RRD-----S-----ELGPG-----	629
FRL2	579	AETVPA--PPLAPPLPSAPP-----L--PGTS-----SPT-----V-----VFNSGLA-----	612
FRL3	540	-----APP-----L--PG-A-----APS-----V-----VLTVGLS-----	557
WHIF1	499	CPPPPPPPLPGMGWGP PPPP-----PPLLPTC-----SPPV--AGGMEE-----VIVAQVDHG-----	545
INF1	69	-EPIP--PPPPGL-PP-----	81
FHOD1		-----	
FHOD3		-----	
DELPH	817	-----GLG-----	819
FMN1	718	-GPPA--PPPPGLAPPPP-----	734
FMN2	1184	IPPPPP--LPVGI PPPPLPGAGIPPPPLPGMGI PPAPPLPPPGTGIPPPPLPVSGPPLPQVGSSTLPTPQVCG	1261
DIA1	761	---PVLPGFLT-----PKKLYKPEVQLRRPNWSKLVAE <sup>DL</sup> LSQ-DC-----FWTKVKEDRFEN-NELFAK-	814
DIA2	629	---ILPFLK-----PKKEFKPEISMRRLNWLKIRPHEMTE-NC-----FWIKVNEKYNEN-VDLLCK-	681
DIA3	620	---LNLPGYMK-----QKKMYKPEVSMKRINWSKIEPT <sup>EL</sup> SE-NC-----FWLRVKEDKFEN-PDLFAK-	673
DAAM1	598	-----LK-----KKSIPQPTNALKSFNWSKLPENKLE--GT-----VWTEIDDKVFK-ILDLED-	644
DAAM2	593	-----LR-----KKRVPQPSHPLKSFNWKLE <sup>ERV</sup> P--GT-----VWNEIDDMQVFR-ILDLED-	639
FRL1	630	-----VK-----AKKPIQTKFRMPLLNWV <sup>AL</sup> KPSQIT--GT-----VFTELNDEKVLQ-ELDMSD-	676
FRL2	613	-----AVK-----IKKPIKTKFRMPVFNWV <sup>AL</sup> KPNQIN--GT-----VFNEIDDERILE-DLNVE-	660
FRL3	558	-----AIR-----IKKPIKTKFRLPVFNWV <sup>AL</sup> KPNQIS--GT-----VFSELDDKILE-DLDDK-	605
WHIF1	546	---LGS <sup>AW</sup> VPS-----HRRVNPPTLRMKLNWQK <sup>LP</sup> SNVAREHNS-----MWASLSSPDAAEAVEPDFSS-	601
INF1	82	-----TTHMGYSHLGKKRMRSF <sup>FW</sup> KTIP--EEQVRGKTN-----IW <sup>TL</sup> AARQEHYQ-IDTKT-	133
FHOD1	618	-----S-ALPTKRKTVKLFW <sup>REL</sup> KL <sup>AG</sup> GHGVSASRFGPCAT-LWASLDVSV-----DTAR-	666
FHOD3	901	-----QPTFTKKKTIRLFWNEVRPFDWPC <sup>KNN</sup> RR--CREFLW <sup>SK</sup> LEPIK-----DTSR-	948
DELPH	820	-----HRRSETSHMS <sup>VK</sup> RLR <sup>WE</sup> QVENSEGT-----IW <sup>QL</sup> LGEDSDYDKLSDMVKY	864
FMN1	735	-----GLFFGLGSSSSQCPRKPAIEPSCP <sup>MK</sup> PLYWTRIQISDRSQ <sup>NAT</sup> PT-----LWDSLEEPDIRDP-SEFEY-	797
FMN2	1262	FLPPPLPSGLF-GLGMNQDKGSRKQPIEPC <sup>RM</sup> K <sup>PLY</sup> WTRIQ <sup>LH</sup> SKRDSSTSL-----IWEKIEEPI-DC-HEFEE-	1330
<b>FH2</b>			
DIA1	815	--LTLTFS <sup>AQ</sup> T <sup>TK</sup> S-----KAKKQEGEGEEKS-VQKKVKELKVLDSKTAQNLSIFLGSFRMPYQEIKNVILEVNEA	884
DIA2	682	--LENTFCCQ <sup>QK</sup> ER-----RE--EEDIEEKS--IKKKIKELKFLDSKIAQNLSIFLSSFRVPEEIRMMILEVDET	747
DIA3	674	--LALNFATQ <sup>IK</sup> VQ-----KN--AEALEEKTGPTKKVKELRILDPKTAQNLSIFLGSFRMPYEDIRNVILEVNEA	741
DAAM1	645	--LERTFSAYRQ <sup>QD</sup> FFVNSNSKQKEADAIDD <sup>TL</sup> S--SKLKV <sup>EL</sup> SVIDGRRQNCNILLSR <sup>LK</sup> LSNDEIKR <sup>ALL</sup> TM <sup>DE</sup> C	720
DAAM2	640	--FEKMF <sup>SAY</sup> QRHQ-----KELGSTEDIYL--ASR <sup>KV</sup> ELSVIDGRRQNCIILLSK <sup>LK</sup> LSNEIRQ <sup>AIL</sup> KM <sup>DE</sup> C	705
FRL1	677	--FEEQ <sup>FK</sup> TKSQGP-----SLDLSALKSKAA--QKAPKATLIEANRAKNLAITLRKGNLGAERICQAI <sup>EAY</sup> DLQ	742
FRL2	661	--FEEIF <sup>FK</sup> TKAQGP-----AIDLSSSKQ <sup>KI</sup> P--QKGSNKVTLLEANRAKNLAITLRKAGKTADEICKAIHVPDLK	726
FRL3	606	--FEEL <sup>FK</sup> TKAQGP-----ALDLIC <sup>SK</sup> NKTA--QKAASKVTLLEANRAKNLAITLRKAGRS <sup>AE</sup> EICRAIHTFDLQ	671
WHIF1	602	--IERLFS <sup>F</sup> PAAKP-----KEPTMVAPRAK <sup>EP</sup> KEITFLDAK <sup>SL</sup> NLNIFL <sup>KQ</sup> FKCSNEEVAAMIRAGDTT	665
INF1	134	--IEELFG <sup>Q</sup> EDTT-----KSSLPRGR <sup>T</sup> LNSS <sup>FE</sup> AREEITILDAKRSMNIGIFL <sup>KQ</sup> FKKSPRSIVEDIHQ <sup>GK</sup> SE	202
FHOD1	667	--LEHLFES <sup>R</sup> AKEV-----LPS-----KK-AGEG-RRTMTTVLDPKRSNAINIGL <sup>TTL</sup> -PPVHVIKAALLNFDEY	726
FHOD3	949	--LEHLFES <sup>K</sup> SKEL-----SVS-----KTAADG-KRQEIIVLDSKRSNAINIGL <sup>TVL</sup> -PPRTIKIAILNFDEY	1009
DELPH	865	LDLELHFG <sup>T</sup> QKPAK-----PVP-----GP-EPFR-KKEVVEILSHK <sup>KAY</sup> NTSILLAH <sup>LK</sup> LSPAELRQV <sup>LMS</sup> MEPR	927
FMN1	798	--LFSKDT <sup>T</sup> Q <sup>Q</sup> KKK-----PLS--ETYE <sup>K</sup> KNK--VKKIKLLDGKRSQ <sup>TV</sup> GILISSLH <sup>LE</sup> MKDIQ <sup>QAI</sup> FN <sup>V</sup> DDS	860
FMN2	1331	--LFSK <sup>T</sup> AVKERKK-----PIS--DTIS <sup>K</sup> TKA--KQVVKLLSNKRSQ <sup>AV</sup> GILMSSLH <sup>LD</sup> MKDIQ <sup>H</sup> AVVNL <sup>D</sup> NS	1392

## Chapter 2: Formin expression patterns

DIA1	885	V-LTESMIGNLIKQMPPEPEQLKMLSEL---KDE---YDDLAESEQFGVVMGTVPRLRPRLNAILFKLQFSEQVENIKPEI	957
DIA2	748	R-LAESMIGNLIKHLDPQEQNLNSLSQF---KSE---YSNLCEPEQFVVMVSNVKKRLRPRLSAILFKLQFEEQVNNIKPDI	820
DIA3	742	M-LSEALIGNLVKHLPEQKILNELAEL---KNE---YDDLCEPEQFVVMSSVKMLQPRSSILFKLTFEEHINNPKPSI	814
DAAM1	721	EDLFLKDMLEQLLKFVPEKSDIDLLEE---KHE---LDRMAKADRFLFEMSRINHYQRLQSLYFKKKFAERVAEVKPKV	794
DAAM2	706	EDLAKDMLEQLLKFVPEKSDIDLLEE---KHE---IERMARADRFLFEMSRIDHYQRLQALFFKKKQFQERLAEAKPKV	779
FRL1	743	A-LGLDFLELLMRFLPTEYERSLITRF---EREQRPMEELSEEDRFMLCFSRIPRLPERMTTLTFLGNFPDTAQLLMPQL	818
FRL2	727	T-LPVDVFECLMRFLPTENEVKVLRLY---ERERKPLENLSDEDRFMMQFSKIERLMQKMTIMAFIGNFAESIQLMTPQL	802
FRL3	672	T-LPVDVFECLMRFLPTEAEVKLLRQY---ERERQPLEELAAEDRFMLLFSKVERLTQRMAGMAFLGNFQDNLQMLTPQL	747
WHIF1	666	K-FDVEVLKQLKLLPEKHIEINLRAF---TEE---RAKLASADHFYLLLLAIPCYQLRIECLMLCEGAAAVLDMVRPKA	738
INF1	203	H-YGSETLREFLKFPESEEVKLLKAF-----SGDVSKLSLADSFLYGLIQVPNYSLRIEAMVLKKEFLPSCSSLYTDI	275
FHOD1	727	A-VSKDGEIKLLTMMPTEEERQKIEEA-----QLANPDIPLGPAENFLMTLASIGGLAARLQLWAFKLDYDSMEREIAEPL	801
FHOD3	1010	A-LNKEGIEKILTIPTDEEKQKIQEA-----QLANPEIPLGSAEQFLTLTSSISELSARLHLWAFKMDYETTEKEVAEPL	1084
DELPH	928	R-LEPAHLAQLLTFAPDADEEQRYQ-----AFREAPGRLSEPDQFVLQMLSVPEYKTRLRSLHFAQATLQEKTEEIRGSL	1000
FMN1	861	V-VDLETLAALYENRAQDEDELVKIRKYETSK--EELKLLDKPEQFLHELAQIPNFAERAQCIIFRSVFSSEGITSLHRKV	938
FMN2	1393	V-VDLETQALYENRAQSDLEKIEKHGRSSKDKENAKSLDKPEQFLYELSLIPNFSERVFICILFQSTFSESICSIIRKRL	1471
DIA1	958	VSVTAACEELRKSSEFSNLEITLLVGNMAGSRN-AGAFGFNISFLCKLRDTKST-DQKMTLLHFLAELCEN-----D	1030
DIA2	821	MAVSTACEEIKKSKSFSKLELVLMLGNMAGSRN-AQTFGFNLSSLCKLKDTKSA-DQKTTLLHFVLEICEE-----K	893
DIA3	815	IAVSTLACEELKKSSEFNRLLELVLVGNMAGSRN-AQSLGPKINFLCKIRDTKSA-DQKTTLLHFVLEICEE-----K	887
DAAM1	795	EAIRSGSEEVFRSGALKQLLEVVLAFGNMNGKQR--GNAYGFKISSLNKIADTKSSIDKNIITLLHYLITIVEN-----K	867
DAAM2	780	EAILLASRELVRSKRLRQMLEVILAIGNFMNGKQR--GGAYGFRVASLNKIADTKSSIDRNIISLLHYLLMILEK-----H	852
FRL1	819	NAIIAASMSIKSSDKLRQILEIVLAFGNMNSKR--GAAYGFRQLQSLDALLEMKST-DRKQTTLLHYLVKVAIE-----K	890
FRL2	803	HAIIAASVSIKSSQKLLKILEIILALGNMNSKR--GAVYGFKLQSLDLDLDTKST-DRKQTTLLHYISNVVKE-----K	874
FRL3	748	NAIIAASASVKSSQKLLKQMLEIILALGNMNSKR--GAVYGFKLQSLDLDLDTKST-DRKMTLLHFIALTVKE-----K	819
WHIF1	739	QLVLAACESLLTSRQLPFCQLILRIGNFLNYGSH--GDADGFKISTLLKLETQKSK-QNRVTLHHVLEEEAEK-----S	811
INF1	276	TVLRTAIKELMSCEELHSILHLVLQAGNIMNAGGYA-GNAVGFKLSSLLKLADTKAN-KPGMNLHFVAQEAQK-----K	348
FHOD1	802	FDLKVGMEQLVQNFATFRICILATLLAVGNFLNGSQ-----SSGFELSYLEKVSVEKDT-VRRQSLHHLLCSLVLQ-----T	870
FHOD3	1085	LDLKEGIDQLENNTLGFILSTLLAIGNFLNGTN-----AKAFELSYLEKVSVEKDT-VHKQSLHHVCTMVE-----N	1153
DELPH	1001	ECLRQASLELKNRKLAKILEFVLAMGNVLDGQPKTKTTGFKINFLTTELNSTKTV-DGKSTFLHILAKLSLQ-----H	1074
FMN1	939	EIIITRASKDLLHVKSVDILALILAFGNMNGNRTRGQADGYSLEILPKLKDVKSR-DNGINLVVYVVKYLYRYDQEA	1017
FMN2	1472	ELLQKLCETLKNGGVGMQVLGLVLAFGNVMNGNKTGQADGFLDILPKLKDVKSS-DNSRSLLSYIVSYLRFNDFEDA	1550
DIA1	1031	YPDVLKFP-DELAHVEKASRVSAENLQKNLDQMKQIISDVERDVQNFPA--ATDEKDKFVEKMTSFVKDAQEQYNKLRMM	1107
DIA2	894	YPDILNFV-DDLEPLDKASKVSVETLEKNLRQMGRLQOLEKELETFFP--PEDLHDKFVTKMSRFVISAQEQYETLSKL	970
DIA3	888	YDILKFP-EELHVESASKVSAQILKSNLASEQQIVHLERDIKKFPQ--AENQHKFVEKMTSFTKTAREYQEKLSM	964
DAAM1	868	YPSVLNLN-EELRDIQAAKVNMTELDKEISTLRSGLKAVETELEYQKSQ-PPQPGDKFVSVVSQFITVASFSFSDVEDL	945
DAAM2	853	FDPDILNMP-SELQHLPEAAKVNLALEKEVEGNLRRGLRAVEVELEYQRRQ-VREPSDKFVPMVSDFITVSSFSFSELEDQ	930
FRL1	891	YQPLTGFH-SDLHFLDKAGSVSLDSVLADVRSLQRGELTQREFVRQD-----CMVLKEFLRANSPMDKLLAD	959
FRL2	875	YHQVSLFY-NELHYVEKAAAVSLENVLLDVKELQRGMDLTKRYETMHDH-----NTLLKEFILNNEGKLLKQLQD	943
FRL3	820	YPDLANFW-HELHFVEKAAAVSLENVLLDVKELGRGMELIRRECSIHD-----NSVLRNFLTSTNEGKLDKLRD	887
WHIF1	812	HPDLLQLP-RDLEQPSQAAGINLEIRSEASSNLKLLLETERKVSASVA---EVQEQYTERLQASISA---FRALDEL	882
INF1	349	DTILLNFS-EKLHHVQKTARLSLENTEAELHLLFVRTKSLKENIQRDGE-----LCQQMEDFLQFAIEKLRLELCW	418
FHOD1	871	PRESSDLY-SEIPALTRCAKVDQFQLENTENLQLENSRAEESLRSRAK---HELAPALRARLTHFLDQCARRVAMLRIV	946
FHOD3	1154	FDPSSDLY-SEIGAITRSKAVDFDQLQDNLQCMERRCKASWDHLKAIK---HEMKPVLKQRMSEFLDKCAERIIILKIV	1229
DELPH	1075	FPELLGFA-QDLPVPLAAKVNQRALTSDLADLHGTISEIQDACQSISSP---SSEDKFAMVMSFLETAQPALRALDGL	1149
FMN1	1018	GTEKSVFPLPEPQDFFLASQVKFEDLIKDLRKLKRQLEASEKQMVVVCESPKYEQPFKDKLEEFFQKAKKEHKMEESH	1097
FMN2	1551	GKEQCLFPLPEPQDLFQASQMKFEDFQKDLRKLKDKLACEVEAGKVYQVSSKEHMQPFKFNMEQFI IQAKIDQEAEEENS	1630
DIA1	1108	HSNMETLYKELGEYFLDFPKK---LSVEEFFMDLHNFNMFLQAVKEN-QKRRETEEKMRRAKLAKEA-----	1172
DIA2	971	HENMEKLYQSIIGYYAIDVKK---VSVEDFLTDLNNFRITTFMQAIKEN- IKKREAEKEKRVRIAKELA-----	1035
DIA3	965	HNNMMKLYENLGEYFIDFSKT---VSEIEFFGLDNNFRITFLAVREN-NKRREMEKTRRAKLAKEA-----	1029
DAAM1	946	LAEAKDLFTKAVKHFGEEAGK---IQPDEFFGIFDQFLQAVSEAKQENENMRKKKEEERRARMEAQLK-----	1011
DAAM2	931	LNEARDKFAKALMHFGEDSK---MQPDEFFGIFDQFLQAFSEARQDLEAMRRRKEEERRARMEAMLK-----	996
FRL1	960	SKTAQEAFAFESVVEYFGENPKT---TSPGLFFSLFSRFIKAYKAEQEV-EQWKK-EAAAQEAQADTPGKGEPPAPKSP	1033
FRL2	944	AKTAAQADFDVVKYFGENPKT---TPPSVFFVVFVFRVRSYKAEQEEEN-ELRKKQEALMEKLLQEALMEQDQPKSP	1018
FRL3	888	AKTAAEYNAVVRVYFGENPKT---TPPSVFFVVFVFRVRSYKAEQEEEN-EARKKQEVMEKQALQEA--KKLDAKTPS	960
WHIF1	883	FEAIEQKQRELADYLCEAQQ---LSLEDFTSTMKAFRDLFLRALKEN---KDRKEQAAKAERRKQQLA-----	945
INF1	419	KQELQDEAYTLIDFFCEDKKT---MKLDECQIFRDFCTKFNKAVKDN--HDREAQELRQLRQLKEQEQ-KQRSWATGE	491
FHOD1	947	HRVRCNRFHAFLLYLGYPQAA--REVRIMQFCHTLREFALEYRTCRERV--LQQQKQATYRERNKTRGR-MITE--TEK	1020
FHOD3	1230	HRRIINRFHSFLFMGHPPYAI--REVINNKFCRIISEFALEYRTTRERV--LQQQKQKRNHRERNKTRGR-MITD--SGK	1303
DELPH	1150	QREAMEELGKALAFFGEDSKA---TTSEAFFGIFAEFMSKF---ERA--LSDLQA-----GE-GLRS--SGM	1205
FMN1	1098	LENAQKSFETTVRYFGMKPKSGEKIEITPSYVFMVWYFPCSDFK-----	1140
FMN2	1631	LTETHKCFLETTAYFFMKPKLGEKEVSPNAFFSIIWHEFSDFK-----	1673

## Chapter 2: Formin expression patterns

DIA1	1173	-----EKERLEKQKREQLIDMNAEGDETVGMDLLEALQSGAAF-----R--RKRGRPQA-----	1221
DIA2	1036	-----ERERLERQKKKRLLEMKTEGDETVGMDNLLLEALQSGAAF-----RDRRKRTMPKDVRQSLSPMSQRPV	1100
DIA3	1030	-----EQEKLERQKKKQLIDINKEGDETVGMDNLLLEALQSGAAF-----RDRRKRI PR-----	1078
DAAM1	1012	-----EQRERERKMRKAK-----ENSEESGEFDDLVSALRSGEVFDKDLCKL--KRNKRITNQM----TDSRRERPI	1073
DAAM2	997	-----EQRERERWQRQRKVLAAAGSSLEEGGEFDDLVSALRSGEVFDKDLCKL--KRSRKRSGSQA----LEVTRERAI	1063
FRL1	1034	-KARRPQMDLISELKRRQKKEPLIYESDRDGAIEDIITVIKTVPFT-----A--RTGKRTS--RLLCEASL----GHEM	1098
FRL2	1019	HKSKRQQQELIAELRRRQVKDNHRHVEGDKGAIEDIIITDLRNQPYR-----R--ADAVRRSVRRRFDQNLRSVNGAEI	1090
FRL3	961	QRNKWQQQELIAELRRRQAKEHRPVYEGKDGTIEDIITVLKSVPT-----A--RTAKRGS--RFFCD----AAHDES	1026
WHIF1	946	-----EEEARRPRGEDGKPVKGPQKQEEVVCVIDALLADIRKGFQLRRTA-----RGRGDTGGSKAASMDPPRATFP	1013
INF1	492	LGAFGRSSSENDVELLTKKAEG-----LLPFLHPRPISPSSPSYRPPNTRRSRLSLGPSADRELLTFLEST	559
FHOD1	1021	FSGVAGEAPSNPSPVAVSSGPRGDADSHASKSLL--TSRP--EDTT-----HNRRSRGMVQSSSP--IMPTVGPST	1088
FHOD3	1304	FSG--SSPAPPSQPGLSYAE---DAAEHENMKAVLKTSSPSVEDATPALGVTRRSRASRGSTSSW-----T	1365
DELPH	1206	VSPLAW-----	1211
FMN1		-----	
FMN2		-----	
DIA1	1222	-----NRKAGCAVTSLLASELTKDDAMAAPAKVSKNSETFPTI-----LEEAKELVGRAS-----	1272
DIA2	1101	LKVCNHNQKVLTEGSRSHYNINCNSTRTPVAKELNYNLDTHSTGRIKAAEKKEACNVESNRKKETELLSFSKNEVS	1180
DIA3	1079	---NPDNRRVPL-ERSRSRHN-----GAISSK---	1101
DAAM1	1074	TKL-NF-----	1078
DAAM2	1064	NRL-NY-----	1068
FRL1	1099	PL-----	1100
FRL2	1091	TM-----	1092
FRL3	1027	NC-----	1028
WHIF1	1014	VATSNPAGDPVVGSTRCPASEPGLDATTASESRGWDLVDAVTPGPPQ--TLEQLEEGGPRPLERSSWYVDASDLTTEDPQ	1092
INF1	560	GSPEEPNK-----FHSLPRSSPRQARPTIA--CLEPAEVRHQDSSFAHK---PQASGGQEEAPNPPSAQAHLA	623
FHOD1	1089	ASPEEPPGSSLPDTSDEIMDLLVQSVTKSSPRALA--ARERKRSRGNRKSRLRT--LKSGLGDDLQALGLSKGPGLE	1163
FHOD3	1366	MGTDDSP--NVTDDAADEIMDRIVKSATQVPSQRVV--PRERKRSRANRKSRLRT--LKSGLTPEEARALGLVGTSELQ	1438
DELPH		-----	
FMN1		-----	
FMN2		-----	
DIA1		-----	
DIA2	1181	PEVEALLARLRAL-----	1193
DIA3		-----	
DAAM1		-----	
DAAM2		-----	
FRL1		-----	
FRL2		-----	
FRL3		-----	
WHIF1	1093	CPQPLEGAWPVTLGDAQALKPLKFSNQPPAAGSSRQDAKDPSTSLGLVQAEADSTSEGLEDAVHSRGARPPAAGPGGDE	1172
INF1	624	AAQPENHASAFPRARRQGVSVLRKRYSEPVSLGSAQSPPLSPLAL-GIKEHEL-VTGLAQFNLQGSQGMETSQTLTSD	701
FHOD1	1164	V-----	1164
FHOD3	1439	L-----	1439
DELPH		-----	
FMN1		-----	
FMN2	1674	-----DF	1675
DIA1		-----	
DIA2		-----	
DIA3		-----	
DAAM1		-----	
DAAM2		-----	
FRL1		-----	
FRL2		-----	
FRL3		-----	
WHIF1	1173	DEDEEDTAPESALDTSLDKSFSEDAVTDSSSGTLPRARGRASKGTGKRKRKPSRSQEEVPPDSDDNKTKKLCVIQ---	1249
INF1	702	SPMELESVGHGRG-PQSLASASSSLTPMGRDALGSLSPALEDGKAAPDEPGSAALGSGVSSDPENKDPRLFCISDTTDCS	780
FHOD1		-----	
FHOD3		-----	
DELPH		-----	
FMN1		-----	
FMN2		-----	

## Chapter 2: Formin expression patterns

```

DIA1 -----
DIA2 -----
DIA3 -----
DAAM1 -----
DAAM2 -----
FRL1 -----
FRL2 -----
FRL3 -----
WHIF1 -----
INF1 781  LTLDCSEGTDSRPRGGDPEEGEGDGSMSGSGVEMGDSQVSSNPTSSPPGEAPAPVSDSEPSCKGGLPRDKPTKRKDVV 860
FHOD1 -----
FHOD3 -----
DELPH -----
FMN1 -----
FMN2 -----

DIA1 -----
DIA2 -----
DIA3 -----
DAAM1 -----
DAAM2 -----
FRL1 -----
FRL2 -----
FRL3 -----
WHIF1 -----
INF1 861  APKRGSLKEASPGASKPGSARRSQGAVAKSVRTLTAENESMRKVMPITKSSRGAGWRRPELSSRGPSQNPPSSTDTVWS 940
FHOD1 -----
FHOD3 -----
DELPH -----
FMN1 1141 -----TIWK 1144
FMN2 1676 -----WK 1677

DIA1 -----
DIA2 -----
DIA3 -----
DAAM1 -----
DAAM2 -----
FRL1 -----
FRL2 -----
FRL3 -----
WHIF1 -----
INF1 941  RQNSVRRASTGAEEQRLPRGSSGSSSTRPGRDVPLQPRGSFKKPSAKPLRNLPRQKPEENKTCRAHSEGPESPKKEEPKTP 1020
FHOD1 -----
FHOD3 -----
DELPH -----
FMN1 1145  RE-----SKNISKERL-----KMAQESVSKLTSEKKVETK----- 1174
FMN2 1678  KENKL-----LLQERV-----KEAEVCRQKKGKSLY----- 1704

DIA1 -----
DIA2 -----
DIA3 -----
DAAM1 -----
DAAM2 -----
FRL1 -----
FRL2 -----
FRL3 -----
WHIF1 -----
INF1 1021  SVPSVPHELPRVPSFARNTVASSRSRMTDLPVAKAPGITRTRVTSRQLRVKGDPEDAAPKDSSTLRRASSARAPKKRPE 1100
FHOD1 -----
FHOD3 -----
DELPH -----
FMN1 -----
FMN2 -----

```

```

DIA1      -----
DIA2      -----
DIA3      -----
DAAM1     -----
DAAM2     -----
FRL1      -----
FRL2      -----
FRL3      -----
WHIF1     -----
INF1      1101  SAEGPSANTEAPLKARGAGERASLRKDSRRTLGRILNPLRK  1143
FHOD1     -----
FHOD3     -----
DELPH     -----
FMN1      1175  -----KINPTASLKER-----LRQKEASVTN-----  1196
FMN2      1705  -----KIKPR---HDSGIKAKISMKT-----  1722

```

**Figure 1S – Human formin amino acid alignment.**

Formin alignment was performed using COBALT on 3/30/2012 with the accession numbers listed in Methods. Amino acids highlighted in yellow are translations of forward primers and amino acids highlighted in green are translations of reverse primers used for PCR and qPCR as described in Methods. Two additional sets of primers were made against delphilin, with the amino acids encoded by the forward primers highlighted in pink and those encoded by the reverse primers highlighted in blue.

**Figure 2S –Quality Control and Quantification of RNA**

Figure 2SA-V2: RNA was obtained as described in Methods. The “Electropherogram Summary” visualizes the analysis of total RNA, where peaks between and underneath the 18S and 28S ribosomal subunits indicate degraded RNA, and higher peaks correspond to a higher concentration of RNA. The rectangular box to the right of the “Electropherogram Summary” is a visual representation of RNA degradation. The RNA Integrity Number (RIN) is calculated using an algorithm based on a Bayesian analysis of nine distinct features of the electropherogram of 1208 samples of RNA of varying degrees of degradation using the Agilent 2100 bioanalyzer system (Agilent Technologies, Santa Clara, CA) (Schroeder et. al., 2006).

Figure 2SW: Statistical analysis of RIN from 2SA – 2V2

Set 1 including all RINs shows the average and standard deviation off all cell types.

Set 2 excludes RINs of monocytic cells.

Set 3 excludes RINs of monocytic cells and platelets.

2SA	HeLa
2SB	Macrophage
2SC	Cerebellum
2SD	U2OS
2SE	HCN
2SF	Skeletal muscle
2SG	THP
2SH	differentiated THP
2SI	U937
2SJ	K562
2SK	Cardiac muscle
2SL	HaCaT
2SM	MDA
2SN	HK-2
2SO	HUVEC
2SP	HEK
2SQ	Meg-01
2SR1	Neutrophil
2SR2	Neutrophil
2SR3	Neutrophil
2SS	Platelet
2ST	Monocyte
2SU	HT1080
2SV1	Jurkat
2SV2	Jurkat
2SW	RNA Integrity Number Analysis

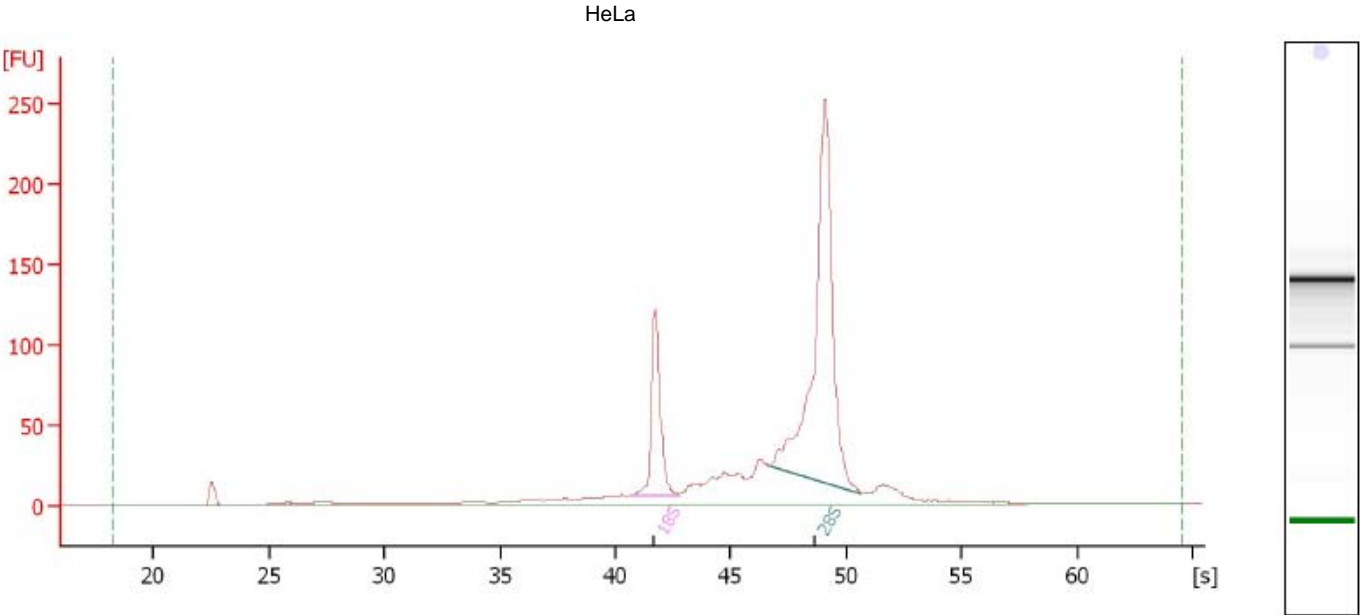
Figure 2SA

Blystone\_2011-03-01\_001.xad

Assay Class: EukaryoteTotal RNA Nano  
Data Path: C:\...00 bioanalyzer\2100 expert\data\Blystone\_2011-03-01\_001.xad

Created: 3/1/2011 3:28:50 PM  
Modified: 3/1/2011 4:11:35 PM

Electropherogram Summary Continued ...



Overall Results for sample 2 : 2

RNA Area:	1,019.5	RNA Integrity Number (RIN):	9.4 (B.02.05)
RNA Concentration:	480 ng/ $\mu$ l	Result Flagging Color:	<span style="background-color: #ccccff; border: 1px solid black; display: inline-block; width: 20px; height: 10px;"></span>
rRNA Ratio [28s / 18s]:	3.5	Result Flagging Label:	RIN: 9.40

Fragment table for sample 2 : 2

Name	Start Time [s]	End Time [s]	Area	% of total Area
18S	40.60	42.75	123.0	12.1
28S	46.64	50.66	429.7	42.1

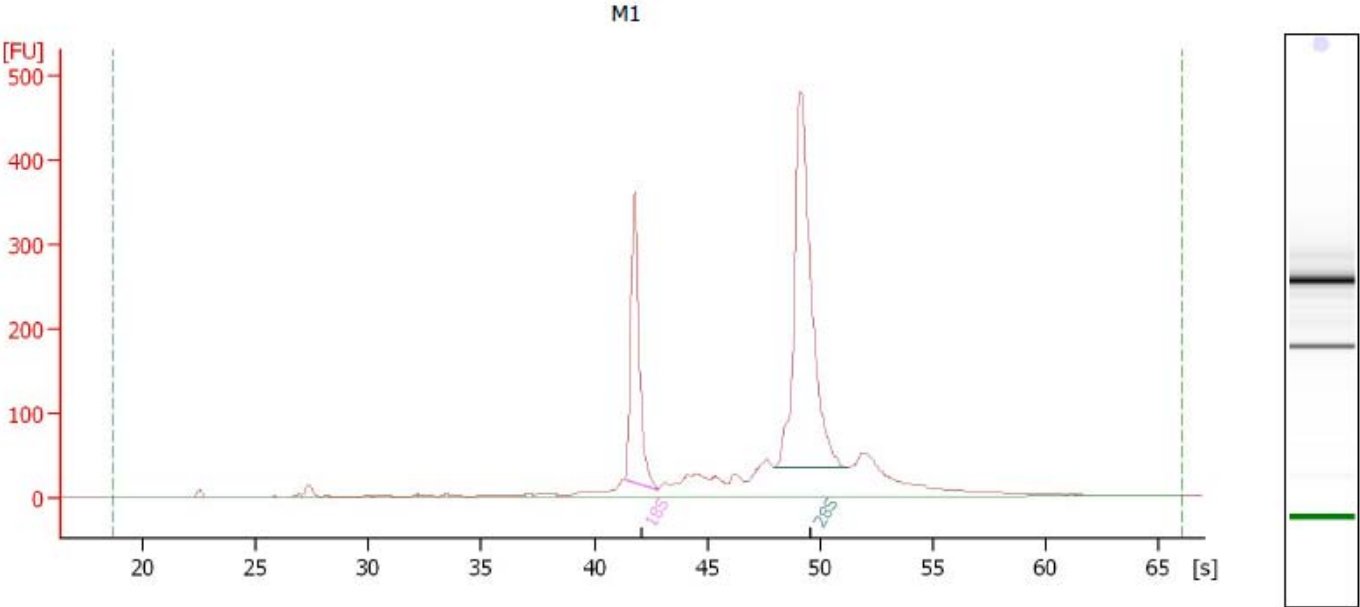
Figure 2SB

Blystone\_M1\_M2\_2011-03-30\_001.xad

Assay Class: EukaryoteTotal RNA Nano  
Data Path: C:\...analyzer\2100 expert\Data\Blystone\_M1\_M2\_2011-03-30\_001.xad

Created: 3/30/2011 12:48:59 PM  
Modified: 3/30/2011 1:59:13 PM

Electropherogram Summary



Overall Results for sample 1 : M1

RNA Area:	2,052.2	RNA Integrity Number (RIN):	9.9 (B.02.05)
RNA Concentration:	1,627 ng/ $\mu$ l	Result Flagging Color:	<span style="background-color: #ccccff; border: 1px solid black; display: inline-block; width: 20px; height: 10px;"></span>
rRNA Ratio [28s / 18s]:	2.2	Result Flagging Label:	RIN: 9.90

Fragment table for sample 1 : M1

Name	Start Time [s]	End Time [s]	Area	% of total Area
18S	41.36	42.85	349.1	17.0
28S	47.97	51.27	784.6	38.2

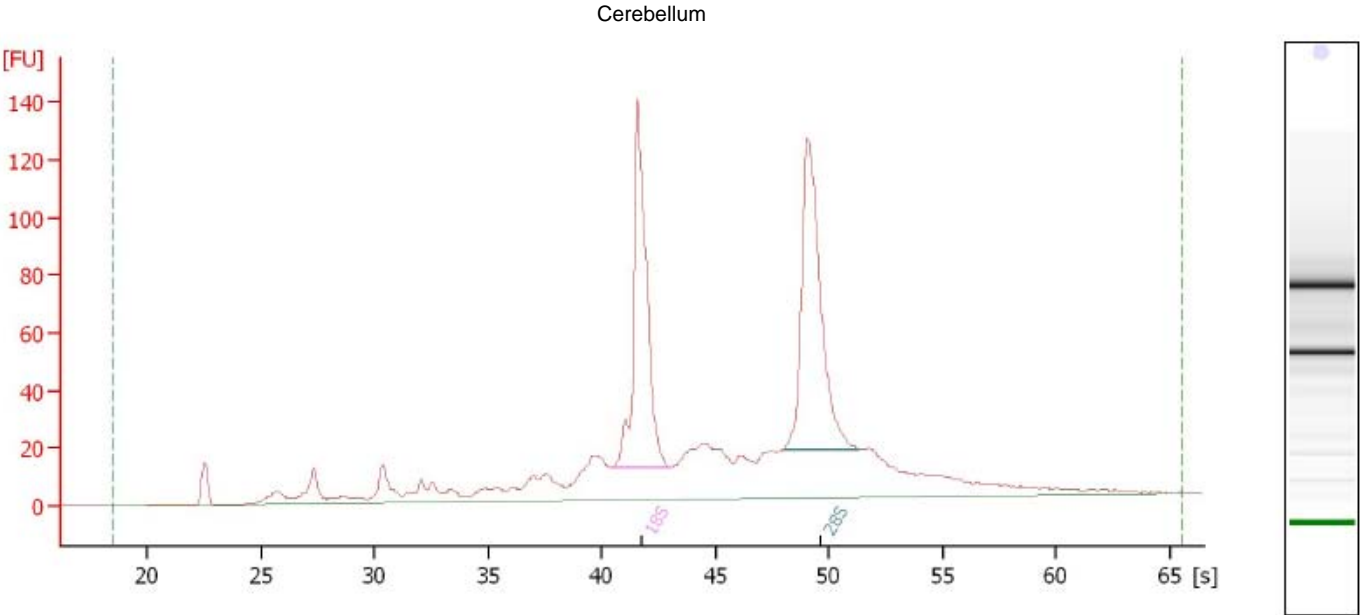
Figure 2SC

Blystone\_2011-03-01\_001.xad

Assay Class: EukaryoteTotal RNA Nano  
Data Path: C:\...00 bioanalyzer\2100 expert\data\Blystone\_2011-03-01\_001.xad

Created: 3/1/2011 3:28:50 PM  
Modified: 3/1/2011 4:11:35 PM

Electropherogram Summary Continued ...



Overall Results for sample 6 : 6

RNA Area:	1,103.7	RNA Integrity Number (RIN):	8.3 (B.02.05)
RNA Concentration:	520 ng/ $\mu$ l	Result Flagging Color:	<span style="border: 1px solid black; background-color: #ccccff; display: inline-block; width: 20px; height: 10px;"></span>
rRNA Ratio [28s / 18s]:	1.0	Result Flagging Label:	RIN: 8.30

Fragment table for sample 6 : 6

Name	Start Time [s]	End Time [s]	Area	% of total Area
18S	40.44	43.05	202.5	18.3
28S	47.99	51.31	210.0	19.0

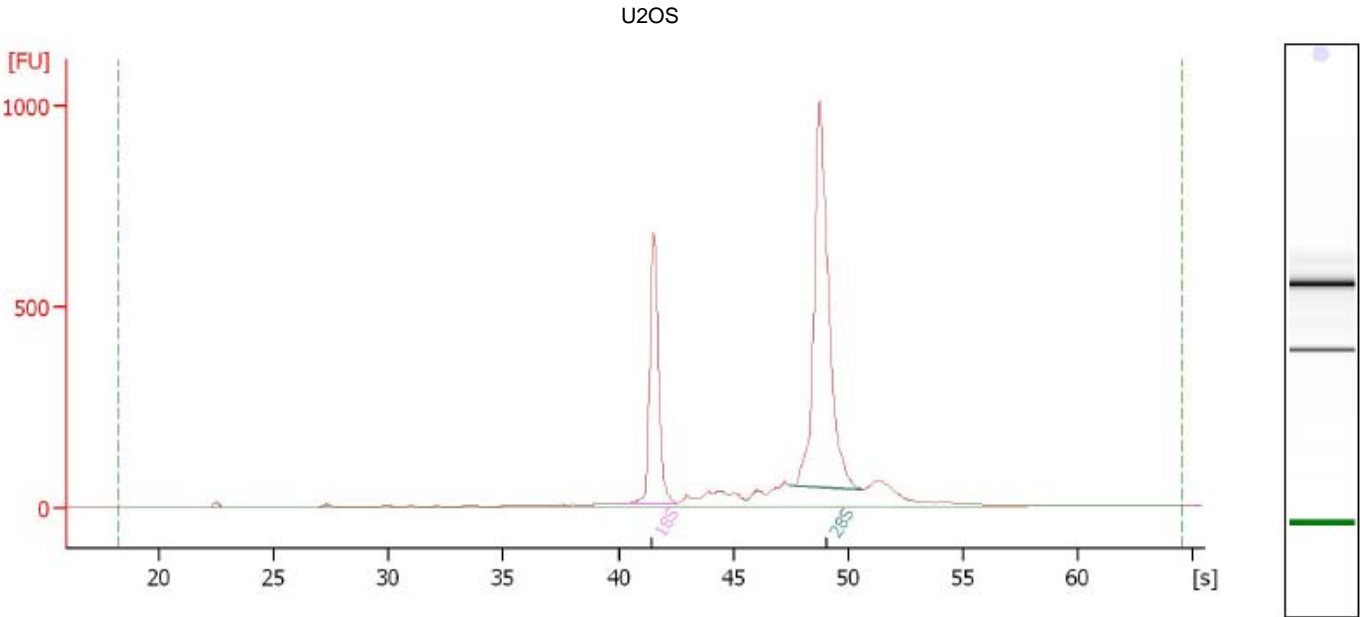
Figure 2SD

Blystone\_2011-03-01\_001.xad

Assay Class: EukaryoteTotal RNA Nano  
Data Path: C:\...00 bioanalyzer\2100 expert\data\Blystone\_2011-03-01\_001.xad

Created: 3/1/2011 3:28:50 PM  
Modified: 3/1/2011 4:11:35 PM

Electropherogram Summary Continued ...



Overall Results for sample 4 : 4

RNA Area:	3,186.6	RNA Integrity Number (RIN):	10.0 (B.02.05)
RNA Concentration:	1,500 ng/ $\mu$ l	Result Flagging Color:	<span style="background-color: #ccccff; border: 1px solid black; display: inline-block; width: 20px; height: 10px;"></span>
rRNA Ratio [28s / 18s]:	2.1	Result Flagging Label:	RIN:10

Fragment table for sample 4 : 4

Name	Start Time [s]	End Time [s]	Area	% of total Area
18S	40.37	42.61	699.5	21.9
28S	47.53	50.61	1,455.8	45.7

Figure 2SE

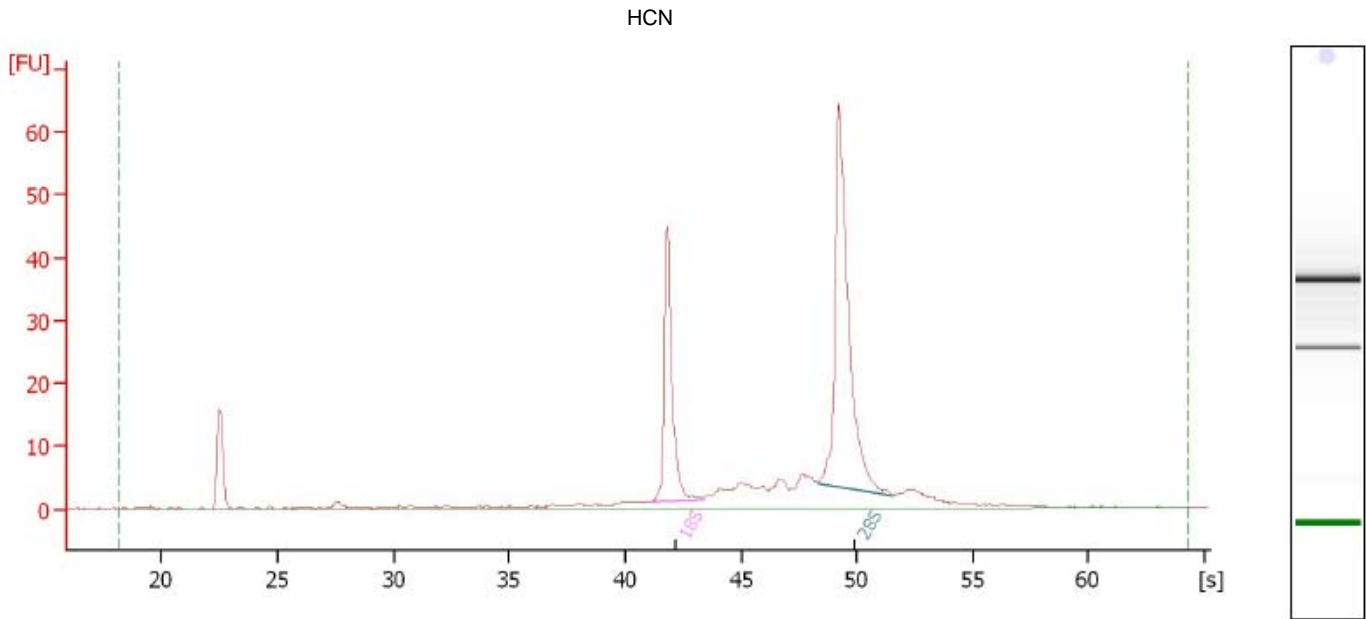
Blystone\_2011-03-01\_001.xad

Page 5 of 9

Assay Class: EukaryoteTotal RNA Nano  
 Data Path: C:\...00 bioanalyzer\2100 expert\data\Blystone\_2011-03-01\_001.xad

Created: 3/1/2011 3:28:50 PM  
 Modified: 3/1/2011 4:11:35 PM

Electropherogram Summary Continued ...



Overall Results for sample 3 : 3

RNA Area:	220.9	RNA Integrity Number (RIN):	9.9 (B.02.05)
RNA Concentration:	104 ng/μl	Result Flagging Color:	<span style="background-color: #ccccff; border: 1px solid black; display: inline-block; width: 20px; height: 10px;"></span>
rRNA Ratio [28s / 18s]:	2.0	Result Flagging Label:	RIN: 9.90

Fragment table for sample 3 : 3

Name	Start Time [s]	End Time [s]	Area	% of total Area
18S	41.04	43.37	40.1	18.2
28S	48.31	51.52	82.2	37.2

Figure 2SF

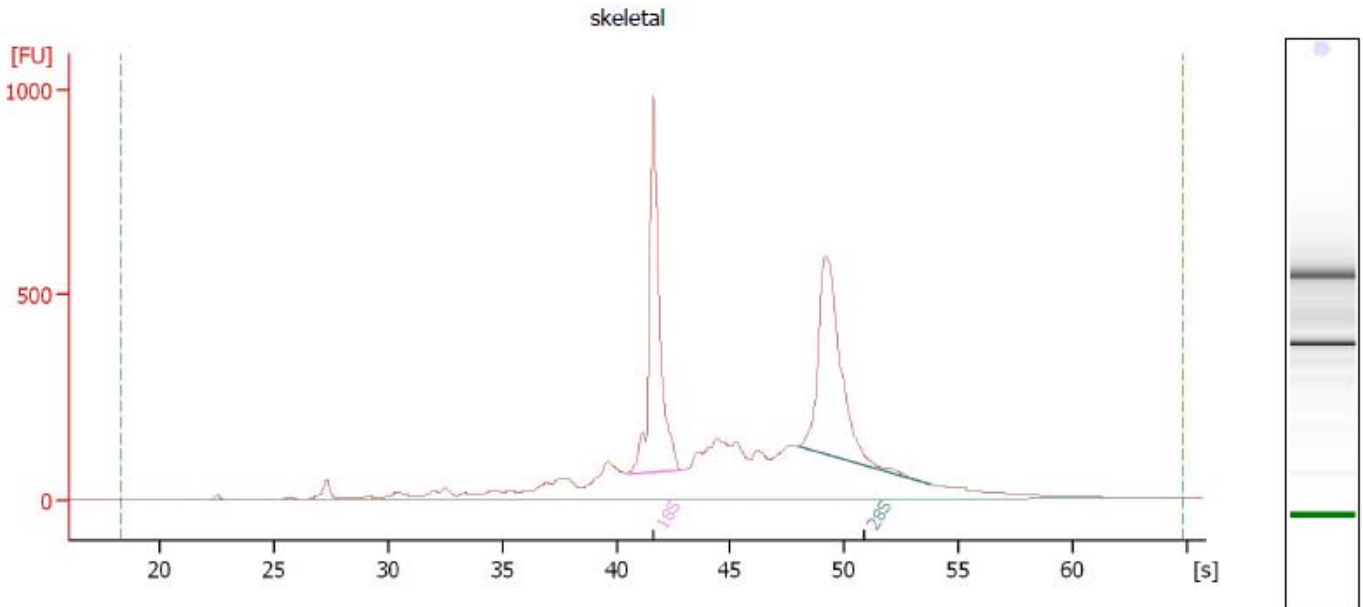
Blystone\_2011-03-15\_001.xad

Page 4 of 5

Assay Class: EukaryoteTotal RNA Nano  
 Data Path: C:\...00 bioanalyzer\2100 expert\Data\Blystone\_2011-03-15\_001.xad

Created: 3/15/2011 4:05:09 PM  
 Modified: 3/15/2011 5:14:30 PM

**Electropherogram Summary Continued ...**



**Overall Results for sample 2 : skeletal**

RNA Area:	6,046.2	RNA Integrity Number (RIN):	8.3 (B.02.05)
RNA Concentration:	4,668 ng/µl	Result Flagging Color:	<span style="background-color: #ccccff; border: 1px solid black; display: inline-block; width: 20px; height: 10px;"></span>
rRNA Ratio [28s / 18s]:	1.0	Result Flagging Label:	RIN: 8.30

**Fragment table for sample 2 : skeletal**

Name	Start Time [s]	End Time [s]	Area	% of total Area
18S	40.49	42.89	1,099.6	18.2
28S	47.96	53.78	1,126.2	18.6

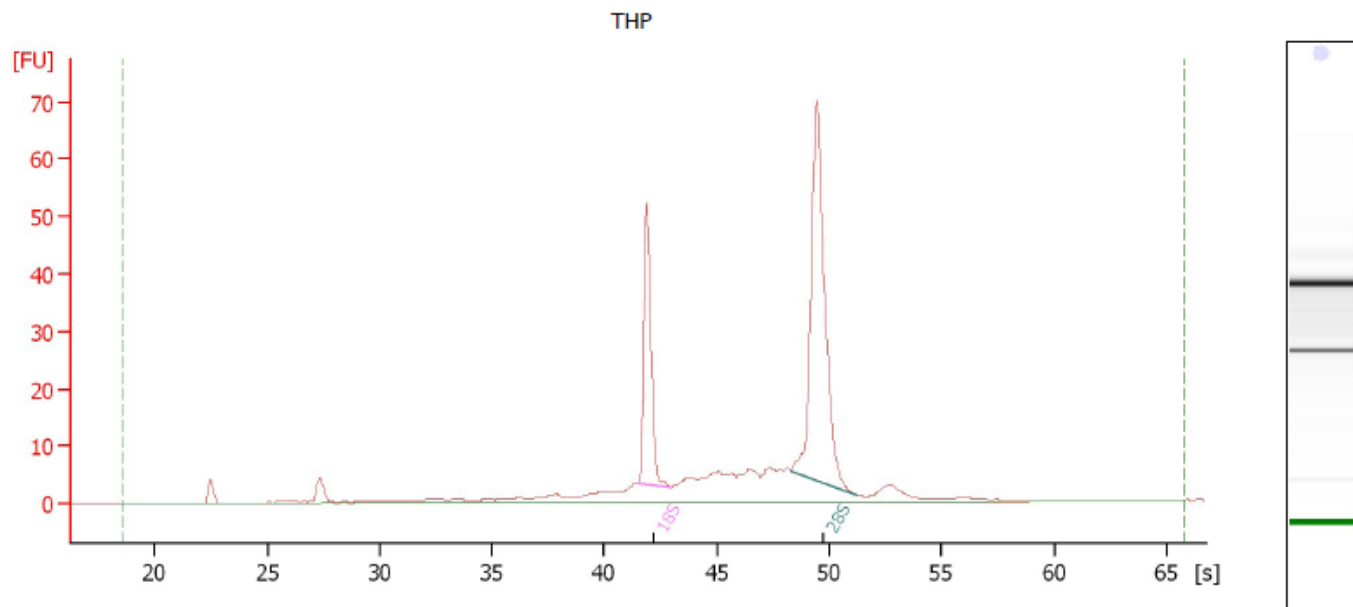
Mooney9\_Blystone\_2011-03-24\_001.xad

Page 7 of 9

Assay Class: EukaryoteTotal RNA Nano  
 Data Path: C:\...alyzer\2100 expert\Data\Mooney9\_Blystone\_2011-03-24\_001.xad

Created: 3/24/2011 5:04:59 PM  
 Modified: 3/24/2011 5:22:06 PM

**Electropherogram Summary Continued ...**



**Overall Results for sample 5 : THP**

RNA Area:	266.9	RNA Integrity Number (RIN):	9.3 (B.02.05)
RNA Concentration:	314 ng/μl	Result Flagging Color:	<span style="background-color: #ccccff; border: 1px solid black; display: inline-block; width: 20px; height: 10px;"></span>
rRNA Ratio [28s / 18s]:	2.2	Result Flagging Label:	RIN: 9.30

**Fragment table for sample 5 : THP**

Name	Start Time [s]	End Time [s]	Area	% of total Area
18S	41.47	42.95	42.0	15.7
28S	48.29	51.24	94.5	35.4

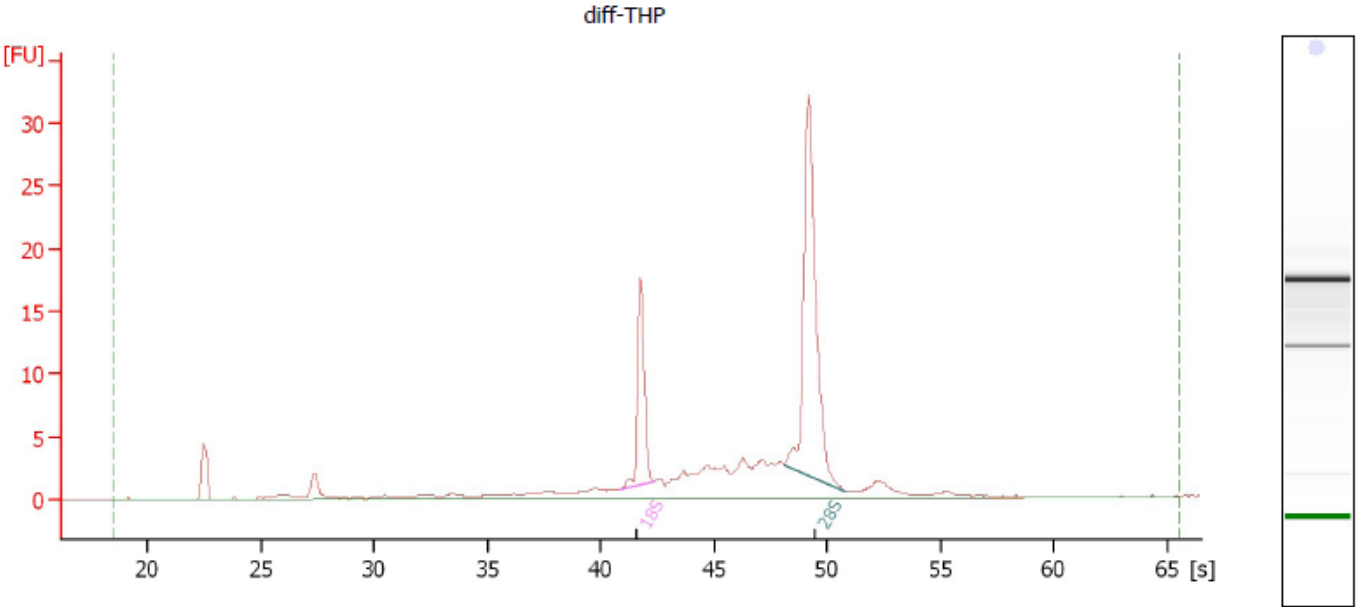
Figure 2SH

Mooney9\_Blystone\_2011-03-24\_001.xad

Assay Class: EukaryoteTotal RNA Nano  
Data Path: C:\...alyzer\2100 expert\Data\Mooney9\_Blystone\_2011-03-24\_001.xad

Created: 3/24/2011 5:04:59 PM  
Modified: 3/24/2011 5:22:06 PM

Electropherogram Summary Continued ...



Overall Results for sample 4 : diff-THP

RNA Area:	109.8	RNA Integrity Number (RIN):	9.3 (B.02.05)
RNA Concentration:	129 ng/μl	Result Flagging Color:	<span style="background-color: #ccccff; border: 1px solid black; display: inline-block; width: 20px; height: 10px;"></span>
rRNA Ratio [28s / 18s]:	2.9	Result Flagging Label:	RIN: 9.30

Fragment table for sample 4 : diff-THP

Name	Start Time [s]	End Time [s]	Area	% of total Area
18S	40.82	42.34	13.0	11.8
28S	48.09	50.79	37.7	34.3

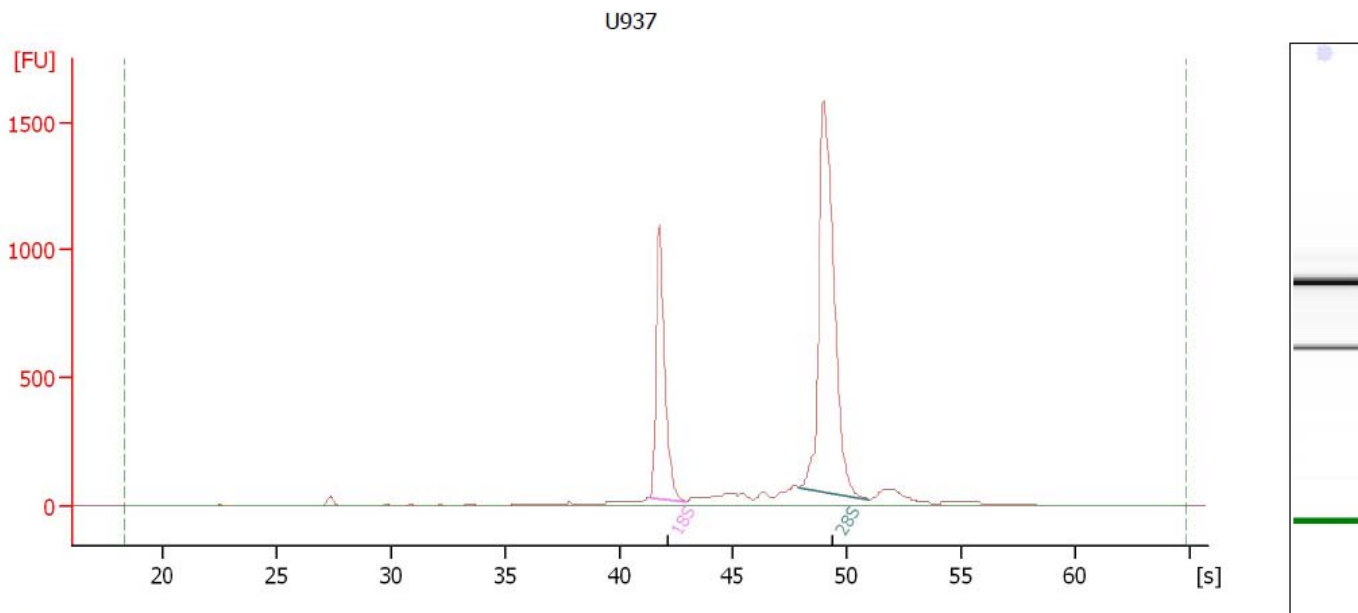
Blystone\_2011-03-30\_001.xad

Page 3 of 4

Assay Class: EukaryoteTotal RNA Nano  
 Data Path: C:\...00 bioanalyzer\2100 expert\Data\Blystone\_2011-03-30\_001.xad

Created: 3/30/2011 12:28:46 PM  
 Modified: 3/30/2011 12:43:24 PM

**Electropherogram Summary**



**Overall Results for sample 1 : U937**

RNA Area:	4,995.9	RNA Integrity Number (RIN):	6.9 (B.02.05)
RNA Concentration:	3,997 ng/μl	Result Flagging Color:	<span style="background-color: #ccccff; border: 1px solid black; display: inline-block; width: 20px; height: 10px;"></span>
rRNA Ratio [28s / 18s]:	2.1	Result Flagging Label:	RIN: 6.90

**Fragment table for sample 1 : U937**

Name	Start Time [s]	End Time [s]	Area	% of total Area
18S	41.34	42.93	1,161.4	23.2
28S	47.87	50.92	2,431.7	48.7

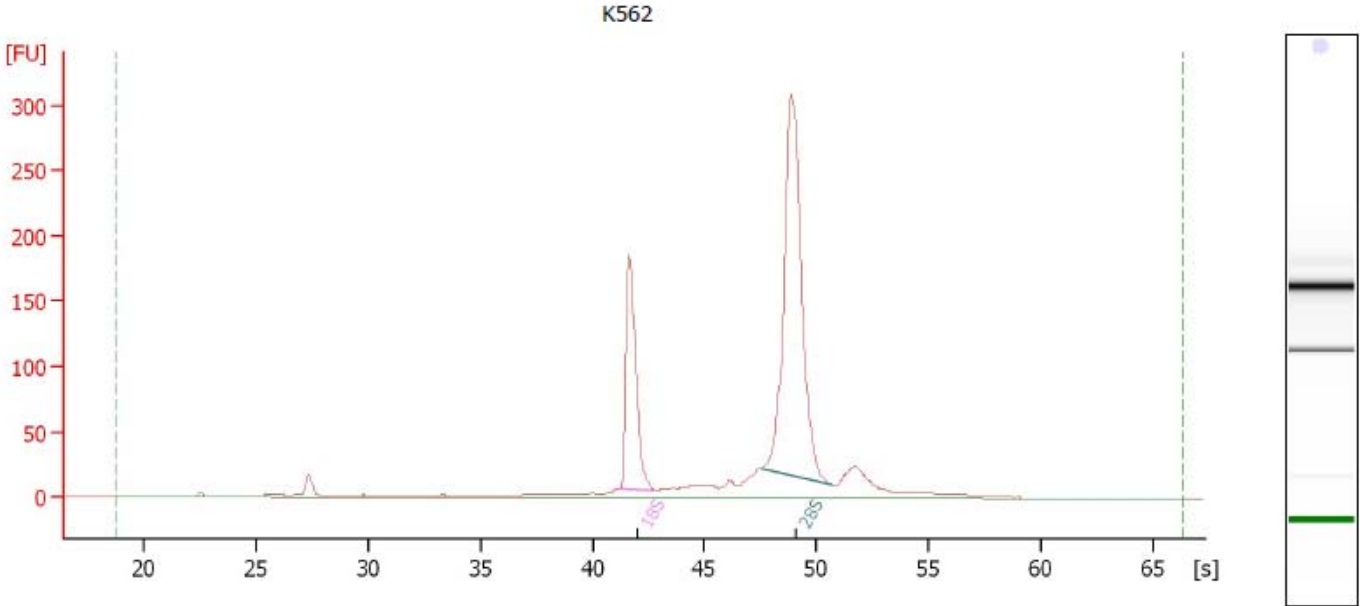
Figure 2SJ

Mooney9\_Blystone\_2011-03-24\_001.xad

Assay Class: EukaryoteTotal RNA Nano  
Data Path: C:\...alyzer\2100 expert\Data\Mooney9\_Blystone\_2011-03-24\_001.xad

Created: 3/24/2011 5:04:59 PM  
Modified: 3/24/2011 5:22:06 PM

Electropherogram Summary Continued ...



Overall Results for sample 6 : K562

RNA Area:	1,185.2	RNA Integrity Number (RIN):	10.0 (B.02.05)
RNA Concentration:	1,394 ng/μl	Result Flagging Color:	<span style="background-color: #ccccff; border: 1px solid black; display: inline-block; width: 20px; height: 10px;"></span>
rRNA Ratio [28s / 18s]:	2.5	Result Flagging Label:	RIN:10

Fragment table for sample 6 : K562

Name	Start Time [s]	End Time [s]	Area	% of total Area
18S	41.20	42.84	218.7	18.5
28S	47.60	50.67	546.1	46.1

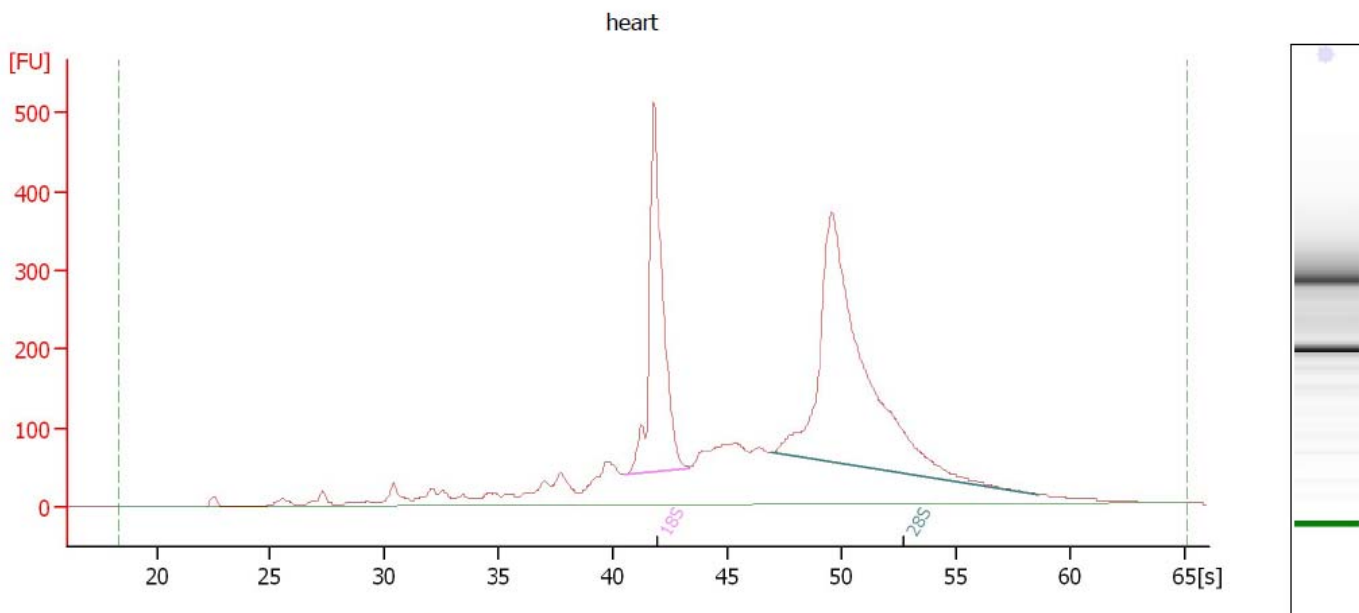
Blystone\_2011-03-15\_001.xad

Page 3 of 5

Assay Class: EukaryoteTotal RNA Nano  
 Data Path: C:\...00 bioanalyzer\2100 expert\Data\Blystone\_2011-03-15\_001.xad

Created: 3/15/2011 4:05:09 PM  
 Modified: 3/15/2011 5:14:30 PM

**Electropherogram Summary**



**Overall Results for sample 1 : heart**

RNA Area:	4,630.6	RNA Integrity Number (RIN):	8.9 (B.02.05)
RNA Concentration:	3,575 ng/μl	Result Flagging Color:	<span style="background-color: #ccccff; border: 1px solid black; display: inline-block; width: 20px; height: 10px;"></span>
rRNA Ratio [28s / 18s]:	1.9	Result Flagging Label:	RIN: 8.90

**Fragment table for sample 1 : heart**

Name	Start Time [s]	End Time [s]	Area	% of total Area
18S	40.47	43.35	763.5	16.5
28S	46.93	58.63	1,416.7	30.6

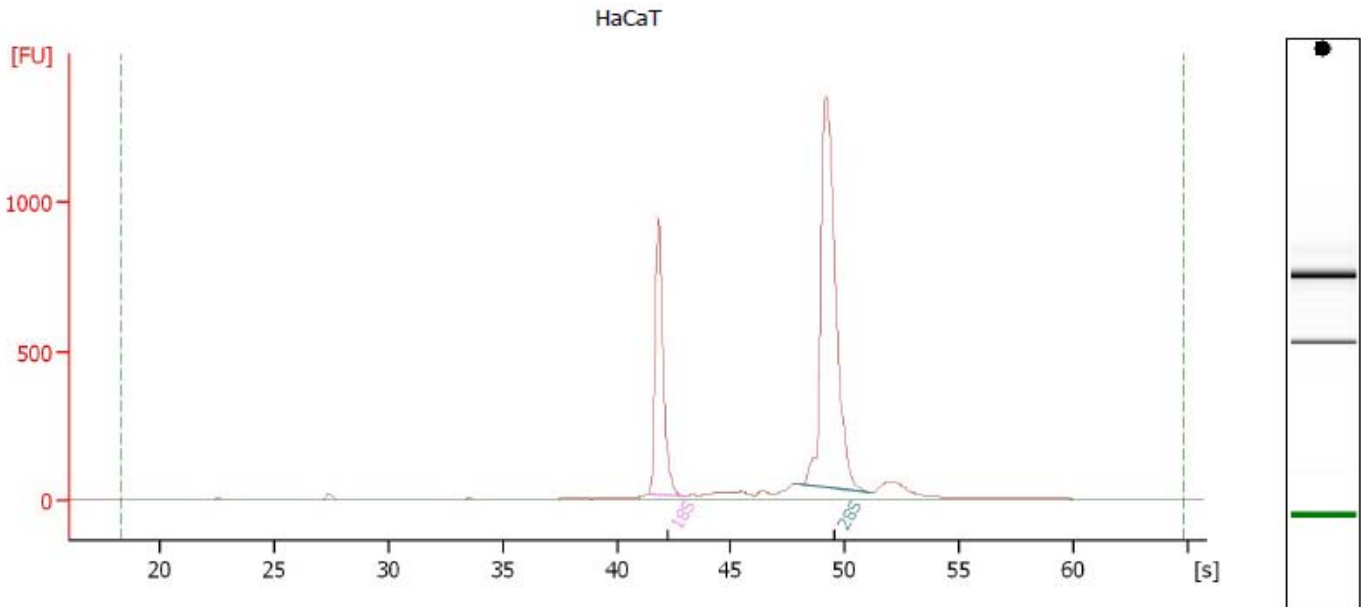
Blystone\_2011-04-01\_001.xad

Page 4 of 6

Assay Class: EukaryoteTotal RNA Nano  
 Data Path: C:\...00 bioanalyzer\2100 expert\Data\Blystone\_2011-04-01\_001.xad

Created: 4/1/2011 3:01:01 PM  
 Modified: 4/1/2011 3:12:51 PM

**Electropherogram Summary Continued ...**



**Overall Results for sample 2 : HaCaT**

RNA Area:	3,863.9	RNA Integrity Number (RIN):	10.0 (B.02.05)
RNA Concentration:	2,801 ng/μl	Result Flagging Color:	<span style="background-color: black; color: black;">████████</span>
rRNA Ratio [28s / 18s]:	2.2	Result Flagging Label:	

**Fragment table for sample 2 : HaCaT**

Name	Start Time [s]	End Time [s]	Area	% of total Area
18S	41.43	42.98	922.0	23.9
28S	48.05	51.06	2,000.6	51.8

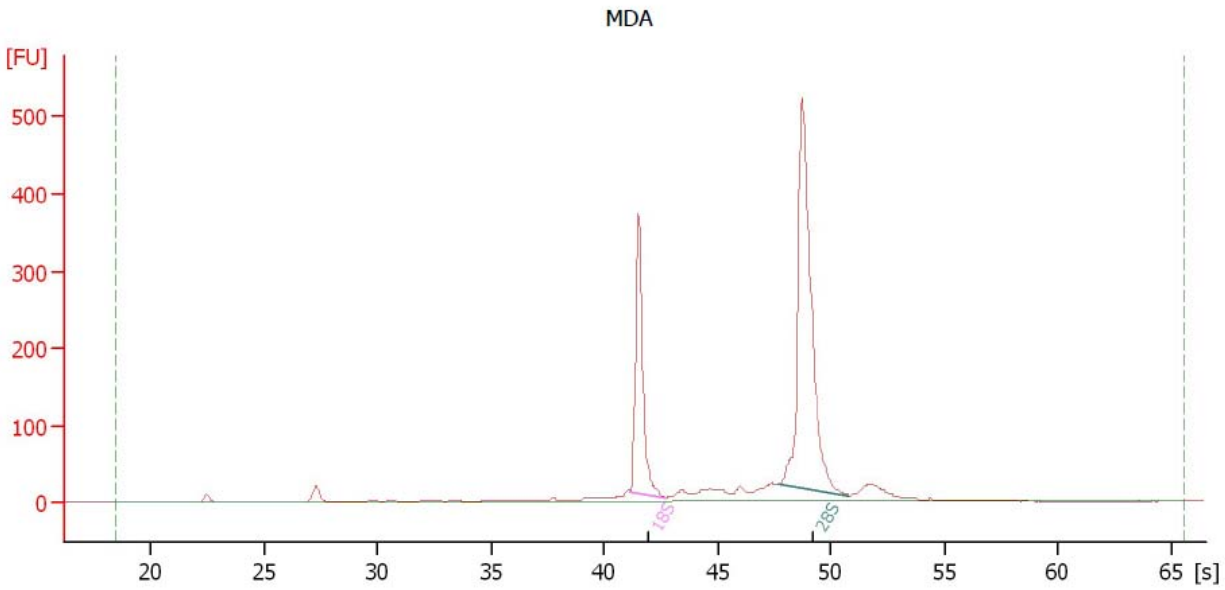
Blystone\_MDA\_2011-03-28\_001.xad

Page 3 of 4

Assay Class: EukaryoteTotal RNA Nano  
 Data Path: C:\...ioanalyzer\2100 expert\Data\Blystone\_MDA\_2011-03-28\_001.xad

Created: 3/28/2011 11:16:12 AM  
 Modified: 3/28/2011 11:30:04 AM

**Electropherogram Summary**



**Overall Results for sample 1 : MDA**

RNA Area:	1,515.3	RNA Integrity Number (RIN):	10.0 (B.02.05)
RNA Concentration:	1,096 ng/μl	Result Flagging Color:	<span style="background-color: #ccccff; border: 1px solid black; display: inline-block; width: 20px; height: 10px;"></span>
rRNA Ratio [28s / 18s]:	2.2	Result Flagging Label:	RIN:10

**Fragment table for sample 1 : MDA**

Name	Start Time [s]	End Time [s]	Area	% of total Area
18S	41.15	42.67	320.0	21.1
28S	47.66	50.79	713.8	47.1

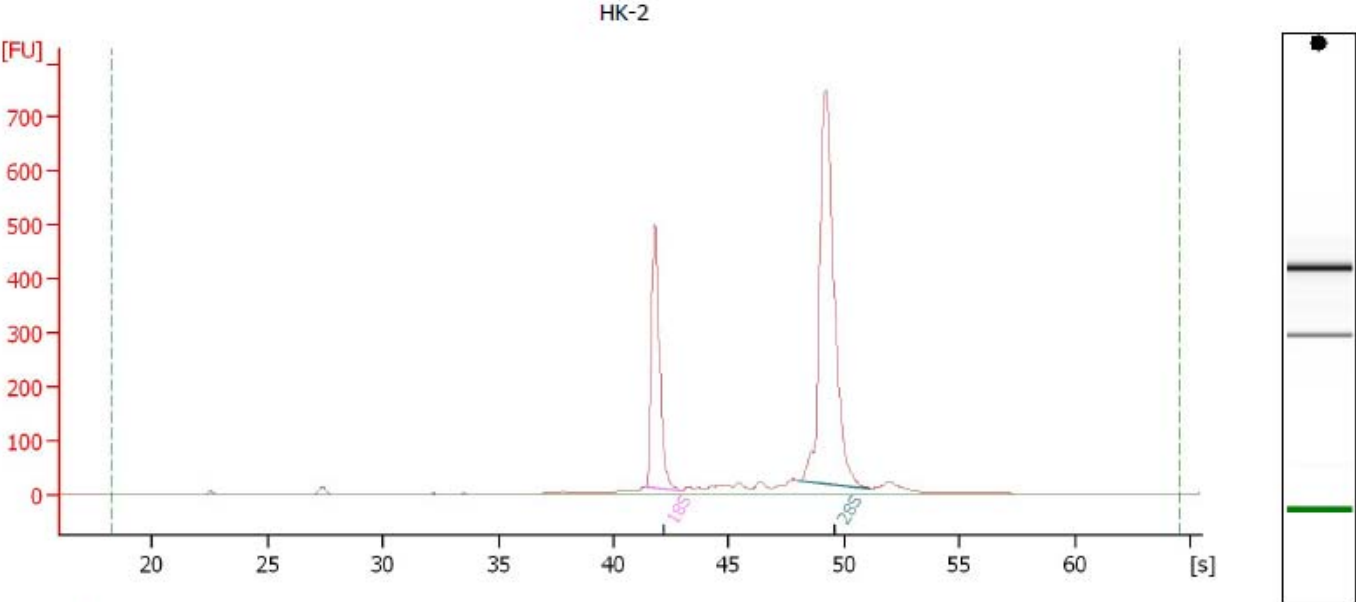
Figure 2SN

Blystone\_2011-04-01\_001.xad

Assay Class: EukaryoteTotal RNA Nano  
Data Path: C:\...00 bioanalyzer\2100 expert\Data\Blystone\_2011-04-01\_001.xad

Created: 4/1/2011 3:01:01 PM  
Modified: 4/1/2011 3:12:51 PM

Electropherogram Summary Continued ...



Overall Results for sample 3 : HK-2

RNA Area:	2,086.7	RNA Integrity Number (RIN):	10.0 (B.02.05)
RNA Concentration:	1,513 ng/μl	Result Flagging Color:	<span style="background-color: black; color: black;">████████</span>
rRNA Ratio [28s / 18s]:	2.3	Result Flagging Label:	

Fragment table for sample 3 : HK-2

Name	Start Time [s]	End Time [s]	Area	% of total Area
18S	41.40	42.94	480.9	23.0
28S	48.04	51.17	1,083.8	51.9

Figure 2SO

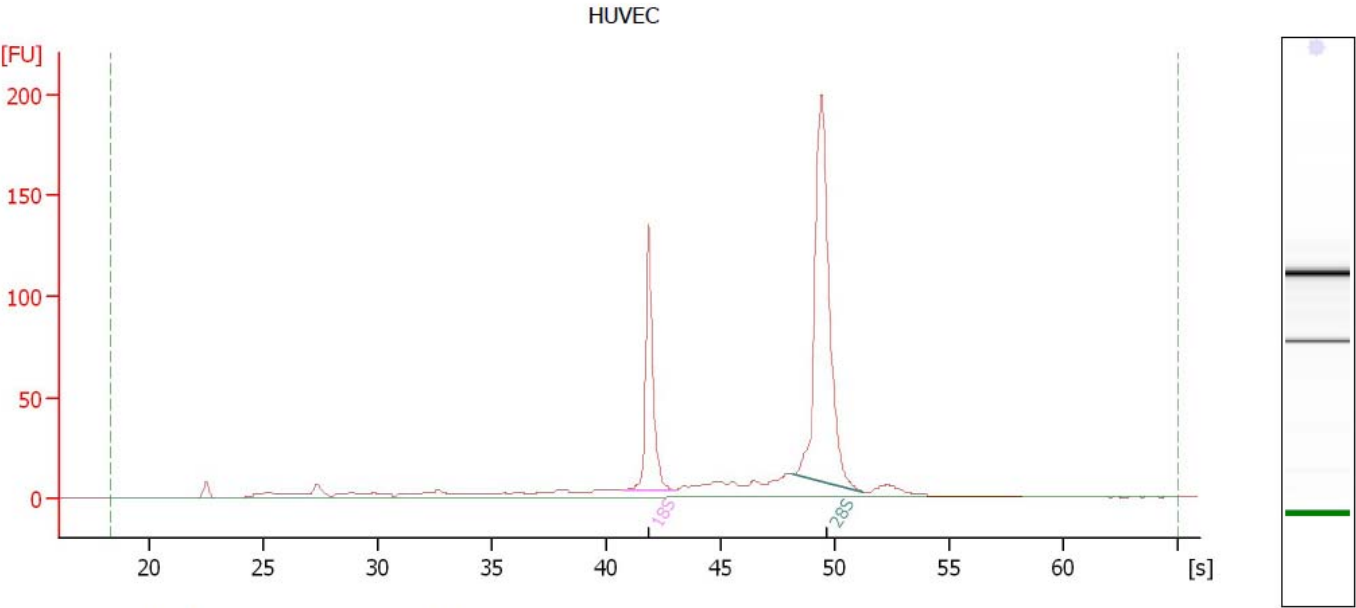
Blystone\_2011-04-18\_001.xad

Page 3 of 4

Assay Class: EukaryoteTotal RNA Nano  
 Data Path: C:\...00 bioanalyzer\2100 expert\Data\Blystone\_2011-04-18\_001.xad

Created: 4/18/2011 3:37:15 PM  
 Modified: 4/18/2011 3:47:03 PM

**Electropherogram Summary**



**Overall Results for sample 1 : HUVEC**

RNA Area:	700.8	RNA Integrity Number (RIN):	9.6 (B.02.05)
RNA Concentration:	567 ng/μl	Result Flagging Color:	<span style="background-color: #ccccff; border: 1px solid black; display: inline-block; width: 20px; height: 10px;"></span>
rRNA Ratio [28s / 18s]:	2.2	Result Flagging Label:	RIN: 9.60

**Fragment table for sample 1 : HUVEC**

Name	Start Time [s]	End Time [s]	Area	% of total Area
18S	40.67	43.02	125.8	18.0
28S	48.11	51.21	279.3	39.8

Figure 2SP

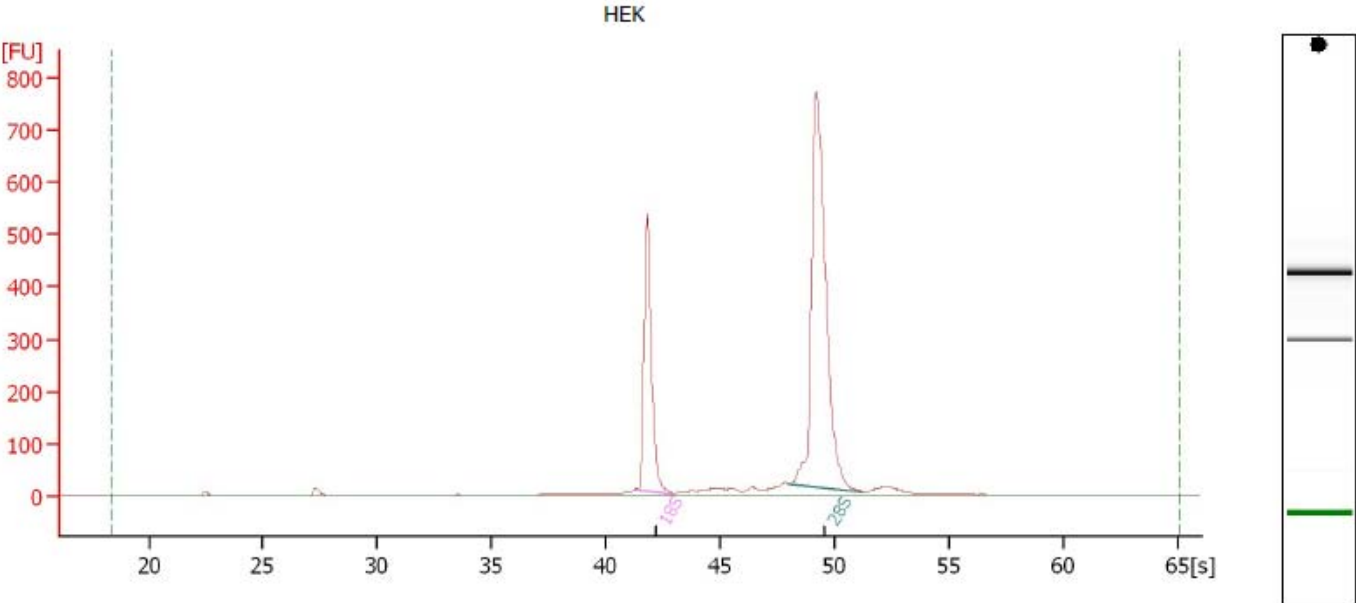
Blystone\_2011-04-01\_001.xad

Page 3 of 6

Assay Class: EukaryoteTotal RNA Nano  
Data Path: C:\...00 bioanalyzer\2100 expert\Data\Blystone\_2011-04-01\_001.xad

Created: 4/1/2011 3:01:01 PM  
Modified: 4/1/2011 3:12:51 PM

Electropherogram Summary



Overall Results for sample 1 : HEK

RNA Area:	2,053.9	RNA Integrity Number (RIN):	10.0 (B.02.05)
RNA Concentration:	1,489 ng/μl	Result Flagging Color:	████████
rRNA Ratio [28s / 18s]:	2.3	Result Flagging Label:	

Fragment table for sample 1 : HEK

Name	Start Time [s]	End Time [s]	Area	% of total Area
18S	41.42	42.97	481.3	23.4
28S	47.97	51.23	1,109.7	54.0

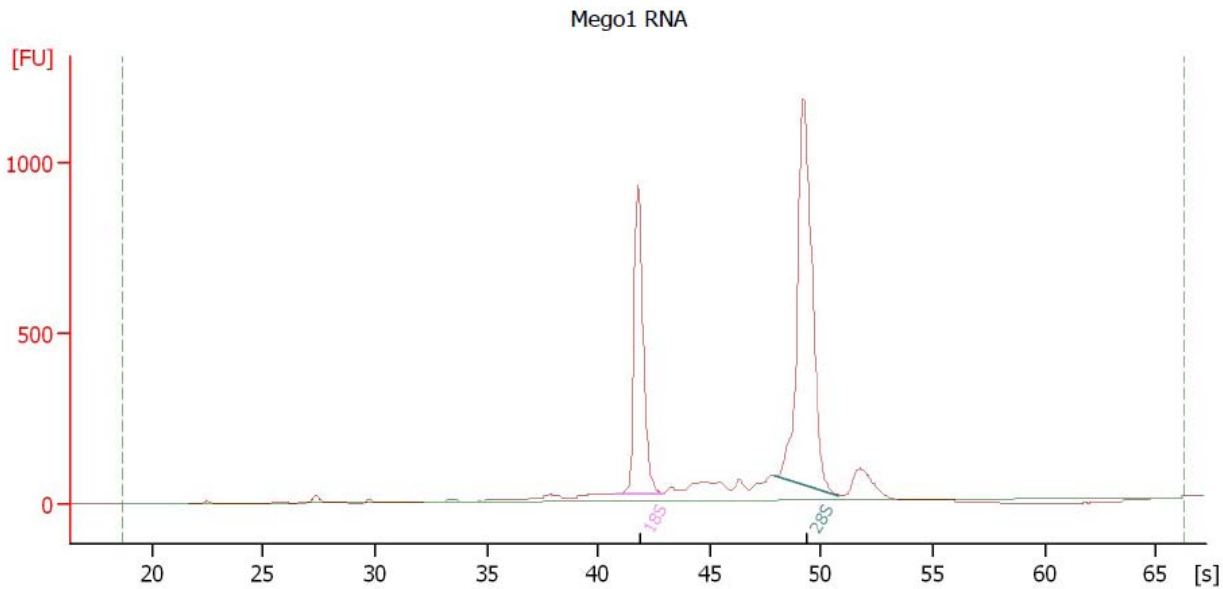
Blystone\_2011-05-13\_001.xad

Page 6 of 8

Assay Class: EukaryoteTotal RNA Nano  
 Data Path: C:\...00 bioanalyzer\2100 expert\Data\Blystone\_2011-05-13\_001.xad

Created: 5/13/2011 2:12:42 PM  
 Modified: 5/13/2011 2:32:41 PM

**Electropherogram Summary Continued ...**



**Overall Results for sample 4 : Mego1 RNA**

RNA Area:	3,988.8	RNA Integrity Number (RIN):	9.7 (B.02.05)
RNA Concentration:	1,941 ng/μl	Result Flagging Color:	<span style="background-color: #ccccff; border: 1px solid black; display: inline-block; width: 20px; height: 10px;"></span>
rRNA Ratio [28s / 18s]:	1.8	Result Flagging Label:	RIN: 9.70

**Fragment table for sample 4 : Mego1 RNA**

Name	Start Time [s]	End Time [s]	Area	% of total Area
18S	40.78	42.94	994.9	24.9
28S	47.93	50.80	1,768.5	44.3

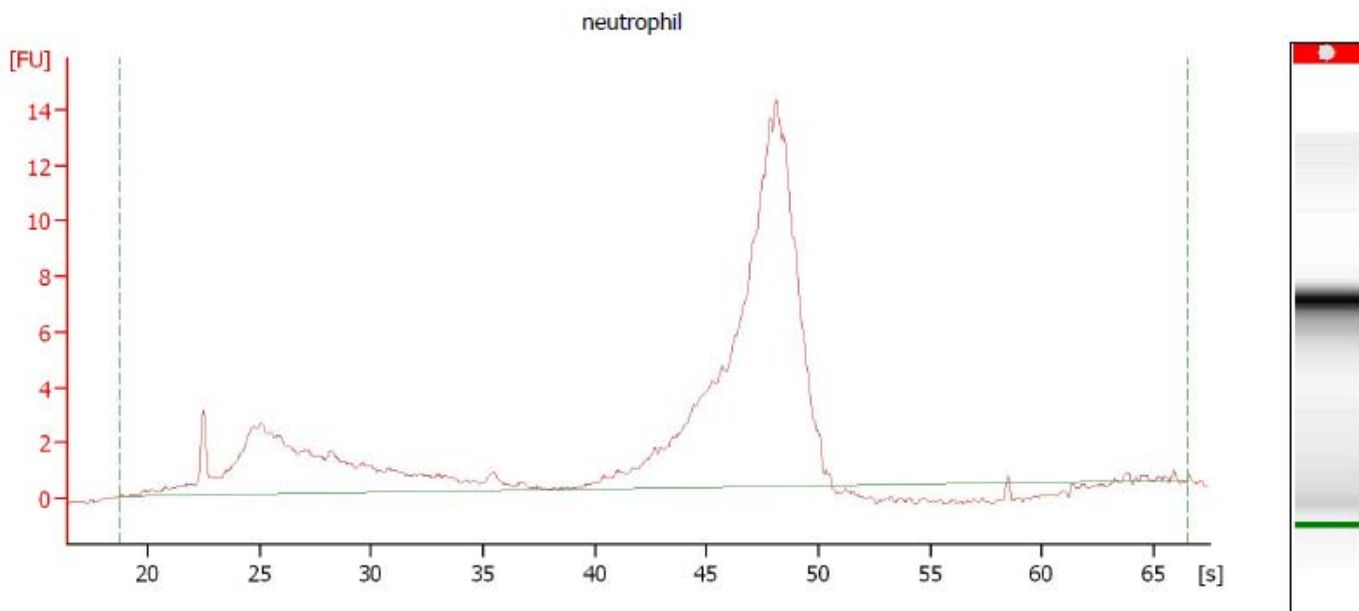
Blystone\_2011-05-24\_001.xad

Page 3 of 5

Assay Class: EukaryoteTotal RNA Nano  
 Data Path: C:\...00 bioanalyzer\2100 expert\Data\Blystone\_2011-05-24\_001.xad

Created: 5/24/2011 2:29:50 PM  
 Modified: 5/24/2011 2:44:59 PM

**Electropherogram Summary**



**Overall Results for sample 1 : neutrophil**

RNA Area:	149.3	RNA Integrity Number (RIN):	N/A (B.02.05)
RNA Concentration:	188 ng/ $\mu$ l	Result Flagging Color:	<span style="border: 1px solid gray; display: inline-block; width: 20px; height: 10px;"></span>
rRNA Ratio [28s / 18s]:	0.0	Result Flagging Label:	RIN N/A

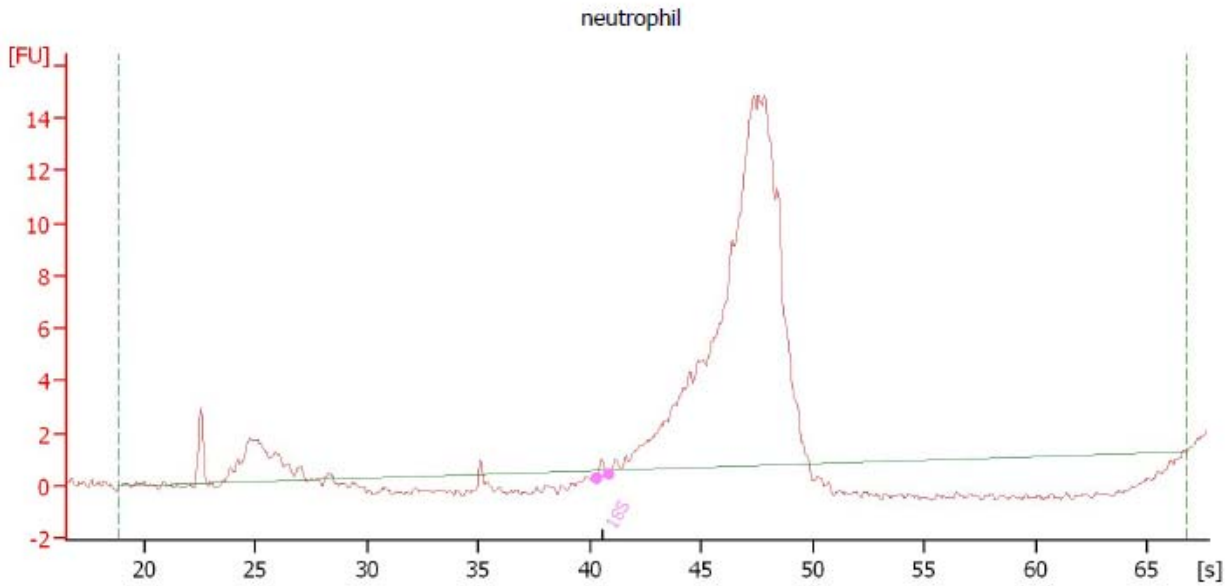
Blystone\_2011-05-24\_001.xad

Page 4 of 5

Assay Class: EukaryoteTotal RNA Nano  
 Data Path: C:\...00 bioanalyzer\2100 expert\Data\Blystone\_2011-05-24\_001.xad

Created: 5/24/2011 2:29:50 PM  
 Modified: 5/24/2011 2:44:59 PM

**Electropherogram Summary Continued ...**



**Overall Results for sample 2 : neutrophil**

RNA Area:	106.9	RNA Integrity Number (RIN):	N/A (B.02.05)
RNA Concentration:	135 ng/μl	Result Flagging Color:	<span style="background-color: #cccccc; border: 1px solid black; display: inline-block; width: 20px; height: 10px;"></span>
rRNA Ratio [28s / 18s]:	0.0	Result Flagging Label:	RIN N/A

**Fragment table for sample 2 : neutrophil**

Name	Start Time [s]	End Time [s]	Area	% of total Area
18S	40.26	40.84	0.3	0.3

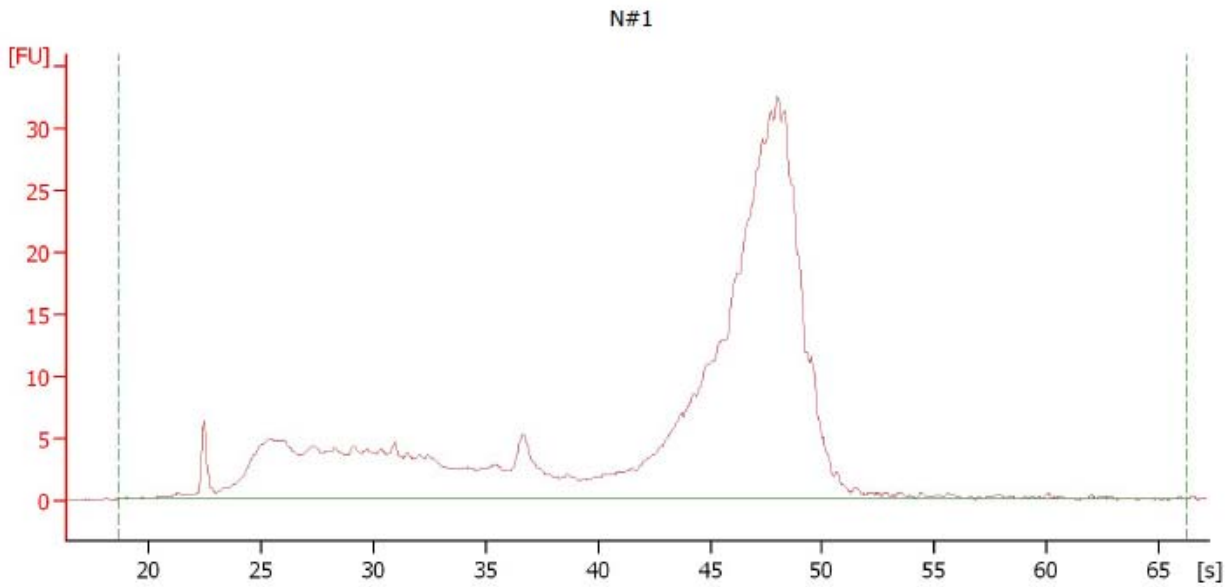
Blystone\_2011-05-27\_001.xad

Page 3 of 13

Assay Class: EukaryoteTotal RNA Nano  
 Data Path: C:\...00 bioanalyzer\2100 expert\Data\Blystone\_2011-05-27\_001.xad

Created: 5/27/2011 1:52:03 PM  
 Modified: 5/27/2011 2:13:33 PM

**Electropherogram Summary**



**Overall Results for sample 1 : N#1**

RNA Area:	445.0	RNA Integrity Number (RIN):	N/A (B.02.05)
RNA Concentration:	241 ng/μl	Result Flagging Color:	<span style="background-color: #cccccc; border: 1px solid black; display: inline-block; width: 20px; height: 10px;"></span>
rRNA Ratio [28s / 18s]:	0.0	Result Flagging Label:	RIN N/A

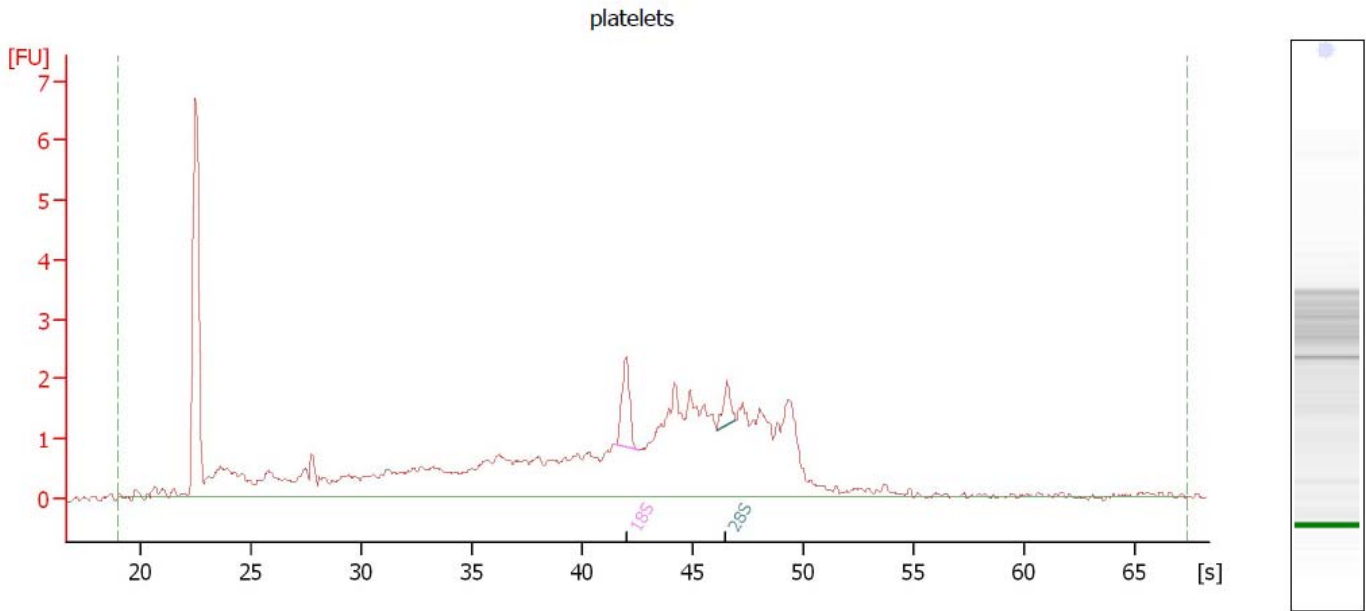
Blystone\_2011-05-20\_001.xad

Page 4 of 5

Assay Class: EukaryoteTotal RNA Nano  
 Data Path: C:\...00 bioanalyzer\2100 expert\Data\Blystone\_2011-05-20\_001.xad

Created: 5/20/2011 12:46:30 PM  
 Modified: 5/20/2011 1:02:17 PM

**Electropherogram Summary Continued ...**



**Overall Results for sample 2 : platelets**

RNA Area:	53.5	RNA Integrity Number (RIN):	3.8 (B.02.05)
RNA Concentration:	37 ng/µl	Result Flagging Color:	<span style="background-color: #ccccff; border: 1px solid black; display: inline-block; width: 20px; height: 10px;"></span>
rRNA Ratio [28s / 18s]:	0.3	Result Flagging Label:	RIN: 3.80

**Fragment table for sample 2 : platelets**

Name	Start Time [s]	End Time [s]	Area	% of total Area
18S	41.53	42.51	1.4	2.7
28S	46.07	46.95	0.4	0.7

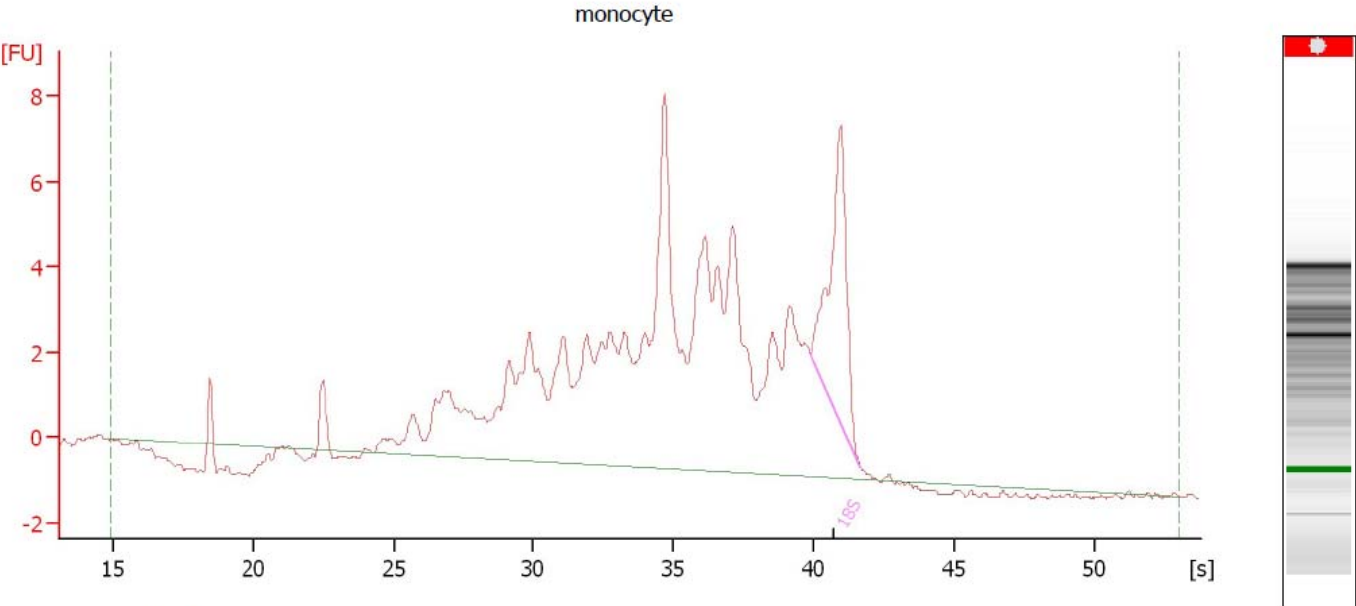
Figure 2ST

Blystone\_2011-06-03\_001.xad

Assay Class: EukaryoteTotal RNA Nano  
Data Path: C:\...00 bioanalyzer\2100 expert\Data\Blystone\_2011-06-03\_001.xad

Created: 6/3/2011 11:13:23 AM  
Modified: 6/3/2011 11:44:26 AM

Electropherogram Summary



Overall Results for sample 1 : monocyte

RNA Area:	132.3	RNA Integrity Number (RIN):	N/A (B.02.05)
RNA Concentration:	273 ng/μl	Result Flagging Color:	<span style="background-color: #cccccc; border: 1px solid black; display: inline-block; width: 20px; height: 10px;"></span>
rRNA Ratio [28s / 18s]:	0.0	Result Flagging Label:	RIN N/A

Fragment table for sample 1 : monocyte

Name	Start Time [s]	End Time [s]	Area	% of total Area
18S	39.85	41.66	11.3	8.5

Figure 2SU

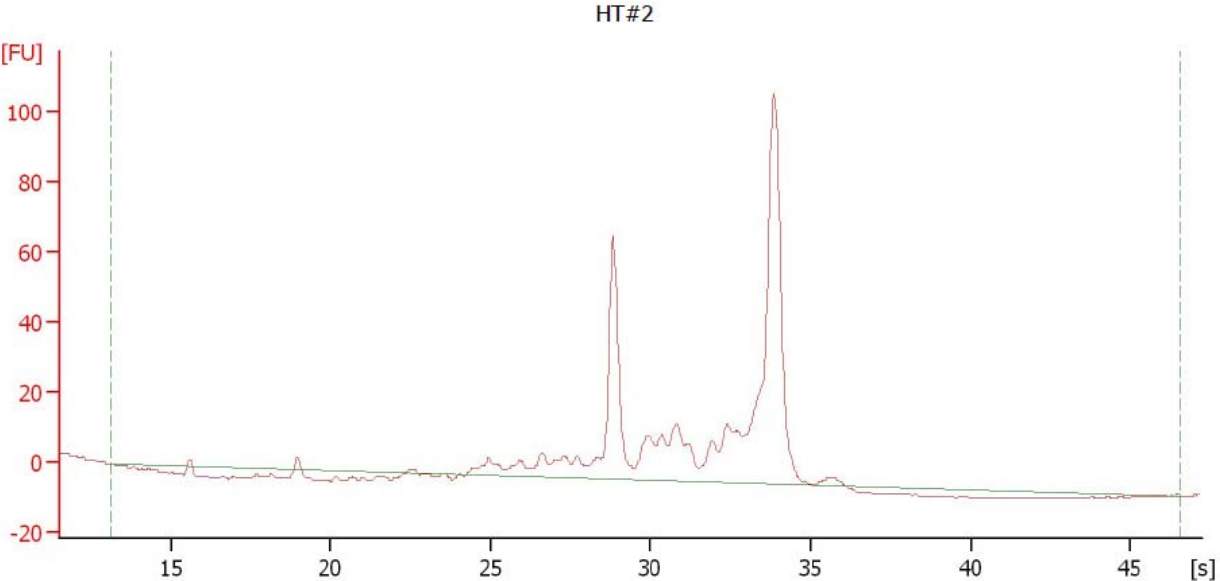
Blystone\_2011-05-27\_001.xad

Page 12 of 13

Assay Class: EukaryoteTotal RNA Nano  
Data Path: C:\...00 bioanalyzer\2100 expert\Data\Blystone\_2011-05-27\_001.xad

Created: 5/27/2011 1:52:03 PM  
Modified: 5/27/2011 2:13:33 PM

Electropherogram Summary Continued ...



Overall Results for sample 10 : HT#2

RNA Area:	453.8	RNA Integrity Number (RIN):	8.3 (B.02.05)
RNA Concentration:	246 ng/μl	Result Flagging Color:	<span style="background-color: #ccccff; border: 1px solid black; display: inline-block; width: 20px; height: 10px;"></span>
rRNA Ratio [28s / 18s]:	0.0	Result Flagging Label:	RIN: 8.30

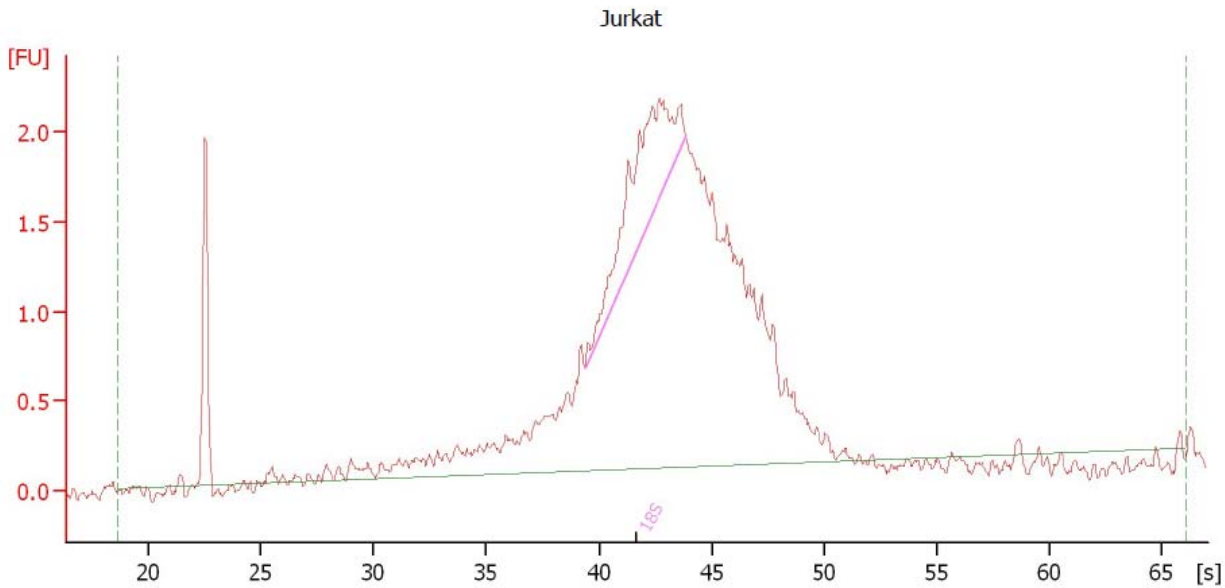
Blystone\_2011-07-08\_001.xad

Page 3 of 5

Assay Class: EukaryoteTotal RNA Nano  
 Data Path: C:\...00 bioanalyzer\2100 expert\Data\Blystone\_2011-07-08\_001.xad

Created: 7/8/2011 2:19:28 PM  
 Modified: 7/8/2011 2:40:02 PM

**Electropherogram Summary**



**Overall Results for sample 1 : Jurkat**

RNA Area:	34.3	RNA Integrity Number (RIN):	2.5 (B.02.05)
RNA Concentration:	61 ng/μl	Result Flagging Color:	<span style="background-color: black; color: black;">████████</span>
rRNA Ratio [28s / 18s]:	0.0	Result Flagging Label:	

**Fragment table for sample 1 : Jurkat**

Name	Start Time [s]	End Time [s]	Area	% of total Area
18S	39.40	43.85	3.0	8.8

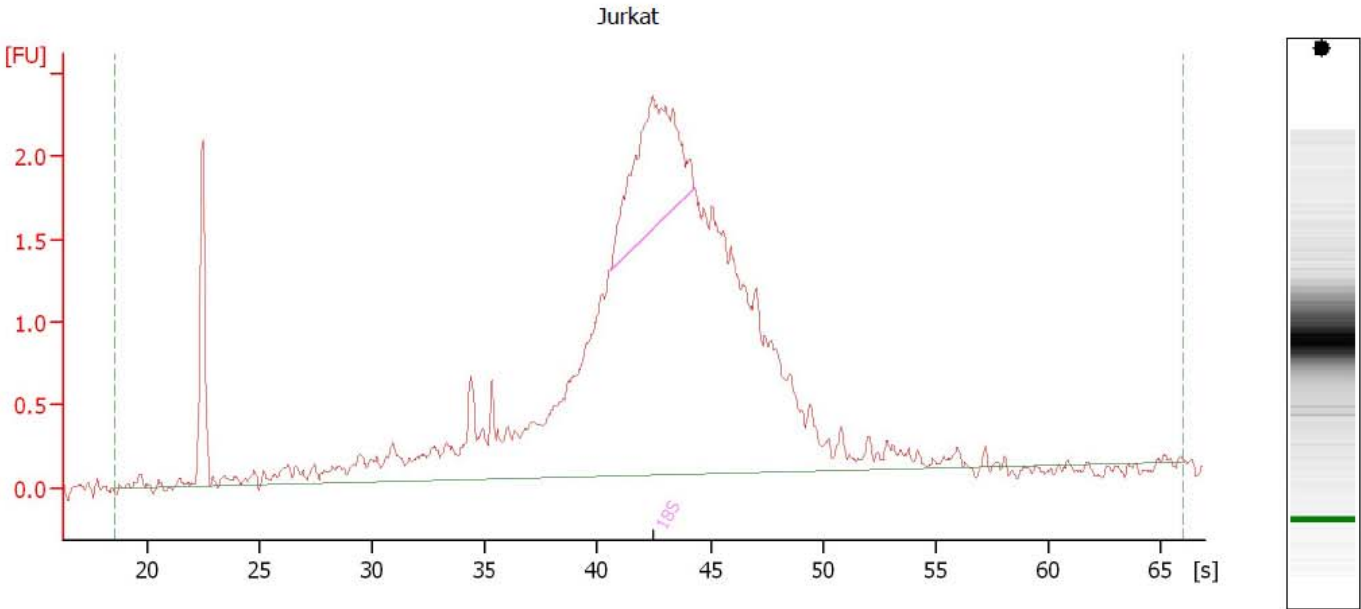
Figure 2SV2

Blystone\_2011-07-08\_001.xad

Assay Class: EukaryoteTotal RNA Nano  
Data Path: C:\...00 bioanalyzer\2100 expert\Data\Blystone\_2011-07-08\_001.xad

Created: 7/8/2011 2:19:28 PM  
Modified: 7/8/2011 2:40:02 PM

Electropherogram Summary Continued ...



Overall Results for sample 2 : Jurkat

RNA Area:	42.2	RNA Integrity Number (RIN):	2.5 (B.02.05)
RNA Concentration:	75 ng/μl	Result Flagging Color:	████████
rRNA Ratio [28s / 18s]:	0.0	Result Flagging Label:	

Fragment table for sample 2 : Jurkat

Name	Start Time [s]	End Time [s]	Area	% of total Area
18S	40.56	44.28	4.0	9.4

Figure 2SW

1 - all RINs		2 - RINs excluding monocytes		3 - RINs excluding monocytes & platelets	
Cell type	RIN	Cell type	RIN	Cell type	RIN
HeLa	9.4	HeLa	9.4	HeLa	9.4
Macrophage	9.9	Macrophage	9.9	Macrophage	9.9
Cerebellum	8.3	Cerebellum	8.3	Cerebellum	8.3
U2OS	10	U2OS	10	U2OS	10
HCN	9.9	HCN	9.9	HCN	9.9
Skeletal muscle	8.3	Skeletal muscle	8.3	Skeletal muscle	8.3
THP	9.3	THP	9.3	THP	9.3
differentiated THP	9.3	differentiated THP	9.3	differentiated THP	9.3
U937	6.9	U937	6.9	U937	6.9
K562	10	K562	10	K562	10
Cardiac muscle	8.9	Cardiac muscle	8.9	Cardiac muscle	8.9
HaCaT	10	HaCaT	10	HaCaT	10
MDA	10	MDA	10	MDA	10
HK-2	10	HK-2	10	HK-2	10
HUVEC	9.6	HUVEC	9.6	HUVEC	9.6
HEK	10	HEK	10	HEK	10
Meg-01	9.7	Meg-01	9.7	Meg-01	9.7
Neutrophil	N/A	Neutrophil	N/A	Neutrophil	N/A
Neutrophil	N/A	Neutrophil	N/A	Neutrophil	N/A
Neutrophil	N/A	Neutrophil	N/A	Neutrophil	N/A
Platelet	3.8	Platelet	3.8	Platelet	3.8
Monocyte	N/A	Monocyte	N/A	Monocyte	N/A
HT1080	8.3	HT1080	8.3	HT1080	8.3
Jurkat	2.5	Jurkat	-	Jurkat	-
Jurkat	2.5	Jurkat	-	Jurkat	-
average RIN	8.41	average RIN	9.03	average RIN	9.32
st. dev.	2.44	st. dev.	1.52	st. dev.	0.87

## References

Aspenstrom P. 2010. Formin-binding proteins: modulators of formin-dependent actin polymerization. *Biochim Biophys Acta* 1803:2174-182.

Block J, Breitsprecher D, Kuhn S. 2012. FMNL2 drives actin-based protrusion and migration downstream of Cdc42. *Curr Biol Elsevier Ltd*22:111005-1012.

Blystone SD, Williams MP, Slater SE and Brown EJ. 1997. Requirement of integrin beta3 tyrosine 747 for beta3 tyrosine phosphorylation and regulation of alphavbeta3 avidity. *J Biol Chem* 272:4528757-28761.

Bustin SA, Benes V, Garson JA. 2009. The MIQE guidelines: minimum information for publication of quantitative real-time PCR experiments. *Clin Chem* 55:4611-622.

Bustin SA. . 2002. Quantification of mRNA using real-time reverse transcription PCR (RT-PCR): trends and problems. *J Mol Endocrinol* 29:123-39.

Campellone KG and Welch MD. 2010. A nucleator arms race: cellular control of actin assembly. *Nat Rev Mol Cell Biol* 11:4237-251.

Castrillon DH and Wasserman SA. 1994. Diaphanous is required for cytokinesis in *Drosophila* and shares domains of similarity with the products of the limb deformity gene. *Development* 120:123367-3377.

Chae SC, Inazu Y, Amagai A and Maeda Y. 1998. Underexpression of a novel gene, *dia2*, impairs the transition of *Dictyostelium* cells from growth to differentiation. *Biochem Biophys Res Commun Academic Press*252:1278-283.

Chesarone MA, DuPage AG and Goode BL. 2010. Unleashing formins to remodel the actin and microtubule cytoskeletons. *Nat Rev Mol Cell Biol* 11:162-74.

Chhabra ES and Higgs HN. 2007. The many faces of actin: matching assembly factors with cellular structures. *Nat Cell Biol* 9:101110-1121.

Chhabra ES and Higgs HN. 2006. INF2 Is a WASP homology 2 motif-containing formin that severs actin filaments and accelerates both polymerization and depolymerization. *J Biol Chem* 281:3626754-26767.

Colon-Franco JM, Gomez TS and Billadeau DD. 2011. Dynamic remodeling of the actin cytoskeleton by FMNL1gamma is required for structural maintenance of the Golgi complex. *J Cell Sci* 124:Pt 183118-3126.

Copeland JW, Copeland SJ and Treisman R. 2004. Homo-oligomerization is essential for F-actin assembly by the formin family FH2 domain. *J Biol Chem* 279:4850250-50256.

Evangelista M, Zigmond S and Boone C. 2003. Formins: signaling effectors for assembly and polarization of actin filaments. *J Cell Sci* 116:Pt 132603-2611.

Goode BL and Eck MJ. 2007. Mechanism and function of formins in the control of actin assembly. *Annu Rev Biochem* 76:593-627.

Habas R, Kato Y and He X. 2001. Wnt/Frizzled activation of Rho regulates vertebrate gastrulation and requires a novel Formin homology protein Daam1. *Cell* 107:7843-854.

Harris ES, Gauvin TJ, Heimsath EG and Higgs HN. 2010. Assembly of filopodia by the formin FRL2 (FMNL3). *Cytoskeleton (Hoboken) Wiley-Liss, Inc* 67:12755-772.

Higgs HN and Peterson KJ. 2005. Phylogenetic analysis of the formin homology 2 domain. *Mol Biol Cell* 16:11-13.

Jones SL, Wang J, Turck CW and Brown EJ. 1998. A role for the actin-bundling protein L-plastin in the regulation of leukocyte integrin function. *Proc Natl Acad Sci U S A* 95:169331-9336.

Katoh M and Katoh M. 2004a. Identification and characterization of human FHDC1, mouse Fhdc1 and zebrafish fhdc1 genes in silico. *Int J Mol Med* 13:6929-934.

Katoh M and Katoh M. 2004b. Identification and characterization of the human FMN1 gene in silico. *Int J Mol Med* 14:1121-126.

Katoh M and Katoh M. 2004c. Characterization of FMN2 gene at human chromosome 1q43. *Int J Mol Med* 14:3469-474.

Katoh M and Katoh M. 2003a. Identification and characterization of human FMNL1, FMNL2 and FMNL3 genes in silico. *Int J Oncol* 22:51161-1168.

Katoh M and Katoh M. 2003b. Identification and characterization of human DAAM2 gene in silico. *Int J Oncol* 22:4915-920.

Katoh M and Katoh M. 2003c Identification and characterization of human GRID2IP gene and rat Grid2ip gene in silico. *Int J Mol Med* 12:61015-1019.

Kida Y, Shiraishi T and Ogura T. 2004. Identification of chick and mouse Daam1 and Daam2 genes and their expression patterns in the central nervous system. *Brain Res Dev Brain Res* 153:1143-150.

Kovar DR. 2006. Molecular details of formin-mediated actin assembly. *Curr Opin Cell Biol* 18:111-17.

Lee HK and Deneen B. 2012. Daam2 is required for dorsal patterning via modulation of canonical Wnt signaling in the developing spinal cord. *Dev Cell Elsevier Inc* 22:1183-196.

Matsuda K, Matsuda S, Gladding CM and Yuzaki M. 2006. Characterization of the delta2 glutamate receptor-binding protein delphilin: Splicing variants with differential palmitoylation and an additional PDZ domain. *J Biol Chem* 281:3525577-25587.

Mersich AT, Miller MR, Chkourko H and Blystone SD. 2010. The formin FRL1 (FMNL1) is an essential component of macrophage podosomes. *Cytoskeleton (Hoboken) Wiley-Liss, Inc* 67:9573-585.

Miyagi Y, Yamashita T, Fukaya M. 2002. Delphilin: a novel PDZ and formin homology domain-containing protein that synaptically colocalizes and interacts with glutamate receptor delta 2 subunit. *J Neurosci* 22:3803-814.

Nolan T, Hands RE and Bustin SA. 2006. Quantification of mRNA using real-time RT-PCR. *Nat Protoc* 1:31559-1582.

Paul AS and Pollard TD. 2009. Energetic requirements for processive elongation of actin filaments by FH1FH2-formins. *J Biol Chem* 284:1812533-12540.

Paul AS and Pollard TD. 2008. The role of the FH1 domain and profilin in formin-mediated actin-filament elongation and nucleation. *Curr Biol* 18:19-19.

Peng J, Wallar BJ, Flanders A, Swiatek PJ and Alberts AS. 2003. Disruption of the Diaphanous-related formin Drf1 gene encoding mDia1 reveals a role for Drf3 as an effector for Cdc42. *Curr Biol* 13:7534-545.

Schonichen A and Geyer M. 2010. Fifteen formins for an actin filament: a molecular view on the regulation of human formins. *Biochim Biophys Acta* 1803:2152-163.

Schroeder A, Mueller O, Stocker S, Salowsky R, Leiber M, Gassmann M, Lightfoot S, Menzel W, Granzow M and Ragg T. 2006. The RIN: an RNA integrity number for assigning integrity values to RNA measurements. *BMC Mol Biol* 7:3.

Ståhlberg A, Hakansson J, Xian X, Semb H and Kubista M. 2004. Properties of the reverse transcription reaction in mRNA quantification. *Clin Chem* 50:3509-515.

Wallar BJ and Alberts AS. 2003. The formins: active scaffolds that remodel the cytoskeleton. *Trends Cell Biol* 13:8435-446.

Watanabe-Kaneko K, Sonoda T, Miyagi Y, Yamashita T, Okuda K and Kawamoto S. 2007. The synaptic scaffolding protein Delphilin interacts with monocarboxylate transporter 2. *Neuroreport* 18:5489-493.

Westendorf JJ, Mernaugh R and Hiebert SW. 1999. Identification and characterization of a protein containing formin homology (FH1/FH2) domains. *Gene* 232:2173-182.

Zigmond SH, Evangelista M, Boone C, Yang C, Dar AC, Sicheri F, Forkey J and Pring M. 2003. Formin leaky cap allows elongation in the presence of tight capping proteins. *Curr Biol* 13:201820-1823.

**Chapter 3:**

**Immunohistochemical Localization of  
Fhod1 and Fhod3 in the Sarcomere**

## Introduction

Formin Homology Domain containing proteins 1 and 3 (FHOD1 and FHOD3) were found to be expressed in both cardiac and skeletal muscle at high levels compared to other formins (Krainer, et al, 2013). The same study found FHOD1 to be the most highly expressed formin across 22 different human cell lines and tissues, while FHOD3 was the least highly expressed formin, posing the question why two closely related formins would have such strikingly different expression profiles across a wide range of cells and tissues, but have similarly high expression in striated muscle (Krainer, et al., 2013).

The microscopic structure of striated muscles is highly preserved across species, with the structure of the smallest contractile unit, the sarcomere, virtually unchanged between lower invertebrates and humans (Huxley H and Hanson J, 1954). While the structure of sarcomeres is fairly well understood, the formation of myofibrils and sarcomeres is much less clear. Specifically, the process by which actin, the main thin filament component is incorporated into the sarcomere remains unknown. The thin filament starts at an integrin-based adhesion site near the cell membrane called Z-bodies, Z-disk precursors, and are anchored at the barbed end and appear similar to stress-fiber like actin filaments (Sparrow and Schöck, 2009; Moerman and Williams, 2006; Volk, et al., 1990). However, it has not been determined which actin nucleation factor or factors (ANF) are responsible for the assembly and maintenance of the actin filament, but three candidates seem likely: neuronal Wiskott–Aldrich Syndrome protein (N-WASP), tropomodulin-related leomodulin-2 (Lmod), and formins (Takano, et al., 2010;

### Chapter 3 – Endogenous Fhod1 and Fhod3 in the Sarcomere

Chereau, et al., 2008; Tanaguchi, et al., 2009). Based on previous findings of high expression levels of FHOD1 and FHOD3 in striated muscle, this chapter focuses on the localization of FHOD1 and FHOD3 within the sarcomere to determine if they could play a role in the formation or stabilization of the actin filament.

## Methods

### Quantitative real-time PCR (qPCR) Analysis of Formin Expression

Methods as described in Chapter 2.

### C2C12 Cell Culture

To prepare glass coverslips, they were washed in 70% Ethanol, coated with 10% Poly-L-Lysine (Sigma-Aldrich, St. Louis, MO) for 20 minutes, washed with phosphate-buffered saline (Life Technologies, Grand Island, NY) twice after removing Poly-L-Lysine, washed with sterile water twice, and placed under UV light for 18 hours. Glass coverslips were then coated with 3mg/ml Type I rat tail collagen (Corning Incorporated Life Sciences, Tewksbury, MA) and dried under UV light for three hours. The mouse myoblast cell line C2C12 (ATCC<sup>®</sup> Manassas, VA), isolated from the thigh muscles of dystrophic mice (Yaffe and Saxel, 1977) was seeded on prepared coverslips in growth medium containing Dulbecco's modified eagle medium, DMEM (Life Technologies, Grand Island, NY) containing 10% Fetal Bovine Serum (Gemini Bio-Products, West Sacramento, CA), 1% Penicillin Streptomycin (Life Technologies, Grand Island, NY) and 1% GlutaMAX<sup>™</sup> (Life Technologies, Grand Island, NY). To differentiate C2C12 cells the media was changed to differentiation medium containing DMEM 4% horse serum (Life Technologies, Grand Island, NY), 1% Penicillin Streptomycin and 1% GlutaMAX<sup>™</sup>, which was changed every 48 hours until cells were fully differentiated.

### **FHOD1 and FHOD3 Expression**

FHOD1 and FHOD3 levels in differentiating C2C12 cells were analyzed using SDS-PAGE and Western blot analysis between zero and 193 hours of differentiation. Cells were grown to 90% confluency in growth media, changing the media to differentiation media was marked as time point 0 of differentiation. Cells were lysed using 4°C lysis buffer containing 10% Glycerol (Fischer, Pittsburgh, PA), 1% NP40 (Merck, Germany), 1mM DTT (Bio-Rad Laboratories, Hercules, CA), 0.1mM EDTA (Sigma-Aldrich, St. Louis, MO), 1mM PMSF (Sigma-Aldrich, St. Louis, MO), 10µg/ml Aprotinin (Sigma-Aldrich, St. Louis, MO), 10µg/ml Leupeptin (Sigma-Aldrich, St. Louis, MO), 150mM NaCl<sub>2</sub>, 50mM MgCl<sub>2</sub> and 50mM HEPES (Life Technologies, Grand Island, NY). The antibodies used for Western Blot analysis were Fhod1 (C-14) and Fhod3 (K-19 and E-20) and transaldolase (T-20) (Santa Cruz, Dallas, TX). Western blots for FHOD1 and FHOD3 were normalized against transaldolase and analyzed in Image J (National Institutes of Health, Bethesda, MD). A total of 29 time points were used for each protein's intensity graph.

### **Sample Preparation for Microscopy**

Cells were washed with room temperature phosphate buffered saline, (PBS, Life Technologies, Grand Island, NY) twice, incubated with 3.7% Formaldehyde (Fischer, Pittsburgh, PA), 1% TX-100 (Fischer, Pittsburgh, PA) in PBS for 10 minutes at 4°C, washed with PBS twice, incubated with 1M Glycine

## Chapter 3 – Endogenous Fhod1 and Fhod3 in the Sarcomere

(Fischer, Pittsburgh, PA) in PBS for 20 minutes at room temperature, washed with PBS twice, incubated with 3% Bovine Serum Albumin (BSA, Sigma-Aldrich, St. Louis, MO) 1% TX-100 for 2 hours at room temperature, washed with PBS twice, and incubated with primary antibody for two hours at 37°C. Primary antibodies for Fhod1 C-14, Fhod3 K-19 and E-20 (Santa Cruz, Dallas, TX), alpha-actinin (Sigma-Aldrich, St. Louis, MO) were incubated in 1% BSA 0.5% TX-100 for 2 hours at 37°C. Myomesin antibody was isolated from supernatant obtained from mMaC myomesin B4 (Developmental Studies Hybridoma Bank, University of Iowa) grown in Iscove's DMEM (Life Technologies, Grand Island, NY) containing 20% FBS and 1% Gentamicin. C2C12 cells were incubated with myomesin supernatant for 2 hours at 37°C. After primary antibody incubation, cells were washed with PBS three times, and incubated with secondary antibodies anti-goat FITC and TRITC and anti-mouse TRITC (Jackson ImmunoResearch Laboratories, West Grove, PA) and DAPI (Life Technologies, Grand Island, NY) in 1% BSA 0.5% TX-100 for 1 hour at 37°C.

### **Microscopy & Image Analysis**

Images were captured using a Nikon Eclipse E800 microscope and analyzed using NIS-Elements AR 3.10 software (Nikon Instruments Inc. Melville, NY). Intensity profile analysis was performed using NIS Elements AR 3.10.

## Results

### FHOD1 and FHOD3 Expression levels.

FHOD1 and FHOD3 were found to be the most and least expressed formins, respectively, across 22 different human tissues and cell lines, with levels of expression of 54% and 26% of the expression of the 18S ribosomal subunit, as shown in Figure 1.

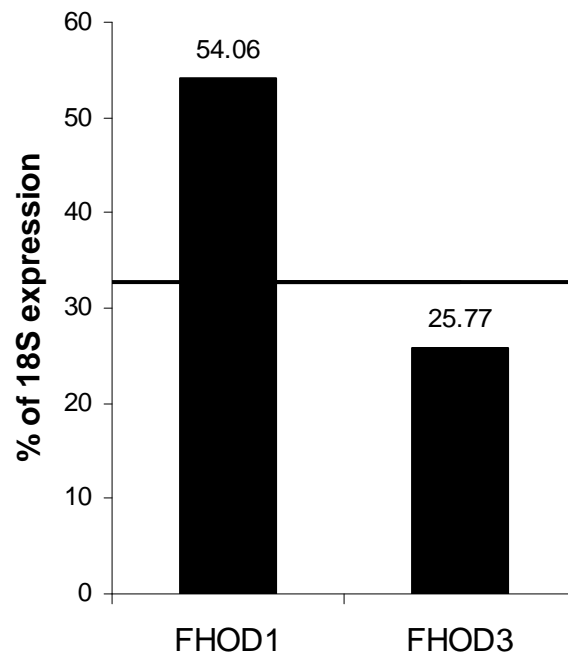


### Figure 1: FHOD1 and FHOD3 expression in 22 cell types and tissues

The levels of formin expression in all cell and tissue types analyzed in chapter 2 were analyzed. Two formins, FHOD1 and FHOD3, were notable for consistently high and low expression, respectively. Line indicates the average expression of all 15 formins in all cells. Data are reported as the average percentage of expression of 18S ribosomal subunit,  $p < 0.05$ . FHOD1 and FHOD3 data points have a  $p$ -value of  $< 0.05$ . (Krainer, et al., 2013)

### Formin Expression in Skeletal and Cardiac Muscle

An expression analysis of all 15 human formins in cardiac and skeletal muscle showed that FHOD1 and FHOD3 were both highly expressed, with expression levels of 20% and 32% in skeletal muscle and 28% and 23%, respectively, as shown in Figure 2.

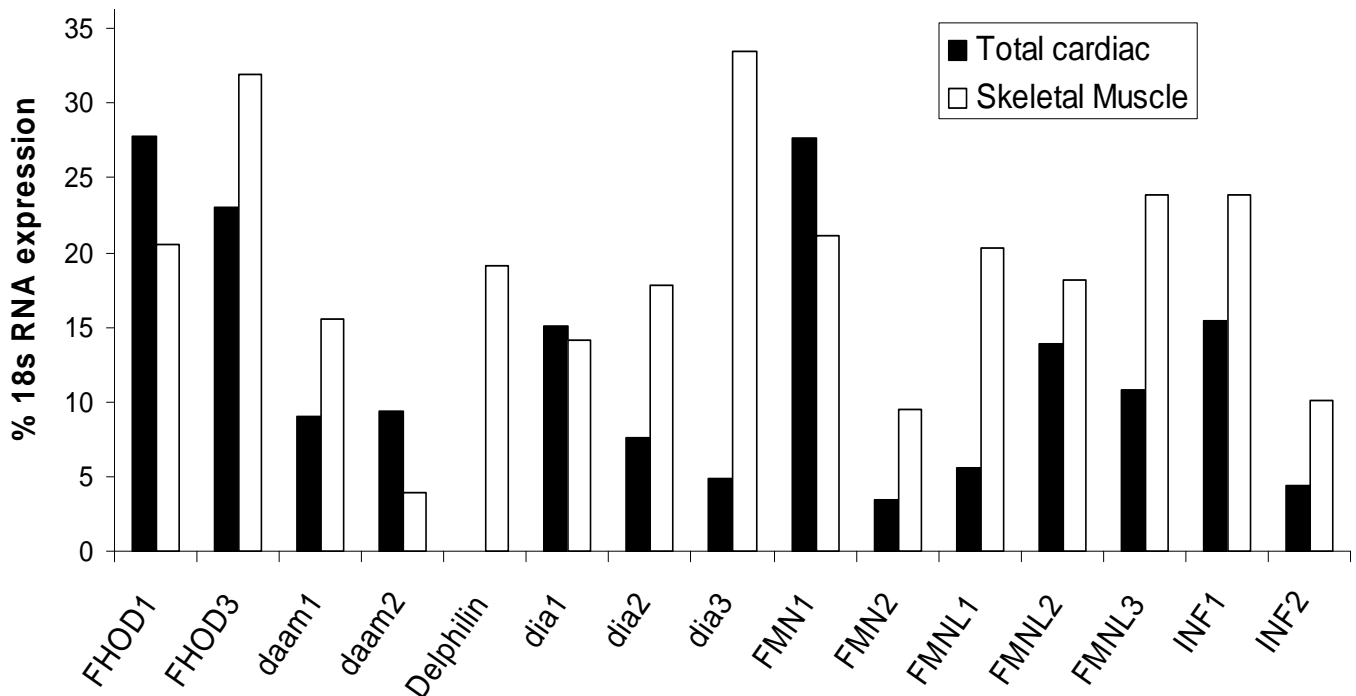


**Figure 2: Formin expression in cardiac and skeletal muscle.**

As analyzed in chapter 2, the level of expression of all formins in cardiac and skeletal muscle. Data are reported as the average percentage of expression of 18S ribosomal subunit,  $p < 0.05$ . (Krainer, et al., 2013)

### Protein Expression Analysis of FHOD1 and FHOD3 in C2C12 Cells

The expression levels of FHOD1 and FHOD3 were tracked throughout C2C12 development until full differentiation was achieved. Western Blot analysis shows increasing levels of FHOD1 and FHOD3 throughout C2C12 differentiation, as shown in Figure 3A. After normalizing the levels against transaldolase visually, a graph was constructed to show the relative levels of FHOD1 and FHOD3, as shown in Figure 3B. A clear increase in the level of both proteins can be seen throughout differentiation, but no further significant increase was observed after day 8 or 200 hours.

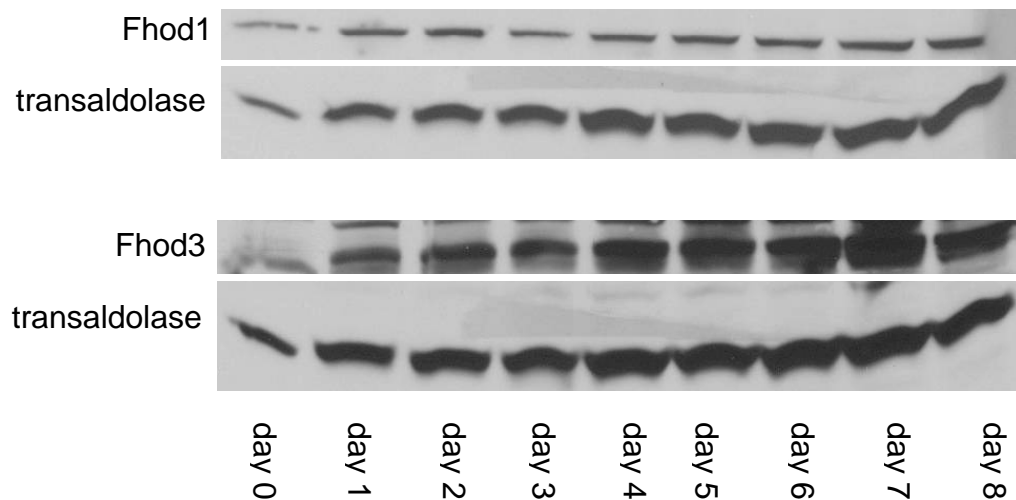


**Figure 3A: FHOD1 and FHOD3 during C2C12 differentiation**

Western Blot analysis of FHOD1 and FHOD3 with transaldolase control.

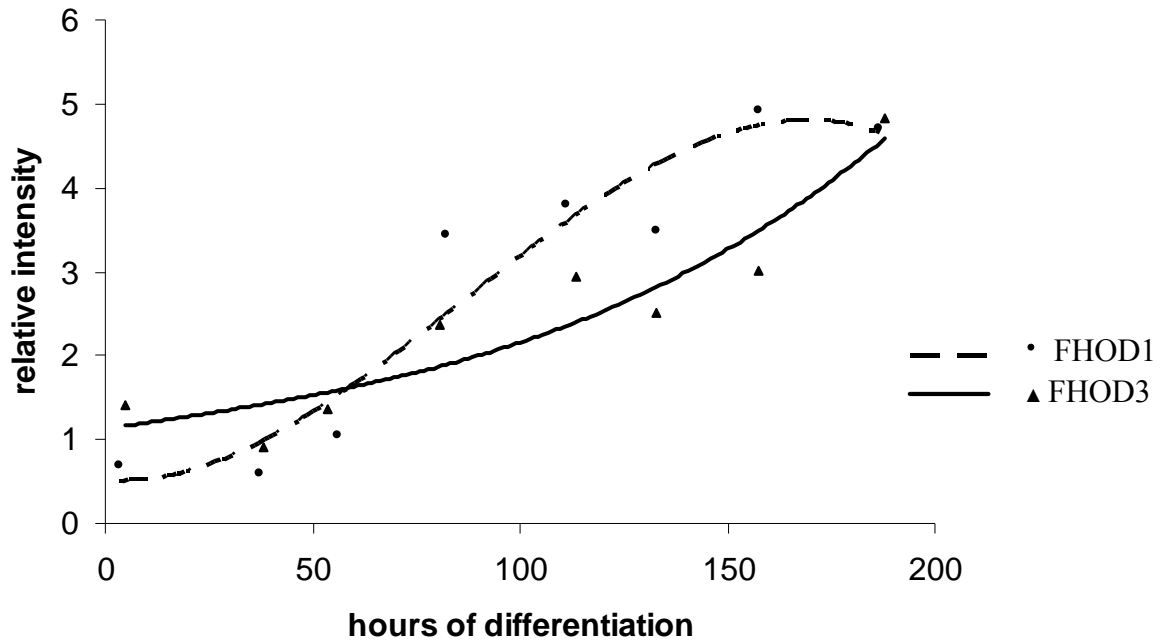


**Figure 3B: FHOD1 and FHOD3 intensity throughout C2C12 differentiation**

FHOD1 and FHOD3 relative levels of intensity are shown over the course of C2C12 cell differentiation between zero and 193 hours. The graph is a polynomial function of the third order of 29 time points for each protein.

### **Localization of Endogenous FHOD1 in the Sarcomere**

Figure 4 shows the localization of FHOD1 in relationship to the M-line marker myomesin. Myomesin localizes to the very center of the sarcomere, and as seen in the merged images, there is a periodic pattern, indicating the sarcomeric arrangement of myomesin, with FHOD1 localizing in between myomesin bands. The line intensity analysis shows that red and green spikes alternate, confirming that FHOD1 alternates with myomesin in the sarcomere, indicating that FHOD1 localizes to the area of the Z-disk in mature myotubes. Note that the fluorescent overlap of FITC and TRITC emission creates some bleed-through of TRITC in the FITC channel.

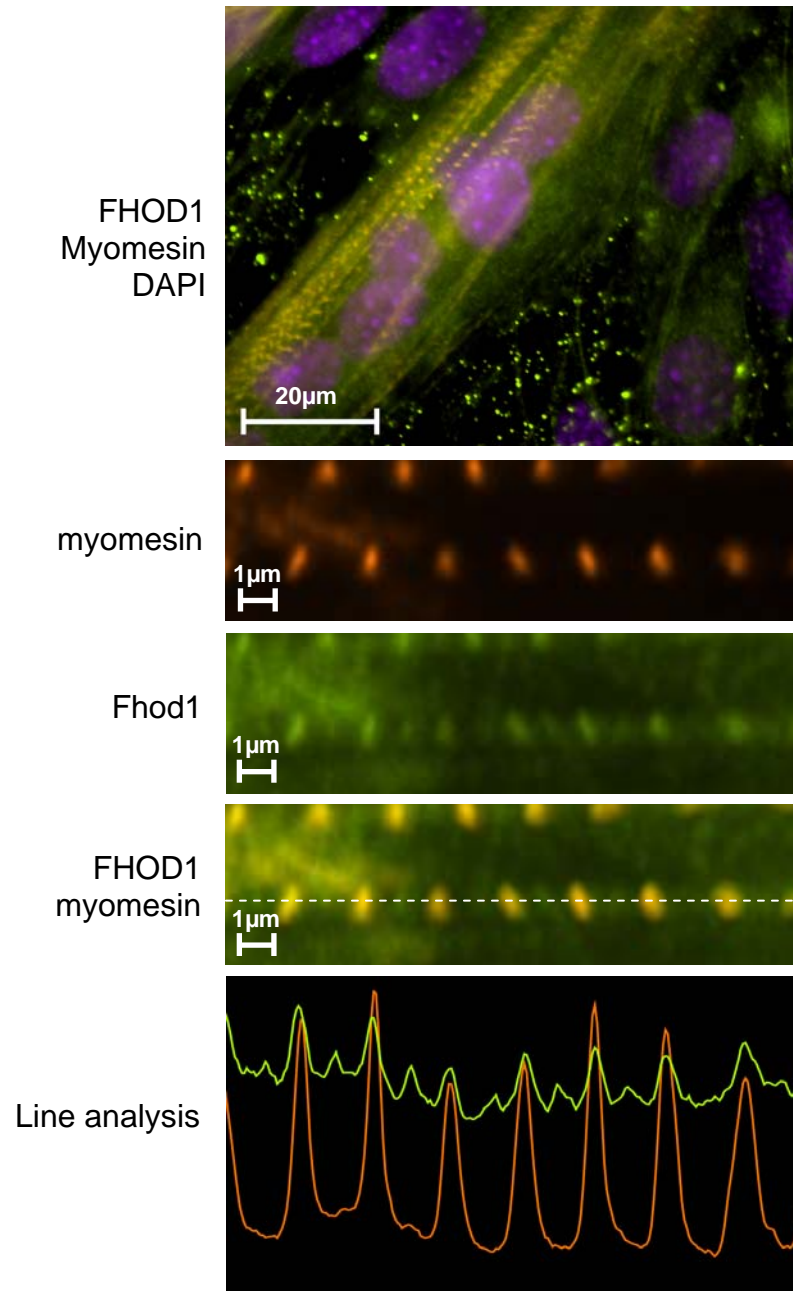
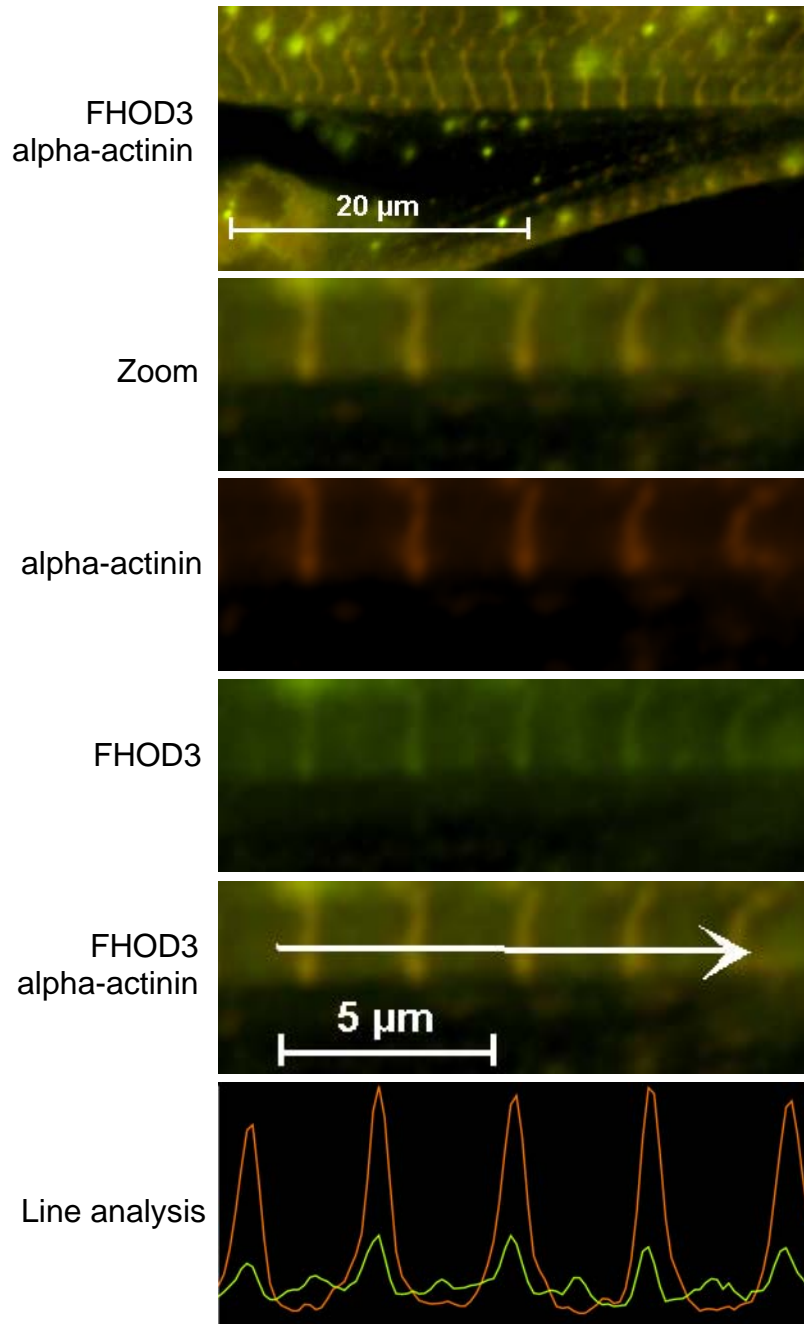


**Figure 4: FHOD1 immunohistochemistry in C2C12 cells with myomesin**  
FHOD1 localization compared to the M-line marker myomesin shows FHOD1 to localize near the Z-line.

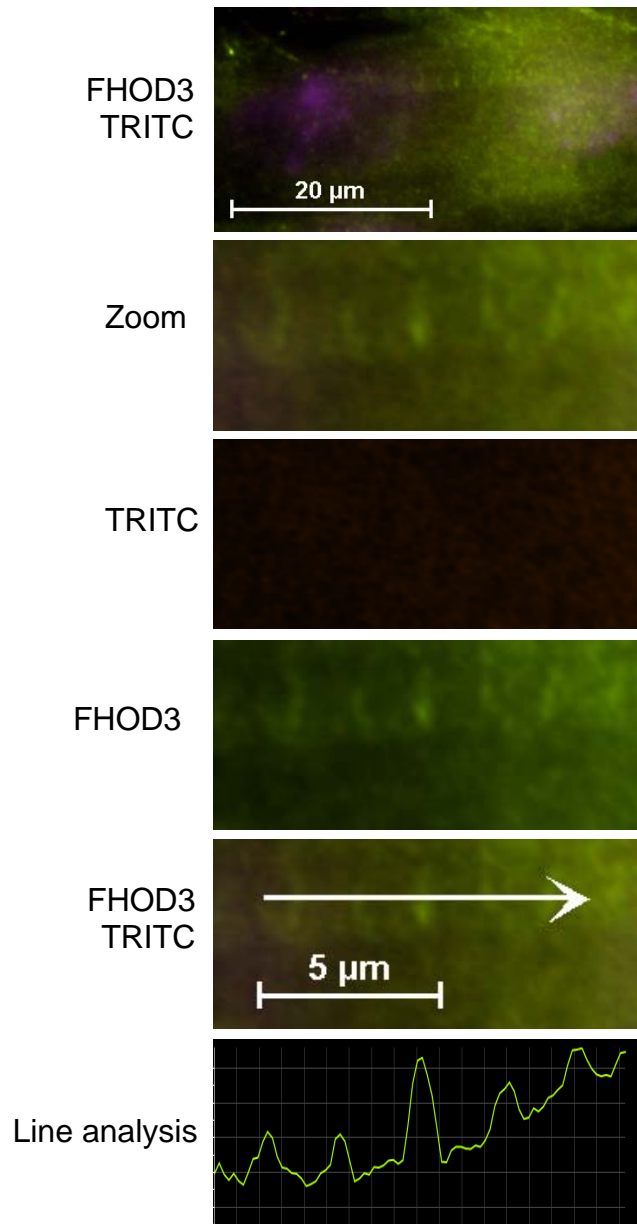
### **Localization of Endogenous FHOD3 in the Saromere**

Figure 5 shows that localization of FHOD3 in relationship to the Z-disk marker alpha-actinin. The first image in Figure 5 shows the periodic arrangement of alpha-actinin, with the zoomed images showing a pattern of alternating green and red. FHOD3 appears to localize right in between the lines of alpha actinin, indicating that it localizes to the area of the center of the sarcomere where the M-line and the H-band can be found. In the line analysis, considering the spaces between the first and second and the fourth and fifth alpha actinin peak it looks as if FHOD3 has a slight double-peak, indicating that there may be two thin lines of FHOD3 at the center of the sarcomere, most likely on either side of the M-line, considering the regular arrangement of the sarcomere. Note that the fluorescent overlap of FITC and TRITC emission creates some bleed-through of TRITC in the FITC channel.

Figure 6 shows FHOD3 by itself without any other sarcomeric markers. The images and line analysis show a periodic sarcomeric pattern of FHOD3 bands, with an average distance of 1.74 $\mu$ m between bands, confirming that FHOD3 localizes to a specific part of the sarcomere.



**Figure 5: FHOD3 immunohistochemistry in C2C12 with alpha actinin**  
FHOD3 co-localization with Z-disc marker alpha-actinin. Fhod3 seems to localize to the space between the Z-discs.



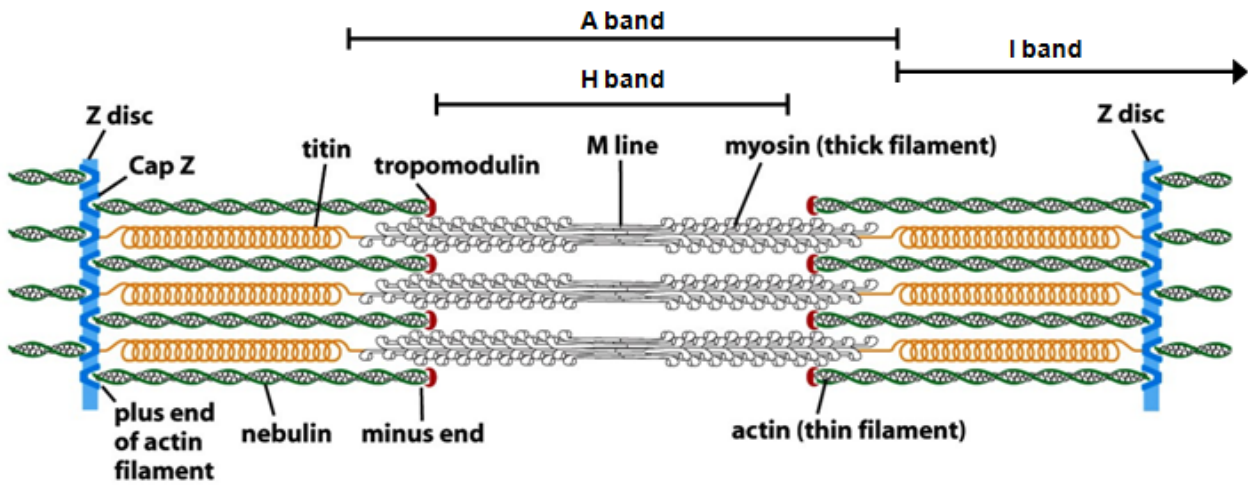
**Figure 6: FHOD3 immunohistochemistry in C2C12 cells**

FHOD3 antibody showing sarcomeric arrangement. Average distance between FHOD3 bands is 1.74μm, confirming sarcomeric patterning.

### **Models for FHOD1 and FHOD3 Localization in the Sarcomere**

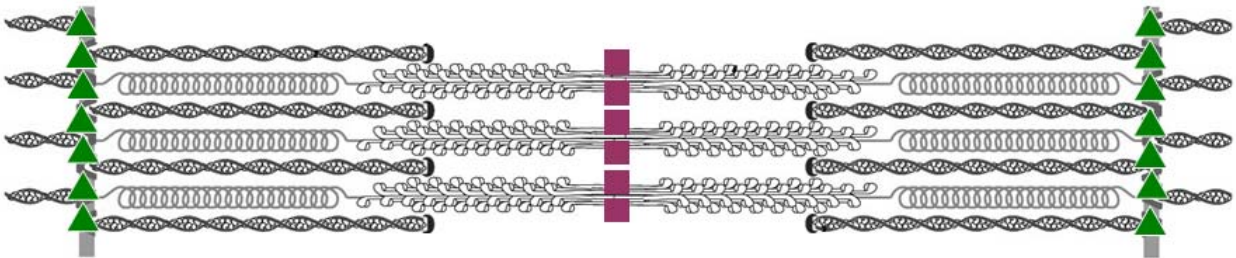
Based on the fluorescent microscopy data presented, Figure 7 shows two proposed models for FHOD1 and FHOD3 localization in the sarcomere. Figure 7a shows a non-contracted sarcomere, as seen by the small area of overlap between thin and thick filaments and the wide H-band. A contracted sarcomere has an almost non-existent H-band and almost complete overlap of the thin and thick filaments. When fixing cells for immunohistochemical analysis, cells contract, the space in the H-band is greatly compressed, making it difficult to distinguish between the pointed end of the actin filament and the M-line. Thus we present two alternate possibilities for FHOD3 localization. For ease of visualization, a relaxed sarcomere is shown in Figure 7b and 7c.

Figure 7b shows the localization as it appears in the microscopy image analysis, with FHOD1 localizing in between the M-bands, to the area of the Z-disk and FHOD3 localizing in between bands of alpha actinin, to the area at or near the M-band. Based on the first and fourth of the FHOD3 peaks in Figure 5, it seems possible that FHOD3 localizes as two thin bands on either side of the M-band. The level of resolution attained with the equipment used does not allow for any further actual discrimination, such as whether FHOD1 localizes exactly to the Z-disk or to the barbed ends of actin that are anchored at the Z-disk. However, based on the function of formins, the model in Figure 7c shows what could be the likely localization of FHOD1 and FHOD3 inside the sarcomere: FHOD1 at the barbed ends of actin along either side of the Z-disk, and FHOD3 at the pointed end of actin towards the center of the sarcomere.



**Figure 7a: Components of the Sarcomere**

adapted from: Alberts, et al, 2003, p 963



**Figure 7b: FHOD1 and FHOD3 localization in the sarcomere model 1**

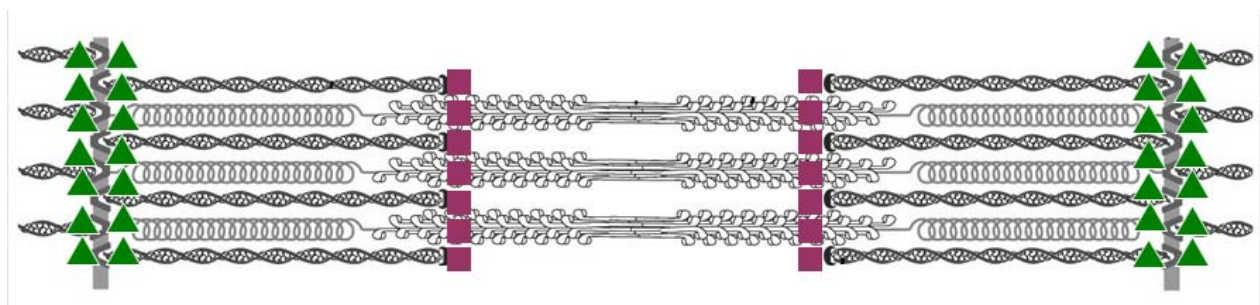


**Figure 7c: FHOD1 and FHOD3 localization in the sarcomere model 2**

- ▲ endogenous FHOD1
- endogenous FHOD3

**Figure 7: Endogenous FHOD1 and FHOD3 localization in the sarcomere**

## Discussion

High levels of expression of FHOD1 and FHOD3 in muscle as compared to other formins suggests a function for these proteins related to either sarcomere assembly or maintenance. To elucidate the possible roles of FHOD1 and FHOD3, this study aimed to determine the sarcomeric localization of endogenous FHOD1 and FHOD3 in murine C2C12 cells.

### FHOD1 Localization

Based on the results of this study, FHOD1 appears to localize with sarcomeric periodicity between M-lines, which corresponds to the area of the Z-disk. As shown in Figures 7a and 7b, the exact location of FHOD1 in the sarcomere is unclear because of the limitations of microscopic resolution. While the fluorescent microscopy analysis places FHOD1 at the Z-disk, based on the actin-binding motif in FHOD1's FH2 domain, it appears likely that FHOD1 localizes to the barbed ends of actin, which are anchored at the Z-disk. The arrangement of proteins at the Z-disk is such that the barbed end of the actin filament and the Z-disk itself are very difficult to distinguish using light microscopy. This localization to or near the Z-disk is congruent with the findings of other studies in murine cardiac muscle and *Caenorhabditis elegans* (Dwyer, et al., 2014; Mi-Mi, et al., 2012). To further clarify the exact localization of FHOD1 in the sarcomere using immunohistochemical methods, co-localization with alpha-actinin or CapZ may help to determine how close to the Z-disk FHOD1 localizes.

Other possible antibodies that could help narrow the range of localizations for FHOD1 include actin and the thin filament markers troponin and tropomyosin.

### **FHOD3 Localization**

Based on the data presented in this study, endogenous FHOD3 appears to localize periodically between the Z-disks, placing it at the center of the sarcomere at the area of the M-line. As part of the data in Figure 5 suggests, it seems likely that FHOD3 localizes to the pointed end of actin, which, in a contracted sarcomere, appears as two closely spaced lines on either side of the M-line. This localization has been seen in studies in both embryonic and adult murine cardiomyocytes, but to date has not been demonstrated in skeletal muscle (Taniguchi, et al., 2009; Kan-o, et al., 2010). Other studies have suggested that FHOD3 does not localize to the pointed end of actin, but between the ends of actin filaments and the M-line, to the area of overlap between thin filaments and thick filaments (Kan-o, et al., 2010). Such a localization would be completely new to FHOD3 and formins in general, as no formins have been shown to bind to myosin. To clarify the exact localization of FHOD3, further immunohistochemical studies could be performed using other sarcomeric markers, such as thin filament markers (actin, troponin, tropomyosin) and the M-line marker myomesin.

## References

Alberts B, Johnson A, Lewis J, Raff M, Roberts K and Walter P. 2002. *Molecular Biology of the Cell*. Garland Science, p963.

Chandhoke SK, Williams M, Schaefer E, Zorn L and Blystone SD. 2004. Beta 3 integrin phosphorylation is essential for Arp3 organization into leukocyte alpha V beta 3-vitronectin adhesion contacts. *J Cell Sci* 117:Pt 81431-1441.

Chereau D, Boczkowska M, Skwarek-Maruszczyńska A, Fujiwara I, Hayes DB, Rebowski G, Lappalainen P, Pollard TD and Dominguez R. 2008. Leiomodin is an actin filament nucleator in muscle cells. *Science* 320:5873239-243.

Dwyer J, Pluess M, Iskratsch T, Dos Remedios CG and Ehler E. 2014. The formin FHOD1 in cardiomyocytes. *Anat Rec (Hoboken) Wiley Periodicals, Inc* 297:91560-1570.

Huxley H and Hanson J. 1954. Changes in the cross-striations of muscle during contraction and stretch and their structural interpretation. *Nature* 173:4412973-976.

Kan-o M, Takeya R, Taniguchi K, Tanoue Y, Tominaga R and Sumimoto H. 2012. Expression and subcellular localization of mammalian formin Fhod3 in the embryonic and adult heart. *PLoS One* 7:4e34765.

Krainer EC, Ouderkirk JL, Miller EW, Miller MR, Mersich AT and Blystone SD. 2013. The multiplicity of human formins: Expression patterns in cells and tissues. *Cytoskeleton (Hoboken) Wiley Periodicals, Inc.* 70(8):424-38.

Mi-Mi L, Votra S, Kempfues K, Bretscher A and Pruyne D. 2012. Z-line formins promote contractile lattice growth and maintenance in striated muscles of *C. elegans*. *J Cell Biol* 198:187-102.

### Chapter 3 – Endogenous Fhod1 and Fhod3 in the Sarcomere

Moerman DG and Williams BD. 2006. Sarcomere assembly in *C. elegans* muscle. *WormBook* 1-16.

Sparrow JC and Schock F. 2009. The initial steps of myofibril assembly: integrins pave the way. *Nat Rev Mol Cell Biol* 10:4293-298.

Taniguchi K, Takeya R, Suetsugu S, Kan-O M, Narusawa M, Shiose A, Tominaga R and Sumimoto H. 2009. Mammalian formin fhod3 regulates actin assembly and sarcomere organization in striated muscles. *J Biol Chem* 284:4329873-29881.

Takano K, Watanabe-Takano H, Suetsugu S, Kurita S, Tsujita K, Kimura S, Karatsu T, Takenawa T and Endo T. 2010. Nebulin and N-WASP cooperate to cause IGF-1-induced sarcomeric actin filament formation. *Science* 330:60101536-1540.

Volk T, Fessler LI and Fessler JH. 1990. A role for integrin in the formation of sarcomeric cytoarchitecture. *Cell* 63:3525-536.

Yaffe D and Saxel O. 1977. Serial passaging and differentiation of myogenic cells isolated from dystrophic mouse muscle. *Nature* 270:5639725-727.

**Chapter 4:**

**Exogenous FHOD1 and FHOD3 in the Sarcomere**

## **Introduction**

FHOD1 and FHOD3 both have high levels of expression in striated muscle and both proteins have distinct localizations in the sarcomere (Kan-o, et al., 2012; Krainer, et al., 2013; Taniguchi, et al., 2009). In order to further determine the possible roles of FHOD1 and FHOD3 in sarcomere formation or maintenance, GFP-tagged cDNAs of both proteins are used for actin-binding mutant studies. In this study full-length FHOD1 and FHOD3 are introduced into the established C2C12 model system, as well as FHOD1 and FHOD3 actin-binding mutants.

## **Methods**

### **C2C12 Cell Culture**

To prepare glass coverslips, they were washed in 70% Ethanol, coated with 10% Poly-L-Lysine (Sigma-Aldrich, St. Louis, MO) for 20 minutes, washed with phosphate-buffered saline (Life Technologies, Grand Island, NY) twice after removing Poly-L-Lysine, washed with sterile water twice, and placed under UV light for 18 hours. Glass coverslips were then coated with 3mg/ml Type I rat tail collagen (Corning Incorporated Life Sciences, Tewksbury, MA) and dried under UV light for three hours. The mouse myoblast cell line C2C12 (ATCC<sup>®</sup> Manassas, VA), isolated from the thigh muscles of dystrophic mice (Yaffe and Saxel, 1977) was seeded on prepared coverslips in growth medium containing Dulbecco's modified eagle medium, DMEM (Life Technologies, Grand Island, NY) containing 10% Fetal Bovine Serum (Gemini Bio-Products, West Sacramento, CA), 1% Penicillin Streptomycin (Life Technologies, Grand Island, NY) and 1% GlutaMAX<sup>™</sup> (Life Technologies, Grand Island, NY). To differentiate C2C12 cells the media was changed to differentiation medium containing DMEM 4% horse serum (Life Technologies, Grand Island, NY), 1% Penicillin Streptomycin and 1% GlutaMAX<sup>™</sup>, which was changed every 48 hours until cells were fully differentiated.

### **Sample Preparation for Microscopy**

Cells were washed with room temperature phosphate buffered saline, (PBS, Life Technologies, Grand Island, NY) twice, incubated with 3.7%

Formaldehyde (Fischer, Pittsburgh, PA), 1% TX-100 (Fischer, Pittsburgh, PA) in PBS for 10 minutes at 4°C, washed with PBS twice, incubated with 1M Glycine (Fischer, Pittsburgh, PA) in PBS for 20 minutes at room temperature, washed with PBS twice, incubated with 3% Bovine Serum Albumin (BSA, Sigma-Aldrich, St. Louis, MO) 1% TX-100 for 2 hours at room temperature, washed with PBS twice, and incubated with primary antibody for two hours at 37°C. Primary antibodies for Fhod1 C-14, Fhod3 K-19 and E-20 (Santa Cruz, Dallas, TX), alpha-actinin (Sigma-Aldrich, St. Louis, MO) were incubated in 1% BSA 0.5% TX-100 for 2 hours at 37°C. Myomesin antibody was isolated from supernatant obtained from mMaC myomesin B4 (Developmental Studies Hybridoma Bank, University of Iowa) grown in Iscove's DMEM (Life Technologies, Grand Island, NY) containing 20% FBS and 1% Gentamicin. C2C12 cells were incubated with myomesin supernatant for 2 hours at 37°C. After primary antibody incubation, cells were washed with PBS three times, and incubated with secondary antibodies anti-goat FITC and TRITC and anti-mouse TRITC (Jackson ImmunoResearch Laboratories, West Grove, PA) and DAPI (Life Technologies, Grand Island, NY) in 1% BSA 0.5% TX-100 for 1 hour at 37°C.

### **HeLa Cell Lipofection**

HeLa cells (ATCC® Manassas, VA) were grown on glass coverslips at a density of 75,000 cells per well in a 24-well plate in growth media containing 1ml of Dulbecco's modified eagle medium (DMEM, Life Technologies, Grand Island, NY) containing 10% Fetal Bovine Serum (Gemini Bio-Products, West

Sacramento, CA), 1% Penicillin Streptomycin (Life Technologies, Grand Island, NY) and 1% GlutaMAX™ (Life Technologies, Grand Island, NY) for 24 hours. After 24 hours the media was changed to 0.5ml of growth media. 25 µg DNA and 25 µL of Lipofectamine® 2000 (Life Technologies, Grand Island, NY) were incubated separately, each in a total of 150µl Opti-MEM® I Reduced Serum Media (Life Technologies, Grand Island, NY) and combined after five minutes, incubated for 20 minutes at room temperature and added to the cells. Cells were fixed after a 24 hour lipofection incubation.

### **C2C12 Lipofection**

C2C12 cells were grown to 75% confluency. The media was changed to 1ml 37°C DMEM containing 10% Fetal Bovine Serum and 1% GlutaMAX™. DNA plasmids in concentrations ranging from 1µg to 15µg and Lipofectamine® 2000 (Life Technologies, Grand Island, NY) were incubated separately, each in a total of 150µl Opti-MEM® I Reduced Serum Media (Life Technologies, Grand Island, NY) and combined after five minutes, incubated for 20 minutes at room temperature and added to the cells. After 24 hours 0.5ml of DMEM containing 10% Fetal Bovine Serum and 1% GlutaMAX™ was added, and after 48 hours the media changed to 3ml DMEM containing 4% horse serum (Life Technologies, Grand Island, NY), 1% Penicillin Streptomycin and 1% GlutaMAX™ for cell differentiation. The media was changed to 3ml DMEM containing 4% horse serum, 1% Penicillin Streptomycin and 1% GlutaMAX™ every 48 hours until cells fully differentiated.

### **siRNA Treatment of C2C12 cells**

C2C12 cells were grown to 75% confluency. The media was changed to 1ml 37°C DMEM containing 10% Fetal Bovine Serum and 1% GlutaMAX™. siRNA against FHOD1 (sc-155893, Santa Cruz, Dallas, TX) and FHOD3 (sc-75016, Santa Cruz, Dallas, TX) in concentrations ranging from 200 to 800µg per well in a 6 well-plate and 5-15µl of Lipofectamine® 2000 (Life Technologies, Grand Island, NY) were incubated separately, each in a total of 150µl Opti-MEM® I Reduced Serum Media (Life Technologies, Grand Island, NY) and combined after five minutes, incubated for 20 minutes at room temperature and added to the cells. After 24 hours 0.5ml of DMEM containing 10% Fetal Bovine Serum and 1% GlutaMAX™ was added, and after 48 hours the media changed to 3ml DMEM containing 4% horse serum (Life Technologies, Grand Island, NY), 1% Penicillin Streptomycin and 1% GlutaMAX™ for cell differentiation. The media was changed to 3ml DMEM containing 4% horse serum, 1% Penicillin Streptomycin and 1% GlutaMAX™ every 48 hours until cells fully differentiated.

### **FHOD1 cDNA and Mutants**

Full-length human FHOD1 cDNA (OriGene Technologies, Rockville, MD) was introduced into a GFP-Zeocin vector (Chandhoke et al., 2004) C-terminally to the GFP domain. Mutations at conserved actin-binding sites were introduced in the FH2-domain. Isoleucine 705 and Lysine 851 were changed to Alanine, resulting in the following mutants: GFP-Fhod1-705A, GFP-Fhod1-851A and the

double mutant GFP-Fhod1-705+851A (Xu, et al., 2004; Otomo, et al., 2005; Lu, et al., 2007).

### **FHOD3 cDNA and Mutants**

A partial C-terminal human FHOD3 (imaGenes, Berlin, Germany) clone was inserted into pCMV6-Sport (Adagene, Cambridge, MA) via restriction enzyme digestions of Sall-HF and AflIII (New England Biolabs, Ipswich, MA). The partial human Fhod3 clone was then inserted into pBluescript KS2 together with a novel DNA sequence obtained from oligomers containing restriction enzyme sites for AflIII and AsuII via NotI and Sall (New England Biolabs, Ipswich, MA). N-terminus Fhod3 was obtained by cloning skeletal muscle cDNA obtained through reverse transcription PCR using human skeletal muscle poly A<sup>+</sup> RNA (Clontech, Mountain View, CA) with primers 5'GGGCTGTCTTCACCACCAGGCGG3' 5'GGATATCGTCGTTTCGAACATGGCCACGCTGGC3' and inserted into pBluescript KS2 containing the C-terminus of Fhod3 via AsuII and AflIII. Full-length Fhod3 was then moved into a GFP-Zeocin vector via AsuII and NotI and subsequently into pcDNA3.1 (Adagene, Cambridge, MA) via BstI and NheI (New England Biolabs, Ipswich, MA). Mutations at known actin-binding sites were introduced in the FH2-domain. Isoleucine 971 and Lysine 1117 were changed to Alanine, resulting in the following mutants: GFP-Fhod3-971A and GFP-Fhod3-1117A (Xu, et al., 2004; Otomo, et al., 2005; Lu, et al., 2007).

### **Microscopy & Image Analysis**

Images were captured using a Nikon Eclipse E800 microscope and analyzed using NIS-Elements AR 3.10 software (Nikon Instruments Inc. Melville, NY). Intensity profile analysis was performed using NIS Elements AR 3.10 and intensity peaks were analyzed by finding the mid-point between the highest and lowest values of a peak and the width of the peak measured at the mid-point.

## Results

To ensure that these GFP-tagged cDNAs could be successfully expressed, GFP-tagged FHOD1 and FHOD3 were introduced into HeLa cells using lipofection, with Figure 1 showing expression of control GFP and GFP-FHOD1 and GFP-FHOD3. Column one shows all nuclei using DAPI, column two shows the GFP expression in certain cells and column three shows the merged view, demonstrating detectable levels of expression of both FHOD1 and FHOD3 in HeLa cells.

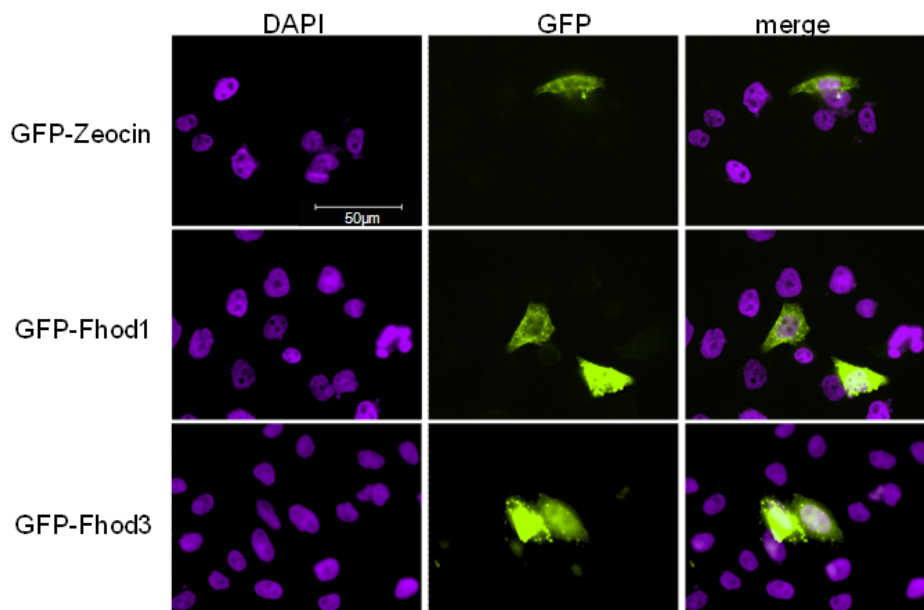


**Figure 1: GFP-tagged plasmids expressed in HeLa cells**

Control GFP and GFP-tagged FHOD1 and GFP-tagged FHOD3 plasmids expressed in HeLa cells.

### **Localization of GFP-FHOD1 and Actin-binding Mutants in the Sarcomere**

In order to determine whether actin-binding is important to FHOD1 localization, we first expressed wild type GFP-FHOD1, as shown in the first column in Figure 2. Note that the fluorescent overlap of FITC and TRITC emission creates some bleed-through of TRITC in the FITC channel. The M-line marker myomesin localizes to the center of the sarcomere, with GFP-FHOD1 localizing in two bands on either side of myomesin. The line analysis shows two GFP spikes on either side of the myomesin TRITC spike, confirming the localization of GFP-FHOD1 to the center of the sarcomere on either side of myomesin.

The actin-binding mutant GFP-FHOD1-705A, shown in Figure 2, column 2, also localizes in two bands on either side of myomesin. There is slightly more diffuse, non-descript localization than with full-length FHOD1, but the mutation at amino acid 705 does not completely interfere with localization of GFP-FHOD1-705A in the sarcomere.

The second actin-binding mutant GFP-FHOD1-851A, column 3 in Figure 2, does not appear to have any distinct localization within the sarcomere. Random, diffuse spots of GFP appear throughout the cell, but there is no periodicity or detectable co-localization with myomesin, as shown in the line analysis graph.

The double actin-binding mutant GFP-FHOD1-705A+851A, shown in column 4 of Figure2, has no detectable localization in the sarcomere. The protein

## Chapter 4 – Exogenous Fhod1 and Fhod3 in the Sarcomere

is still expressed as the cell has diffuse GFP expression throughout, but GFP does not aggregate at any specific points inside the cell.

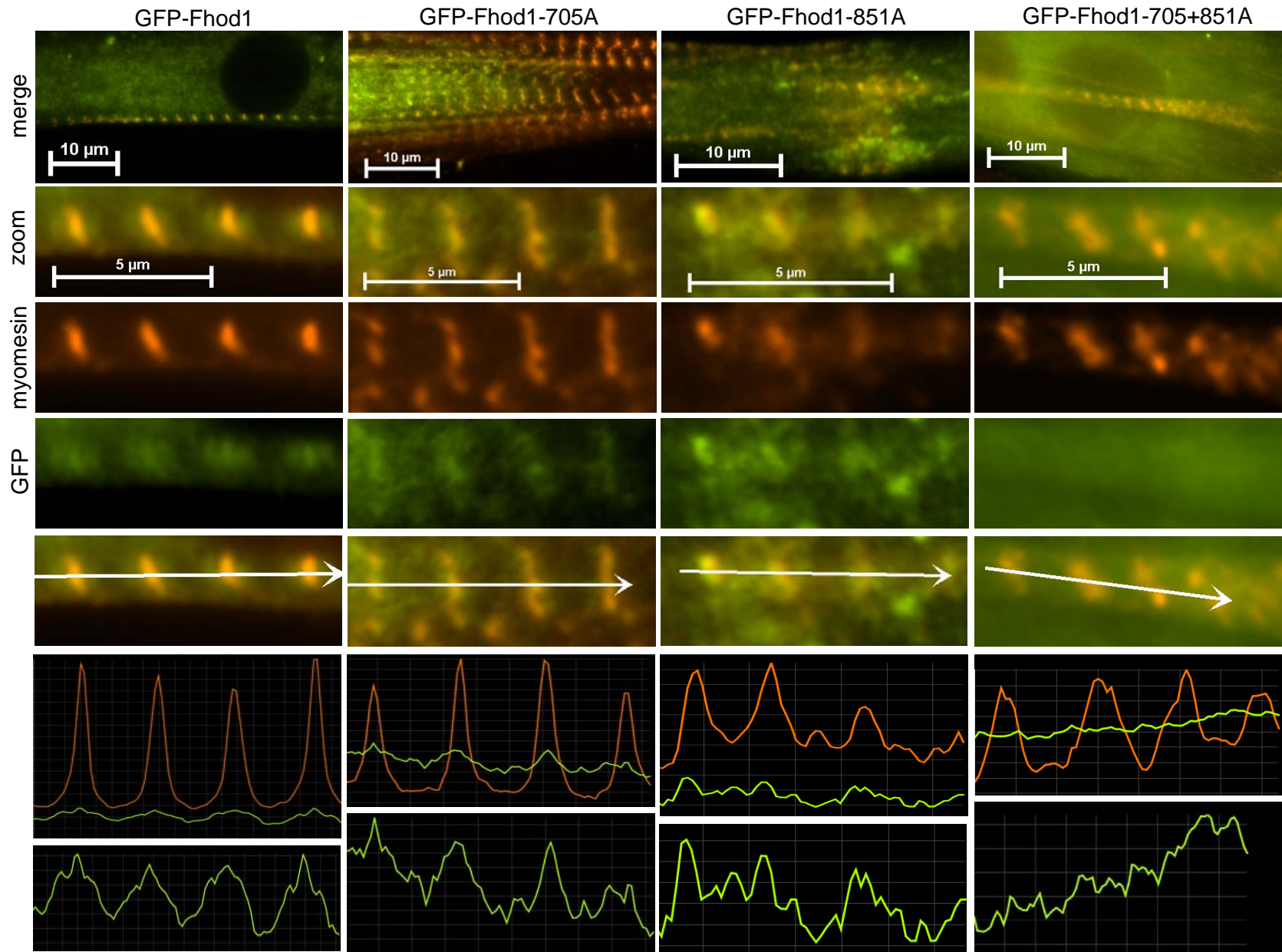


**Figure 2: Localization of GFP-Fhod1 and GFP-Fhod1 actin-binding mutants**

Figure 2 shows the expression of GFP-FHOD1 in column 1, single actin-binding mutant GFP-FHOD1-705A in column 2, single actin-binding mutant GFP-FHOD1-851A in column three and the double actin-binding mutant GFP-FHOD1-705A+851A in column four. All samples were stained for the M-line marker myomesin. The first row shows an overview of the transfected cells, the second column shows several sarcomeres with both GFP and myomesin-TRITC, the third row shows the myomesin-TRITC only to show the M-line, the fourth row shows the GFP-tagged formin and formin mutants, the fifth row indicates the line at which the line analysis was performed, which can be seen in row 6, with an amplified view of the GFP line analysis in row 7 to show the distribution of the GFP-tagged FHOD1 and FHOD1 mutants.

### Analysis of Sarcomeric Patterning in GFP-tagged Plasmid Expression

To determine whether the introduction of GFP-FHOD1 and GFP-FHOD1 mutants had any effect on the sarcomere itself, measurements were performed on the sarcomere as well as the intensity profile. While there was no statistically significant difference between full-length FHOD1 and the two single-point actin-binding mutants, there was a statistically significant difference between the full-length and single-point mutants and the double-point mutant, as shown in Figure 3. The width of the myomesin peak in the cells expressing the double mutant was significantly wider.

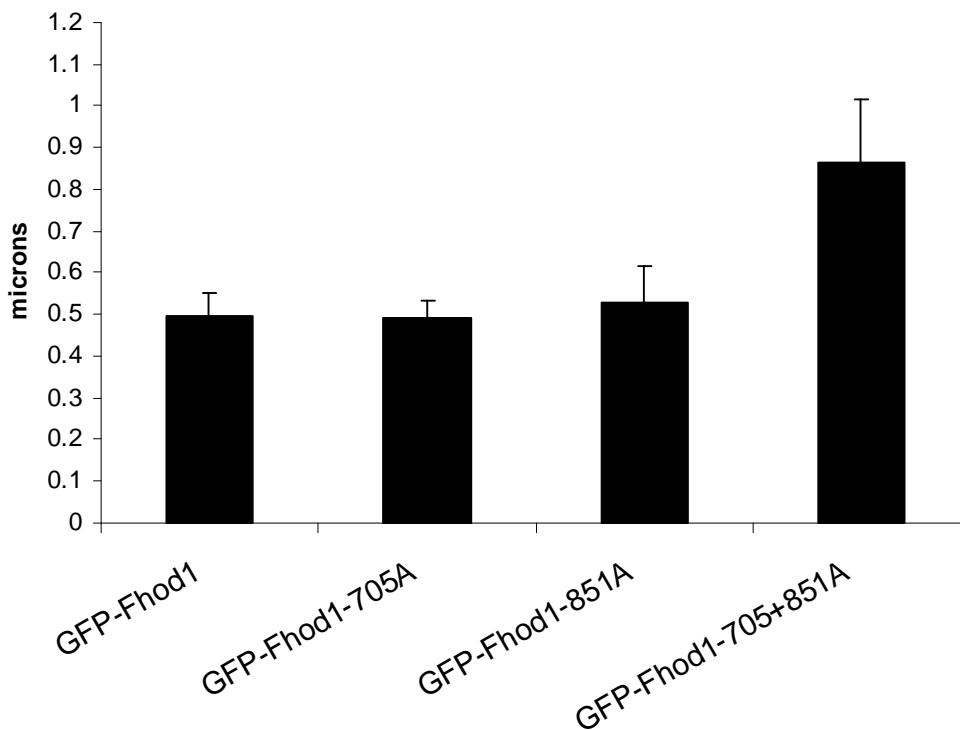


**Figure 3: Width of Intensity Profile Peaks at mid-point with standard deviation**

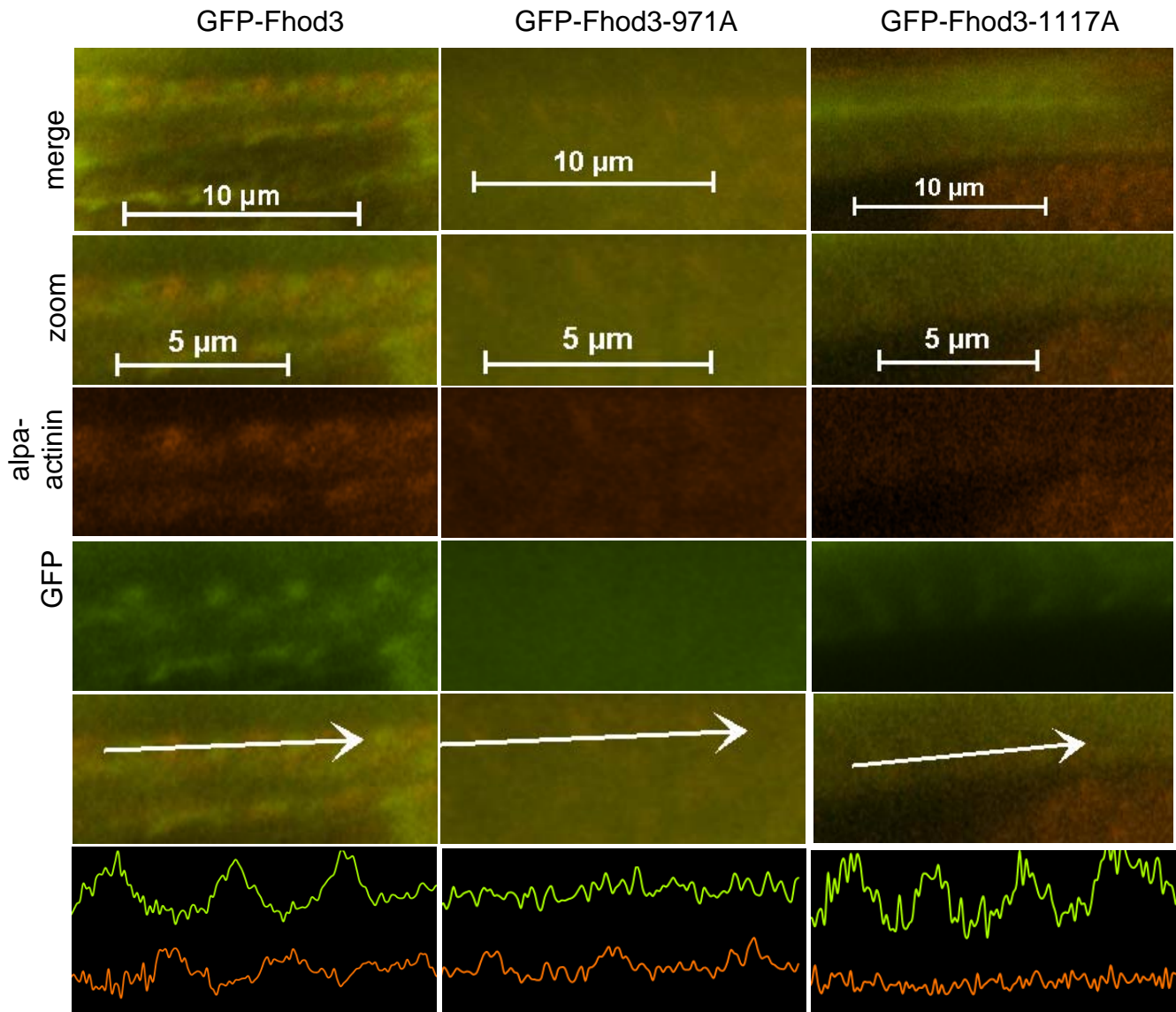
The width of the intensity profile peaks of myomesin were measured at the vertical mid-point, showing one standard deviation in the error bars.

### **Localization of GFP-FHOD3 and Actin-binding Mutants in the Sarcomere**

Full-length GFP-FHOD3 localizes to the area at the center of the sarcomere, as shown in Figure 4. Note that the fluorescent overlap of FITC and TRITC emission creates some bleed-through of TRITC in the FITC channel. The alpha-actinin and GFP-FHOD3 peaks in the intensity profile have an alternating periodic pattern, with the GFP-FHOD3 peaks falling in between alpha-actinin peaks, which indicate the location of the Z-disk.

The single-point actin-binding mutant GFP-FHOD3-971A does not show any distinct localization within the sarcomere. The diffuse non-specific distribution of GFP in column 2 in Figure 4 does not indicate any sarcomerically patterned localization for GFP-FHOD3-917A. The intensity profile analysis shows sarcomeric patterning for the Z-disk marker alpha-actinin, but no periodic pattern for GFP-FHOD3-917A.

The single-point actin-binding mutant GFP-FHOD3-1117A exhibits sarcomeric patterning, as shown in column three of Figure 4. Column three is not stained for alpha-actinin, indicated by the diffuse level of TRITC and lack of sarcomeric patterning of TRITC. However, GFP-FHOD3-1117A shows a typical sarcomeric arrangement, as seen in the periodic GFP-peaks in the intensity profile analysis. While the lack of co-localization with another sarcomeric marker means that there is no definitive answer to where GFP-FHOD3-1117A localizes, it can safely be assumed that this single-point actin mutant localizes to the same area of the sarcomere as full-length GFP-FHOD3, the center of the sarcomere.



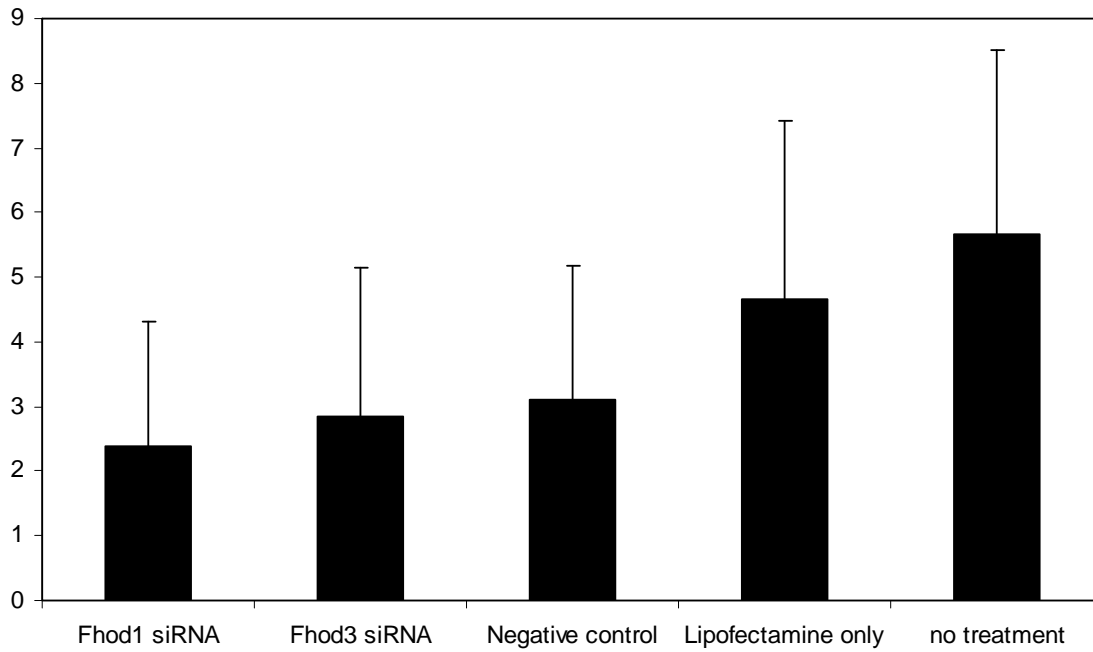
**Figure 4: Localization of GFP-Fhod3 and GFP-Fhod3 actin-binding mutants**

Figure 4 shows the expression of GFP-FHOD3 in column 1, single-point actin-binding mutant GFP-FHOD3-971A in column 2 and single-point actin-binding mutant GFP-FHOD3-1117A in column 3. Columns one and two were co-stained for the Z-disk marker alpha-actinin. The first row shows an overview of the cell, with a zoomed in view in the second row. The third row shows alpha-actinin localization, the fourth row GFP localization, and the fifth row indicates at which line the intensity analysis shown in row six was performed.

### **FHOD1 and FHOD3 siRNA**

After establishing the sarcomeric localization of endogenous and exogenous FHOD1 and FHOD3 and determining that the ability to bind actin via the FH2 domain effected their localization, we sought to test whether full-length and actin-binding mutants would be able to reverse the effects of knocking down the expression of endogenous FHOD1 and FHOD3.

FHOD1 and FHOD3 siRNAs were introduced into C2C12 cells using lipofection. Myotube formation was analyzed for lipofections with FHOD1 siRNA, FHOD3 siRNA and negative control siRNA, as well as for samples that received only Lipofectamine and samples that were untreated. Proper myotube formation was evaluated based on the size of myotubes and the number of nuclei per myotube. All experiments were performed in triplicates and myotube formation was analyzed by selecting three separate areas on each slide. A two tailed student's T-test showed that while Lipofectamine alone had no statistically significant effect on myotube formation, all siRNAs including the negative control siRNA affected myotube formation. As shown in Figure 5, the introduction of experimental siRNA had no statistically significant different effect than the negative control siRNA, making any siRNA experiments invalid due to the lack of a negative control that does not effect myotube formation. No further siRNA experiments were conducted.



**Figure 5: Average Number of Nuclei per Myotube for Fhod1 and Fhod3 siRNA treatments and controls**

Experiments were performed in triplicates, and myotube analysis was performed on three randomly selected areas in each sample.

p-values:

Fhod1 against negative control = 0.309

Fhod3 against negative control = 0.743

Negative control against no treatment = 0.004

Lipofectamine against negative control = 0.290

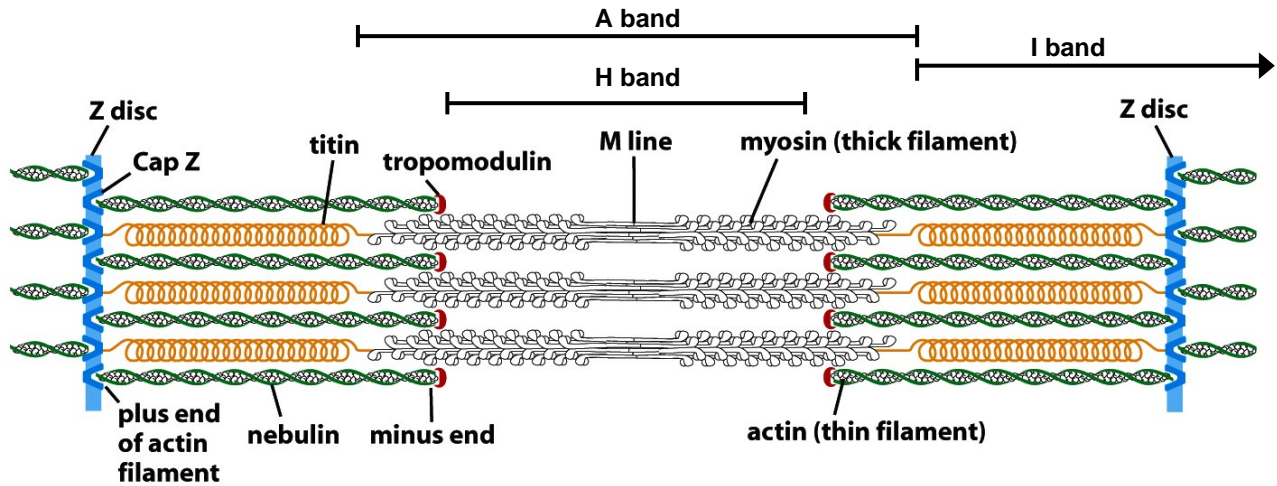
No treatment NA

### **Model of GFP-FHOD1 and GFP-FHOD3 Localization in the Sarcomere**

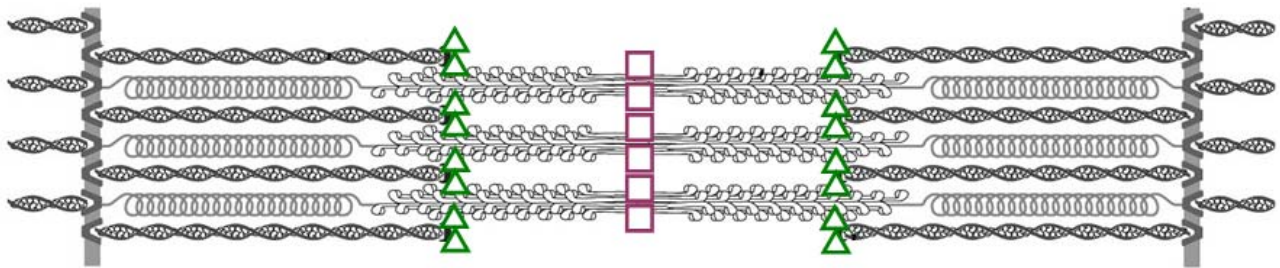
Based on the fluorescent microscopy data presented, Figure 6 shows two proposed models for GFP- FHOD1 and GFP-FHOD3 localization in the sarcomere. The figure shows a non-contracted sarcomere, as seen by the small area of overlap between thin and thick filaments and the wide H-band. A contracted sarcomere has an almost non-existent H-band and almost complete overlap of the thin and thick filaments. When fixing cells for immunohistochemical analysis, cells contract, and the space in the H-band is greatly compressed, making it difficult to distinguish between the pointed end of the actin filament and the M-line. For ease of visualization, a relaxed sarcomere is shown in Figure 6.

Figure 6b shows the localization of GFP-FHOD1 and GFP-FHOD3 as it appears in the image analysis. GFP-FHOD1 localizes in two bands on either side of the M-band, which is the pointed end of the actin filament in a contracted sarcomere. GFP-FHOD3 localizes in between bands of alpha-actinin, also placing it near the center of the sarcomere at the M-line.

Figure 6c shows an alternate model of GFP-FHOD1 and GFP-FHOD3 localization that takes into account the diminished localization of their actin-binding mutants. GFP-FHOD1 localizes in two bands on either side of the M-line, which is confirmed by intensity profile analysis in Figure 2. FHOD3, however, as proposed here, does not localize directly at the M-line, as suggested in Figure 6b, but also localizes to the pointed end of actin in the thin filament. The lack of sarcomeric localization of the single-point actin-binding mutant GFP-FHOD3-971 confirms this localization, since there is no actin directly at the M-line.



**Figure 6a – Components of the Sarcomere**  
 adapted from: Alberts, et al, 2003, p 963



**Figure 6b – GFP-FHOD1 and GFP-FHOD3 in the Sarcomere Model 1**

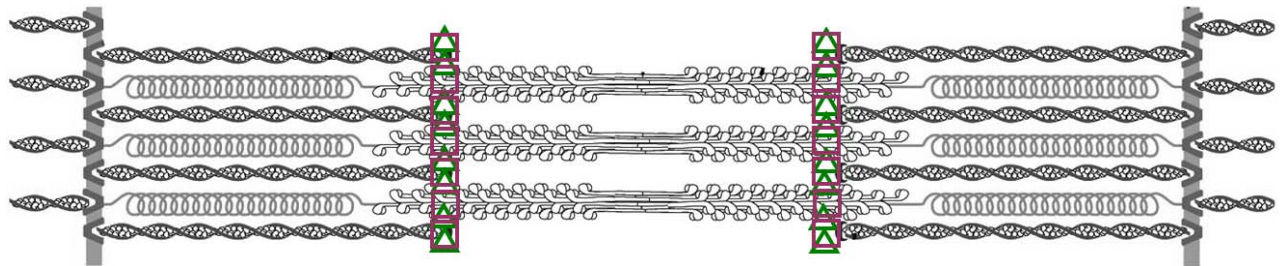


**Figure 6c – GFP-FHOD1 and GFP-FHOD3 in the Sarcomere Model 2**

- △ GFP-FHOD1
- GFP-FHOD3

**Figure 6: Exogenous FHOD1 and FHOD3 localization in the sarcomere**

## Discussion

Full-length GFP-FHOD1 and GFP-FHOD3 as well as actin-binding mutants were successfully introduced into the C2C12 model system. Based on the findings of localization of GFP-FHOD1 and GFP-FHOD3 and their actin-binding mutants, this study suggests that both proteins rely on the actin-binding motifs inside the FH2 domain for localization in the sarcomere.

### **GFP-FHOD1 Localization is Actin-binding Dependent**

GFP-FHOD1 localizes in bands on either side of the M-line in the sarcomere. This is in contrast to the localization of endogenous FHOD1, which is seen at the area of the Z-disk, and is likely at the barbed ends of the actin filament that are anchored at the Z-disk, as discussed in Chapter 3. This disparity could be due to a host of different factors. The addition of GFP to the FHOD1 molecule could affect the protein structure in a way that would make it incompatible with the space available at the Z-disk, thus forcing GFP-FHOD1 to bind to the next-best site in the sarcomere, which could be the pointed end of actin. Considering that FHOD3 localizes to the pointed end of actin it is not unreasonable to assume that FHOD1 would have enough structural and molecular similarities to mimic FHOD3 binding. Another reason could be the turn-over rate of endogenous FHOD1. Since no knock-down of endogenous FHOD1 was performed in conjunction with the introduction of GFP-FHOD1, the exogenous protein had to compete with the endogenous form. The turn-over rate of endogenous FHOD1 could be very slow, perhaps several days, and so the binding site that endogenous FHOD1 occupies at the barbed end of actin at the Z-disk is occupied and exogenous FHOD1 is

not able to bind in its place. Despite the inability of the exogenous FHOD1 to localize as endogenous FHOD1 does, the findings of the actin-binding study remain valid. The actin-binding mutant GFP-FHOD1-705A retains some of its actin-binding ability, while the mutant GFP-FHOD1-851A loses most of its actin-binding ability. The double-mutant GFP-FHOD1-705A+581A loses its ability to localize in the sarcomere altogether and appears to be present diffusely throughout the cell without any aggregates. This leads to the conclusion that both Isoleucine 705 and Lysine 851 are required for proper actin-binding of the FHOD1's FH2 domain.

The pointed end of actin in the thin filament is capped by tropomodulin, but even at the slow-growing end there is a steady exchange of actin-monomers, with tropomodulin forming a leaky cap controlled by the interaction of nebulin, nebulin and tropomodulin (Littlefield and Fowler, 1998; Littlefield and Fowler, 2008). Findings in *Drosophila melanogaster* and *Gallus gallus domesticus* have shown that in non-immortalized striated muscle cells, significant turn-over and growth of the actin filament occurs at the pointed end of actin (Littlefield, et al., 2001; Mardahl-Dumesnil and Fowler, 2001; Bai, et al., 2007). C2C12 cells are non-immortalized primary muscle cells, and it can safely be assumed that there is significant exchange of actin monomers at the pointed end. This turn-over of monomers, combined with the leaky tropomodulin cap means that the pointed end could easily be accessible to an actin-binding protein such as FHOD1. While the non-endogenous localization of GFP-FHOD1 does not allow for conclusions based on its physiological functions within the sarcomere, the diminished actin-binding capacity does suggest that full-length FHOD1 is capable of binding actin at or near the pointed end, and that the conserved actin-binding sites 705 and 851 are

necessary for FHOD1 to bind actin at or near the pointed end. The linear localization of GFP-FHOD1 to the middle of the sarcomere suggests that rather than binding the sides of the actin filament, GFP-FHOD1 binds the ends of the filament. Whether there is a competitive binding mechanism with tropomodulin or both proteins act as pointed end cappers is unclear.

Another possibility is that GFP-FHOD1 binds to the side of the actin filament. A constitutively active form of FHOD1 has been shown to bundle 5-10 parallel actin filaments, indicating that FHOD1 may be able to bind to the sides of actin filaments (Schönichen, et al., 2003). Furthermore, another DRF, FMNL1, has been shown to have actin-binding residues located outside of the conserved actin-binding FH2 domain to bind to the sides of actin filaments, and as shown in appendix 1, GFP-FMNL1 is likely capable of binding the sides of actin filaments in the sarcomere (Harris, et al., 2006). The demonstrated inability of FHOD1 to polymerize actin combined with a slow rate of turnover of endogenous FHOD1 at the Z-disk could make such a side-binding localization of GFP-FHOD1 likely. However, if GFP-FHOD1 uses residues outside of the conserved actin-binding residues in the FH2 domain, the mutation of those conserved actin-binding residues in the mutants GFP-FHOD1-705A and GFP-FHOD1-851A would not have any effect on its ability to bind to actin. The conserved residues Isoleucine and Lysine were replaced with Alanine residues, which are not known to cause any conformational change, so the decreased localization is not likely due to a change in the protein's folding.

The C2C12 model system is of murine origin, while the constructs introduced are based on human sequences. The protein sequences of human (NP\_037373) and

murine FHOD1 (NP\_808367) share 91% identity and 94% similarity, with the conserved actin-binding residues being identical. While there is a possibility that the difference in species may be the cause of the different localization of the endogenous murine FHOD1 and the exogenous human FHOD1, the degree of similarity and identity, especially with the actin-binding sites conserved makes this unlikely. The best way to confirm this would be to create murine constructs and introduce them into C2C12 cells, or, to introduce the human constructs into human skeletal muscle cells, the latter of which would be much quicker. If the human FHOD1 cDNA localizes to the barbed end of the actin filament in a human cell, the difference in localization in C2C12 cells is most likely due to the difference in human and murine FHOD1.

### **Myomesin Band Wider in GFP-FHOD1 Double Mutant**

The question of why the myomesin bands appear to be wider in the double-point actin-binding mutant of GFP-FHOD1 in Figure 3 remains unanswered. One explanation may be that the lack of GFP-FHOD1 binding on either side of the M-band removes the fluorescent overlap present in the other images and more of the myomesin TRITC band is visible and distinguishable. The reason could be a molecular spring inside myomesin, allowing it to stretch. Myomesin has been found to contain stretches of molecular spring-like motifs that can stretch when sustained or high stretching forces are present in the sarcomere (Schoenauer, et al., 2005). Considering this elasticity of myomesin, it could be possible that the introduction of the non-localizing double-point actin-binding mutant disturbs the sarcomere in a way that causes stretching of the sarcomere. The width of the sarcomeres in cells expressing the GFP-FHOD1 double actin-binding

mutant is similar to the width of all other cells shown, no extreme stretching of the sarcomere appears to be present, making this an unlikely explanation. The lack of localization of the double actin-binding mutant makes it unlikely that the protein itself interferes with or disturbs proper sarcomere formation and maintenance.

### **GFP-FHOD3 Localization is Actin-binding Dependent**

Exogenous FHOD3 localizes the same way endogenous FHOD3 does, to the area at the center of the sarcomere near the M-line. Similar to the endogenous localization, GFP-FHOD3 appears to be in one line at the center of the sarcomere. This localization is greatly diminished in one of the single-point actin-binding mutants, GFP-FHOD3-971A, but undisturbed in another single-point actin-binding mutant, GFP-FHOD3-1117A. This diminished localization eliminated the need to produce a double-point actin binding mutant, since one of the single-point mutants confirmed that the FH2 actin binding ability is necessary in order for GFP-FHOD3 to localize properly in the sarcomere. As the models in Figure 6 show, the likely localization of FHOD3 as well as GFP-FHOD3 in the sarcomere is in bands on either side of the M-line. There are no known binding sites for formins at the M-line, and based on known formin functions and other studies that have showed FHOD3 localizing to the pointed ends of actin near the M-line, the results in this study suggest that FHOD3, as well as GFP-FHOD3 localize to the pointed ends of actin in the sarcomere. This localization is dependent on the actin-binding ability of conserved regions in the FH2 domain, as shown by the loss of localization in the single-point actin-binding mutant GFP-FHOD3-971A. Similarly to GFP-FHOD1, it is unclear how exactly GFP-FHOD3 binds to the pointed end of actin,

but the high rate of turnover of actin monomers at the pointed end and the leaky tropomodulin cap suggest that the actin monomers at the pointed end of the filament are exposed enough for GFP-FHOD3 to bind to them (Littlefield, et al., 2001; Mardahl-Dumesnil and Fowler, 2001; Bai, et al., 2007).

## References

- Alberts B, Johnson A, Lewis J, Raff M, Roberts K and Walter P. 2002. *Molecular Biology of the Cell*. Garland Science, p293.
- Bai J, Hartwig JH and Perrimon N. 2007. SALS, a WH2-domain-containing protein, promotes sarcomeric actin filament elongation from pointed ends during *Drosophila* muscle growth. *Dev Cell* 13:6828-842.
- Chandhoke SK, Williams M, Schaefer E, Zorn L and Blystone SD. 2004. Beta 3 integrin phosphorylation is essential for Arp3 organization into leukocyte alpha V beta 3-vitronectin adhesion contacts. *J Cell Sci* 117:Pt 81431-1441.
- Harris ES, Rouiller I, Hanein D and Higgs HN. 2006. Mechanistic differences in actin bundling activity of two mammalian formins, FRL1 and mDia2. *J Biol Chem* 281:2014383-14392.
- Kan-o M, Takeya R, Taniguchi K, Tanoue Y, Tominaga R and Sumimoto H. 2012. Expression and subcellular localization of mammalian formin Fhod3 in the embryonic and adult heart. *PLoS One* 7:4e34765.
- Krainer EC, Ouderkirk JL, Miller EW, Miller MR, Mersich AT and Blystone SD. 2013. The multiplicity of human formins: Expression patterns in cells and tissues. *Cytoskeleton* (Hoboken) Wiley Periodicals, Inc. 70(8):424-38.
- Littlefield R and Fowler VM. 1998. Defining actin filament length in striated muscle: rulers and caps or dynamic stability? *Annu Rev Cell Dev Biol* 14:487-525.
- Littlefield R, Almenar-Queralt A and Fowler VM. 2001. Actin dynamics at pointed ends regulates thin filament length in striated muscle. *Nat Cell Biol* 3:6544-551.

Littlefield RS and Fowler VM. 2008. Thin filament length regulation in striated muscle sarcomeres: pointed-end dynamics go beyond a nebulin ruler. *Semin Cell Dev Biol* 19:6511-519.

Lu J, Meng W, Poy F, Maiti S, Goode BL and Eck MJ. 2007. Structure of the FH2 domain of Daam1: implications for formin regulation of actin assembly. *J Mol Biol* 369:51258-1269.

Mardahl-Dumesnil M and Fowler VM. 2001. Thin filaments elongate from their pointed ends during myofibril assembly in *Drosophila* indirect flight muscle. *J Cell Biol* 155:61043-1053.

Otomo T, Tomchick DR, Otomo C, Panchal SC, Machius M and Rosen MK. 2005. Structural basis of actin filament nucleation and processive capping by a formin homology 2 domain. *Nature* 433:7025488-494.

Schoenauer R, Bertoncini P, Machaidze G, Aebi U, Perriard JC, Hegner M and Agarkova I. 2005. Myomesin is a molecular spring with adaptable elasticity. *J Mol Biol* 349:2367-379.

Schönichen A, Mannherz HG, Behrmann E. 2013. FHOD1 is a combined actin filament capping and bundling factor that selectively associates with actin arcs and stress fibers. *J Cell Sci* 126:Pt 81891-1901.

Taniguchi K, Takeya R, Suetsugu S, Kan-O M, Narusawa M, Shiose A, Tominaga R and Sumimoto H. 2009. Mammalian formin fhod3 regulates actin assembly and sarcomere organization in striated muscles. *J Biol Chem* 284:4329873-29881.

Xu Y, Moseley JB, Sagot I, Poy F, Pellman D, Goode BL and Eck MJ. 2004. Crystal structures of a Formin Homology-2 domain reveal a tethered dimer architecture. *Cell* 116:5711-723.

Yaffe D and Saxel O. 1977. Serial passaging and differentiation of myogenic cells isolated from dystrophic mouse muscle. *Nature* 270:563-727.

**Chapter 5:**

**Discussion**

## Discussion

Formin proteins have been found to modify filamentous actin by polymerizing, nucleating, capping, severing and bundling. The ability to effect linear actin filament places them in a unique position to effect a large range of cellular functions, such as cell morphology, cell migration, cell invasion, cytokinesis, microtubule dynamics, phagocytosis, intracellular transport, plasma membrane blebbing, filopodia, invadopodia and podosome formation and focal adhesions. To gain a broad overview of formin expression levels across different cell and tissue types, a quantitative real-time PCR analysis allowed us to see larger patterns and identify possible formins or model systems for future studies.

### Formin Expression Analysis

The expression analysis of formins performed across 22 different human cell and tissue types using quantitative real-time PCR produced not only a broad analysis for the expression of an entire protein family across many commonly studied cell and tissue types, but also provided a spring board for further, more detailed study. The findings regarding FHOD1 and FHOD3 were particularly noteworthy, as FHOD1 and FHOD3 are closely related, yet were found to be the most and the least expressed formin, respectively. While FHOD1 was fairly highly expressed across many cell and tissue types, FHOD3 had very low levels of expression except in striated muscle cells. This finding warranted further investigation into the possible roles for FHOD1 and FHOD3 in skeletal muscle,

starting with a localization study and the creation of full-length GFP-tagged cDNAs.

### **Difference in Localization of Endogenous FHOD1 and FHOD3**

Endogenous FHOD1 localizes to the area of the Z-disk in the sarcomere, as shown in Chapter 3. This finding coincides with other studies of FHOD1 and FHOD1 orthologs and we are quite confident that we correctly identified endogenous FHOD1 and placed it near the Z-disk (Dwyer, et al., 2014; Mi-Mi, et al., 2012). The limitations of our microscopy place FHOD1 at the Z-disk, as shown in Figure 1b. However, based on the known binding ability of FHOD1 and the complex structure of the Z-disk, we are proposing that FHOD1 binds to the barbed end of the actin in the thin filament, which is anchored at the Z-disk. This localization is in line with formins being barbed-end actin polymerizing proteins. Unlike FHOD1, FHOD3 does not localize how a barbed-end actin binding protein would be expected to localize in the sarcomere. Instead of being near the Z-disk, FHOD3 is found near the center of the sarcomere, at the pointed ends of the actin filament, as shown in Figure 1, which is in line with other findings of FHOD3 in striated muscles (Taniguchi, et al., 2009, Kan-o, et al., 2010). Studies on FHOD3 localization have been performed primarily in cardiac muscle, and as far as we know, this is the first study confirming this sarcomeric localization of FHOD3 in skeletal muscle.

These different localizations raise the question why two closely related formins would localize so differently in the same model system. FHOD1 and

FHOD3 are 50% identical and 61% similar. An obvious reason could be that they have different functions in the sarcomere. FHOD1 at the barbed end could act as an actin capper, as has been suggested by other studies (Schönichen, et al., 2013), or perhaps even play a role in thin filament anchoring at the Z-disk. While it is possible that FHOD1 polymerizes actin at the barbed end, based on *in vitro* findings of FHOD1 not being able to polymerize actin, this function is somewhat unlikely, though possible. What function FHOD3 performs at the pointed end, or even how it localizes in relation to other proteins at the pointed end is equally unclear. The pointed end is capped by tropomodulin, which is a leaky capper, so it is entirely possible that FHOD3 binds to the pointed end of the actin filament in the presence of tropomodulin. FHOD3 mostly likely is not binding to the side of the actin filament, because side-binding would result in a very broad band of FHOD3 along the entire thin filament, but our findings suggest a narrow band equivalent to the pointed ends of actin pointed ends lining up at the M-line. FHOD3 could be playing a role in actin monomer exchange and the slow-growing, yet highly dynamic pointed end of actin. It could simply be part of the capping complex, interacting with tropomodulin somewhere outside the FH2 domain and the actin filament with its FH2 domain.

To further determine the role of FHOD1 and FHOD3 at their respective locations within the sarcomere, a number of experiments could be performed. A series of domain-based studies could help to determine if any other domains are necessary for proper localization. A constitutively active mutant lacking the DAD domain could provide insight into both whether the DAD domain is necessary for

proper localization, and whether a constitutively active formin would have an effect on the sarcomere. Perhaps the active form of FHOD1 would turn from an actin-capping protein into an actin-polymerizing protein and thin filament length increases. To avoid any possible side-effects of removing the DAD domain, alternatively, monoclonal antibodies could be designed for FHOD1 and FHOD3 that bind the proteins in a way that forces them into a constitutively active conformation, allowing us to see the effects of full-length active FHOD1 and FHOD3 on the sarcomere.

### **Creation of Full-length FHOD1 and FHOD3 cDNA**

As part of the analysis of FHOD1 and FHOD3 localization in the sarcomere, we needed full-length cDNA for FHOD1 and FHOD3. Full-length FHOD1 cDNA was commercially available and introduced into a GFP-Zeocin expression vector. The entire construct was sequenced, ensuring GFP-FHOD1 expression was in-frame.

Two studies have been published using full-length FHOD3 cDNAs, but repeated attempts to contact the authors for sample cDNA were fruitless (Taniguchi, et al., 2009, Kan-o, et al., 2010). Both *in vivo* and *in vitro* formin studies are often performed using partial constructs or domain-based constructs, and the availability of full-length cDNAs, especially of some of the lesser studied formins, such as FHOD1 and FHOD3 has been scarce. A partial C-terminal clone of FHOD3 was available commercially, and we added the missing N-terminal portion through a combination of novel cDNA created by fusing oligomers and

using reverse transcription PCR on human skeletal muscle poly A<sup>+</sup> RNA.

Mutations at known actin-binding sites were introduced into the full-length GFP-FHOD3 cDNA.

One of the results of this study is the availability of full-length, fully sequenced cDNAs of FHOD1 and FHOD3 tagged with GFP, as well as single actin binding mutants for both formins and a double actin-binding mutant for FHOD3. We will make these novel cDNAs available to other laboratories after publishing our current findings, which will hopefully further the study of full-length human formins.

### **Actin-binding Required for Localization of GFP-FHOD1 and GFP-FHOD3**

The localization of both GFP-FHOD1 and GFP-FHOD3 was disturbed by mutations of conserved actin-binding sites within the FH2 domain. For GFP-FHOD1 single-point mutants (GFP-FHOD1-705A and GFP-FHOD1-851A) only partially diminished actin-binding ability, while a double-point mutant completely abolished it. GFP-FHOD3's actin-binding ability was not disturbed by one single-point mutant (GFP-FHOD3-1117A), but was completely eradicated by another single-point mutant (GFP-FHOD3-971A). This actin-binding study shows that the localization of GFP-FHOD1 and GFP-FHOD3 is actin-dependent, but it allows further insight into the nature of the actin-binding of these two formins. Perhaps FHOD1 binds actin via both conserved residues (Isoleucine 705 and Lysine 851), while FHOD3 binds actin only at Isoleucine 971. Such a difference could explain why they bind to opposite ends of the actin filament, with the Isoleucine required

to bind to the pointed end and either Isoleucine and Lysine required to properly bind to the barbed end.

Introducing mutations into the full-length FHOD1 and FHOD3 cDNAs could potentially disrupt proper folding of the protein, and the diminished localization could be due to a conformational change rather than a lack of actin-binding ability. However, these mutations have been shown to hinder actin-binding in other formins, Bni1p in *Saccharomyces cerevisiae* and human DAAM1 in (Otomo, et al., 2005; Lu, et al., 2007; Xu, et al., 2007), so the chance that these mutations cause a conformational change that interferes with actin-binding, rather than changing the residues that bind with actin is rather low. The conserved Lysine and Isoleucine residues were replaced with Alanine, which is not known to cause conformational changes, further indicating that the decrease in actin-binding ability in these mutants is due to the mutation of the actin-binding residues rather than a change in the protein's shape.

### **Difference in Localization of Endogenous and Exogenous FHOD1**

The most surprising finding of these studies is the difference in localization of endogenous and exogenous FHOD1. While endogenous FHOD1 localizes to the barbed end of the actin filament, exogenous GFP-tagged FHOD1 localizes to the exact opposite end of the actin filament. In fact, GFP-FHOD1 localizes the same way endogenous and GFP-FHOD3 localize. While we do not have a definitive explanation for this difference, there are a number of reasons that could explain it. The addition of the GFP to FHOD1 may increase its size or change its

shape in a way that makes it unable to fit into the space around the Z-disk. Compared to the M-line, the Z-disk is a very tightly packed structure. During muscle contraction, the space around the Z-disk becomes even more crowded than it is in a relaxed state, with the thick filament approaching the Z-disk, while the pointed ends of actin at the center of the sarcomere become very exposed during muscle relaxation, allowing much easier access for a protein to bind to the pointed end. Another reason for the different localization could be the half-life of endogenous FHOD1. If FHOD1 is highly stable and has a half life of several days, there would be few opportunities for exogenous FHOD1 to bind in its place, forcing GFP-FHOD1 to bind somewhere else. Being that FHOD1 and FHOD3 are closely related it would make sense for FHOD1 to bind where FHOD3 binds.

The C2C12 model system is of murine origin, while the cDNA constructs introduced into this system are human. The protein sequences of human (NP\_037373) and murine FHOD1 (NP\_808367) share 91% identity and 94% similarity. Differences between the two species could be a reason for the different localization of endogenous murine FHOD1 and exogenous human FHOD1. The actin-binding sites in the FH2 domain that were mutated in the actin-binding study are the same in human and murine FHOD1.

Exogenous FHOD1 has an additional GFP domain, which increases the size of the FHOD1 protein by approximately 80 amino acids or 7%. This is a significant increase in size, and the location of the GFP domain could impact the protein's shape. The GFP was added N-terminally, placing it near the GBD and DID domains, which are involved in the activation of formins. The addition of GFP

could interfere with the proper activation of FHOD1 by interfering with effector-binding to the GBD or with DID-DAD interaction. Formins undergo a conformational change when they switch between their inactive and active states. It is possible that the GFP of the exogenous FHOD1 interferes with the binding of the DID and DAD domains, which results in an autoinhibited state, making GFP-FHOD1 constitutively active. If endogenous FHOD1 at the barbed end of actin is in an autoinhibited state while capping actin, the active form of FHOD1 as GFP-FHOD1 may not be able to bind correctly. Endogenous GFP-FHOD3 could be in an active state more often than FHOD1 at the barbed end, making the FHOD3 spot at the pointed end a more fitting localization for the active GFP-FHOD1. To eliminate or significantly decrease the possibility of the GFP-tag interfering with proper protein folding and function, a smaller tag, such as a polyhistidine-tag containing 6 amino acids could be used. The likelihood of such a small tag interfering with protein folding and function is much smaller than the 80 amino acid GFP causing a change that effects localization or function. Alternatively, a C-terminal tag could be introduced to minimize interference with the GBD and DID domains.

### **Determining the Rate of Turn-over of FHOD1 and FHOD3**

To determine the half-life of FHOD1 and FHOD3 in the sarcomere, a series of FRAP (fluorescence recovery after photobleaching) experiments could be carried out. After introducing the GFP-tagged cDNAs, an area in the sarcomere is photobleached and the gradual return of fluorescence is measured

and extrapolated to calculate the half-life of FHOD1 and FHOD3 in the sarcomere. A long half-life for FHOD1, meaning that FHOD1 proteins stay at the barbed end for many days before being replaced could explain why exogenous FHOD1 could not bind at the barbed end of actin. The rate of dissociation of FHOD1 from the barbed end could be so slow that there are very few opportunities for GFP-FHOD1 to bind in its place.

### **Knock-down and Rescue Experiments**

The siRNA knock-down attempted in this study showed a statistically significant effect of the negative control on myofibril formation, and did not allow us to carry out any further knock-down and rescue experiments. To overcome this effect of raw oligonucleotides on the proper formation of myotubes, an alternate system of decreasing endogenous FHOD1 and FHOD3 could be used. Two options for the introduction of silencing RNA would be a viral expression system or CRISPR (clustered regularly interspaced short palindromic repeats).

### **Other Formins in the Sarcomere**

As shown in chapter 6, GFP-FMNL1 localizes to the sides of the thin filament. This finding prompts the question where other formins localize that have high levels of expression in skeletal muscle, such as Dia3, which has a similar level of expression to FHOD3 in skeletal muscle (Krainer, et al., 2013). Dia formins have been shown to polymerize actin *in vitro* by binding to the barbed end of the actin filament. If Dia3 localizes to the barbed end of actin it would co-

localize with FHOD1, or perhaps the presence of FHOD1 would make it difficult for another formin with the same actin-binding domains to bind to the barbed end of actin. Another question that arises is why the level of expression of Dia3 is twice as high in skeletal muscle as that of Dia1 and Dia2. Dia3 has not been studied in detail, and so far the only specific finding is that it is required, along with Dia1 and Dia2 for invadopodia formation *in vitro* (Lizarraga, et al., 2009). No studies exist on the localization or role of Dia3 in striated muscles, but based on its high level of expression and its capability to bind actin it is likely that Dia3 binds the actin in the thin filament of the sarcomere. This raises the bigger question of which other formins localize within the sarcomere. Perhaps formin function in the sarcomere is dependent upon other nearby formins, or the proper functioning of one formin at the barbed end and a different formin at the pointed end, as could be the case with FHOD1 and FHOD3. Further localization studies with formin antibodies could help shed light on the possible presence and role of other formins in the sarcomere.

### **Implications for Muscle Diseases**

There are 40 to 50 muscle disorders and myopathies in humans, varying from in-utero to geriatric onset. (Ozawa, E, 2010). A simple blood test for cytoplasmic proteins, such as lactate dehydrogenase and creatine kinase, which leak out of muscle cells due to membrane damage can determine the presence of a muscular dystrophy or myopathy (McNally and Pytel, 2007). The exact mechanisms and involved proteins have been determined for only a few

disorders, such as the most common genetic muscular disorder, Duchenne Muscular Dystrophy, but treatments remain palliative at best (McNally and Pytel, 2007).

One particular class of muscle diseases in which formins could potentially play a curative or stabilizing role are nemaline myopathies. Nemaline myopathy is a skeletal muscle disease that affects the thin filament, caused by one of seven identified genetic mutations that destabilize thin filament proteins (Wallgren-Pettersson, et al., 2011). While no clear pathway or connection has been established, formins' ability to bind the actin inside the thin filament of the sarcomere could allow formins, such as FMNL1 which likely binds to the sides of the actin filament, to aid in stabilizing the thin filament in the presence of mutations that disrupt proteins that surround actin in the thin filament, such as tropomyosin and troponin.

The cardiac isoform of FHOD3 specifically has been associated with two different cardiac myopathies: dilated cardiomyopathy and hypertrophic cardiomyopathy (Arimura, et al., 2013; Wooten, et al., 2013).

### **Model of FHOD1, FHOD3, GFP-FHOD1, GFP-FHOD3 and GFP-FMNL1 in the Sarcomere**

Based on the findings in this study, we have proposed a model for the sarcomeric localization of FHOD1, GFP-FHOD1, FHOD3, GFP-FHOD3 and GFP-FMNL1, as shown in Figure 1. Figure 1b shows the localization of all formins included in this study as they appear in fluorescent microscopy images.

FHOD1 localizes to the area of the Z-disk, FHOD3 to the center of the sarcomere, GFP-FHOD1 in two lines on either side of the M-line, GFP-FHOD3 to the center of the sarcomere and GFP-FMNL1 to the length of the thin filament. The resolution constraints and considerable fluorescent overlap between FITC, GFP and TRITC channels does not allow us to pinpoint the exact sarcomeric localization of these proteins. However, based on the results of our microscopy and actin-binding studies and the likely function of these formins, we have proposed a working model in Figure 1c.

We propose that FHOD1 localizes to the barbed ends of the actin filament in the sarcomere. FHOD1 has highly conserved actin-binding sites in the FH2 domain and we hypothesize that these motifs bind to the barbed end of actin. FHOD1 has no demonstrated ability to polymerize actin *in vitro*, and assuming this inability to polymerize actin holds true *in vivo*, we believe that FHOD1 likely serves as an actin capping protein in the sarcomere. While consistent in length, the thin filament is dynamic and actin monomers depolymerize and polymerize at both the barbed and pointed ends of the thin filament. FHOD1 would make an ideal capping protein, due to its ability to remain associated with the barbed end of the actin filament while also adding actin monomers at the barbed end. Even though FHOD1 has not been shown to polymerize actin in actin polymerization assays *in vitro*, a very slow polymerization activity that allows the thin filament to retain its set length remains possible.

GFP-FHOD1 does not localize the way endogenous FHOD1 does, but instead localizes to the center of the sarcomere. We propose that GFP-FHOD1

binds to the pointed end of the actin filament in the sarcomere, based on our findings in the actin-binding study. We were able to disturb the localization of GFP-FHOD1 with the mutation of two actin-binding residues in the FH2 domain. Single-point mutations decreased its localization, while a double-point mutation completely abolished the sarcomeric localization of GFP-FHOD1. This diminished ability to localize when unable to bind to actin led us to the conclusion that GFP-FHOD1 binds to the barbed end of the actin filament in an FH-2 dependent manner. Specifically, the residues Isoleucine 705 and Lysine 851 are necessary for actin-binding.

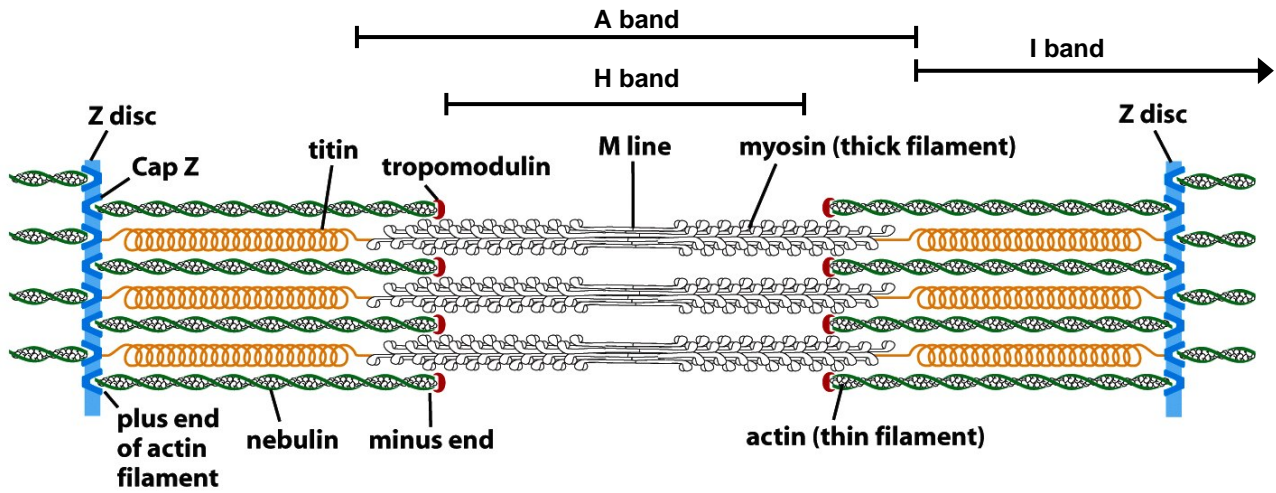
GFP-FHOD3 also localizes to the center of the sarcomere, and similarly to GFP-FHOD1, we hypothesize that it binds to the pointed ends of the actin filament located towards the center of the sarcomere. This exogenous localization is the same as the localization of endogenous FHOD3. Furthermore, the results of our actin-binding study confirmed the pointed end of actin as the most likely binding site for FHOD3. A single-point mutant was able to completely disturb the localization of FHOD3 in the sarcomere, which led us to conclude that GFP-FHOD3 localization is dependent on actin-binding in the FH2 domain, with Isoleucine 971 primarily responsible for the sarcomeric localization of GFP-FHOD3 to the pointed end of the actin filament.

GFP-FMNL1 was included in this study because we found this formin to have a very particular localization during the process of establishing the C2C12 model system. To optimize the introduction of cDNA into C2C12 cells, we introduced full-length GFP-tagged formins that had already been successfully

expressed in other cells. GFP-FMNL1 not only expressed successfully in C2C12 cells, but it localized in a sarcomeric pattern to the thin filaments, as shown in Appendix 1. Diaphanous related formins have been shown to have actin-binding sites outside of the FH2 domain in the DAD domain, and FMNL1 has been found to have residues outside of the FH2 domain capable of binding to the sides of actin filaments (Harris, et al., 2006; Gould, et al., 2011). Mutations of conserved actin-binding sites in the FH2 domain do not disturb FMNL1's ability to bind to the sides of actin filaments (Harris, et al., 2006). Furthermore, our own laboratory has found that full-length FMNL1, with mutations in the FH2 domain that interfere with actin binding is able to rescue an actin-dependent function *in vivo*, further supporting the idea that there are additional actin-binding sites outside the FH2 (Blystone Lab, unpublished observations). To determine whether the localization of GFP-FMNL1 mimics the localization of endogenous FMNL1 a series of immunohistochemical co-localization studies could be performed, to rule out a possible difference in localization, such as is the case with FHOD1 and GFP-FHOD1. Introducing GFP-FMNL1 actin-binding mutants could confirm whether or not the sarcomeric localization of GFP-FMNL1 is actin-binding dependent. If actin-binding mutants localize to the sides of the actin filament the same way GFP-FMNL1 does, we could conclude that this localization is most likely due to actin-binding sites located outside of the FH2 domain, and likely in the DAD domain.

Overall we feel that this model of formin localization in the sarcomere, besides providing a comparative analysis of FHOD1 and FHOD3, is a good

starting point to place other formins in the sarcomere. A series of antibody-studies could help to determine the localization of other formins in the sarcomere. While localizing formins in the sarcomere may not provide any immediate conclusions as to their possible function in the sarcomere, the directional arrangement of actin in the sarcomere would allow for a quick determination which end of the actin filament a formin is binding *in vivo*. The C2C12 model system could be used as a supplemental approach to determining full-length cDNA or endogenous formin binding of the actin filament.





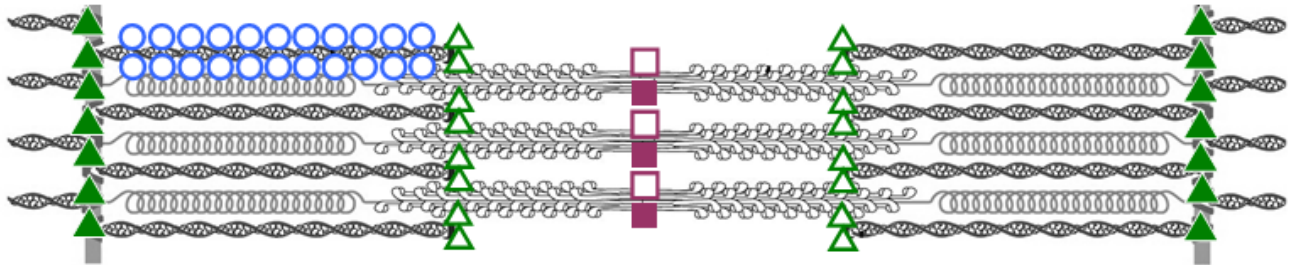



**Figure 1a – Components of the Sarcomere**  
 adapted from: Alberts, et al, 2003, p 963

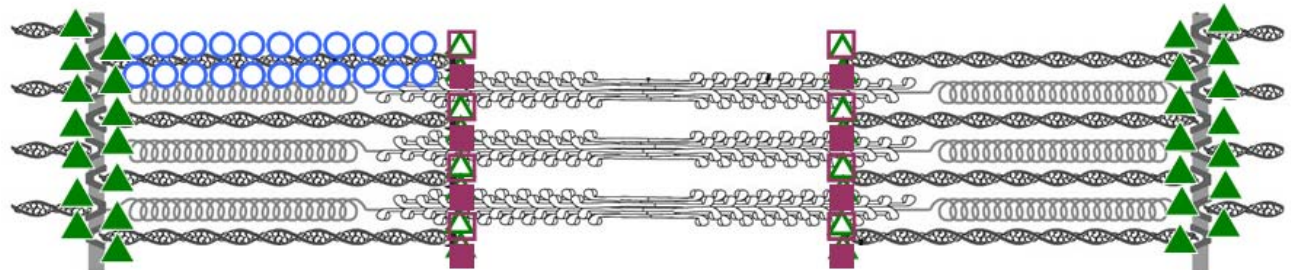


**Figure 1b – Formin localization in the sarcomere model 1**



**Figure 1c – Formin localization in the sarcomere model 2**

- |   |                  |   |           |
|---|------------------|---|-----------|
|  | endogenous FHOD1 |  | GFP-FHOD1 |
|  | endogenous FHOD3 |  | GFP-FHOD3 |
|   |                  |  | GFP-FMNL1 |

**Figure 1 - Proposed localization of endogenous FHOD1 and FHOD3, and GFP-FHOD1, GFP-FHOD3 and GFP-FMNL1**

## Summary

The first part of this study yielded a comprehensive expression analysis of all 15 human formins across 22 different human cell and tissue types. The results led us to initiate a comparative study of FHOD1 and FHOD3 in skeletal muscles, but this was just one of many findings in the expression analysis that could be used as a preliminary finding to further investigate specific formins in certain cell and tissue types.

The second part of this study focused on the localization of endogenous and exogenous FHOD1 and FHOD3 in the sarcomere. We found that endogenous FHOD1 and FHOD3 localize to opposite ends of the actin filament at the core of the thin filament, with FHOD1 at the barbed end and FHOD3 at the pointed end. Full-length GFP-tagged cDNAs were created for both formins and introduced into the sarcomere. While GFP-FHOD3 localized in the same manner as FHOD3, GFP-FHOD1 localized to the opposite end of the actin filament as the endogenous form. Despite this difference in localization we were able to show that the sarcomeric localization of both GFP-tagged formins depends on highly conserved actin-residues inside the FH2 domain.

## References

Alberts B, Johnson A, Lewis J, Raff M, Roberts K and Walter P. 2002. *Molecular Biology of the Cell*. Garland Science.

Arimura T, Takeya R, Ishikawa T, Yamano T, Matsuo A, Tatsumi T, Nomura T, Sumimoto H and Kimura A. 2013. Dilated cardiomyopathy-associated FHOD3 variant impairs the ability to induce activation of transcription factor serum response factor. *Circ J* 77:122990-2996.

Dwyer J, Pluess M, Iskratsch T, Dos Remedios CG and Ehler E. 2014. The formin FHOD1 in cardiomyocytes. *Anat Rec (Hoboken) Wiley Periodicals, Inc* 297:91560-1570.

Gould CJ, Maiti S, Michelot A, Graziano BR, Blanchoin L and Goode BL. 2011. The formin DAD domain plays dual roles in autoinhibition and actin nucleation. *Curr Biol Elsevier Ltd* 21:5384-390.

Harris ES, Rouiller I, Hanein D and Higgs HN. 2006. Mechanistic differences in actin bundling activity of two mammalian formins, FRL1 and mDia2. *J Biol Chem* 281:2014383-14392.

Kan-o M, Takeya R, Taniguchi K, Tanoue Y, Tominaga R and Sumimoto H. 2012. Expression and subcellular localization of mammalian formin Fhod3 in the embryonic and adult heart. *PLoS One* 7:4e34765.

Lizarraga F, Poincloux R, Romao M, Montagnac G, Le Dez G, Bonne I, Rigail G, Raposo G and Chavrier P. 2009. Diaphanous-related formins are required for invadopodia formation and invasion of breast tumor cells. *Cancer Res* 69:72792-2800.

Lu J, Meng W, Poy F, Maiti S, Goode BL and Eck MJ. 2007. Structure of the FH2 domain of Daam1: implications for formin regulation of actin assembly. *J Mol Biol* 369:51258-1269.

McNally, E. M., and P. Pytel. 2007. Muscle diseases: The muscular dystrophies. *Annual Review of Pathology* 2, : 87-109.

Mi-Mi L, Votra S, Kempfues K, Bretscher A and Pruyne D. 2012. Z-line formins promote contractile lattice growth and maintenance in striated muscles of *C. elegans*. *J Cell Biol* 198:187-102.

Otomo T, Tomchick DR, Otomo C, Panchal SC, Machius M and Rosen MK. 2005. Structural basis of actin filament nucleation and processive capping by a formin homology 2 domain. *Nature* 433:7025488-494.

Ozawa E. Our trails and trials in the subsarcolemmal cytoskeleton network and muscular dystrophy researches in the dystrophin era. *Proc Jpn Acad Ser B Phys Biol Sci.* 2010; 86(8): 798-821.

Schönichen A and Geyer M. 2010. Fifteen formins for an actin filament: a molecular view on the regulation of human formins. *Biochim Biophys Acta* 1803:2152-163.

Taniguchi K, Takeya R, Suetsugu S, Kan-O M, Narusawa M, Shiose A, Tominaga R and Sumimoto H. 2009. Mammalian formin fhod3 regulates actin assembly and sarcomere organization in striated muscles. *J Biol Chem* 284:4329873-29881.

Wallgren-Pettersson C, Sewry CA, Nowak KJ and Laing NG. 2011. Nemaline myopathies. *Semin Pediatr Neurol Elsevier Inc*18:4230-238.

Wooten EC, Hebl VB, Wolf MJ. 2013. Formin homology 2 domain containing 3 variants associated with hypertrophic cardiomyopathy. *Circ Cardiovasc Genet* 6:110-18.

Xu Y, Moseley JB, Sagot I, Poy F, Pellman D, Goode BL and Eck MJ. 2004. Crystal structures of a Formin Homology-2 domain reveal a tethered dimer architecture. *Cell* 116:5711-723.

**Appendix 1:**

**Localization of Exogenous FMNL1**

## **Introduction**

To develop the C2C12 model system and introduce GFP-tagged plasmids, several constructs that had been successfully expressed in other cell types were introduced into C2C12 cells via lipofection. These included non-formin constructs, such as GFP and Paxillin, as well as full-length formins. This was intended simply as a method of establishing parameters for the introduction of exogenous DNA, and to show that full-length formins can be successfully expressed in this model. Surprisingly, GFP-FMNL1 localized to a specific part of the sarcomere.

## **Methods**

### **C2C12 Cell Culture**

To prepare glass coverslips, they were washed in 70% Ethanol, coated with 10% Poly-L-Lysine (Sigma-Aldrich, St. Louis, MO) for 20 minutes, washed with phosphate-buffered saline (Life Technologies, Grand Island, NY) twice after removing Poly-L-Lysine, washed with sterile water twice, and placed under UV light for 18 hours. Glass coverslips were then coated with 3mg/ml Type I rat tail collagen (Corning Incorporated Life Sciences, Tewksbury, MA) and dried under UV light for three hours. The mouse myoblast cell line C2C12 (ATCC<sup>®</sup> Manassas, VA), isolated from the thigh muscles of dystrophic mice (Yaffe and Saxel, 1977) was seeded on prepared coverslips in growth medium containing Dulbecco's modified eagle medium, DMEM (Life Technologies, Grand Island, NY) containing 10% Fetal Bovine Serum (Gemini Bio-Products, West Sacramento, CA), 1% Penicillin Streptomycin (Life Technologies, Grand Island, NY) and 1% GlutaMAX<sup>™</sup> (Life Technologies, Grand Island, NY). To differentiate C2C12 cells the media was changed to differentiation medium containing DMEM 4% horse serum (Life Technologies, Grand Island, NY), 1% Penicillin Streptomycin and 1% GlutaMAX<sup>™</sup>, which was changed every 48 hours until cells were fully differentiated.

### **Sample Preparation for Microscopy**

Cells were washed with room temperature phosphate buffered saline, (PBS, Life Technologies, Grand Island, NY) twice, incubated with 3.7%

Formaldehyde (Fischer, Pittsburgh, PA), 1% TX-100 (Fischer, Pittsburgh, PA) in PBS for 10 minutes at 4°C, washed with PBS twice, incubated with 1M Glycine (Fischer, Pittsburgh, PA) in PBS for 20 minutes at room temperature, washed with PBS twice, incubated with 3% Bovine Serum Albumin (BSA, Sigma-Aldrich, St. Louis, MO) 1% TX-100 for 2 hours at room temperature, washed with PBS twice, and incubated with primary antibody for two hours at 37°C. Primary antibodies for Fhod1 C-14, Fhod3 K-19 and E-20 (Santa Cruz, Dallas, TX), alpha-actinin (Sigma-Aldrich, St. Louis, MO) were incubated in 1% BSA 0.5% TX-100 for 2 hours at 37°C. Myomesin antibody was isolated from supernatant obtained from mMaC myomesin B4 (Developmental Studies Hybridoma Bank, University of Iowa) grown in Iscove's DMEM (Life Technologies, Grand Island, NY) containing 20% FBS and 1% Gentamicin. C2C12 cells were incubated with myomesin supernatant for 2 hours at 37°C. After primary antibody incubation, cells were washed with PBS three times, and incubated with secondary antibodies anti-goat FITC and TRITC and anti-mouse TRITC (Jackson ImmunoResearch Laboratories, West Grove, PA) and DAPI (Life Technologies, Grand Island, NY) in 1% BSA 0.5% TX-100 for 1 hour at 37°C.

### **C2C12 Lipofection**

C2C12 cells were grown to 75% confluency as previously described. The media was changed to 1ml 37°C DMEM containing 10% Fetal Bovine Serum and 1% GlutaMAX™. GFP-FMNL1 in a GFP-Zeocin vector (Chandhoke, et al., 2004) in concentrations ranging from 1µg to 15µg and Lipofectamine® 2000 (Life

Technologies, Grand Island, NY) were incubated separately, each in a total of 150µl Opti-MEM® I Reduced Serum Media (Life Technologies, Grand Island, NY) and combined after five minutes, incubated for 20 minutes at room temperature and added to the cells. After 24 hours 0.5ml of DMEM containing 10% Fetal Bovine Serum and 1% GlutaMAX™ was added, and after 48 hours the media changed to 3ml DMEM containing 4% horse serum (Life Technologies, Grand Island, NY), 1% Penicillin Streptomycin and 1% GlutaMAX™ for cell differentiation. The media was changed to 3ml DMEM containing 4% horse serum, 1% Penicillin Streptomycin and 1% GlutaMAX™ every 48 hours until cells fully differentiated.

### **Microscopy & Image Analysis**

Images were captured using a Nikon Eclipse E800 microscope and analyzed using NIS-Elements AR 3.10 software (Nikon Instruments Inc. Melville, NY). Intensity profile analysis was performed using NIS Elements AR 3.10

## Results

### **GFP-FMNL1 Localization in the Sarcomere**

Full-length GFP-FMNL1 was found to localize in a sarcomeric pattern in C2C12 cells. Co-localization with the Z-disk marker alpha-actinin shows FMNL1 to localize in a wide double band between Z-disks, with no FMNL1 seen at the very center of the sarcomere. This pattern suggests that FMNL1 localizes to the sides of the actin filament in the sarcomere. No similar studies with FMNL1 antibodies have been carried out. Note that the fluorescent overlap of FITC and TRITC emission creates some bleed-through of TRITC in the FITC channel.

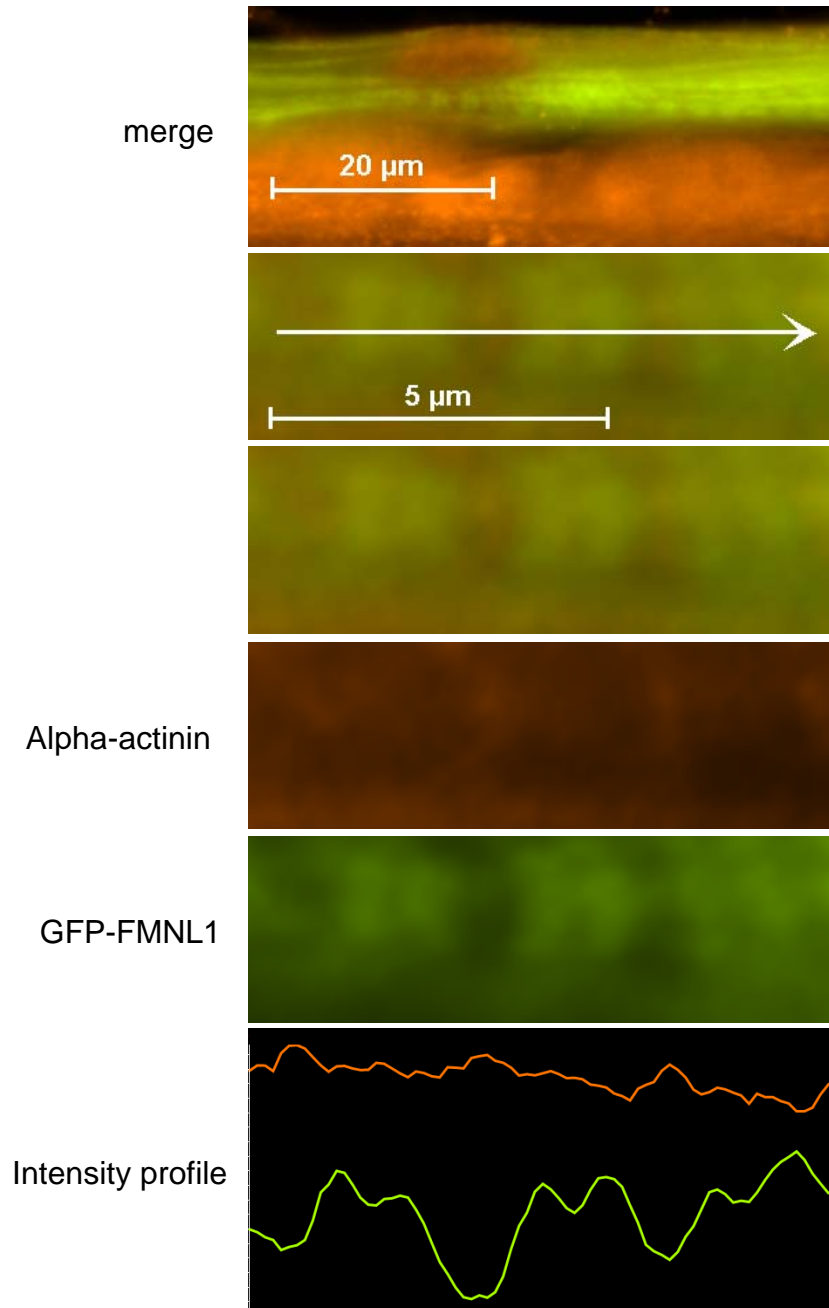


**Figure 1 – GFP-FMNL1 localization with sarcomeric alpha-actinin.** GFP-FMNL1 localizes in a sarcomeric pattern with Z-disk marker alpha-actinin.

### **Model of GFP-FMNL1 Localization in the Sarcomere**

Based on the findings in this study, Figure 2 presents a model of the proposed sarcomeric localization of GFP-FMNL1. The figure shows a non-contracted sarcomere, as seen by the small area of overlap between thin and thick filaments and the wide H-band. A contracted sarcomere has an almost non-existent H-band and almost complete overlap of the thin and thick filaments. When fixing cells for immunohistochemical analysis, cells contract, the space in the H-band is greatly compressed. For ease of visualization, a relaxed sarcomere is shown in Figure 7.

As shown in Figure 2b, it is proposed that GFP-FMNL1 localizes to the length of the part of the thin filament, made up of an actin core and surrounded by troponin and tropomyosin. The width of the GFP-FMNL1 suggests that it is binding to the sides of the actin filament. A localization to either the pointed or the barbed end would yield a much narrower band, such as the alpha-actinin band in Figure 1.

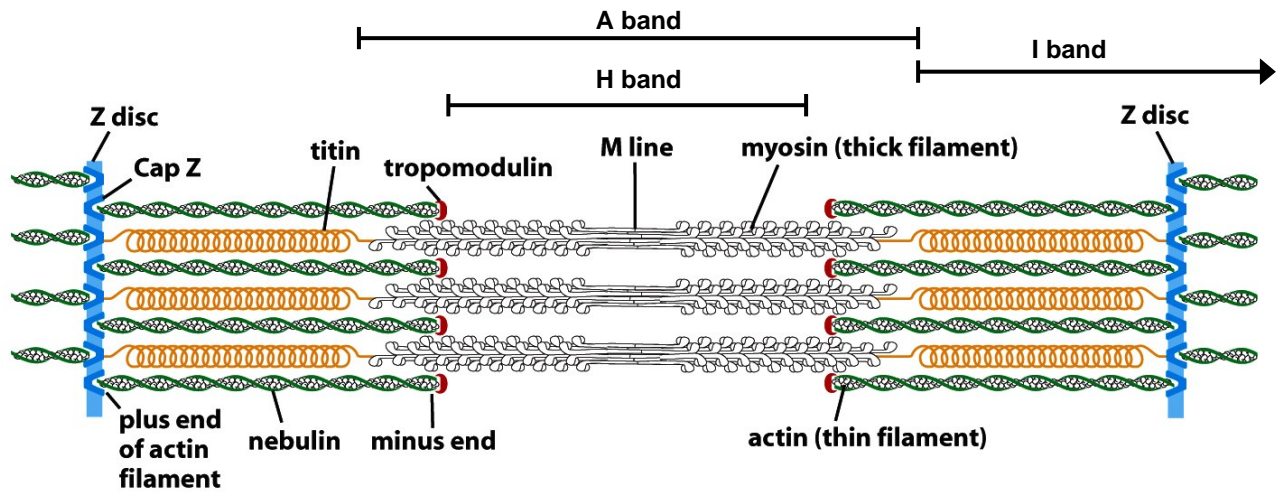


**Figure 2a – Components of the Sarcomere**  
adapted from: Alberts, et al, 2003, p 963

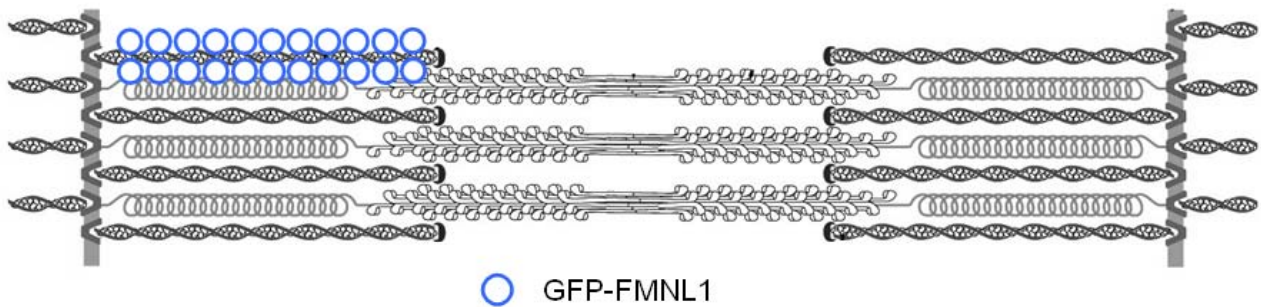


**Figure 2b – Model of GFP-FMNL1 Localization in the Sarcomere**

**Figure 2 – GFP-FMNL1 in the Sarcomere**

Proposed model of GFP-FMNL1 localization in the sarcomere

## Discussion

FMNL1 is a diaphanous-related formin, which, traditionally bind actin via the FH2 domain as homo-dimers. However, recent findings suggest that DRFs may have actin-binding sites outside the FH2 domain in the DAD domain (Gould, et al., 2011). Furthermore, FMNL1 has been found to have residues outside of the FH2 domain capable of binding to the sides of actin filaments (Harris, et al., 2006). This side-binding ability of FMNL1 holds true when the conserved FH2 domain actin binding domains are mutated (Harris, et al., 2006). Full-length FMNL1, with mutations in the FH2 domain that interfere with actin binding has been shown to rescue an actin-dependent function *in vivo*, further supporting the idea that there are additional actin-binding sites outside the FH2 (Blystone Lab, unpublished observations).

The findings in this study that FMNL1 localizes to the sides of the actin filament in the sarcomere are likely due to these alternative actin-binding sites in FMNL1. No studies exist to show how FMNL1 is involved in striated muscle architecture, formation or maintenance, and expression analysis of FMNL1 in skeletal and cardiac muscle do not suggest a prominent role of FMNL1 in these tissues (Krainer, et al., 2013). FMNL1 likely has no function in the sarcomere and forcing its expression via exogenous cDNA introduction could force a localization that is not present endogenously. To confirm endogenous localization, immunohistochemical studies would need to be performed. If FMNL1 has no endogenous expression in the sarcomere, the forced expression could force the protein to localize in a way that can support binding capabilities of FMNL1, such

as the secondary actin-binding sites in the DAD domain. The traditional localization of FMNL1 would be to the barbed end of the actin filament. However, the barbed end in the sarcomere is anchored to the Z-disk and surrounded by Z-disk proteins. This arrangement could mean that there is simply not enough room for FMNL1 to bind to the barbed end of actin by forming a homo dimer, and the protein localized where it could bind, the side of the actin filaments.

To determine whether GFP-FMNL1 localizes to the sides of the actin filament via its FH2 or DAD domain, actin-binding mutants can be introduced. If actin-binding mutants, with highly conserved regions in the FH2 domain mutated from Isoleucine and Lysine to Alanine, still bind to the sides of the actin filament, this localization is most likely due to a secondary actin binding site possibly located in the DAD domain. If actin-binding mutants are unable to localize to the sides of the actin filament, this localization is most likely due to FMNL1 binding to the sides of the actin filament via the conserved regions inside the FH2 domain.

## References

Alberts B, Johnson A, Lewis J, Raff M, Roberts K and Walter P. 2002. Molecular Biology of the Cell. Garland Science, p963.

Chandhoke SK, Williams M, Schaefer E, Zorn L and Blystone SD. 2004. Beta 3 integrin phosphorylation is essential for Arp3 organization into leukocyte alpha V beta 3-vitronectin adhesion contacts. J Cell Sci 117:Pt 81431-1441.

Gould CJ, Maiti S, Michelot A, Graziano BR, Blanchoin L and Goode BL. 2011. The formin DAD domain plays dual roles in autoinhibition and actin nucleation. Curr Biol Elsevier Ltd21:5384-390.

Harris ES, Rouiller I, Hanein D and Higgs HN. 2006. Mechanistic differences in actin bundling activity of two mammalian formins, FRL1 and mDia2. J Biol Chem 281:2014383-14392.

Krainer EC, Ouderkirk JL, Miller EW, Miller MR, Mersich AT and Blystone SD. 2013. The multiplicity of human formins: Expression patterns in cells and tissues. Cytoskeleton (Hoboken) Wiley Periodicals, Inc. 70(8):424-38.

Yaffe D and Saxel O. 1977. Serial passaging and differentiation of myogenic cells isolated from dystrophic mouse muscle. Nature 270:5639725-727.